

INTERACTIONS OF A SOIL HUMIC ACID
WITH ALKALI METAL CATIONS
AND ALKALINE EARTH METAL CATIONS

Bernadine A. Bonn
B.S., University of Portland, Portland, Oregon, 1979
M.A.T., Lewis and Clark College, Portland, Oregon, 1986

A thesis submitted to the faculty of the
Oregon Graduate Institute of Science & Technology
in partial fulfillment of the requirements for the degree
of Doctor of Philosophy
in
Environmental Science and Engineering

April, 1992

The dissertation "Interactions of a soil humic acid with alkali metal cations and alkaline earth metal cations" by Bernadine A. Bonn has been examined and approved by the following Examination Committee:

William Fish, Thesis Advisor
Assistant Professor

Wesley M. Jarrell
Professor

Thomas Loehr
Professor

Carl D. Palmer
Assistant Professor

ACKNOWLEDGEMENTS

Until recently, the completion of this dissertation seemed overwhelming. In the five-and-a-half years it has taken to get to this point, I have received assistance, support, and reassurance from many individuals and wish to express my sincere appreciation.

I am grateful to my advisor, Bill Fish, for both financial support and encouragement. His personable nature and skills as a conversationalist are particularly appreciated. I would also like to thank all of the members of my examination committee, Bill Fish, Carl Palmer, Wes Jarrell, and Tom Loehr, for their thoughtful reading of this work and their insightful comments. I am also indebted to Maurie Clark for providing financial assistance via the Clark Fellowship.

This research could not have been accomplished without assistance from several individuals and laboratories. Special thanks to Tom Loehr and the chemistry department for the use of the FTIR and the CIRCLE® cell; Laura Andersson for introducing me to the FTIR; Bill Pengelly for the use of equipment in his laboratory; Gloria Maestrojuan, Yitai Lui, and other members of Dave Boone's laboratory for their gracious sharing of the centrifuge. A number of people made my life easier with their helpfulness in innumerable ways. Thank you to Judi Irvine, Don Buchholz, Lorne Isabelle, Pam Locke, Donna Reed, Allan Ryall, Sandy Holt, and Doug Davis.

I was blessed with two wonderful labmates, and friends, who are not only exceptionally bright, but quite entertaining as well. Karel Mesuere is an insightful and caring individual. I will always be in awe of his painstaking lab work. Mike Elovitz combines sincerity and a helpful nature with a talent for research. His ability to combine graduate research with a myriad of adventures is amazing.

My family and friends probably deserve sainthood for listening to my frustrations and reminding me that graduate school is temporary. Their understanding and unconditional support were most valued. I am particularly grateful for the friendship of Margaret Armstrong, who spent two summers maintaining my humor as my "Partner in Science."

The last person acknowledged here is also the most important. My husband, Stewart Rounds, has been my colleague, advisor, editor, closest friend, and keeper of my sanity. I cannot imagine completing this work without his love, understanding, and reassurance.

TABLE OF CONTENTS

Acknowledgements	iii
Table of Contents	v
List of Figures	vii
List of Tables	xii
Abstract	xiii
CHAPTER I. Introduction	1
Background	1
Purpose and relavance of this research	4
Reader's guide to the thesis	5
References	7
CHAPTER II. Variability in Measurements of Carboxyl Content in Humic Substances	9
Abstract	9
Introduction	10
Equilibrium chemistry	16
Experimental methods	19
Results and discussion	21
Summary and conclusions	37
References	39
CHAPTER III. Measurement of electrostatic and site-specific associations of alkali metal cations with humic acid	41
Abstract	41
Introduction	42
Experimental	44
Results and discussion	47
Conclusions	61
References	62

CHAPTER IV. Aqueous CIR-FTIR of Humic Acid I.	
Method description and evaluation	64
Abstract	64
Introduction	65
Experimental	72
Solvent-subtraction program description	76
Results and discussion	81
Conclusions	91
References	92
CHAPTER V. Aqueous CIR-FTIR of Humic Acid II.	
Effects of pH, alkali metal cations, and alkaline earth cations	95
Abstract	95
Introduction	96
Experimental	102
Mathematical data treatment	104
Results and discussion	107
Conclusions	141
References	144
CHAPTER VI. Summary	148
Conclusions	148
Implications for further research	151
APPENDIX A. Computer programs to model humic carboxyl acidity. . . .	153
APPENDIX B. Computer programs to calculate Langmuir parameters . .	163
APPENDIX C. Computer programs for aqueous humic infrared spectral analysis	175
VITA	197

LIST OF FIGURES

Figure 1.	Measured carboxyl content of a soil humic acid as a function of the humic acid to acetate ratio	23
Figure 2.	Measured carboxyl content (using 0.4 M total acetate) of humic acid as a function of the humic acid to acetate ratio . .	25
Figure 3.	The calculated carboxyl content of monoprotic acids as a function of the HA/acetate ratio	27
Figure 4.	The equilibrium speciation diagrams for a mixture of (a) 0.01 M or (b) 0.001 M monoprotic acid (HA, pK = 6.76) and 0.2 M sodium acetate as a function of pH	28
Figure 5.	Calculated dimensionless carboxyl content isopleths for monoprotic acids. For an acid of any specified pK, the isopleths indicate the carboxyl content observed at any specified HA/acetate ratio	30
Figure 6.	Calculated carboxyl content of binary mixtures (50%-50%) of monoprotic acids	32
Figure 7.	Individual dissociated acid fractions and carboxyl content of a 50%-50% mixture of two monoprotic acids	34
Figure 8.	Calculated carboxyl content of a hypothetical humic acid (bimodal distribution: $\mu_1=4.5$, $\mu_2=10$, $\sigma_1=\sigma_2=2$, $X_1=0.6$). Inset pK distributions show the pH and humic acid speciation	36
Figure 9.	Characteristic dilution curves for desorption experiments assuming three sorption models: no sorption, linear sorption, and Langmuir sorption	49
Figure 10.	Aqueous cation concentrations as a function of the dilution ratio for a) desorption experiments with humic acid, and b) control experiments (without humic acid)	51
Figure 11.	The relationship between the pH values of humic solutions before ultrafiltration and the net amount of base added	52

Figure 12.	The relationship between the net base added and the amount of Na ⁺ associated with the humic matter	54
Figure 13.	The relationship between the net base added and the amount of Li ⁺ , Na ⁺ , or K ⁺ associated with the humic matter	55
Figure 14.	The relationship between the net base added and the amounts of Li ⁺ , Na ⁺ , and K ⁺ associated with the humic matter expressed cumulatively	56
Figure 15.	The correlation between the free aqueous anion and cation concentrations for all of the ultrafiltration experiments	58
Figure 16.	A schematic diagram of the diffuse layer model for humic solutions	59
Figure 17.	a) The infrared absorbance spectrum of aqueous lithium humate, pH 8.02. Humic acid concentration: 45 mg/mL b) The absorbance spectrum of water	69
Figure 18.	a) The infrared absorbance spectrum of water in the "fit region", 2250 - 1950 cm ⁻¹ . b) An undersubtracted difference spectrum and the best fit line segments in the fit region. c) The optimal difference spectrum and best fit line segments in the fit region d) An oversubtracted difference spectrum and the best fit line segments in the fit region	77
Figure 19.	a) A representative water-water difference spectrum. b) The standard deviation of 6 water-water difference spectra. c) An undersubtracted water-water difference spectrum. d) An oversubtracted water-water difference spectrum	82
Figure 20.	a) The mean of 3 lithium humate difference spectra obtained on the same day, pH 3.42. b) The standard deviation associated with the mean spectrum shown in a)	84
Figure 21.	a) The mean of 3 lithium humate difference spectra obtained on the same day, pH 8.02. b) The standard deviation associated with the mean spectrum shown in a)	85

Figure 22.	a) The mean of 2 lithium humate difference spectra prepared and recorded 24 days apart day, pH 3.91. b) The standard deviation associated with the mean spectrum shown in a) . . .	87
Figure 23.	a) The difference spectrum between a 0.1 M solution of LiCl and a water background. b) The difference spectrum between a 0.1 M solution of NaCl and a water background. c) The difference spectrum between a 0.1 M solution of KCl and a water background	88
Figure 24.	a) A Li-humate difference spectrum, pH 5.35. b) A Na-humate difference spectrum, pH 5.37. c) A K-humate difference spectrum, pH 5.45	90
Figure 25.	a) The second derivative spectrum of the Lorentzian shaped peak shown immediately below in b). b) A Lorentzian shaped peak	101
Figure 26.	The aqueous spectra of six Li-humate solutions of different pH. All spectra have been background subtracted	108
Figure 27.	Difference spectra formed by subtracting the aqueous Li-humate spectrum at pH 3.0 from spectra of higher pH. Only the features that change with pH are visible	111
Figure 28.	A detailed view of the carboxyl/carboxylate absorbance regions of Li-humate spectra of different pH	114
Figure 29.	The numerically-approximated second derivatives of a set of Li-humate spectra of different pH. Only the carboxyl/carboxylate absorbance region is shown	115
Figure 30.	a) The absorbance spectrum of Li-humate and the fitted synthetic spectrum in the region 1800-1480 cm^{-1} with the 17 individual synthetic peaks. b) The residual spectrum, calculated as the difference of the absorbance data and the fitted values. c) The smoothed, numerically-approximated second derivatives of the absorbance spectrum and the fitted spectrum	119

Figure 31.	The pH dependence of the 16 fitted synthetic peaks for 28 Li-humate spectra	120
Figure 32.	Three difference spectra formed by subtracting pH-matched (pH=4.6) aqueous spectra containing different alkali metal cations. a) Na-humate - Li-humate. b) K-humate - Li-humate. c) K-humate - Na-humate	124
Figure 33.	Difference spectra formed by subtracting an aqueous Na-humate spectrum (pH 3.1) from spectra of higher pH . Only the features that change with pH are visible	125
Figure 34.	The pH dependence of the 16 fitted synthetic peaks for 12 Na-humate spectra	127
Figure 35.	The pH dependence of the 16 fitted synthetic peaks for 13 K-humate spectra	128
Figure 36.	The dependence of the pH of Li-humate on the alkaline earth cation concentration	130
Figure 37.	a) The aqueous spectra of five Li-humate solutions in the presence of increasing amounts of Ba ²⁺ . All spectra have been background subtracted. b) Background subtracted aqueous spectrum of 0.10 M BaCl ₂ (humic-free)	131
Figure 38.	Difference spectra formed by subtracting the aqueous Li-humate spectrum (alkaline earth cation free) from spectra containing increasing amounts of Mg ²⁺ , Ca ²⁺ , or Ba ²⁺ . Only the features that change are visible	133
Figure 39.	The dependence of the fitted synthetic peak areas on the total Mg ²⁺ concentration for 12 aqueous Li-humate samples. Peak areas are normalized to the total area shown in the lower plot, and are displayed cumulatively	135
Figure 40.	The dependence the fitted synthetic peak areas on the total Ca ²⁺ concentration for 12 aqueous Li-humate samples. Peak areas are normalized to the total area shown in the lower plot, and displayed cumulatively	136

- Figure 41.** The dependence the fitted synthetic peak areas on the total Ba^{2+} concentration for 10 aqueous Li-humate samples. Peak areas are normalized to the total area shown in the lower plot, and displayed as **cumulatively** 137
- Figure 42.** Four series of difference spectra formed by subtracting the aqueous spectrum of the most acidic sample in the series from the spectra of samples with higher pH. Three of series contain divalent cations as indicated on the figure 138

LIST OF TABLES

Table I.	Fractions of humic matter.	2
Table II.	Elemental composition of humic matter.	2
Table III.	Optimized Langmuir model parameters.	50
Table IV.	Second derivative peaks of Li-humate spectra.	117

ABSTRACT

Interactions of a Soil Humic Acid with Alkali Metal Cations and Alkaline Earth Cations

Bernadine A. Bonn, Ph.D.

Oregon Graduate Institute of Science & Technology, 1992
Supervising Professor: William Fish

The association between alkali metal cations and humic acid was investigated by aqueous infrared spectroscopy and discontinuous titration. The infrared spectra of aqueous humic solutions were acquired by circular internal reflectance Fourier transform (CIR-FTIR) techniques. An objective, reproducible method of aqueous solvent subtraction was developed and evaluated. Derivative spectra and curve fitting methods were used to improve the resolution of highly overlapping peaks.

Significant quantities of alkali metal cations associated with humic matter. The absolute amount of humic-associated cation depended on the solution alkalinity, rather than the cation concentration. The alkali metal cations (Li^+ , Na^+ , and K^+) behaved equivalently and were essentially interchangeable. Aqueous humic infrared spectra were unaffected by the identity of the alkali metal cation, except for solvent artifacts. In addition, the humate anion did not significantly contribute to the charge balance of the aqueous solution. These results suggest that alkali metal cations neutralize the humate charge by associating electrostatically with the humate anion in a diffuse layer.

Desorption experiments at pH 1, revealed a small amount of site-specific binding of Na^+ and K^+ by the humic acid. No site-specific binding of Li^+ was detected. The number of sites was greater for K^+ than for Na^+ , indicating that

more-hydrated cations may be sterically excluded. The hydrated cation size decreases in order $\text{Li}^+ > \text{Na}^+ > \text{K}^+$.

The infrared spectra of solutions containing low concentrations of alkaline earth cations were essentially identical to those of humic solutions containing only alkali metal cations. Unlike the alkali metal cations, however, humic matter showed a preferential association among the alkaline earth cations. The amount of humic-associated cation decreased in order $\text{Ba}^{2+} > \text{Ca}^{2+} > \text{Mg}^{2+}$. Increasing the alkaline earth cation concentration did not substantively affect the aqueous infrared spectra until a threshold concentration was exceeded. At that concentration, the spectral intensity abruptly decreased and the solution became very viscous. The physical aspect of these changes and their precipitous nature suggest a conformational change facilitated by the alkaline earth cations.

CHAPTER I

Introduction

BACKGROUND

Humic substances are present in virtually all soils, sediments and natural waters as a major component of both dissolved and particulate organic matter. The non-humic fraction of organic matter is typically of low molecular weight and consists primarily of carbohydrates, proteins, peptide fragments, amino acids and fats. Most of these compounds are easily degraded by microorganisms, and exhibit short lifetimes in the environment. In contrast, the humic fraction is of much higher molecular weight and resists degradation. The first known methods to separate soil humic material into distinct fractions were developed by Sprengel (1826) and Berzelius (1833). The procedure has changed very little since then. Sequential extractions are used to separate humic material into three fractions based upon acid-base solubility (Table I.).

The genesis of humic matter is not completely understood. A widely accepted theory postulates that soil micro-organisms slowly degrade lignin into fragments which with small amounts of carbohydrates and proteins coalesce over time to form heterogeneous macromolecules. As these macromolecules age, condensation and degradation reactions occur simultaneously. The macromolecules become progressively larger, more aromatic, less acidic, and more

Table I. Fractions of humic matter.

Fraction	Acid	Base
Fulvic acid	soluble	soluble
Humic acid	insoluble	soluble
Humin	insoluble	insoluble

hydrophobic. Fulvic acids form first and consequently have lower molecular weights, more carboxyl groups and a lesser degree of aromaticity than humic acids (STEVENSON, 1972). Humic and fulvic acids are not unique chemical entities, but rather, **operationally defined** complex mixtures.

Since the 19th century, researchers from a variety of disciplines, including soil science, agriculture, marine and fresh water ecology, chemistry and environmental science, have attacked the problem of humic substance characterization. Although progress has been made, investigations have been severely hampered by one common property of all humic matter: heterogeneity. Humic composition depends upon the environment of origin and the method of isolation. Therefore, determination of exact molecular properties, such as a specific molecular weight, a precise chemical formula, or a definitive structure, is impossible. Typical elemental analyses for fulvic and humic acids are summarized in Table II. Trace amounts of sulfur or phosphorus also may be

Table II. Reported elemental composition ranges of humic matter.

element	per cent by weight	
	fulvic acids	humic acids
Carbon	40.7 - 50.6 %	53.6 - 58.7 %
Hydrogen	4.2 - 7.0 %	3.2 - 5.8 %
Oxygen	43.1 - 48.8 %	32.7 - 38.3 %
Nitrogen	9.0 - 3.3 %	0.8 - 5.5 %

present. Functional group analyses indicate that humic and fulvic acids contain an aromatic core, aliphatic side chains, carboxylic and phenolic groups, and ester and ether linkages. Humic acids have a greater proportion of aromatic carbon, and hence more phenolic groups, than do fulvic acids. The carboxyl content of fulvic acids is greater than that of humic acids. Carboxylic and phenolic functional groups are primarily responsible for the binding of metal cations by humic substances.

Humic substances play a dual role in the environment by influencing both the availability and the transport of metal cations. In soils and aquatic systems, humic and fulvic acids sequester dissolved trace metals, thereby increasing the apparent metal solubility (CHOU DHRY, 1984). Because metal/humate complexes are more labile than their metal/mineral counterparts, humic substances increase the availability of nutrient ions to organisms. It is precisely this labile binding, so vital to plant survival, that is of concern in environments with trace metal contamination. A cation bound to humic matter is *not effectively removed* from its environment. In addition, humic and fulvic acids are mobile and any bound metal cations or sorbed organic molecules will be transported with the humic macromolecules.

Cation-humate association may occur via coordinate-covalent binding at specific sites, or by simple electrostatic attraction. The association equilibrium is significantly complicated by the heterogeneity of humic matter. Cation-humate association is commonly described by one of four models: 1) a set of discrete ligands (HUNSTON, 1975; DZOMB AK, *et al.*, 1986; FISH, *et al.*, 1986), 2) a continuous frequency distribution of ligands (PERDUE, *et al.*, 1984), 3) simple ion exchange (KERNDORF and SCHNITZER, 1980), and 4) ion exchange plus a set of discrete ligands (MARINSKY and EPHRAIM, 1986). All of these models rely heavily upon empirical techniques, especially the ability to fit titration curve data. Conclusions regarding the structure of specific binding sites or the mechanism of association are speculative and not based on direct evidence.

Infrared spectroscopy has been used to probe humic functional groups, directly, especially carboxyl and carboxylate groups (MACCARTHY and RICE, 1985). The infrared spectra of humic substances are surprisingly simple with relatively few, broad absorbance bands. This somewhat featureless nature is due to the overlap of many individual peaks and should be expected. Humic substances are, after all, heterogeneous mixtures, and their spectra must reflect that fact. Interestingly, all humic spectra are strikingly similar, regardless of the origin of the humic substance (STEVENSON, 1982). Such similarity does not imply structural equivalence, but rather, identifies a set of functional groups that are common to all humic substances (MACCARTHY and RICE, 1985).

PURPOSE AND RELEVANCE OF THIS RESEARCH

The intent of this research was to characterize the electrostatic component of cation-humate association. In particular, I was interested in describing this association from the perspective of the humic macromolecule *vis-a-vis* that of the aqueous solution. Unlike empirically-fitted association constants, an understanding of the humic role in cation-humate association is transferable from one environment to another. The primary reason for focusing on an electrostatic association mechanism is its simplicity. Studies of the interactions between transition metals and humic matter have been almost hopelessly complicated by the combination of multiple binding sites and electrostatic effects with humic heterogeneity. I view this study of the electrostatic mechanism of humic-cation association as a basic foundation, and hope that the results will be applied to more complex systems to help resolve competing mechanisms.

The association between a soil humic acid and a suite of alkali metal cations was used to assess the magnitude of electrostatic attraction as a function of pH. The covalent character of bonds with alkali metal cations is minimal. Infrared spectroscopy was employed to probe humic functional group changes that occur due to humic dissociation, and the presence of alkali metal or alkaline

earth metal cations. The humic-interactions with alkaline earth cations and with alkali metal cations can be compared to identify the effects of cation charge. The use of a circular internal reflectance (CIR) accessory facilitated the acquisition of **aqueous** infrared spectra. Almost all previous infrared spectroscopic studies of humic substances utilized dry samples (KBr pellets) that do not accurately represent the natural hydrated state of humic acids.

The suite of cations (Li^+ , Na^+ , K^+ , Mg^{2+} , Ca^{2+} , Ba^{2+}) selected for these experiments are environmentally relevant, despite the fact that they are usually ignored by most researchers. The *macro-cations*, Na^+ , K^+ , Mg^{2+} , and Ca^{2+} , are naturally present at concentrations much higher than those of trace metal cations, such as Cu^{2+} or Pb^{2+} . Although humic binding of trace metals may be much stronger than humic association with macro-cations, the importance of the latter is increased by the number of environmental systems that contain relatively high concentrations of these cations. Understanding the interactions of the macro-cations with humic matter is important in the areas of agriculture, plant physiology, soil science, and estuarine and oceanic ecology. Nowhere is the presence of macro-cations more striking than in estuarine systems. Steep concentration gradients of macro-cations, especially Ca^{2+} , may cause coagulation of humic matter in estuaries (SHOLKOVITZ and COPELAND, 1981). This coagulation may be associated with the concurrent transport of sorbed trace level cations to the sediments, or alternatively, the macro-cation may displace trace cations from humic material.

READER'S GUIDE TO THE THESIS

The next four chapters describe the results of my research with soil humic acid and my interpretations of that research. Pertinent references to the literature are included for background, and to present a context for my work.

My research has taken a number of twists and turns over the past four years; Chapter 2 resulted from one such detour. The acetate method for

determining humic carboxyl content was supposed to be routine, but I could not obtain values that were independent of the solution composition. Chapter Two demonstrates that the acetate method cannot yield constant values for the carboxyl content of humic matter, and explores the effects of humic heterogeneity on acid-base titrations in general.

In Chapter Three, the extent of alkali-metal-cation association with humic acid is explored. The magnitude of the electrostatic association was investigated by performing discontinuous titrations with a soil humic acid and a suite of alkali metal cations (Li^+ , Na^+ , and K^+). In addition, the possibility of specific binding of these cations was assessed by desorption experiments at low pH. The use of ultrafiltration to sample the humic aqueous phase is also described in Chapter Three.

Chapters Four and Five discuss the application of CIR-FTIR (circular internal reflectance Fourier transform infrared spectroscopy) to aqueous suspensions of soil humic acids. The method is described in detail and evaluated in Chapter Four. In particular, the mathematical algorithm for performing optimal aqueous solvent subtraction is developed and tested. In Chapter Five, the results of the aqueous humic infrared studies are reported and discussed. The dependence of the humic spectra on pH, alkali metal cations, and alkaline earth cations is shown. In addition, the application of resolution enhancement methods (second derivative spectra and curve fitting) to aqueous humic spectra is described.

In Chapter Six, the overall conclusions this work are summarized and the implications for other studies of humic materials are discussed. In addition, some possible directions for future work are outlined.

No part of my research seems to have escaped the influence of the microprocessor. I have written a variety of programs in the attempt to wring more information from the data or gain insight into a complex process. The source codes for these programs are listed in the Appendices. Sample input and

output are included as well. All programs are written in Microsoft Professional BASIC. Appendix A contains the program listing for the discrete and the continuous distribution models of humic pK values (from Chapter Two). The optimization routine used to fit the Langmuir parameters for the desorption experiments (Chapter Three) is listed in Appendix B. Finally, Appendix C outlines the manipulation of the humic infrared spectra from the initial translation to an ASCII file format to the fitting of synthetic peaks, and contains all of the associated source code listings.

Chapters Two through Five were written as research papers and have been submitted for publication. Chapter Two appeared in *Environmental Science and Technology* in January of 1991. Chapter Three has been submitted to the *Journal of Soil Science*. Chapters Four and Five have been submitted to *Geochimica Cosmochimica Acta* for publication as a two-paper series.

REFERENCES

- CHOUHRY G.G. (1984) *Humic Substances, Structural, photophysical, photochemical and free radical aspects and interactions with environmental chemicals*. Gordon and Breach Science, New York.
- DZOMBAK D.A., FISH W., and MOREL F.M.M. (1986) Metal-humate interactions. 1. Discrete ligand and continuous distribution models. *Environ. Sci. Technol.* **20**, 669-675.
- FISH W., DZOMBAK D.A., and MOREL F.M.M. (1986) Metal-humate interactions. 2. Applications and comparison of models. *Environ. Sci. Technol.* **20**, 676-683.
- HUNSTON D.L. (1975) Two techniques for evaluating small molecule-macromolecule binding in complex system. *Anal. Biochem.* **63**, 99-109.
- KERNDORFF H. and SCHNITZER M. (1980) Sorption of metals on humic acid. *Geochim. Cosmochim. Acta* **44**, 1701-1708.

MACCARTHY P. and RICE J.A. (1985) Spectroscopic methods (other than NMR) for determining functionality in humic substances. In *Humic Substances in Soil, Sediment, and Water: Geochemistry, Isolation and Characterization* (eds. G.R. AIKEN, D.M. MCKNIGHT, R.L. WERSHAW and P. MACCARTHY), pp. 527-559. Wiley-Interscience, New York.

MARINSKY J.A. and EPHRAIM J. (1986) A unified physicochemical description of the protonation and metal ion complexation equilibria of natural organic acids (humic and fulvic acids). 1. Analysis of the influence of polyelectrolyte properties on protonation equilibria in ionic media: fundamental concepts. *Envir. Sci. Technol.* **20**, 349-354.

PERDUE E.M., REUTER J.H. and PARRISH R.S. (1984) A statistical model of proton binding by humus. *Geochim. Cosmochim. Acta* **48**, 1257-1263.

SHOLKOVITZ E.R. and COPLAND D. (1981) The coagulation, solubility and adsorption properties of Fe, Mn, Cu, Ni, Cd, Co and humic acids in a river water. *Geochim. Cosmochim. Acta* **45**, 181-189.

STEVENSON F.J. (1982) *Humus Chemistry*. Wiley, New York.

CHAPTER II

Variability in Measurements of Carboxyl Content in Humic Substances

ABSTRACT

The acetate reaction method for estimating the operationally defined carboxyl content of humic matter was evaluated via laboratory experiments with a soil-derived humic acid and via computer simulations with hypothetical acids. The behavior of monoprotic acids, mixtures of monoprotic acids and a model humic acid were simulated. Both the experimental data and the theoretical analyses demonstrated that the acetate reaction method yields a strong acidity index that varies inversely with the ratio of equivalents of acidity to equivalents of acetate. Unless the exact reaction conditions are known, individual carboxyl content measurements cannot be compared. The equilibrium chemistry of the acetate reaction was examined with particular attention to the influence of acids that partially dissociate in acetate solution. For acids with continuous pK distributions such as humic acids, neither the acetate method, nor any other titration method can be assumed to quantitate acidic groups described by a particular pK or pK range.

INTRODUCTION

Humic substances are heterogeneous polyfunctional macromolecules present in virtually all soils, sediments, and natural waters as a major component of both dissolved and particulate organic matter. Because they are weakly acidic, humic substances help buffer soils and eutrophic waters, and account for a portion of the cation exchange capacity. Most of the acidity in humic and fulvic acids is due to carboxylic and phenolic functional groups, both of which can act as ligands for dissolved metals.

The transport and fate of metal cations in aquatic systems and soils can be dramatically affected by humic matter. Humate complexation can enhance the solubility of otherwise insoluble metal cations, such as Fe^{3+} or Pb^{2+} , allowing them to be advected with the natural flow (RASHID, 1985). Because some metal humate complexes are labile, the effect of complexation on transport can be variable. For example, the precipitation of humic matter in estuarine systems increases the transport of tightly bound metal cations to the sediments, while the weakly bound cations are liberated into the water column (SHOLKOVITZ and COPELAND, 1981). The effect of humate-cation interactions on the bioavailability of ions is also determined by this labile behavior. In humus-rich soils, Cs^+ -humate association is strong enough to resist leaching, but not strong enough to prevent the uptake of Cs^+ by plants (CAWSE, 1983).

In order to accurately model metal transport, a description of the acidic behavior of humic matter is necessary. Measures of the total acidity can be used as an upper limit of the cation exchange capacity of the humic material. The phenolic groups, however, will not be dissociated in the pH range of most natural environments. Consequently, an estimate of the average number of carboxyl groups in the humic macromolecule provides a better indication of the complexing potential of humic matter than does the total acidity measurement. In addition, site specific binding will depend heavily on the identity of the

humic functional group. Knowledge of the distribution of binding sites is needed to model interactions of metal cations with humate ligands.

Acidity of humic material is most often measured by direct or indirect titration. These methods have been reviewed by STEVENSON (1982), PERDUE (1985), and FLAIG *et al.* (1975). The direct titration of humic material is associated with a variety of problems. Direct potentiometric titration of humic matter (in either aqueous or non-aqueous solvents) typically produces curves that lack distinguishable inflection points, making the selection of the endpoint, and therefore the determination of acidity, somewhat arbitrary. Usually specific pH values are chosen to indicate the titration endpoints. For example, PERDUE *et al.* (1980) selected pH 7 as the endpoint for the titration of carboxyl groups; similarly, McKNIGHT *et al.* (1988) estimated that 50% of the phenolic groups were titrated between pH 8 and 10. In their non-aqueous systems, EPHRAIM *et al.* (1986) titrated fulvic acids in a dimethylformamide solvent spiked with parahydroxybenzoic acid. They used the inflection points corresponding to the neutralization of the parahydroxybenzoic acid to mark the titration endpoints for the fulvic acid carboxyl and phenol groups. Direct calorimetric titration has been successfully employed (PERDUE, 1978), however, calorimetric methods are experimentally more cumbersome than potentiometric methods. In contrast to direct methods, indirect potentiometric titrations of humic material are simple to perform and analyze; consequently, they are widely used. Two such methods are the barium hydroxide method for the determination of total acidity, and the acetate method for the determination of carboxyl content. Both methods were originally described for the analysis of coal (FUCHS, 1927; IHNATOWICZ, 1952; BROOKS and STERNHELL, 1957) and later adapted for use with humic materials (SCHNITZER and GUPTA, 1965).

The determination of total acidity via indirect titration is performed by reacting humic matter with 0.1 M Ba(OH)₂, filtering the mixture to remove the barium humate precipitate, and then titrating the excess base in solution

(SCHNITZER and KHAN, 1972). The titration endpoint is sharp because the barium humate is removed. Total acidity is calculated from the difference between the concentration of the reagent base solution and that of the filtrate. Provided that care is taken to maintain CO₂-free solutions, total acidity measured by the barium hydroxide method is reproducible for a given sample (BROOKS and STERNHELL, 1957). Although exceedingly weak acidic groups will not react in this procedure, the pK of such groups is greater than 13 and they are therefore of little significance in natural systems. These very weak acidic groups are evident only in non-aqueous titrations employing solvents that are weaker acids than water, such as dimethylformamide or ethylenediamine (EPHRAIM, *et al.* 1986; WRIGHT and SCHNITZER, 1960).

The acetate reaction is an indirect titration method that is routinely utilized to estimate the portion of acidity attributable to carboxylic functional groups. This method is based upon proton exchange between humic carboxyl groups and the acetate anion. Protons, liberated from the dissociation of carboxyl groups on the humic material, react with acetate to form acetic acid. In the widely used procedure described by SCHNITZER and KHAN (1972), humic material is mixed with excess aqueous calcium acetate, allowed to equilibrate, and then filtered to remove the calcium humate precipitate. The acidity in the filtrate is quantified by titration with strong base to a predetermined endpoint (pH 9.8). A blank titration of the acetate reagent is also performed to correct for background acidity. The carboxyl content is calculated as the corrected acidity of the filtrate divided by the mass of humic material used in the analysis.

Because no convenient independent method exists to measure the phenol content of humic material, the calcium acetate method is frequently used with the barium hydroxide method to calculate the fraction of the total acidity that is due to phenolic functional groups. The phenol content is calculated as the total acidity less the carboxyl content. Any errors in the carboxyl content determination therefore, are carried directly into the value for phenol content.

The relative proportions of carboxylic and phenolic functional groups are used as one indicator of the degree of humification or evolution of the humic matter. Typically, fulvic acids have a greater total acidity and a larger proportion of carboxyl groups than humic acids.

Like all other titration methods, the acetate method distinguishes acidic functional groups by their relative acidity rather than their actual molecular structure. For this method to accurately measure the acidity due to carboxyl groups, the carboxyl acidity of the humic material must be quantitatively converted to acetate acidity. This will occur only if the following two conditions are met when the humic acid/acetate mixture reaches equilibrium: (1) **all humic carboxylic functional groups are completely dissociated**, and (2) **all other acidic functional groups in the humic material are completely undissociated**.

In polyfunctional macromolecules such as humic or fulvic acids, steric constraints, neighboring constituents, and electrostatic interactions influence the acidity of each functional group, causing a distribution of acidity constants. Although the average carboxyl group will be more acidic than the average phenol group, the two distributions of pK will overlap (PERDUE, *et al.*, 1980; DUBACH, *et al.*, 1964). Some carboxylic and phenolic groups will therefore dissociate simultaneously. In addition, although spectroscopic evidence indicates that carboxyl and phenol groups are the predominant acidic functional groups in humic matter, they are not the only source of acidity. Other functional groups, such as sulfonyl groups and hydroxyquinones, are acidic enough to dissociate in the acetate reaction and therefore be included in the measure of carboxyl content (DUBACH, *et al.*, 1964; HOLTZCLAW and SPOSITO, 1979). Consequently the acetate method does not quantify the number of carboxyl functional groups. Instead, it divides the acidity into two categories distinguished by their relative behavior with respect to acetate. *Carboxyl content* and *phenol content* are strictly designations of the operationally defined categories of strong and weak acidity, respectively. Any acidic moiety on the humic

macromolecule that dissociates in the acetate reaction will be categorized as strong acidity and included in the carboxyl content. For consistency and convenience, this operational definition is retained throughout this discussion.

The calcium acetate method is sensitive to any artifact that alters the amount of base required in the titration of the filtrate. The calcium acetate procedure was examined in detail by PERDUE and coworkers (1980). They found that the carboxyl content determined by the calcium acetate method was 43% higher than that measured by direct calorimetric titration. Two problems with the Ca-acetate method are primarily responsible for this difference in apparent acidity: (1) incomplete removal of humic species before titration and (2) the formation of calcium humate complexes.

To accurately quantify the amount of humic matter that is dissociated, only acetate acidity must be titrated. At equilibrium with calcium acetate, the weakly acidic fraction of the humic material is undissociated and remains in solution. If this humic acid is not removed during filtration, it will be titrated with the acetic acid, increasing the apparent carboxyl content and obscuring the inflection point in the titration curve. The effect of filterable humic acidity is particularly significant when the filtrate is titrated to the recommended endpoint of pH 9.8, rather than pH 8.9, which is the theoretical endpoint for a 0.2 M acetate solution. HOLTZCLAW and SPOSITO (1979) eliminated the separation problem by substituting steam distillation for filtration. Steam distillation, however, introduces problems of its own. PERDUE, *et al.* (1980) employed ultrafiltration using a membrane with a nominal 1000 dalton cutoff to minimize filterable humic acidity. Both groups of researchers titrated to the theoretical acetate endpoint.

The formation of calcium humate complexes can significantly influence the amount of acetic acid that is present at equilibrium. When a Ca^{+2} -humate complex forms (whether it precipitates or not), the activity of the dissociated humate decreases, causing the humic acid equilibrium to shift toward the

dissociated species. This shift causes an increase in the measured carboxyl content. When Ca^{+2} -humate complexation occurs, the carboxyl content value reflects the combination of two equilibria: acid dissociation and Ca^{+2} -complexation (VAN DIJK, 1966). In addition to this effect, the net negative charge of the humic species is reduced upon complexation with a calcium cation. Partial charge neutralization of the polyanion increases the relative acidities of all the remaining undissociated acidic functional groups by decreasing the energy required for dissociation. This progression toward greater acidity elevates the apparent carboxyl content further. Because any cation that forms stable complexes with humic material will augment the apparent carboxyl content similarly, PERDUE, *et al.* (1980) recommended that an alkali-metal acetate be substituted for calcium acetate. Alkali-metal cations form very weak complexes with humic material (PERDUE, *et al.*, 1980; GAMBLE, 1973).

Despite its recognized limitations, the acetate method is widely used as an empirical means of characterizing the approximate distribution of strongly and weakly acidic functional groups in humic matter. The numerical value of carboxyl content, while not a quantitative measure of the number of carboxyl functional groups, has been believed to be a unique and reproducible index that facilitates the comparison of humic materials from different sources. However, through experimentation and theoretical examination we have found that the acetate method yields an index of strong acidity that is **not unique** and **cannot be reproduced** unless the exact experimental conditions are known.

In this paper the pertinent acid-base equilibrium chemistry of the acetate method is examined. The effects of variations in the solution composition (ratio of humic matter to acetate) as well as the inherent pK distribution of the humic acid on the measured carboxyl content are explored. To our knowledge such an analysis has not appeared previously in the literature, even though the acetate method has been used for more than 60 years. Several examples involving the acetate reaction with simple monoprotic acids and monoprotic acid mixtures are

considered as well as a reaction with a model humic acid. The analysis of the equilibrium between acetate and a model humic acid illustrates a larger problem common to all titrations of humic matter: **titration data alone cannot uniquely determine a continuous pK distribution.**

EQUILIBRIUM CHEMISTRY

Simple Monoprotic Acid System

The chemical equilibrium that applies to the reaction of a monoprotic acid, HA, with aqueous sodium acetate and the associated proton balance equation (PBE) are



$$[\text{H}^+] + [\text{CH}_3\text{COOH}] = [\text{A}^-] + [\text{OH}^-] \quad (1)$$

where the brackets indicate molar concentration. The expression for the dissociation constant of a monoprotic acid HA is

$$K = \frac{\{\text{H}^+\}\{\text{A}^-\}}{\{\text{HA}\}} = \frac{[\text{H}^+]\gamma_{\text{H}^+}[\text{A}^-]\gamma_{\text{A}^-}}{[\text{HA}]\gamma_{\text{HA}}} \quad (2)$$

The braces indicate the chemical activity of the enclosed species and each γ represents the activity coefficient of the species indicated by the subscript. This expression yields an explicit equation for $[\text{A}^-]$ in terms of the total HA concentration ($[\text{HA}] + [\text{A}^-]$), the acid-dissociation constant, and the pH.

$$[\text{A}^-] = [\text{Total HA}] \frac{K\gamma_{\text{HA}}}{K\gamma_{\text{HA}} + \{\text{H}^+\}\gamma_{\text{A}^-}} \quad (3)$$

Similar equations can be derived for the concentrations of OH^- and CH_3COOH in terms of their respective total concentrations and equilibrium constants. The

pK of acetic acid is 4.76 (MARTELL and SMITH, 1977). Substituting expressions (2) and (3) into the PBE yields

$$\frac{\{H^+\}}{\gamma_{H^+}} + [\text{Total Acetate}] \frac{\{H^+\} \gamma_{CH_3COO^-}}{10^{-4.76} \gamma_{CH_3COOH} + \{H^+\} \gamma_{CH_3COO^-}} = \frac{10^{-14}}{\{H^+\} \gamma_{OH^-}} + [\text{Total HA}] \frac{K \gamma_{HA}}{K \gamma_{HA} + \{H^+\} \gamma_{A^-}} \quad (4)$$

Given the equilibrium constant for HA and the solution composition, equation (4) can be solved for the equilibrium $\{H^+\}$ analytically or by using simple iterative techniques.

The carboxyl content is determined by titrating the solution to the acetate endpoint after A^- and HA are removed. This solution will contain only acetate acidity, defined as

$$\text{acetate acidity} = [H^+] + [CH_3COOH] - [OH^-] \quad (5)$$

The carboxyl content, when expressed as acetate acidity per mole of HA, is mathematically equivalent to the fraction of HA that is dissociated, α_1 . This can be demonstrated by a simple rearrangement of the PBE

$$\text{Carboxyl Content} = \frac{[CH_3COOH] + [H^+] - [OH^-]}{[\text{Total HA}]} = \frac{[A^-]}{[\text{Total HA}]} = \alpha_1 \quad (6)$$

Once the equilibrium $\{H^+\}$ is known, the carboxyl content can be easily calculated using equation (6) and the appropriate equilibrium constants.

Monoprotic Acid Mixtures

When a mixture of monoprotic acids reacts with aqueous acetate the appropriate proton balance equation is

$$[\text{H}^+] + [\text{CH}_3\text{COOH}] = [\text{OH}^-] + \sum_{i=1}^n [\text{A}_i^-] \quad (7)$$

where each A_i^- is the conjugate base of the monoprotic acid HA_i , and n is the number of monoprotic acids in the mixture. An equation analogous to equation (4) can be obtained by substituting the appropriate equilibrium expressions into the PBE.

$$\frac{\{\text{H}^+\}}{\gamma_{\text{H}^+}} + [\text{TotalAcetate}] \frac{\{\text{H}^+\} \gamma_{\text{CH}_3\text{COO}^-}}{10^{-4.76} \gamma_{\text{CH}_3\text{COOH}} + \{\text{H}^+\} \gamma_{\text{CH}_3\text{COO}^-}} = \frac{10^{-14}}{\{\text{H}^+\} \gamma_{\text{OH}^-}} + [\text{Total HA}] \sum_{i=1}^n \frac{X_i K_i \gamma_{\text{HA}_i}}{K_i \gamma_{\text{HA}_i} + \{\text{H}^+\} \gamma_{\text{A}_i^-}} \quad (8a)$$

where

$$[\text{Total HA}] = \sum_{i=1}^n ([\text{HA}_i] + [\text{A}_i^-]) \quad \text{and} \quad X_i = \frac{[\text{HA}_i] + [\text{A}_i^-]}{[\text{Total HA}]} \quad (8b)$$

Equation (8) is implicit in $\{\text{H}^+\}$ and can be solved using simple iterative methods.

Continuous pK Distributions

When the dissociation properties of an acid are described by a continuous distribution of pK the PBE becomes

$$\frac{\{\text{H}^+\}}{\gamma_{\text{H}^+}} + [\text{TotalAcetate}] \frac{\{\text{H}^+\} \gamma_{\text{CH}_3\text{COO}^-}}{10^{-4.76} \gamma_{\text{CH}_3\text{COOH}} + \{\text{H}^+\} \gamma_{\text{CH}_3\text{COO}^-}} = \frac{10^{-14}}{\{\text{H}^+\} \gamma_{\text{OH}^-}} + [\text{Total HA}] \int_{-\infty}^{\infty} \frac{f(\text{pK}) 10^{-\text{pK}} \gamma_{\text{HA}}}{10^{-\text{pK}} \gamma_{\text{HA}} + \{\text{H}^+\} \gamma_{\text{A}^-}} d\text{pK} \quad (9)$$

$f(\text{pK})$ is a probability distribution function where the fraction of functional groups with $a \leq \text{pK} \leq b$ is given by

$$\int_a^b f(\text{pK}) d\text{pK}$$

If the functionality of $f(\text{pK})$ is known, the integral in equation (9) can be approximated using Gaussian quadrature; equation (9) is then solved iteratively.

The probability distribution used in this paper is a bimodal distribution formed by taking the weighted average of two normal distributions with means μ_1 and μ_2 , and standard deviations σ_1 and σ_2 . The fraction of the total distribution, $f(\text{pK})$, due to the distribution defined by μ_1 and σ_1 is X_1 . The total distribution is truncated so that the domain of pK values reflects the leveling effect of water, *i.e.* $-1.74 \leq \text{pK} \leq 15.74$. This results in a probability distribution function of the form

$$f(\text{pK}) = \frac{\left(\frac{X_1}{\sigma_1}\right) e^{-\frac{1}{2}\left(\frac{\text{pK}-\mu_1}{\sigma_1}\right)^2} + \left(\frac{1-X_2}{\sigma_2}\right) e^{-\frac{1}{2}\left(\frac{\text{pK}-\mu_2}{\sigma_2}\right)^2}}{\int_{-1.74}^{15.74} \left(\frac{X_1}{\sigma_1}\right) e^{-\frac{1}{2}\left(\frac{\text{pK}-\mu_1}{\sigma_1}\right)^2} + \left(\frac{1-X_2}{\sigma_2}\right) e^{-\frac{1}{2}\left(\frac{\text{pK}-\mu_2}{\sigma_2}\right)^2} d\text{pK}} \quad (10)$$

PERDUE, *et al.* (1984) used this distribution function to model humic acids.

EXPERIMENTAL METHODS

Humic Matter

Humic acid was isolated from soil by a procedure adapted from the one used by the International Humic Substances Society (MACCARTHY, pers. comm.). The soil was obtained from the A horizon of a Labish mucky clay (a fine, montmorillonitic mesic Cumulic Humaquept) in an uncultivated area adjoining

an onion field in Sherwood, Oregon. The soil was equilibrated with 0.1 M HCl for 24 hours, after which the supernatant was discarded. The residue was extracted with 1 M NaOH under N₂ for 24 hours and then acidified to pH 1 with 6 M HCl. The humic acid precipitate was separated by centrifugation, re-extracted using a solution of 0.1 M KOH/0.2 M KCl under N₂, and precipitated with HCl. Repeated treatment of the sample with 0.1 M HCl/0.3 M HF was used to reduce the ash content to below 1%. After lyophilization, the humic acid was washed with 0.1 M HCl until the sodium and potassium content were 0.3% and less than 0.01%, respectively, as determined by atomic absorption spectroscopy. The excess mineral acidity was removed by washing the humic acid with ultrapure water (Nanopure System, Barnstead) until no chloride was detected when the supernatant was tested with 1 M AgNO₃. The humic acid was lyophilized and stored in a desiccator.

Reagents

All solutions were prepared using CO₂-free ultrapure water (Nanopure System, Barnstead) and reagent grade chemicals unless otherwise noted. Stock 1 M sodium hydroxide was prepared from Dilut-It ampoules (J.T. Baker) and stored in a desiccator containing Ascarite II (Thomas Scientific). Fresh base titrant was prepared daily from the stock solution and standardized against primary standard potassium hydrogen phthalate. Acid titrant was standardized using a standardized sodium hydroxide solution.

Carboxyl Content

To measure the carboxyl content, 25 or 50 mL of 0.2 M or 0.4 M sodium acetate was added to a 10-500 mg sample of humic acid in a N₂ purged tube. The tube was tightly capped, placed on a rotary shaker, and mixed at a moderate speed for 48 hours. A blank containing only sodium acetate solution was prepared similarly. After this equilibration period the reaction mixture was

decanted into a N₂ purged Amicon ultrafiltration cell fitted with a prewashed UM-2 membrane filter and filtered at 65 psi with constant stirring. The filtrate was collected under N₂. Aliquots of the filtrate were analyzed by titration under N₂ with standardized NaOH to the appropriate endpoint determined by the acetate concentration. An Orion pH meter (EA 920) with a Corning general purpose combination electrode (#4765531) was used to measure the pH. The carboxyl acidity was calculated using

$$\text{Carboxyl Content} = \frac{(\text{mL NaOH}_{\text{humic sample}} - \text{mL NaOH}_{\text{blank}}) \cdot \text{molarity NaOH} \cdot \text{mL acetate}}{\text{g humic acid} \cdot \text{mL aliquot}}$$

The barium hydroxide method (SCHNITZER and KHAN, 1972) was used to estimate a total acidity of 7.3 ± 0.4 meq/g HA.

RESULTS AND DISCUSSION

Laboratory experiments

Experiments were performed to test the dependence of the measured carboxyl content (acetate reaction method) on the mass of humic material and the concentration of acetate. The standard acetate reaction procedure for carboxyl content determination as described by SCHNITZER and KHAN (1972) calls for 50-100 mg of humic material and 10 meq of acetate in a total volume of 50 mL. Since the total acidity of humic material (barium hydroxide method) typically ranges from 5 meq/g to 15 meq/g for soil humic acids and aquatic fulvic acids, respectively, the ratio of equivalents of acid to acetate could vary between about 0.025 and 0.15 in a standard acetate reaction. The acid to acetate ratio also varies considerably among researchers. The following ratios have been reported: 0.5 - 1.0 (IHNATOWICZ, 1952), 0.006 - 0.043 (BROOKS and STERNHELL, 1957), 0.05 - 0.30 (BLOM, *et al.*, 1957). Various acetate concentrations, ranging from 0.2 M to 3 M, have also been employed. A relationship between the carboxyl content measurement and the humic acid/acetate ratio has been noted by PERDUE (1985).

The measured carboxyl content of our humic acid decreased significantly (rank correlation coefficient, $r' = -0.90$; $\alpha = 0.005$) as the ratio of equivalents of humic acidity to equivalents of acetate increased from 0.02 to 0.19 (Figure 1). This inverse relationship between the carboxyl content and the humic acid/acetate ratio was slightly more pronounced for the determinations employing the less concentrated acetate solution (0.2 M rather than 0.4 M). The difference, however, was not statistically significant. Although the acetate method yielded reproducible results ($\pm 5\%$) for a single set of solution parameters, a substantial variation in the apparent carboxyl content occurred over the range of humic acid/acetate ratios possible for the standard procedure of SCHNITZER and KHAN (1972). The carboxyl content at a ratio of 0.025 was about 20% higher than that measured at a ratio of 0.15, indicating that a greater fraction of the humic acid was dissociated at the lower ratio.

Because all humic matter is inherently heterogeneous, some random error was expected in the carboxyl content determinations. Artifacts associated with the ultrafiltration process probably also contribute to the error as discussed below. Despite the data scatter evident in Figure 1, the dependence of the measured carboxyl content on the humic acid to acetate ratio was clear.

The ultrafiltration of the reaction mixture required approximately 5 hours, during which the ratio of humic acid to acetate in the pressure cell steadily increased. Any such change in the humic acid/acetate ratio potentially alters the measured carboxyl content. The significance of this source of artifacts was assessed by collecting successive aliquots of the ultrafiltrate and titrating each separately. Unexpectedly, the measured carboxyl content did not decrease over the course of the ultrafiltration. Rather, each successive fraction required more base to reach the acetate endpoint than the previous fraction. The titration endpoint also became less distinct with each successive fraction, indicating that some weakly acidic humic matter was being titrated. These observations can be explained by humic matter passing through the filter. That such leakage had

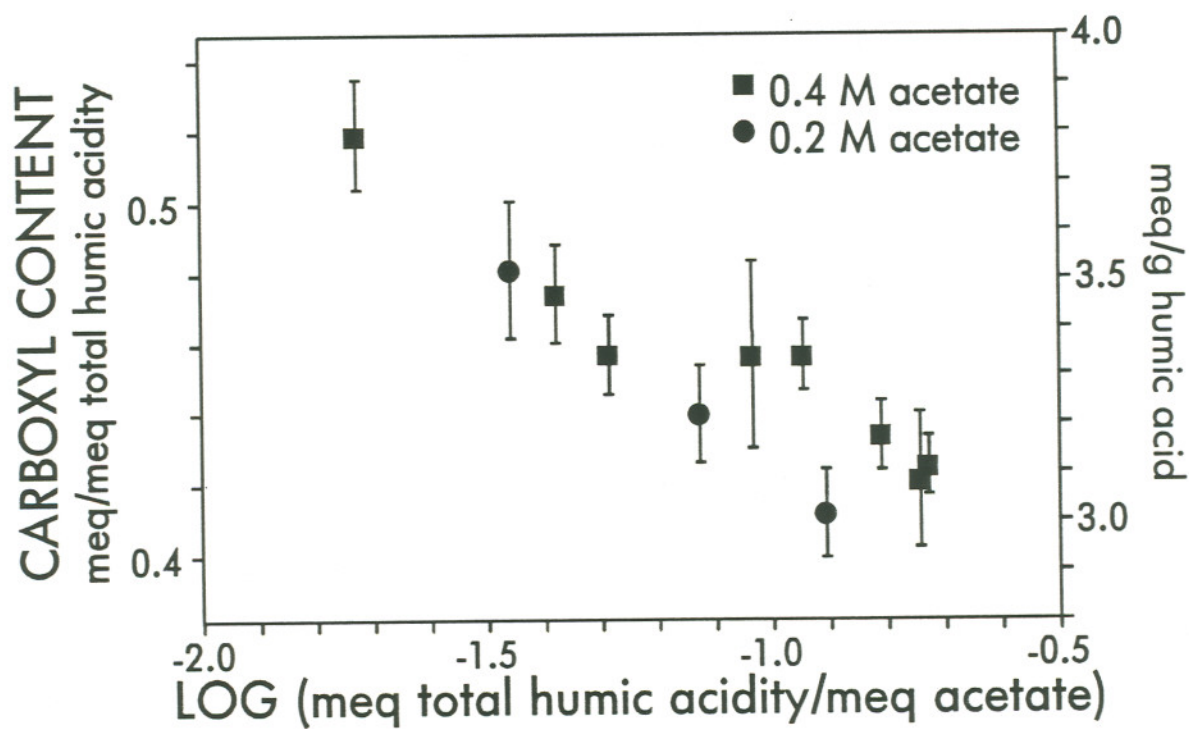


Figure 1. Measured carboxyl content of a soil humic acid as a function of the humic acid to acetate ratio. The left-hand scale is expressed in units of milli-equivalents of apparent carboxyl content per milli-equivalent of total humic acidity in solution; the right hand scale in units of milli-equivalents of carboxyl content per gram (dry weight) of humic acid in solution.

occurred was supported by an increase in both the apparent color (yellowish-brown) and in the light absorbance at 420 nm of successive fractions.

To minimize the effects of humic material leakage through the UM-2 filter, titrations should be performed using an aliquot from the first 10% of the filtrate. Measurements of the carboxyl content of our humic acid were repeated in which only the first 5 mL of filtrate were titrated. The results, shown in Figure 2, indicate that the variability of the acetate method was reduced by minimizing the breakthrough of humic matter. More importantly, Figure 2 reiterates the pronounced relationship between the measured carboxyl content and the humic acid to acetate ratio ($r' = -1.0$; $\alpha = 0.005$). Because of this relationship, comparisons between different humic acid samples or between different laboratories are possible only if the precise reaction conditions are reported. Unfortunately, only the range of conditions is typically provided. The acetate method does not yield an index of acidity that is unique over a range of humic acid sample sizes or acetate concentrations.

Simulations with hypothetical acids

The equilibrium chemistry of the acetate reaction was simulated to show how the relative HA concentration and the pK distribution influence the value obtained for the carboxyl content. These simulations clarify the chemistry underlying the experimental results. Three different types of pK distributions were simulated: (1) a single pK value, representing a simple monoprotic acid, (2) two discrete pKs, representing a mixture of two monoprotic acids, and (3) a continuous distribution of pK, representing a model humic acid. The sodium acetate concentration was 0.2 M in every simulation. The ratio of total equivalents of acid per equivalent of acetate was varied from 0.001 to 1. The standard range (0.025-0.15) used by SCHNITZER and KHAN (1972) is delineated in each subsequent figure with dotted lines. The equilibrium $\{H^+\}$ for each simulated acid-acetate mixture was calculated using the appropriate PBE

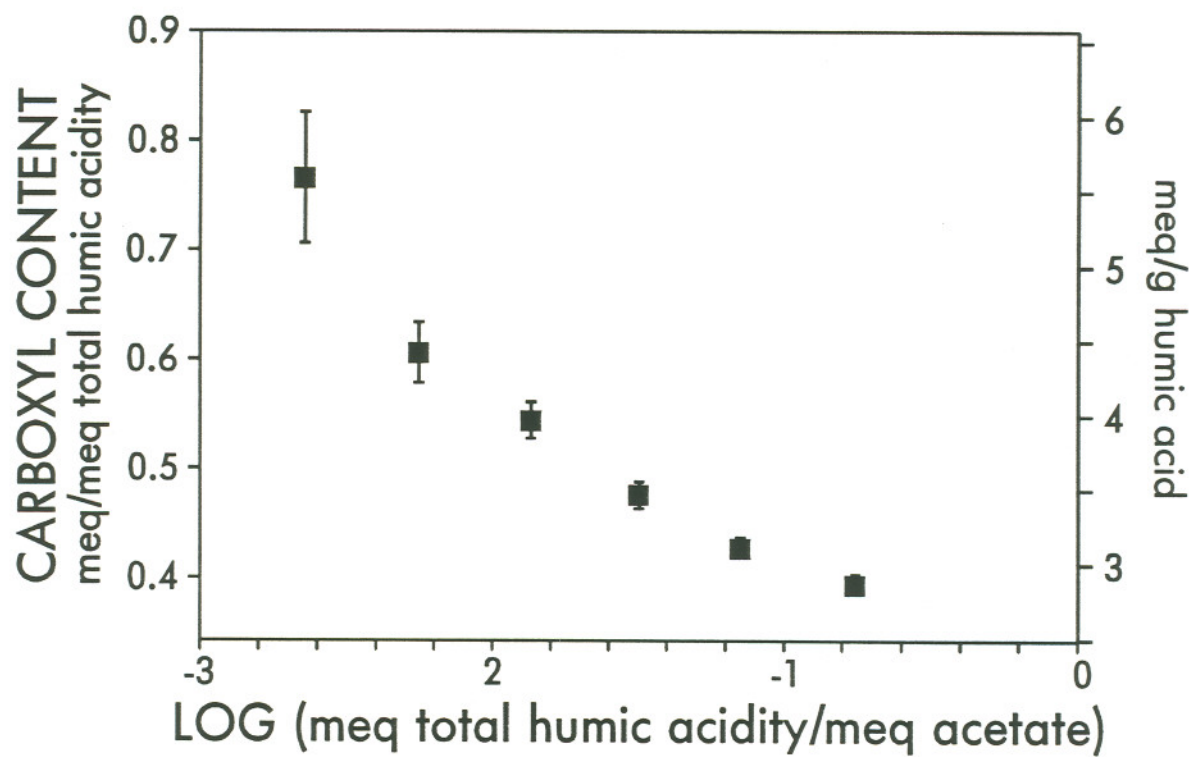


Figure 2. Measured carboxyl content (using 0.4 M total acetate) of humic acid as a function of the humic acid to acetate ratio. Only the first 10% of the filtrate was titrated.

equation (equation (4), (8), or (9)). A dimensionless carboxyl content was then calculated as the acetate acidity divided by the total HA concentration. Activity corrections were performed using the Davies equation (STUMM and MORGAN, 1981).

Monoprotic acids. Four hypothetical monoprotic acids, characterized by pK values of 2.76, 4.76, 6.76, and 8.76, were chosen to model a range of acidities. If the carboxyl content is a measure of the fraction of functional groups more acidic than acetic acid, then the carboxyl content of a monoprotic acid should equal either zero or one. The results of these simulations indicate, however, that only the strongest acid of the four exhibits an invariant carboxyl content equal to 1.0 under the standard conditions of the acetate reaction (Figure 3). For the other three acids, the acetate method divides the acidity into a strongly acidic, or 'carboxyl' fraction, and a weakly acidic, or 'phenol' fraction. Such a division is clearly erroneous because these acids are monoprotic. Furthermore, the division is variable and depends upon the relative concentration of HA with respect to acetate.

To understand why the acetate exchange method produces such paradoxical results, the underlying acid-base equilibria must be examined. The equilibrium speciation diagrams for solutions consisting of 0.2 M total acetate and 0.01 M or 0.001 M total HA (using pK = 6.76 as an example) are depicted in Figures 4a and 4b, respectively. For these conditions, the concentrations of H^+ and OH^- are negligible compared to those of CH_3COOH and A^- . Therefore, the PBE for the acetate exchange reaction can be simplified to $[CH_3COOH] \approx [A^-]$. If activity corrections are ignored, this equation can be solved graphically by inspection of Figures 4a and 4b. The dotted vertical lines indicate the equilibrium pH which determines the speciation. For the two HA/acetate systems depicted in Figures 4a and 4b, the equilibrium pH is near the pK of the acid, and therefore, appreciable quantities of both HA and A^- are present. The operational definition of the carboxyl content as the fraction of the

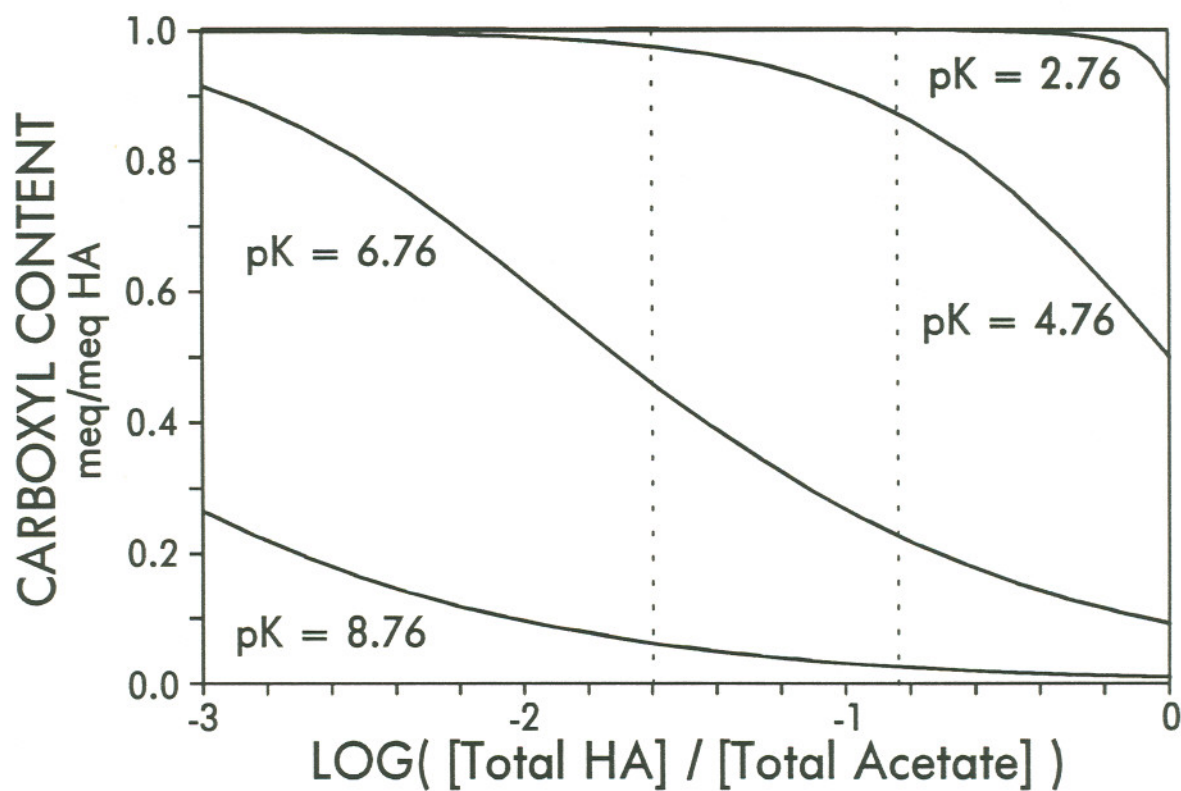


Figure 3. The calculated carboxyl content (using 0.2 M total acetate) of monoprotic acids as a function of the HA/acetate ratio. The dotted lines indicate the standardized range of HA/acetate ratios as described in the text.

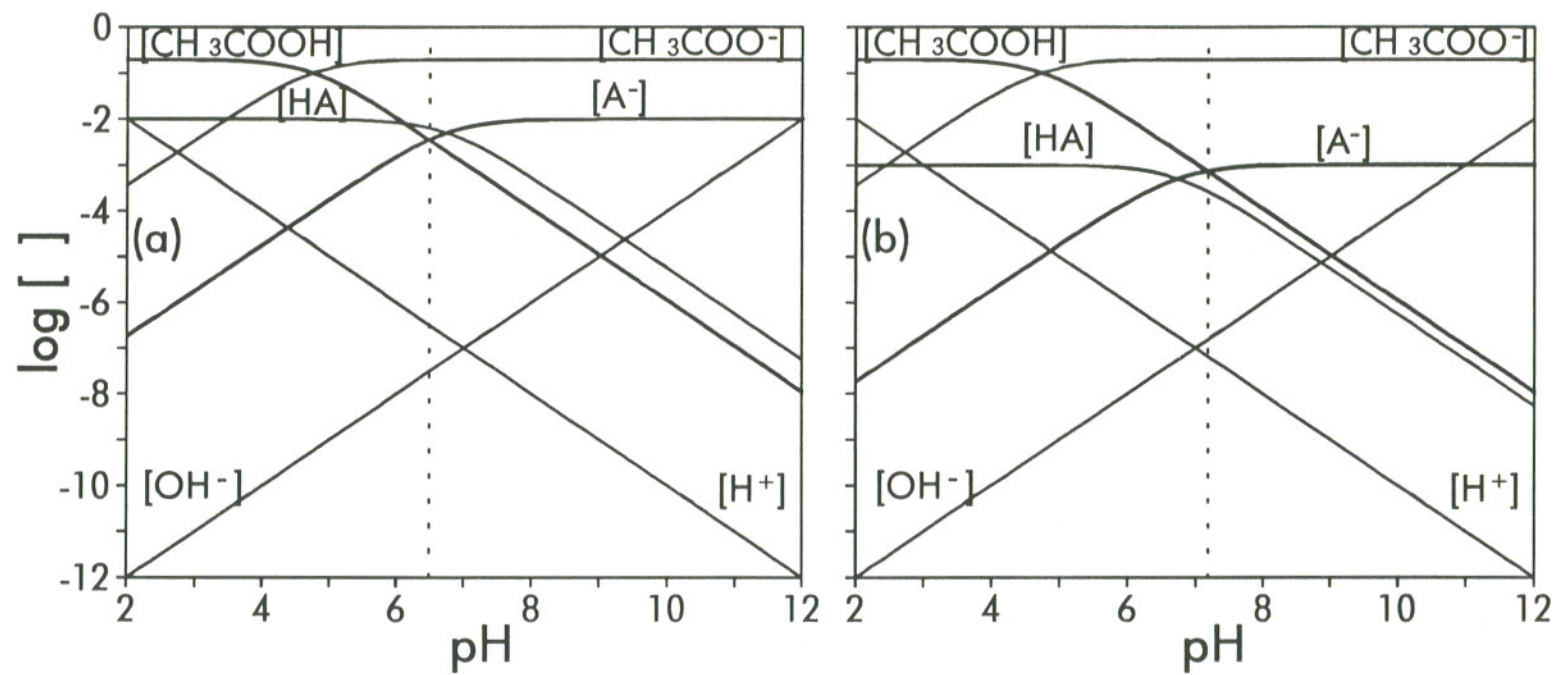


Figure 4. The equilibrium speciation diagrams for a mixture of (a) 0.01 M or (b) 0.001 M monoprotic acid (HA, $pK = 6.76$) and 0.2 M sodium acetate as a function of pH. Each dotted line indicates the equilibrium pH and the speciation at that pH.

acid that is dissociated, coupled with the partial dissociation of HA, causes the acidity of this monoprotic acid to be artificially divided. A non-integral value of carboxyl content suggests that this acid contains a strongly acidic group that has dissociated completely and a weakly acidic group that has not dissociated at all. Clearly this conclusion is wrong.

A comparison of Figures 4a and 4b illustrates the dependence of the carboxyl content on the relative concentrations of HA and acetate. As the total HA concentration decreases from 0.01 M (Figure 4a) to 0.001 M (Figure 4b), the curve corresponding to $[A^-]$ is translated downward and the point where the $[A^-]$ curve and the $[CH_3COOH]$ curve intersect occurs at a higher pH. A greater proportion of the total HA is dissociated at this higher pH, resulting in an increase in the carboxyl content.

The degree of dissociation, α_1 , is a continuous function of the pH and is never identically equal to zero or unity. The carboxyl content, therefore, varies continuously with the HA/acetate ratio. The variation, however, will be imperceptible for very weak or very strong acids. The hypothetical monoprotic acid with $pK = 2.76$ exemplifies this behavior. Over the standard range of HA/acetate ratios (0.025 - 0.15), the equilibrium pH varies from 5.4 to 6.2, corresponding to fractional acid dissociations of 0.9982 and 0.9997, respectively. Because this acid is essentially completely dissociated, the apparent dimensionless carboxyl content remains constant and equal to 1.0. Similarly, the carboxyl content of a very weak acid remains close to zero because the fraction of the acid that dissociates in the acetate reaction is very small. Figure 5 summarizes the dependence of the carboxyl content on the HA/acetate ratio for any monoprotic acid. Clearly, the carboxyl content estimate cannot be associated with a unique pK unless the solution composition is known, and therefore it is not a reliable index of the strength of a monoprotic acid relative to acetic acid.

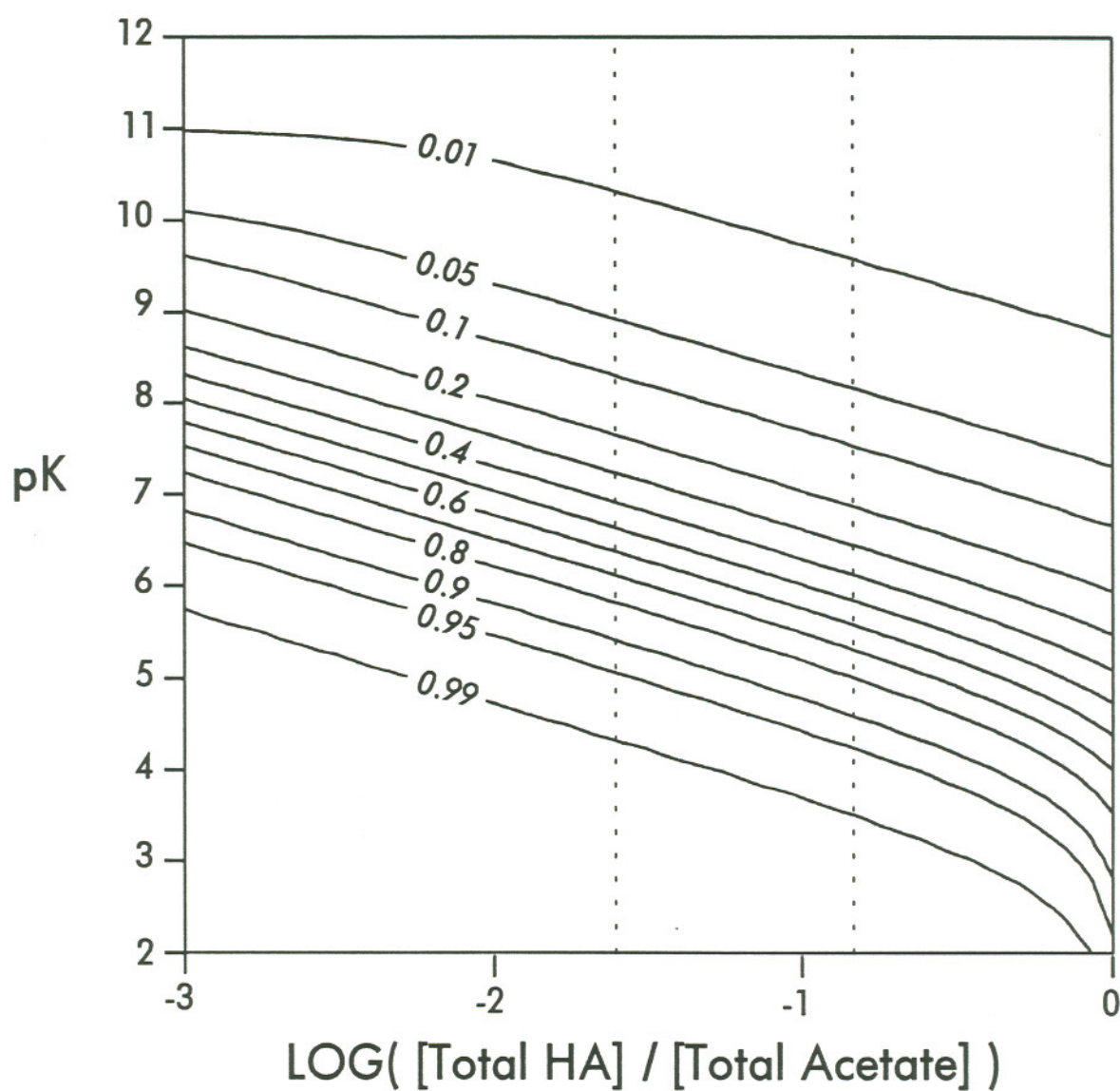


Figure 5. Calculated dimensionless carboxyl content isopleths (using 0.2 M total acetate) for monoprotic acids. For an acid of any specific pK (ordinate axis) the isopleths indicate the carboxyl content observed at any specified HA/acetate ratio (abscissa axis). The dotted lines indicate the standard range of HA/acetate ratios.

Mixtures of monoprotic acids. To assess the ability of the acetate reaction to accurately quantitate the strong acidity in an acid mixture, the HA/acetate equilibrium was simulated using two hypothetical monoprotic acids. Four different monoprotic acid mixtures were chosen in which the relative difference in strength between the two hypothetical acids was progressively smaller. The pK values that characterized the acid pairs were 3 and 11, 4 and 10, 5 and 9, and 6 and 8. The mixtures contained equal amounts of each acid. Figure 6 shows the calculated carboxyl content of each mixture plotted as a function of the ratio of total equivalents of HA to equivalents of acetate. Only for the mixture containing the acids with pKs 3 and 11 is the carboxyl content an accurate and consistent measure of the proportion of acids in the mixture that are stronger than acetic acid. Because one of these acids is very weak and the other is very strong, the dissociation of one is essentially complete while the dissociation of the other remains insignificant. Any mixture containing one strong acid that dissociates completely and one weak acid that remains undissociated will be correctly analyzed by the acetate method. For any other mixture of acids, the pH ranges over which the two acids dissociate will not be sufficiently isolated. If a significant fraction of the weaker acid is dissociated in the acetate reaction, it will contribute to the measured carboxyl content. Similarly, if some of the stronger acid remains undissociated, a lower carboxyl content will be measured. Because the degree of dissociation depends upon the HA/acetate ratio, the measured carboxyl content will not be constant, but will vary as a function of the solution composition.

Examination of Figure 6 might lead one to conclude that a unique HA/acetate ratio exists such that the acetate method can distinguish the two acids and correctly determine that the proportion of each acid in the mixture equals 0.5. This is not the case. The point of intersection in Figure 6 is an artifact due to the symmetrical nature of the simulated pK distributions. No general point of intersection exists for all sets of pK values or acid proportions.

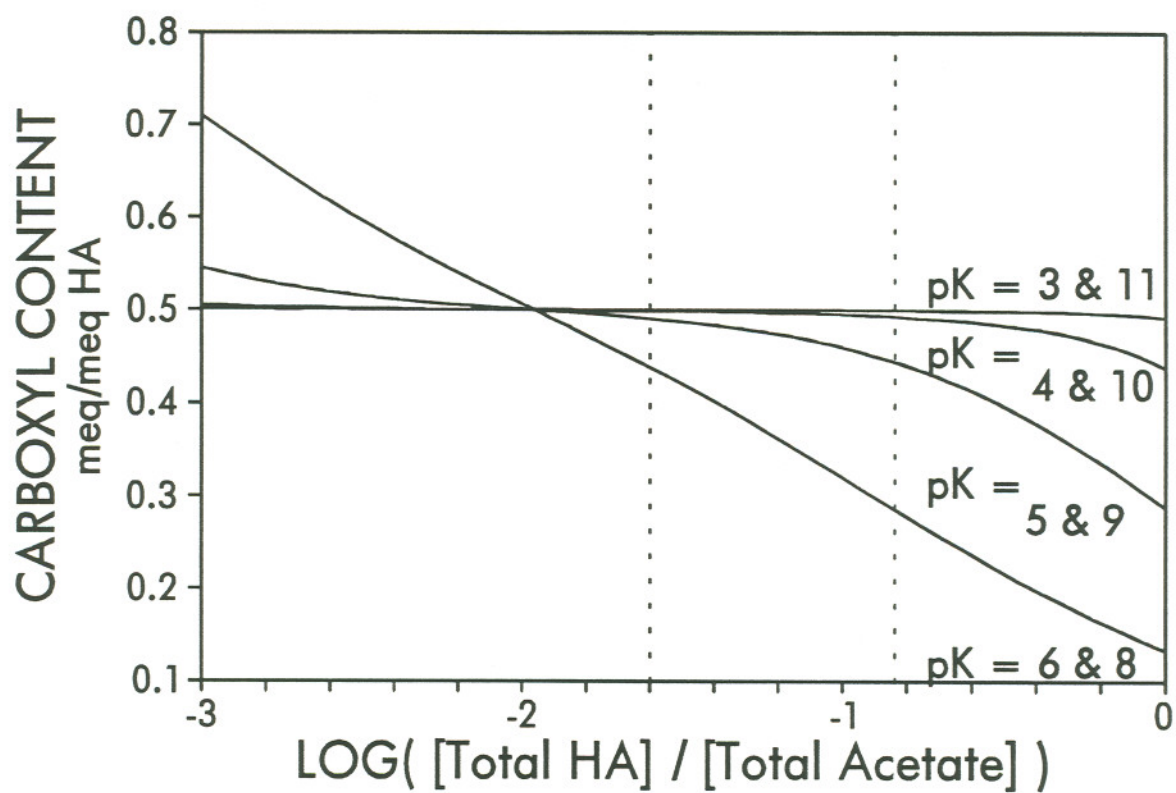


Figure 6. Calculated carboxyl content (using 0.2 M acetate) of binary mixtures (50%-50%) of monoprotic acids. The dotted lines indicate the standard range of HA/acetate ratios.

Furthermore, for two of the mixtures (pKs 5 and 9; pKs 6 and 8) a carboxyl content equal to 0.5 was produced through a cancellation of errors rather than an accurate chemical analysis. The acetate method yields the correct 'answer' for this HA/acetate ratio because the increase in the carboxyl content caused by the fraction of the weaker acid that is dissociated exactly cancels the decrease due to the fraction of the stronger acid that remains undissociated. To illustrate, Figure 7 depicts the dissociated fraction of each acid (pKs 6 and 8). The sum of these fractions equals the carboxyl content. For this mixture of acids, no HA/acetate ratio exists at which essentially all of the weaker acid is dissociated and essentially all of the stronger acid is undissociated. In general, if the pK difference between two acids is less than 3, the acids cannot be distinguished by their relative abilities to dissociate. Such mixtures cannot be accurately analyzed by the acetate method.

Model humic acids. The equilibrium between a model humic acid and sodium acetate was simulated to investigate the ability of the acetate method to estimate the strong acidity of an acid with a complex pK distribution. The pK distribution of the hypothetical humic acid was modeled as a weighted average of two normal distributions as described previously. The strongly acidic functional groups were represented by a distribution with mean pK of 4.5 and accounted for 60% of the total acidity. The mean pK of the distribution representing the weakly acidic groups was 10. These values were chosen because they are the approximate means of the pK distributions of common carboxylic acids and phenols (PERDUE, *et al.*, 1984). A standard deviation of 2 was chosen for each distribution. Of course, this particular distribution does not apply to all humic material (and in fact may not be the actual pK distribution for any particular humus sample), but it is consistent with the general chemical realities of humic matter acidity: a continuum of acidities with a bimodal distribution reflecting the dominant presence of carboxylic and phenolic functional groups. The dependence of the calculated carboxyl content on the

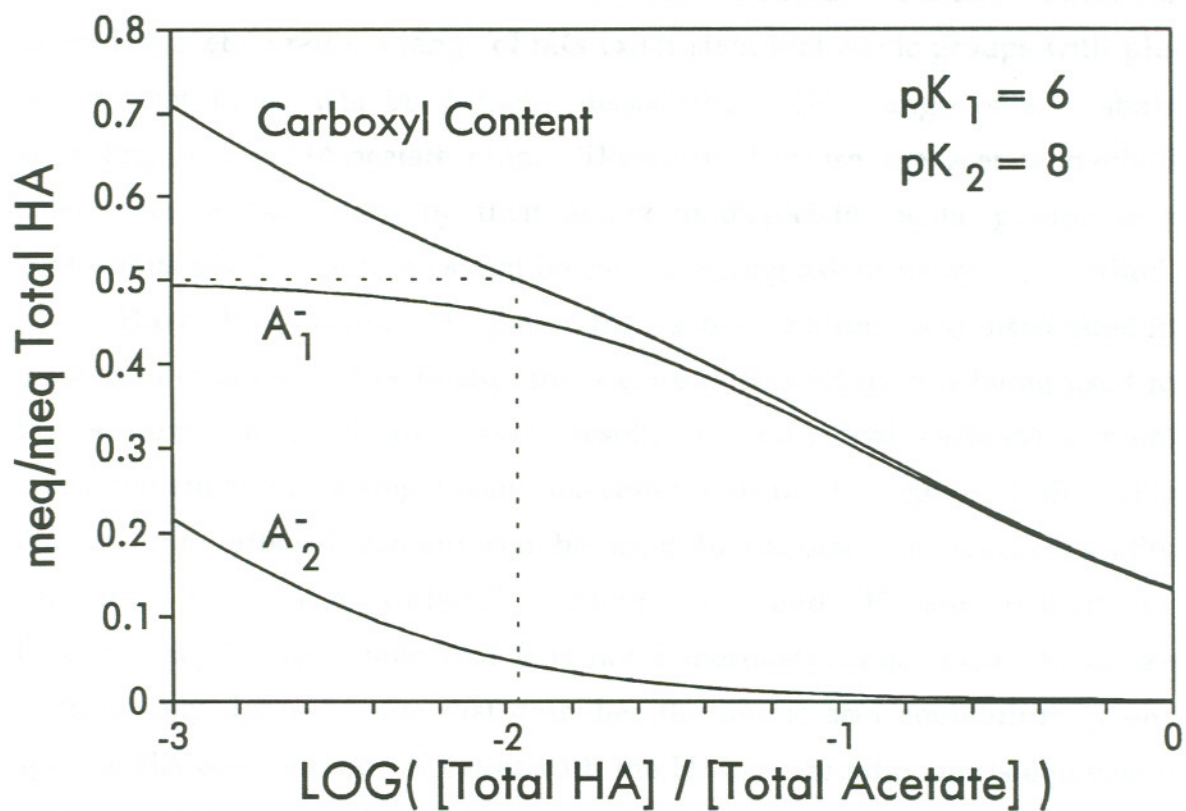


Figure 7. Individual dissociated acid fractions and carboxyl content (0.2 M acetate) of a 50%-50% mixture of two monoprotic acids. Dotted lines indicate the portion of the 0.5 carboxyl content attributable to each acid.

ratio of humic acid to acetate is shown in Figure 8 for this model humic acid. The carboxyl content is not constant over any range of HA/acetate and follows the same general trend observed in the laboratory. The inset pK distributions in Figure 8 depict the dissociation of the humic acid and the predicted pH at various HA/acetate ratios. Examination of these distributions indicates that, for every HA/acetate ratio, a range of pKs exists such that acidic groups with pKs within that range will be partially dissociated. This range of pKs shifts according to the HA/acetate ratio. Therefore, because the acetate method categorizes acidic groups by their ability to dissociate, acidic groups in a continuous pK distribution cannot be clearly distinguished using this method.

The carboxyl content is equal to the fraction of humic acid dissociated in a solution of acetate. Essentially, the acetate in this solution is being used to titrate humic material and, as a result, an individual carboxyl content measurement is only a single point in a continuous titration curve. If the pH is known, the carboxyl content can be used to calculate an average acidity constant, \bar{K} . The carboxyl content, α_1 , and \bar{K} are related by $\bar{K} = \{H^+\}\alpha_1/(1 - \alpha_1)$. Note that \bar{K} is not a thermodynamic constant, but an operationally defined value that describes the humic acid equilibrium at one specific HA/acetate ratio. \bar{K} varies with the HA/acetate ratio and is equivalent to the continuous stability function used by GAMBLE and others (GAMBLE, 1970; GAMBLE and LANGFORD, 1988).

This dependence of the carboxyl content, and \bar{K} , on the HA/acetate ratio illustrates the general problems associated with attempting to use humic acid titration data to infer the pK distribution of the acidic functional groups. For any titration, a unique H^+ activity is associated with each point in the titration curve. The H^+ activity, in turn, determines the speciation of the humic acid. Functional groups with similar acidities are not titrated one at a time in order of pK (DZOMBAK, *et al.*, 1986). Rather, many groups, over a range of pK units, are partially titrated, simultaneously. A comparison of the inset pK distributions in

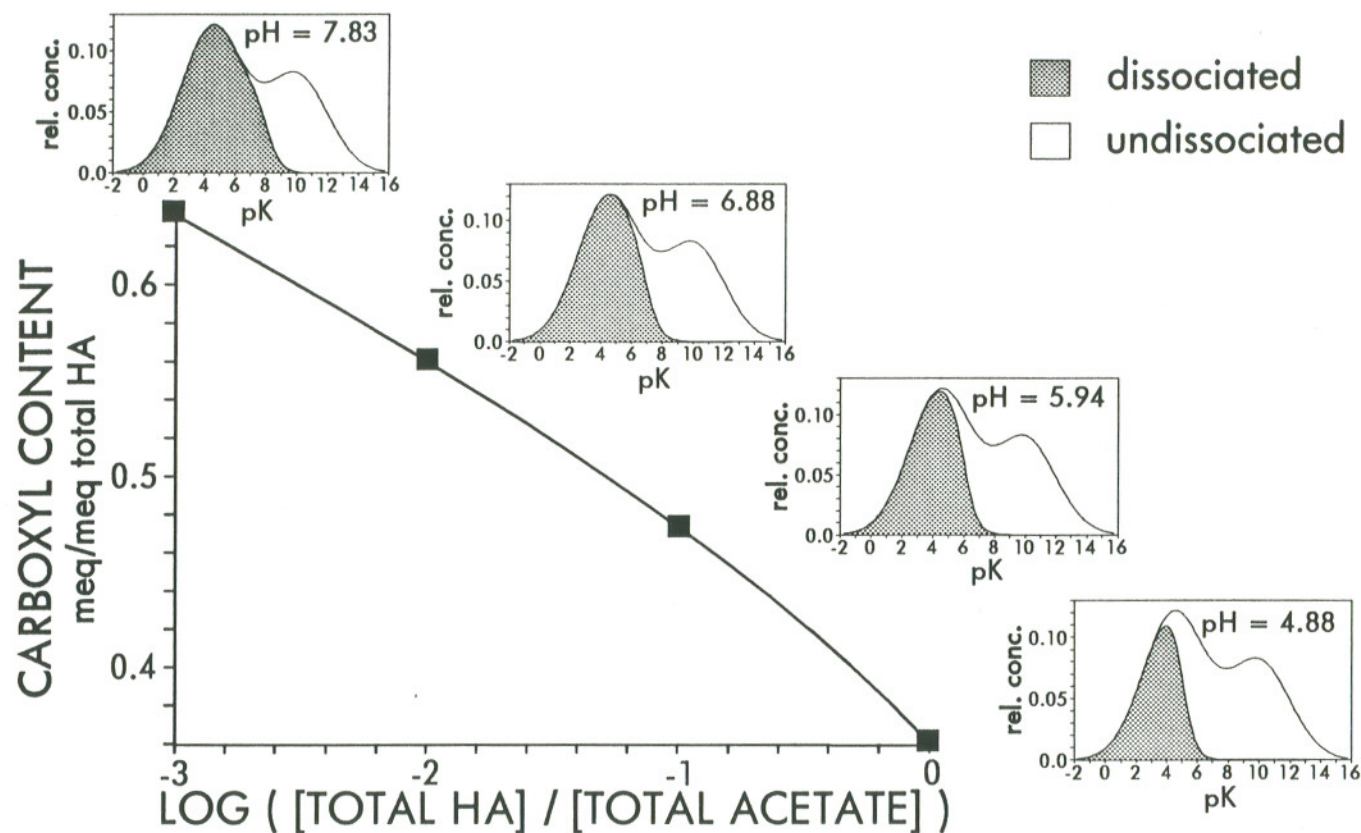


Figure 8. Calculated carboxyl content (using 0.2 M total acetate) of a hypothetical humic acid (bimodal distribution: $\mu_1 = 4.5$, $\mu_2 = 10$; $\sigma_1 = \sigma_2 = 2$; $X_1 = 0.6$). Inset pK distributions show the pH and humic acid speciation at HA/acetate ratios corresponding to the indicated points. Humic acid speciations is illustrated by the relative concentrations of dissociated and undissociated acidic functional groups as functions of their pK values.

Figure 8 illustrates this behavior. Between pH = 4.88 and pH = 5.94, functional groups with pKs between about 3 and 8 were partially titrated. The contribution of each pK to the total fraction of dissociated acid will depend upon the shape of the humic acid pK distribution. Consequently a specific pK or pK range cannot be assigned to the humic acid functional groups that dissociate at a specific pH or over a pH range in a titration. To use titration data to determine the pK distribution the following integral equation must be solved for $f(\text{pK})$

$$\alpha_1(\{\text{H}^+\}) = \int_{-\infty}^{\infty} \frac{f(\text{pK}) 10^{(-\text{pK})} \gamma_{\text{HA}}}{10^{-\text{pK}} \gamma_{\text{HA}} + \{\text{H}^+\} \gamma_{\text{A}^-}} d\text{pK} \quad (11)$$

where $\alpha_1(\{\text{H}^+\})$ is the fraction of humic acid that is dissociated as a function of the H^+ activity. Equation (11) is a Fredholm integral of the first kind; the numerical inversion of this equation is subject to spurious oscillations (DZOMBAK, *et al.*, 1986). Essentially, the fraction of the total acid that dissociates is a datum that is not detailed enough to uniquely characterize a pK distribution. Solving this integral equation is complicated further because the pH range of every titration is limited. Acidic groups whose pKs are more than 2 units outside of the pH range of the titration will be indistinguishable from one another, making the pK distribution in these two regions entirely indeterminate. In the acetate method, typically the pH of the reaction mixture will fall between 4 and 9. The effective pH range is wider for direct aqueous titrations and wider still for non-aqueous titrations employing solvents with larger autoprotolysis constants than water. Regardless of the solvent, however, the inherent limitations of titrations remain.

SUMMARY AND CONCLUSIONS

The ability of the acetate reaction method to quantify the amount of acidity in a solution that is due to acidic groups stronger than acetic acid was tested both experimentally and theoretically. In general, the acetate method

cannot be expected to provide a *strong acidity index* that is constant over the range of reaction conditions that are typically employed. If, when reacted with acetate, the strongly acidic functional groups dissociate completely and the weakly acidic groups remain undissociated, then the measured carboxyl content will be an accurate index of strong acidity. Otherwise, the carboxyl content will vary with the HA/acetate ratio, reflecting the partial dissociation of the various acids.

For humic acids, the acetate method will not yield a unique or constant index of strong acidity. Therefore, if the acetate method is used to analyze humic matter, then the exact conditions of the reaction must be reported. Values of carboxyl content can only be compared if the molarity of the acetate solution and the mass and total acidity of the humic matter are known. In addition, to avoid artifacts due to filterable humic acidity, only the first portion of the ultrafiltered reaction mixture should be analyzed for carboxyl content. The carboxyl content is strictly an operationally defined value equal to the average degree of humic acid dissociation in a particular acetate solution. When the acetate method is performed at several different HA/acetate ratios, the relationship between the carboxyl content and the HA/acetate ratio define a titration curve of the humic matter. The general dependence of the carboxyl content on the ratio of humic acid to acetate as measured in the laboratory was correctly predicted by hypothetical continuous bimodal pK distribution.

Because humic matter has a continuous distribution of pKs, some of the acidic groups will always be partially dissociated over the course of any titration. Therefore, no boundary pK exists, above which all groups are dissociated and below which all groups are undissociated. The assignment of a pK or pK range to the functional groups that dissociate at a particular pH or over a pH range is erroneous. Furthermore, a unique pK distribution cannot be characterized using titration data alone because such data reflects the behavior of functional groups

within a limited pK range and because the mathematical nature of the governing equation is subject to spurious errors.

REFERENCES

- BLOM L., EDELHAUSEN L., and VAN KREVELEN D.W. (1957) Chemical structure and properties of coal XVIII- Oxygen groups in coal and related products. *Fuel* **36**, 135-153.
- BROOKS J.D. and STERNHELL S. (1957) Chemistry of brown coals I. Oxygen-containing functional groups in Victorian brown coals. *Aust. J. App. Sci.* **8**, 206-221.
- CAWSE P.A. (1983) The accumulation of caesium-137 and plutonium-239 + 240 in soils of Great Britain, and transfer to vegetation. In *Ecological Aspects of Radionuclide Release* (eds. P.J. COUGHTREY, J.N.B. BELL and T.M. ROBERTS), pp. 42-62. Blackwell Scientific.
- DUBACH P., METHA N.C., JAKAB T., MARTIN F., and ROULET N. (1964) Chemical investigations on soil humic substances. *Geochim. Cosmochim. Acta* **28**, 1567-1578.
- DZOMBAK D.A., FISH W., and MOREL F.M.M. (1986) Metal-humate interactions. 1. Discrete ligand and continuous distribution models. **20**, 669-675.
- FLAIG W., BEUTELSPACHER H., and RIETZ E. (1975) Chemical composition and physical properties of humic substances. In *Soil Components, Vol 1.: Organic Components*. (ed. J.E. GIESKING), pp. 1-211. Springer-Verlag.
- FUCHS W. (1927) Über die Unterscheidung von Braunkohle und Steinkohle. *Brennst.Chemie* **8**, 337-352.
- GAMBLE D.S. (1970) Titration curves of fulvic acid: the analytical chemistry of a weak polyelectrolyte. *Can. J. Chem.* **48**, 2662-2669.
- GAMBLE D.S. (1973) Na⁺ and K⁺ binding by fulvic acid. *Can. J. Chem.* **51**, 3217-3222.
- GAMBLE D.S. and LANGFORD C.H. (1988) Complexing equilibria in mixed ligand systems: Test of theory with computer simulations. *Environ. Sci. Technol.* **22**, 1325-1336.

- HOLTZCLAW K.M. and SPOSITO G. (1979) Analytical properties of the soluble, metal-complexing fractions in sludge-soil mixtures: IV. Determination of carboxyl groups in fulvic acid. *Soil Sci. Soc. Am. J.* **43**, 318-323.
- IHNATOWICZ A. (1952) Studies on oxygen groups in bituminous coal. *Prace Głównego Inst. Gorn. Komun.* No. 125, p 3. English translation G. NIEMCZYNOW In *English Translations of Polish Works*, p 1-58. U.S. Dept. Interior, N.S.F.
- MACCARTHY P. Colorado School of Mines, personal communication, 1988.
- MARTELL A.E. and SMITH R.M. (1977) *Critical Stability Constants*. Vol.3, p. 3, Plenum Press.
- PERDUE E.M. (1978) Solution thermochemistry of humic substances I. Acid-base equilibria of humic acid. *Geochim. Cosmochim. Acta* **42**, 1351-1358.
- PERDUE E.M., REUTER J.H., and GHOSAL M. (1980) The operational nature of acidic functional group analyses and its impact on mathematical descriptions of acid-base equilibria in humic substances. *Geochim. Cosmochim. Acta* **44**, 1841-1851.
- PERDUE E.M., REUTER J.H., and PARRISH R.S. (1984) A statistical model of proton binding by humus. *Geochim. Cosmochim. Acta* **48**, 1257-1263.
- RASHID M.A. (1985) *Geochemistry of Marine Humic Compounds*, Springer-Verlag.
- SCHNITZER M. and GUPTA U.C. (1965) Determination of acidity in soil organic matter. *Soil Sci. Soc. Am. Proc.* **29**, 274-277.
- SCHNITZER M. and KHAN S.U. (1972) *Humic Substances in the Environment*, Chap. 3, pp. 34-49, Marcel Decker.
- SHOLKOVITZ E.R. and COPELAND D. (1981) The coagulation, solubility and adsorption properties of Fe, Mn, Cu, Ni, Cd, Co and humic acids in a river water. *Geochim. Cosmochim. Acta* **45**, 181-189.
- STEVENSON F.J. (1982) *Humus Chemistry, Genesis, Composition, Reactions*. Wiley-Interscience
- STUMM W. and MORGAN J. (1981) *Aquatic Chemistry*. 2nd edition, p.135, Wiley-Interscience.
- VAN DIJK H. (1966) Some physico-chemical aspects of the investigation of humus. In *The Use of Isotopes in Soil Organic Matter Studies*, pp. 129-141, Pergamon Press.

CHAPTER III

Measurement of Electrostatic and Site-specific Associations of Alkali Metal Cations with Humic Acid

ABSTRACT

A discontinuous acidimetric titration method incorporating ultrafiltration was developed to measure the association of a soil humic acid with Li^+ , Na^+ , and K^+ (pH 3 - 8). In addition, possible site-specific binding of these alkali metal cations was investigated using desorption experiments at pH 1. Lithium, sodium, and potassium cations behaved equivalently in the titrations and the amounts of these cations associated with the humic acid was measureable at all pH values between 3 and 8. Up to 90% of the total alkali metal cation was humate-associated at pH 8. The absolute amount of humic-associated cation did not depend on the alkali metal cation concentration, but rather on the solution alkalinity. In addition, the net charge of the humate polyanion made a negligible contribution to the electroneutrality of the bulk solution under all conditions. These results are consistent with a diffuse layer model of hydrated humic acid in which the alkali metal cations neutralize the humic charge. The association of Na^+ and K^+ with humic acid at pH 1 was successfully described by a Langmuir adsorption model. The number of sites per gram of humic acid

was very small, and greater for K^+ than for Na^+ . Lithium cations exhibited no detectable humic association at pH 1. These differences suggest that humic acids may have a small number of specific binding sites for which the size of the hydrated cation is important.

INTRODUCTION

Most studies of the association between metal cations and natural organic matter focus on the complexation of a few select trace metals. Interactions between humic substances and the major cations such as Na^+ and K^+ have often been either ignored or assumed to be negligible. The need to characterize such interactions is evidenced by the sheer number of systems, both environmental and experimental, which contain appreciable quantities of these cations. In highly organic soils, association with humic matter may decrease the K^+ availability, increasing the need for amendment with K-fertilizers (KONONOVA, 1966). In estuaries, aquatic humic substances are subjected to strong salinity gradients that can influence humic binding of trace metals. In the laboratory, experiments with aqueous humic material often utilize a background electrolyte containing Na^+ or K^+ to control the ionic strength. The extent to which Na^+ or K^+ affect the humate conformation, the electrostatic charge or the binding of other cations is unknown.

Aqueous alkalimetric titration has been used to investigate the association of fulvic and humic acids with Na^+ or K^+ (GAMBLE, 1973; FRIZADO 1979). GAMBLE (1973) showed that the amount of fulvic-associated Na^+ and K^+ increased as the titration progressed. However, alkalimetric titrations present an ambiguous picture of cation-humate association. Because NaOH and KOH were used as titrants the increase in cation association with rising pH may have been due to the greater charge of the dissociating fulvate, the increasing alkali metal cation

concentration, or both. Interestingly, between pH 5 and 10, Na^+ exhibited slightly greater association with fulvic acid than did K^+ .

In this chapter, I describe an investigation of alkali-metal/humate interactions that resolves the ambiguity of pH and cation-concentration effects. Two experimental designs were developed: 1) cation desorption experiments at pH 1, and 2) discontinuous acidimetric titrations with constant alkali metal concentration. At pH 1, humic acid is minimally dissociated, so its electrostatic attraction for aqueous cations should be very small. Association with alkali metal cations at low pH, then, reflects an intrinsic ability of the humate to bind such cations directly, possibly via structures similar to crown ethers or cryptands (LEHN, 1978). In the acidimetric titrations, the humic polyion is negatively charged, and association with alkali metal cations is expected to be primarily by electrostatic attraction. Because a constant alkali metal cation concentration is maintained, the dependence of cation-humate association on the humate charge can be decoupled from the alkali metal cation concentration.

In any study of humate-cation association, some method is needed to determine the amount of cation bound. Fluorescence quenching has sometimes been used to measure the humate-bound cation directly (SAAR and WEBER, 1980; CABANISS and SHUMAN, 1986; FISH, *et al.*, 1986). More often, however, the "free" aqueous cation concentration is measured and the bound cation determined by difference. Several methods have been used in the past to measure the aqueous cation concentration, including ion selective electrodes (ISEs) and anodic stripping voltammetry (TURNER, *et al.*, 1986; SHUMAN and CROMER, 1979). These methods limit the suite of cations amenable to investigation and are subject to interference from humic materials. Recently, ultrafiltration has been described as a technique to sample the aqueous phase of humic solutions (EPHRAIM and MARINSKY, 1990; EPHRAIM and XU, 1989). Ultrafiltration facilitates the investigation of a wide range of metal cations due to the analytical freedom provided by a simple aqueous (humic-free) solution. Atomic absorption spectroscopy (AAS),

for example, is a particularly attractive and sensitive method for the quantitative analysis of many metals. Ultrafiltration and AAS were used to determine aqueous alkali metal concentrations in this study.

EXPERIMENTAL

Materials and analytical methods

All experiments were performed using samples of the same soil humic acid. The origin and isolation of this material has been described by BONN and FISH (1991). The total acidity of the material as measured by the barium acetate method was 7.3 ± 0.4 meq/g. Ash content was 1% (by weight) and the elemental composition (Huffman Laboratories, Golden, CO) was 58% C, 4% H, 35% O, 3% N. The freeze-dried humic acid was stored in a desiccator.

Nitrogen-purged ultrapure water (Nanopure System, Barnstead) and ACS Reagent Grade chemicals were used for all solutions. Base solutions (LiOH, NaOH, and KOH) were prepared daily from 1 M stock solutions that were standardized against potassium hydrogen phthalate. All humic solutions were prepared and equilibrated in polyethylene labware.

Solution pH was measured using a micro-combination electrode (MI-410, Microelectrodes, Inc., Londonderry, NH) and a pH meter (EA 920, Orion, Boston, MA). Alkali metal concentrations (Li, Na, and K) were determined by flame atomic absorption spectrometry (Model 620, Perkin Elmer, Norwalk, CT). Samples for AAS analysis were diluted with 1% $\text{La}(\text{NO}_3)_3$ in 1 M HCl to control ionization.

Desorption experiments

Two-gram humic acid samples were dissolved in 35 mL of 0.28 M base (LiOH, NaOH, or KOH), equilibrated for 4 hours, and then acidified (to pH=1) with 0.5 M HCl. The final volume was approximately 60 mL. The resulting

humic precipitate was mixed overnight and centrifuged at 5000 rpm for 20 minutes ($\sim 2500 \times g$). To effect the desorption of cations, about 30 mL of supernatant was removed, and a comparable volume of 0.1 M HCl dilutant was added. The humic precipitate was then resuspended and allowed to equilibrate overnight. All additions and withdrawals were measured gravimetrically. This process was repeated until the alkali metal cation concentration in the supernatant was undetectable by flame AAS. Humic-free control solutions were treated identically to reveal any artifacts caused by sorption to the polyethylene bottles.

Acidimetric-titration experiments

Approximately 0.1 g humic acid was dissolved in 100 mL of 0.004 M base (LiOH, NaOH, KOH, or a mixture thereof) and equilibrated for 4 hours. Aliquots (10 or 20 mL) were acidified with 0.5 M HCl to yield final net base concentrations between 0 and 4 meq/g humic acid. After mixing overnight, 2 mL samples of each solution were pipeted into previously conditioned ultrafiltration units (see next section). Ultrafiltered, humate-free solution samples were separated from the humic solution. At least 3 replicates were prepared for each humic solution. To minimize contamination with CO₂, all solution transfers were performed under flowing N₂ and into N₂-purged vessels.

The mass of alkali metal that was associated with humic matter was determined by difference using

$$\text{associated cation} = \frac{\text{total cation} - (\text{free aqueous cation concentration} \cdot \text{aqueous mass})}{\text{mass of humic acid}}$$

The aqueous mass was taken as the total mass of the humic solution minus the mass of dry humic acid; no provision was made for a separate humic phase. The free aqueous cation concentration in the humic suspension was calculated

from the alkali metal cation in the ultrafiltrate as described in the following section.

Ultrafiltration

To avoid artifacts, some care must be exercised when using ultrafiltration to sample humic solutions. Only a small fraction of the sample should be filtered to minimize humic conformational changes and shifts in the acid-base and complexation equilibria due to increasing the concentration of humic material (EPHRAIM and MARINSKY, 1990; BONN and FISH, 1991). The humic matter should not interact with the membrane filter, nor should it be transmitted through the filter. The ultrafiltration procedure should also be tested with humic-free cation solutions to determine if the cation of interest is quantitatively transmitted through the filter; if not, a calibration curve must be prepared. The quantitative transfer of cations can sometimes be improved by first "conditioning" the ultrafilter membrane before use.

Centrisart I ultrafiltration units (SM13229, Sartorius, Göttingen, Germany) were used to separate a small amount of the aqueous phase from the humic suspensions. Each unit consisted of an outer tube and an inner, floating tube fitted with a membrane filter (nominal cutoff: 5000 daltons). The humic sample was placed in the outer tube. Separation was accomplished by centrifugation for 30 minutes at 3500 rpm and ambient temperature ($\sim 1200 \times g$). Typically, 200 to 300 μl of ultrafiltrate were produced.

Even after flushing with ultrapure water, new Centrisart units exchanged H^+ for alkali metal cations, significantly altering both the pH and the cation concentration of the ultrafiltrate. Consequently, a procedure was devised that involved "washing" the Centrisart units to remove easily exchangeable cations. Before use, the units were washed twice with phosphate buffer (0.1 M KNaHPO_4 , pH=9), rinsed thoroughly with ultrapure water, and then washed three times with ultrapure water. Each wash consisted of centrifuging a unit with 2 mL of solvent (phosphate buffer or ultrapure water) for 15 minutes and

then discarding both the filtrate and concentrate. The outer tubes and caps were air dried. The inner (filter) tubes were soaked in ultrapure water for 24 hours, removed immediately before use, and dried with Kimwipes (Kimberly-Clark), taking care not to touch the filter membrane. A similar procedure was used to clean the Centrisart units after humic acid experiments. The units were rinsed to remove most of the humic material and then subjected to the wash regimen described for new units. The performance of the ultrafilter membrane in these experiments did not seem to deteriorate with repeated use. The incidence of membrane rupture, however, did increase with age. Generally, a Centrisart unit was used three times and then discarded.

To check for cation sorption by the ultrafiltration system, humic-free LiCl, NaCl, and KCl solutions, spanning a concentration range of 0.5 to 5 M and a pH range of 3 to 9, were prepared and ultrafiltered in conditioned Centrisart units. Cation concentrations were determined in the unfiltered solutions, ultrafiltrates, and concentrates. Despite the conditioning pre-treatment, some ion-exchange occurred during filtration, reducing the cation concentration in the ultrafiltrate by about 5%. An empirical relationship between the concentrations of the unfiltered solutions and their corresponding ultrafiltrates was determined for each alkali metal cation using multiple regression methods. The alkali metal concentration and the product of the alkali metal and H^+ concentrations were determined to be the best predictor variables. These empirical relationships were applied to ultrafiltrate concentration data to obtain the free aqueous alkali metal concentrations.

RESULTS AND DISCUSSION

Desorption experiments

At pH 1, small amounts of alkali metal cations were bound to the humic acid, with the strength and extent depending on the cation type. The results to

these experiments are most easily understood in the context of model representations. Cations in the desorption experiments might be expected to follow one of several models: linear sorption, Langmuirian sorption, or no sorption. The linear and Langmuir models are given by

$$M_s = K \cdot M_{aq} \quad \text{and} \quad M_s = \frac{M_s^\infty b M_{aq}}{1 + b M_{aq}}$$

respectively, where M_s is the mass of sorbed cation per mass of sorbent, M_{aq} is the aqueous cation concentration, K is the linear association constant, M_s^∞ is the maximum sorbed cation concentration, and b is the adsorption coefficient. The general characteristics of each of the three sorption models are illustrated in Figure 9. Notice that the dilution curves for both the linear and no sorption models appear to be linear when plotted on a log-log scale. The slope of the no sorption case will always be unity. The dilution curve of the linear model will deviate from constant slope if the volumes of supernatant removed and dilutant added vary during the desorption experiment. Provided these two volumes are fixed, the dilution curves using the linear sorption model will be linear on a log-log scale and have a slope less than 1. The initial supernatant cation concentration is also significantly reduced for the linear model, due to the mass sorbed to the solid phase. This is not the case, however, for the initial supernatant cation concentration predicted by the Langmuirian model. When the maximum number of sorption sites is much less than the initial total equivalents of cation, the beginning of a Langmuirian dilution curve will be indistinguishable from that of the no sorption model. As the supernatant cation concentration is reduced by repeated dilution, cations begin to desorb from the humate, causing the supernatant concentration to be greater than that expected from dilution alone (no sorption case). As the cation concentration becomes increasingly dilute, sorption is no longer limited by the number of sites and the slope of the Langmuirian dilution curve approaches that of the linear model.

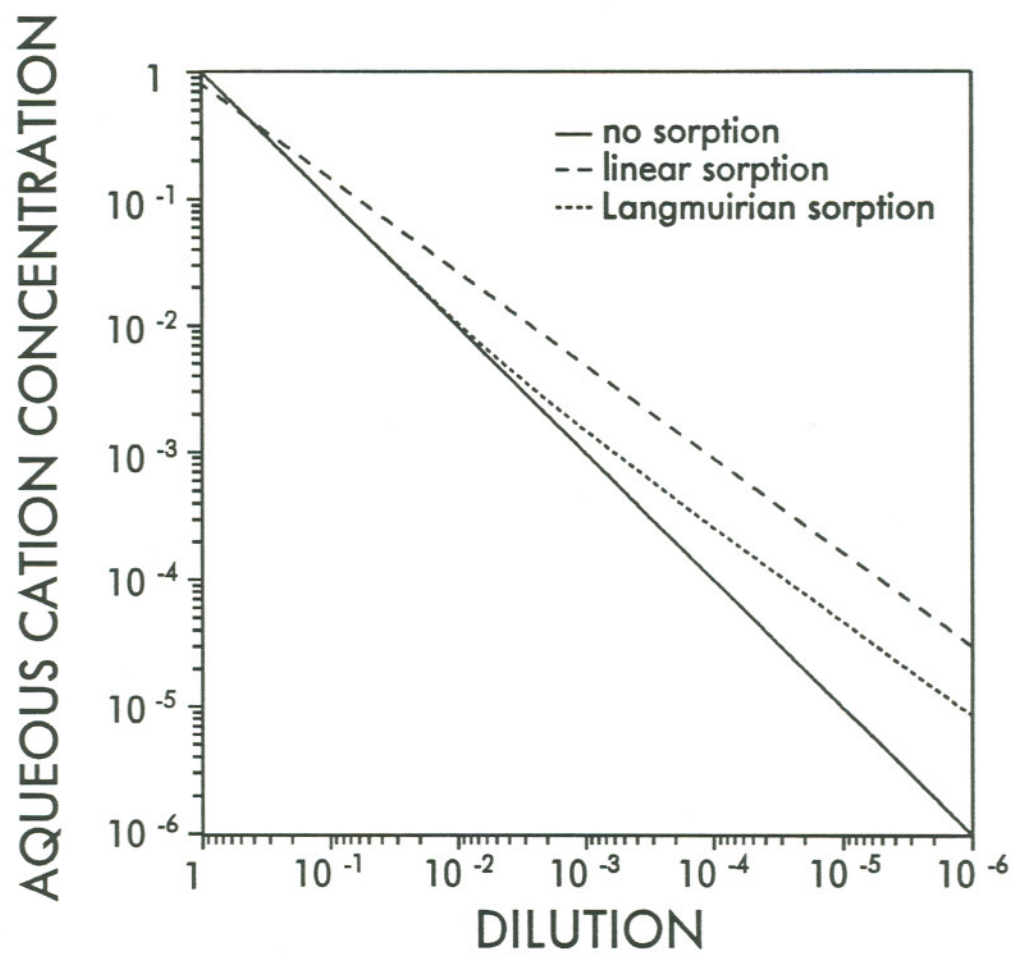


Figure 9. Characteristic dilution curves for desorption experiments assuming three sorption models: no sorption (—), linear sorption (---), and Langmuir sorption (----). Aqueous cation concentrations are expressed in arbitrary, normalized units.

The desorption of Na^+ and K^+ from pH 1 humic acid exhibit dilution curves indicative of Langmuir-type adsorption (Figure 10a). The dilution curve of Li^+ was indistinguishable from control data (Figure 10b), indicating little or no sorption of Li^+ by the humic acid. The data were fitted to a Langmuir model using a non-linear, weighted least squares optimization routine. The downhill simplex method (PRESS, *et al.*, 1989) was used as the optimization technique. The optimized values are given in Table III. Significantly more sites were available for K^+ than for Na^+ perhaps because of steric hindrance of the more highly hydrated Na^+ ion. The adsorption constant for K^+ , however, was less than that for Na^+ , indicating that Na^+ is more tightly bound. This ordering of cation binding strength ($\text{Na}^+ > \text{K}^+$) is typical of coordination complexes with carboxylic acids. Li-carboxylate complexes, however, are generally more stable than either Na^+ or K^+ complexes. The absence of detectable Li^+ binding to the humate polyelectrolyte may be due to steric exclusion of the comparatively large hydrated Li^+ ion.

TABLE III. Optimized Langmuir Model Parameters

cation	$b \times 10^{-3}$, kg/mol		$M_s^\infty \times 10^3$, mmol/gHA	
Na^+	3.7	[3.3 - 4.2] ^a	1.2	[1.1 - 1.3] ^a
K^+	0.51	[0.45 - 0.60] ^a	15	[13 - 16] ^a

^aestimated 95% confidence interval

Discontinuous acidimetric titrations.

The pH values of the humic solutions before ultrafiltration define an acidimetric titration curve for this soil humic acid that exhibited the lack of equivalence points characteristic of humic acid titrations (Figure 11). The moderate amount of scatter in the data is probably due to the discrete nature of

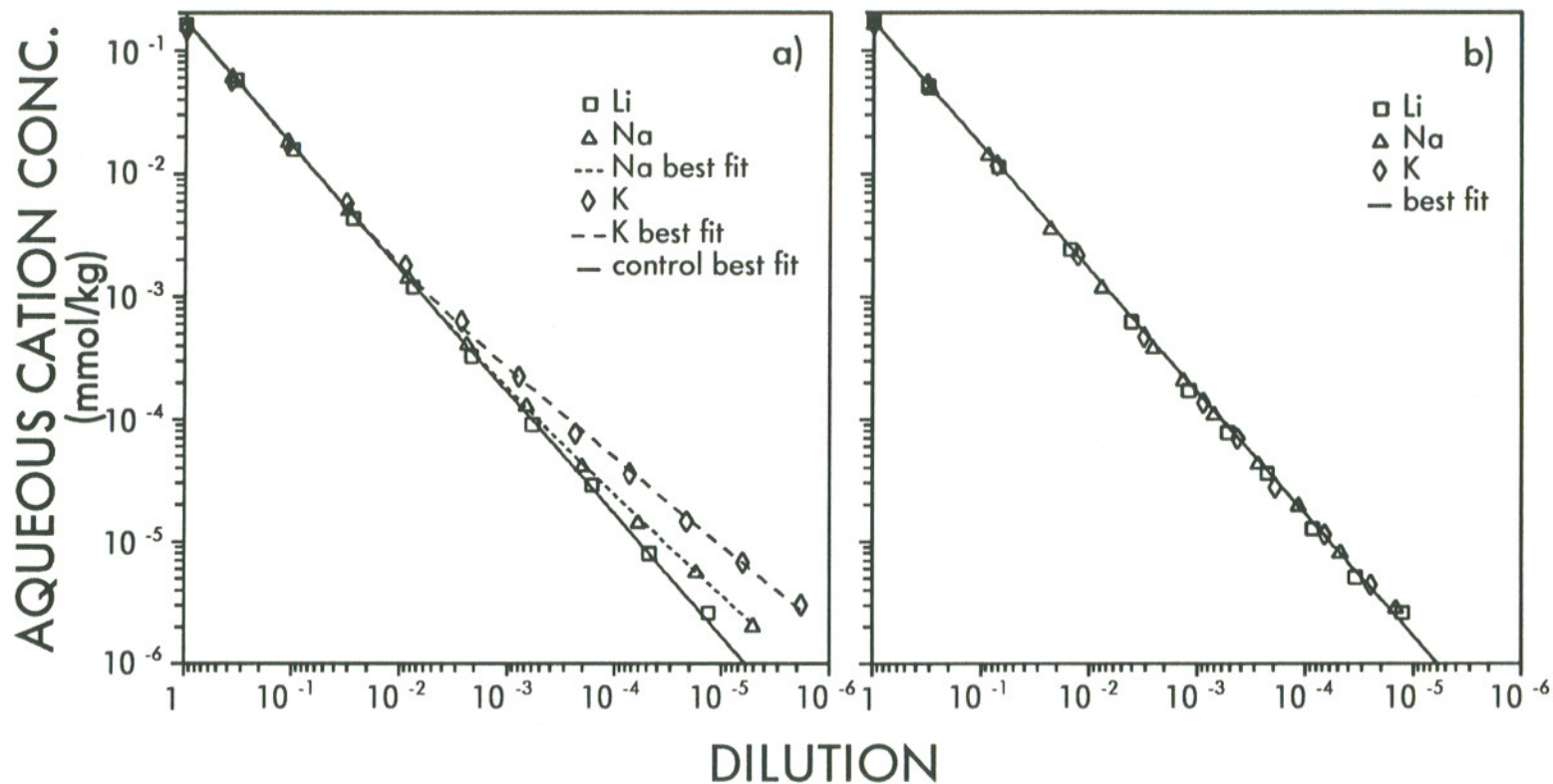


Figure 10. Aqueous cation concentrations as a function of the dilution ratio for a) desorption experiments with humic acid, and b) control experiments (without humic acid). The dashed lines represent the dilution curve calculated using the optimized Langmuir parameters for Na (---) and K (---). The solid line is the best fit of the control data assuming a no sorption model ($r^2=0.999$; slope= $0.996 \pm .008$, $\alpha=0.95$).

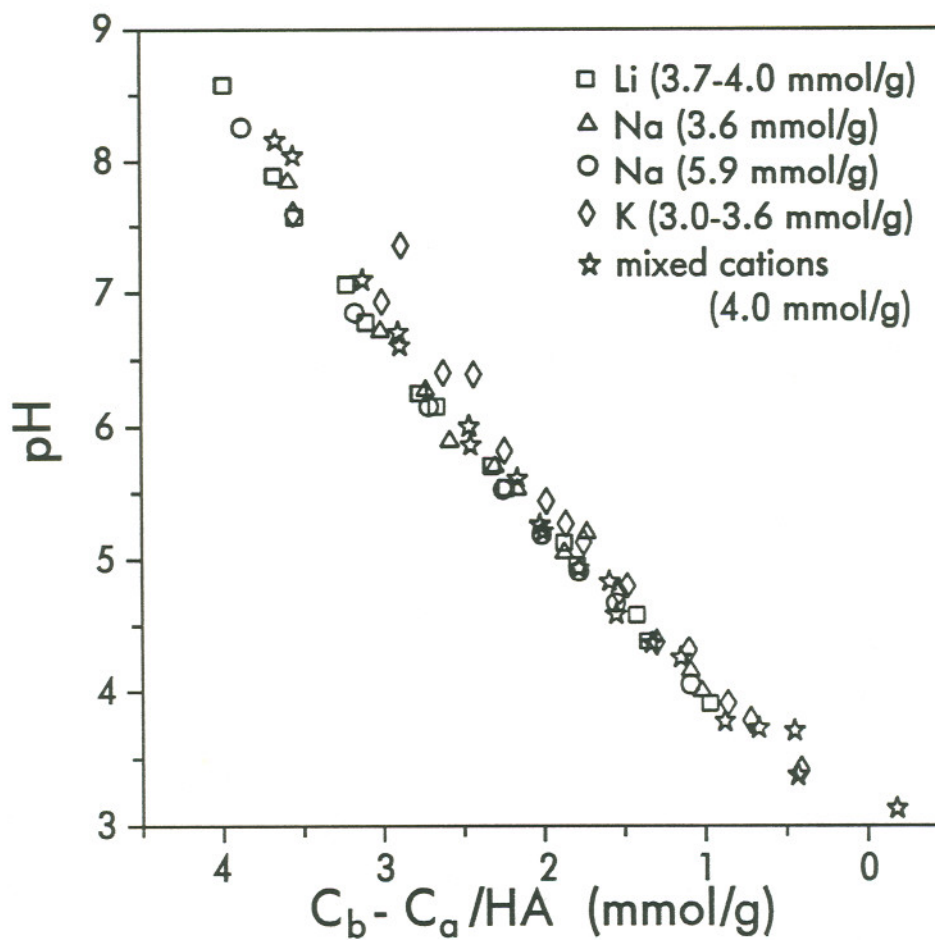


Figure 11. The relationship between the pH values of humic solutions before ultrafiltration and the net amount of base added. The cation concentrations given are the total concentrations and not the free aqueous concentrations. The mixed cation solution is 35% (mol/mol) Li, 31% Na, and 35% K.

these measurements; each data point represents a different sample solution. Notice that the identity of the alkali metal cation did not significantly affect the solution pH. This contrasts with the previous work of GAMBLE (1973) who observed that the pH of K-fulvate solutions was up to three units greater than the pH of Na-fulvate solutions having the same composition (ionic strength, alkalinity, fulvate concentration). Increasing the total concentration of Na^+ by 70% also had no noticeable effect on the pH.

Significant amounts of Na^+ are associated with this soil humic acid over the entire pH range (Figure 12). In solutions that contained no additional neutral Na-salt, over 90% of the total Na^+ was humate-associated at the beginning of the titration (high pH). The amount of humic-associated Na^+ decreased almost linearly with the equivalents of acid added. Even at the end of the titrations ($C_b - C_a / \text{HA} = 1 \text{ meq/g}$; $\text{pH} = 4$), a measurable amount of Na^+ remained in association with the humic acid (0.8 mmol $\text{Na}^+/\text{g HA}$). Contrary to expectation, the addition of a neutral Na-salt did not increase the total amount of humic-associated cation, and may actually have decreased it slightly at high pH. The association of Li^+ or K^+ with humic acid was essentially identical to that of Na^+ (Figure 13). At the beginning of a titration (between 4 and 2 meq base/g HA), each addition of acid decreased the amount of humic-associated cation by an amount approximately equal to the equivalents of acid added. As more acid was added, the size of this decrease steadily declined.

To determine if one of the alkali metal cations preferentially associates with humic acid, titrations were performed using solutions containing all three cations ($\text{Li}^+ = 35\%$ mol/mol, $\text{Na}^+ = 31\%$, and $\text{K}^+ = 35\%$). The total amount of humic-associated cation ($\text{Li} + \text{Na} + \text{K}$) was indistinguishable from that in experiments involving only one of the cations (Figure 14). In addition, the amounts of each alkali metal associated with the humic matter paralleled the total throughout the titration. The composition of the humic-associated fraction

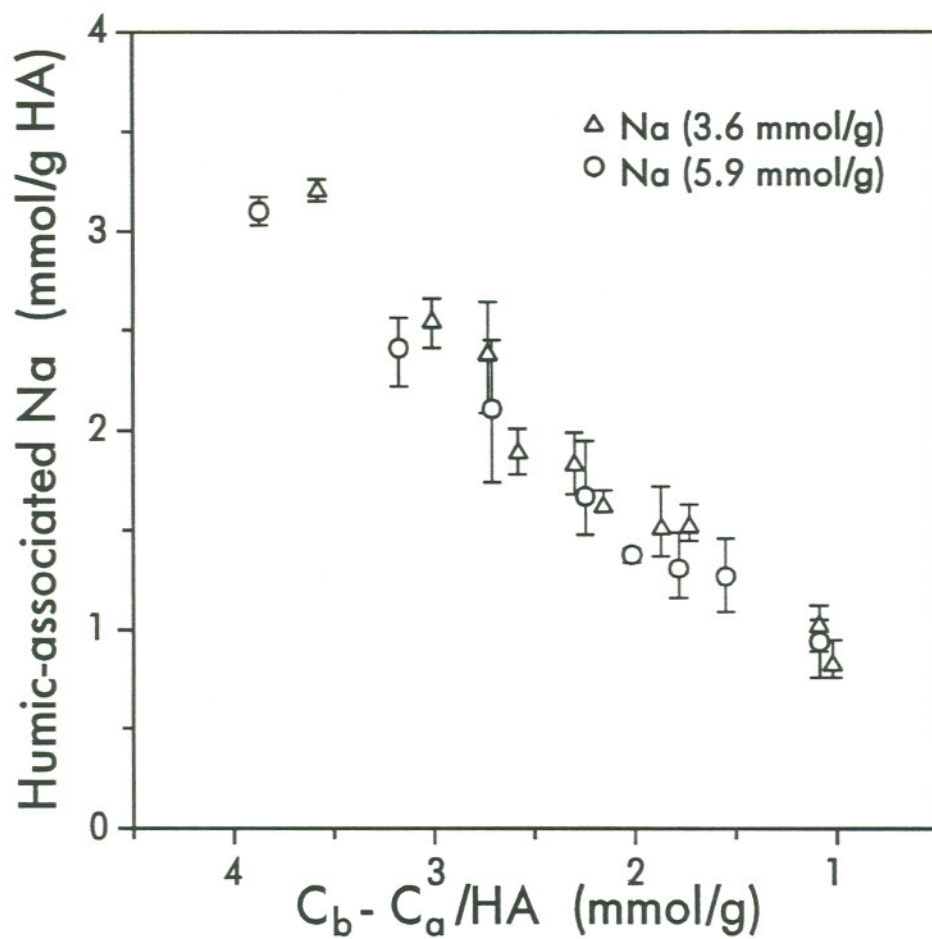


Figure 12. The relationship between the net base added and the amount of Na^+ associated with the humic matter. Humic-associated Na^+ was calculated by difference. The error bars show the range obtained from replicate ultrafiltrations of a given solution. The Na^+ concentrations given are the total Na^+ concentrations and not the free aqueous concentrations.

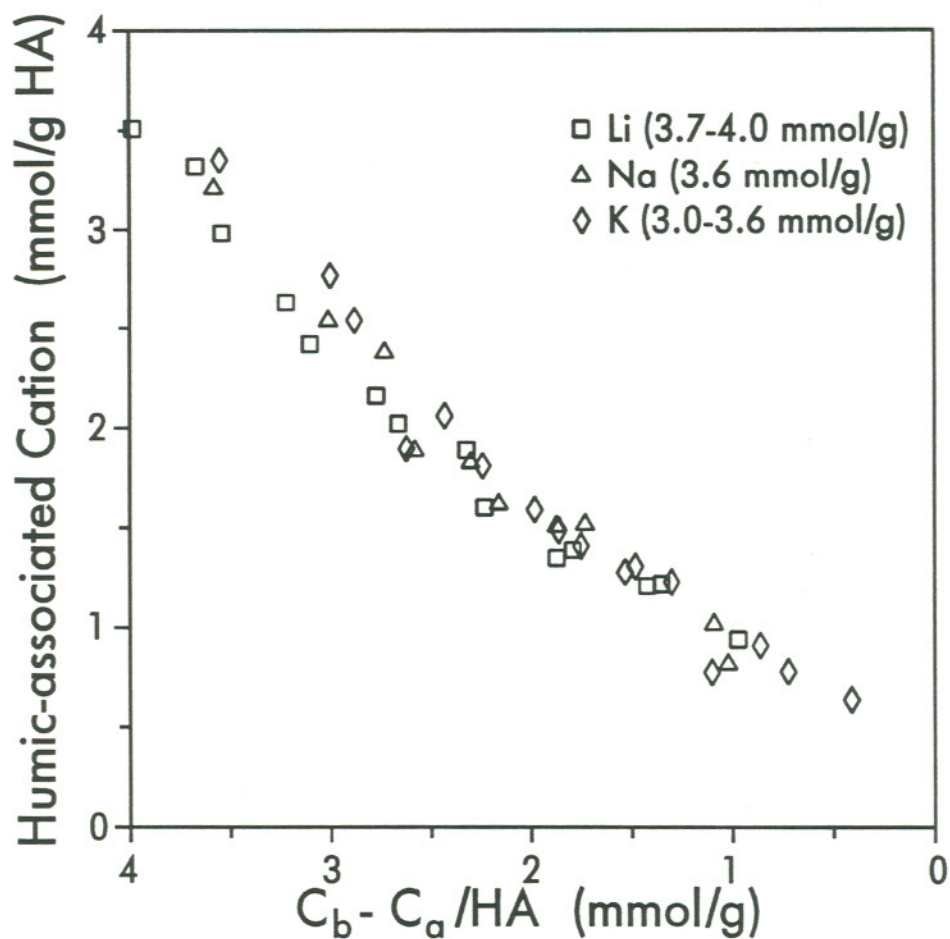


Figure 13. The relationship between the net base added and the amount of Li⁺, Na⁺, or K⁺ associated with the humic matter. Humic-associated cation was calculated by difference. The cation concentrations given are the total concentrations and not the free aqueous concentrations.

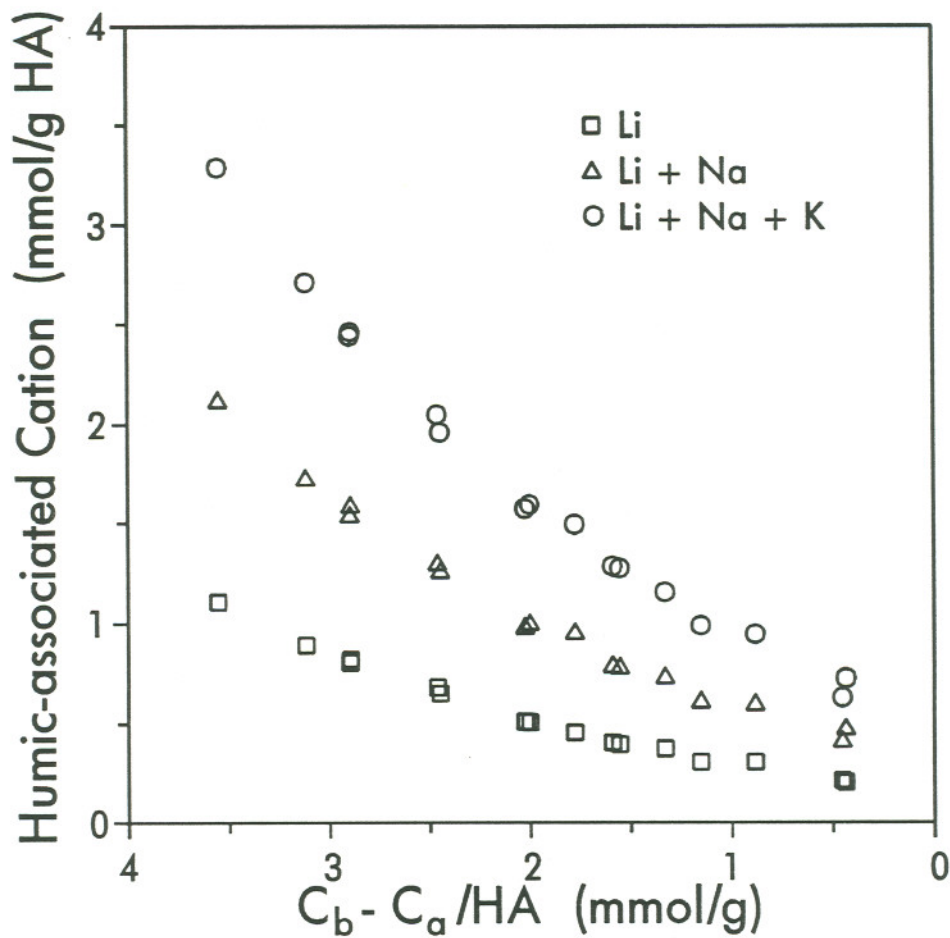


Figure 14. The relationship between the net base added and the amounts of Li^+ , Na^+ , and K^+ associated with the humic matter expressed cumulatively beginning with Li^+ . Humic-associated cation was calculated by difference. The total cation concentration is 4.0 mmol/g HA, composed of 35% (mol/mol) Li^+ , 31% Na^+ , and 35% K^+ .

was constant with respect to pH and reflected the original solution composition (Li: 32% \pm 4, Na: 32% \pm 5, K: 36% \pm 3; $\alpha=0.95$). Clearly, these alkali metal cations compete with one another on an equal basis and appear to be interchangeable.

The association of Li^+ , Na^+ , and K^+ with humic acid seems to be primarily due to a charge neutralization process rather than equilibrium complexation. A charge neutralization model would explain why the humic-associated cation concentration is determined by the net addition of OH^- or H^+ , rather than by the concentration or identity of the alkali metal cation. To assess the validity of such a model, the charge balance of the humic solution was investigated by examining the relationship between the free aqueous anion and cation concentrations. Differences between these two concentration totals reveal the contribution of the humate anion to the bulk solution electrical balance. A plot of the free aqueous anion concentration vs. the free aqueous cation concentration (Figure 15) is linear ($r^2 = 0.98$) with a slope of 1.01 ± 0.04 ($\alpha=0.95$) and an intercept near zero. The small deviation of the intercept from zero (-0.5 ± 0.1 , $\alpha=0.95$) is probably due to a systematic underestimation of the Cl^- concentration which was calculated from the amount of acid added (HCl) and not measured experimentally. This equivalence between the free aqueous anion and cation concentrations for all the titration solutions demonstrates that the humic anion does not contribute to the charge balance of the bulk aqueous solution.

The absence of humate contributions to the electroneutrality of the bulk aqueous solution suggests a model in which cations accumulate near the humic molecule, are not part of the bulk aqueous solution, and therefore, are not sampled by ultrafiltration. Such a model (Figure 16), containing a humic phase with an associated diffuse layer and a bulk aqueous phase has been formulated by TIPPING and HURLEY (1988). The charge on the humic polyion is balanced by the positive counter ions in the diffuse layer so that, together, the humic phase

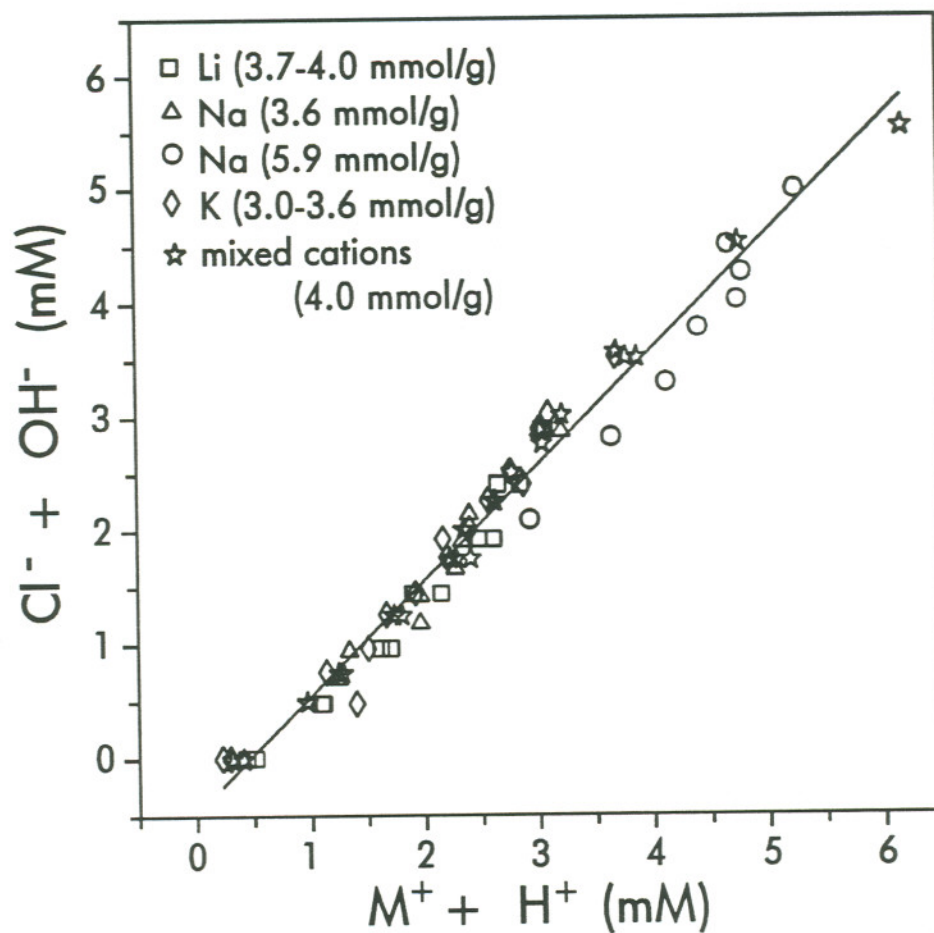


Figure 15. The correlation between the free aqueous anion and cation concentrations for all of the ultrafiltration experiments. The solid line was determined by least squares regression ($r^2 = 0.98$; slope = 1.01 ± 0.04 , intercept = -0.5 ± 0.1 , $\alpha=0.95$). The cation concentrations given are the total concentrations and not the free aqueous concentrations. The mixed cation solution is 35% (mol/mol) Li, 31% Na, and 35% K.

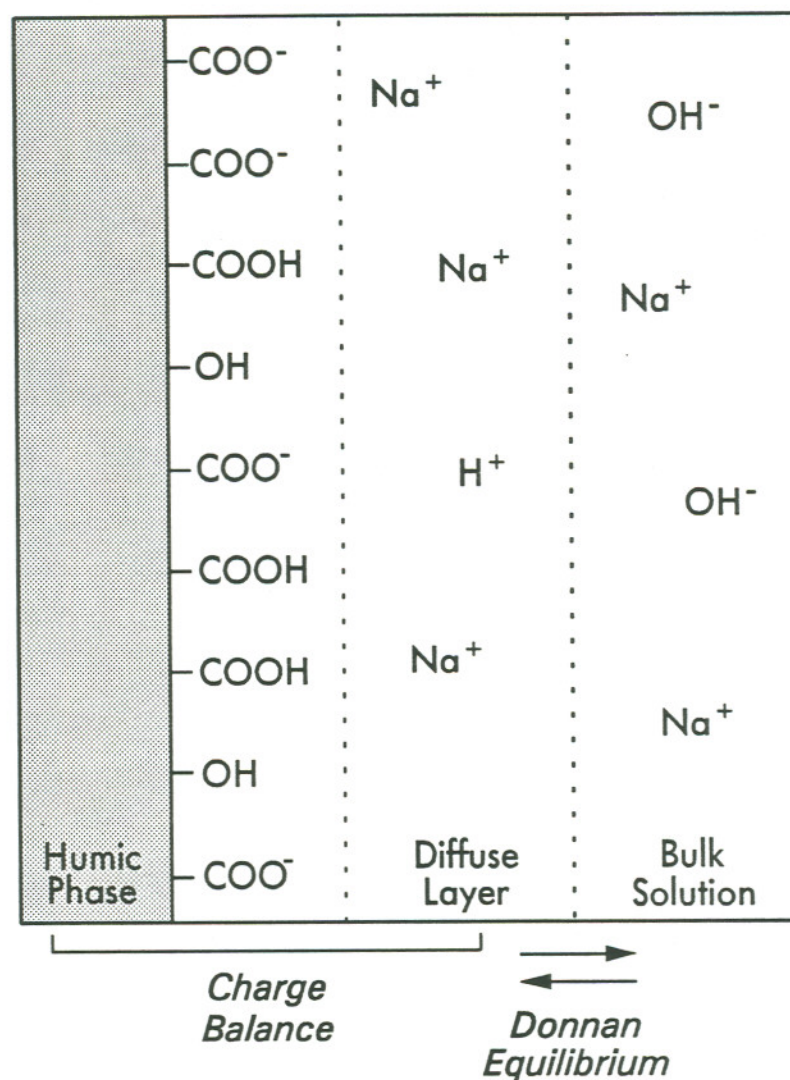


Figure 16. A schematic diagram of the diffuse layer model for humic solutions. Cations are bound to the humic matter directly via specific sites. Cations in the diffuse layer are held by electrostatic attraction. Together, the humic phase and the diffuse layer are electrically neutral. The bulk aqueous phase is also electrically neutral. The diffuse layer and bulk aqueous phase are linked via a Donnan equilibrium.

and diffuse layer are electrically neutral. The diffuse layer and bulk aqueous phase are linked by a Donnan equilibrium

$$\left(\frac{\{X_{diffuse}^{x+}\}}{\{X_{aq}^{x+}\}} \right)^{1/x} = \left(\frac{\{Y_{diffuse}^{y+}\}}{\{Y_{aq}^{y+}\}} \right)^{1/y}$$

where X and Y are representative cations, and the braces indicate activities in the bulk aqueous and diffuse layer phases. The diffuse layer contains some fraction of every charged species in the bulk solution, including H^+ and trace metal cations.

The existence of a diffuse layer which balances the humic charge has implications for the measurement of humic association for all cations. If the mass of humic-associated cation is estimated by difference, two mechanisms of association will be combined: covalent complexation with specific humic functional groups, and non-specific association in the diffuse layer. The usual assumption, that all humic-associated cations are specifically coordinated with humic sites, could lead to erroneous conclusions. The potential for error is greatest in solutions of moderate pH and low ionic strength where a significant fraction of the cations not specifically coordinated to the humic molecule will nonetheless be humic-associated in the diffuse layer. Under such conditions, an increase in the background electrolyte concentration would change the composition of the diffuse layer, and liberate some cations that were assumed to be bound. Because the cations bound to specific humic sites would not be affected, two apparent types of sites are created, exchangeable and non-exchangeable.

The contribution of diffuse layer cations to humic-cation association will be less in solutions with a low pH because cations are required in the diffuse layer to balance the small charge on the humic molecule. In solutions with high ionic strength, the major solution cations will predominate and limit the contribution of trace cations in the diffuse layer. The importance of the diffuse

layer contribution to the total mass of humic-associated cation will depend upon the extent of site-specific binding.

Unfortunately, the composition of the diffuse layer cannot be determined with certainty. Measuring the diffuse layer cation concentration directly is not possible. The Donnan equilibrium links the activities, not the concentrations, of the bulk aqueous phase and the diffuse layer. Even if the concentration of one diffuse layer species could be calculated by difference and the bulk aqueous phase speciation were known, the activity corrections for the two phases could be quite different. Estimating the mass of cations in the diffuse layer is even more problematic because the volume of the diffuse layer surrounding a humic molecule is not well defined, and is expected to change with pH and ionic strength (TIPPING and HURLEY, 1988).

The diffuse layer model may provide a useful mechanism for investigating the dissociation of acidic humic functional groups through the use of Li-humate solutions. Because low pH dilution experiments indicate that site-specific binding of Li^+ to humic matter is virtually non-existent, any Li^+ not present in the bulk aqueous phase can be assumed to be in the diffuse layer. By varying the total Li^+ (using a neutral Li-salt), a data set could be obtained and used with a quantitative chemical model to estimate the humic charge and the diffuse layer volume as functions of alkalinity or pH.

CONCLUSIONS

The association of alkali metal cations with humic material depends upon the solution pH and can be significant. At low pH, the association is well described by a Langmuir model. The number of sites per gram of humic acid is very small and is larger for K^+ than Na^+ . Li^+ exhibited no detectable humic-association at low pH. The differences in the humic-association exhibited by these three cations suggest that some specific-site interaction is possible and may be related to the size of the hydrated cation.

Discontinuous titration with ultrafiltration can be a valuable technique for delineating humate-cation associations. Between pH 3 and 8, significant amounts of Li^+ , Na^+ , and K^+ associate with humic matter. The amount of humic-associated cation depends on the net base added, and not on the cation concentration. The three cations behave equivalently. This behavior suggests a charge neutralization process and is consistent with a diffuse layer model of aqueous humic matter.

Ultrafiltration techniques cannot distinguish between two different association mechanisms: specific site coordination and electrostatic association in the diffuse layer. All other methods in which the humic-associated cation is calculated as the difference of the total cation and a measured free aqueous cation concentration suffer from the same problem. The mass of cations in the diffuse layer could be a significant fraction of the total cation mass, especially if the background electrolyte concentration is low. Cations "bound" in the diffuse layer should be extremely exchangeable and the addition of **any other** cations alters the composition of both the diffuse layer and the bulk aqueous phase. This phenomenon suggests that practical models of humate-metal interactions must take into account the electrostatic properties of the humic polyanion.

REFERENCES

- BONN B.A. and FISH W. (1991) The variable nature of humic carboxyl measurements. *Environ. Sci. Technol.* **25**, 232-240.
- CABANISS, S.E. and SHUMAN M.S. (1986) Combined ion selective electrode and fluorescence quenching detection for copper-dissolved organic matter titrations. *Anal Chem.* **58**, 398-401.
- EPHRAIM J.H. and MARINSKY J.A. (1990) Ultrafiltration as a technique for studying metal-humate interactions: studies with Fe and Cu. *Anal. Chim. Acta* **232**, 171-180
- EPHRAIM J.H. and XU H. (1989) The binding of cadmium by an aquatic fulvic acid: a comparison of ultrafiltration with ion-exchange distribution and ion-selective electrodes. *Sci. Tot. Environ.* **81/82**, 625-634.

- FISH W., DZOMBAK D.A., and MOREL F.M.M. (1986) Metal-humate interactions. 2. Applications and comparison of models. *Environ. Sci. Technol.* **20**, 676-683.
- FRIZADO J.P. (1979) Ion exchange on humic materials- a regular solution approach. In *Chemical Modeling in Aqueous Systems* (ed. E.A.Jenne), pp. 133-145. ACS Symposium Series 93.
- GAMBLE D.S. (1973) Na⁺ and K⁺ binding by fulvic acid. *Can. J. Chem.* **51**, 3217-3222.
- KONONOVA M.M. (1966) *Soil Organic Matter: Its Nature, Its Role in Soil Formation and in Soil Fertility*. 2nd edition. Pergamon, New York. 544 pp.
- LEHN J.M. (1878) Cryptates: the chemistry of macropolycyclic inclusion complexes. *Accts. Chem. Res.* **11**, 49-57.
- PRESS W.H., FLANNERY B.P., TEUKOLSKY S.A. and VETTERLING W.T. (1989) *Numerical Recipes: the art of scientific computing*. Cambridge U. Press, N.Y. Chap. 10.
- SAAR R.A. and WEBER J.H. (1980) Comparison of spectrofluorometry and ion-selective electrode potentiometry for determination of complexes between fulvic acid and heavy-metal ions. *Anal. Chem.* **52**, 2095-2100.
- SHUMAN M.S. and CROMER J.L. (1979) Copper association with aquatic fulvic and humic acids. Estimation of conditional formation constants with a titrimetric anodic stripping voltammetry procedure. *Environ. Sci. Technol.* **13**, 543-545.
- TIPPING E. and HURLEY M.A. (1988) A model of solid-solution interactions in acid organic soils, based on the complexation properties of humic substances. *J. Soil Sci.* **39**, 505-519.
- TURNER D.R., VARNEY M.S., WHITFIELD M., MANTOURA R.F.C. and RILEY J.P. (1986) Electrochemical studies of copper and lead complexation by fulvic acid. I. Potentiometric measurements and a critical comparison of metal binding models. *Geochim. Cosmochim. Acta* **50**, 289-297.

CHAPTER IV

Aqueous CIR-FTIR of Humic Acid

I. Method description and evaluation

ABSTRACT

Humic substances interact with metal cations in soils and aqueous environments both through electrostatic attraction and through coordination with carboxylic and phenolic functional groups. Infrared spectroscopy allows the direct investigation of carboxylic and phenolic functional groups, and consequently can help characterize the acid-base chemistry of these groups and their interactions with metal cations. To accurately reflect the natural hydrated state of humic materials, humic acid-base equilibria and metal-humate association must be investigated in aqueous solution. Infrared spectroscopy of aqueous samples, however, is greatly complicated by the strong absorbance of water. Circular internal reflectance (CIR) Fourier transform infrared spectroscopy (FTIR) and spectral subtraction were used to overcome many of the problems associated with conventional transmission IR spectroscopy of aqueous humic solutions. An objective background subtraction method was required to obtain reproducible difference spectra and to avoid the creation of spurious difference peaks. A general algorithm for background water subtraction was developed in which the elimination of the water band at 2120 cm^{-1} was utilized

as the criterion for optimal subtraction. Corrections for baseline curvature were also incorporated. Difference spectra reproducibility was excellent. Difference spectra quality depended heavily upon the correspondence between the common features of the solution and background spectra. Alkali metal cations can alter the infrared absorbance bands of water thereby causing artifacts in the difference spectra. The signal-to-noise ratio of the difference spectra was large enough to permit peak quantitation throughout the mid-infrared region ($4000\text{-}800\text{ cm}^{-1}$), except between 3600 and 2900 cm^{-1} , where the absorbance of water is extremely intense. The methods described in this paper are general and could be used to study many environmentally important materials in their naturally hydrated state.

INTRODUCTION

Natural organic matter plays a significant role in geochemical cycling in the environment. Humic substances reversibly bind metal cations and thereby alter the solubility of cations and influence their transport. The bioavailability of some trace elements, both toxins and nutrients (*e.g.*, Cu^{2+} and Fe^{3+}), is in part regulated by equilibria involving humic substances. Humic complexation of cations can accelerate the weathering of minerals and transport trace metals through soil horizons. Reversible complexation reactions between humic substances and trace metal cations are thought to be responsible for the transport of trace metals to estuary sediments. In some natural waters, humic substances account for much of the cation exchange capacity and control the pH. Even in aquatic systems with very low concentrations of natural organic matter, complexation of trace metals by humic material can be important. Humic matter also forms aggregates with clay minerals which can bind metal cations and affect speciation and transport in both aquatic and soil systems. Although the precise mechanisms of humic-cation or humic-cation-clay interactions are unknown, oxygen-containing functional groups on the humic macromolecule, specifically

carboxylic and phenolic groups, are thought to be primarily responsible for such interactions (STEVENSON, 1985).

Of the many spectroscopic techniques, infrared spectroscopy has proven to be the method best suited for investigating oxygen-containing functional groups in humic matter (MACCARTHY and RICE, 1985). Infrared absorbance bands due to O-H, C=O and C-O structures have been clearly observed. Changes in the infrared spectra of humic acids due to both neutralization and metal-binding reactions have been documented. Infrared analysis of derivatized oxygen-containing groups has also contributed to understanding humic acid structure (LEENHEER and NOYES, 1989).

Most infrared spectra of humic matter have been obtained using KBr pellets. This method does not reflect the natural wet state of humic matter, and the changes in humic matter that occur upon drying and compression with KBr are unknown. Two early studies by MACCARTHY and co-workers are notable exceptions to the use of KBr pellets (1975). These researchers used a CaF₂ transmission cell and Fourier Transform Infrared (FTIR) technology to record the spectra of humic solutions and suspensions both in D₂O and in H₂O. The spectrum of the solvent-free humic matter was produced by digitally subtracting a background spectrum (either D₂O or H₂O) from each solution spectrum. Subtraction of the solvent spectrum requires the high signal-to-noise ratios and digital data reproduction provided by FTIR technology (GRIFFITHS and DEHASETH, 1986). The CaF₂ cell method, while representing a pioneering effort, inherently contains several experimental complications. It is very difficult to exclude H₂O from all D₂O solutions, background subtraction is inconsistent, and filling a short pathlength sealed transmission cell with humic suspensions is problematic. Because of these problems, the further use of CaF₂ transmission cells to acquire humic spectra has not been pursued.

Significant advantages over transmission-FTIR can be gained by coupling attenuated total reflectance (ATR) sampling techniques with FTIR technology

(HARRICK, 1987). ATR techniques allow samples to be easily investigated in their natural state. Media such as KBr or Nujol are not required. Aqueous spectra can be successfully obtained because the effective path length in ATR-FTIR is very short and reproducible. In addition, ATR accessories are easier to fill and clean than transmission cells.

ATR-FTIR techniques have been applied to a wide variety of substances. The effects of oxidation on the structure of coals were investigated using ATR-FTIR spectra of neat samples (MIELCZARSKI, *et al.*, 1986). TEJEDOR-TEJEDOR, *et al.* (1990) used aqueous ATR-FTIR to study the interactions between goethite and oxygen-containing aqueous ligands. Because aqueous systems can be studied easily with ATR-FTIR, this technique is particularly attractive for environmental applications. Sample preparation is minimal and non-destructive. FTIR instruments are equipped with a computer and the software needed to perform spectral subtraction.

Although the technique is straightforward, aqueous ATR-FTIR is not without problems. Aqueous solvent subtraction seems very simple, but if not carefully conducted, may lead to uninterpretable spectra. We have not found a generally accepted and reliable method for performing solvent subtraction reported in the literature. In addition, most studies that employ ATR-FTIR and solvent subtraction do not discuss the reproducibility of their spectra. This paper describes the procedures we developed and adapted to collect, manipulate and evaluate the spectra of aqueous humic samples. The application of this method to cation-humate interactions is developed here and is explored more completely in a Chapter V. The utility of these procedures is not limited to aqueous humic spectra, but is applicable to ATR-FTIR analysis of aqueous geochemical materials in general. We feel that ATR-FTIR is a very promising technique for examining natural hydrogeochemical systems and hope that the work presented here will lead to a better understanding of and some standardization of solvent subtraction techniques.

Spectral Subtraction Theory

The spectrum of an aqueous humic solution is dominated by the spectrum of the aqueous solvent (Figure 17). In order to examine the features of the humic solute, the background absorbance of water must be removed from the spectrum. Correcting any baseline tilt or curvature is also desirable, especially if several spectra will be compared.

To perform spectral subtraction, the spectrum of a mixture of components must equal the sum of its component spectra. When individual component spectra are available, the fractional composition of diverse mixtures can be routinely determined (GRIFFITHS and DEHASETH, 1975; ANTOON, *et al.*, 1979). Components are assumed to be non-interactive, so that the shape and position of the spectral bands are identical in the component and mixture spectra. By applying the Beer-Lambert Law, each component spectrum (in absorbance units) is multiplied by a constant proportional to its concentration in the mixture. The mixture spectrum is then digitally reproduced by a scaled sum of the individual component spectra. Least squares methods or factor analysis techniques are normally used to calculate the scaling constants.

Scaled subtraction can be applied to remove the spectral features of the solvent from a solution spectrum to yield the difference spectrum of the solute. The spectrum of the solvent must be known. To accomplish this subtraction, features of the solvent spectrum must be chosen that can act essentially as internal standards. That is, one or more solvent peaks must be identified in the solution spectrum with no overlapping or interfering solute peaks. The presence of the solute must not alter the shape and position of these solvent peaks. Using only the absorbance data from these bands, a difference factor is determined. The entire solvent spectrum is then multiplied by that factor before subtraction from the solution spectrum. When the difference factor is chosen correctly, all features of the solvent spectrum are eliminated in the difference spectrum.

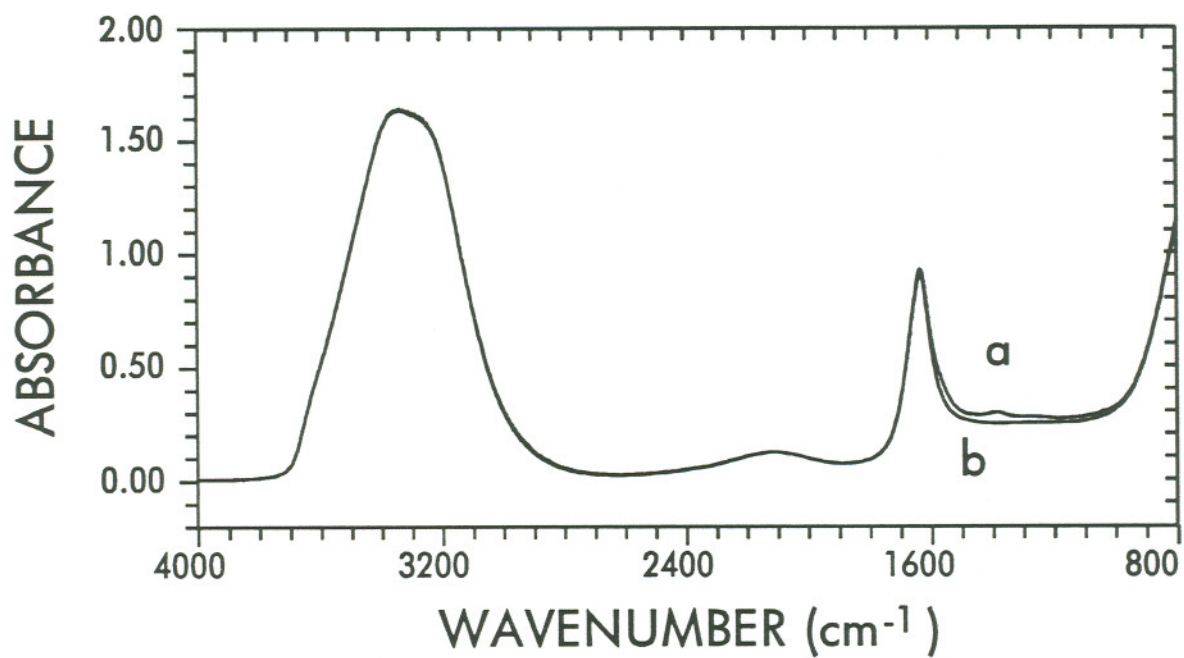


Figure 17. a) The infrared absorbance spectrum of aqueous lithium humate, pH 8.02. Humic acid concentration: 45 mg/mL b) The absorbance spectrum of water.

For aqueous humic spectra in the mid-infrared region, the only water peak usable as a criterion for spectral subtraction is the combination water band at $\sim 2120\text{ cm}^{-1}$. The peak at $\sim 1640\text{ cm}^{-1}$, associated with bending modes of water, overlaps the carbonyl and carboxyl stretching regions of humic matter. The $\sim 3200\text{ cm}^{-1}$ band, associated with hydrogen-bonded O-H stretching, not only overlaps similar humic vibrational modes, but is so intense that the signal-to-noise ratio is too low for reliable spectral subtraction. The 2120 cm^{-1} peak has been used by other researchers as a criterion for aqueous spectral subtraction with both humic and protein solutions (MACCARTHY, *et al.*, 1975 and DOUSSEAU, *et al.*, 1989, respectively).

Because the features of the difference spectrum are very small relative to the solvent spectrum, choosing the correct value for the difference factor is essential. If the difference factor is too small, bands due to water will appear in the difference spectrum (undersubtraction). Similarly, if the factor is too large, negative bands will appear (oversubtraction). In either case, the incorrectly subtracted bands can overlap solute bands, altering their size and shape. This is particularly troublesome with the 1640 cm^{-1} band which overlaps the humic carbonyl and ionized carboxyl bands.

Perhaps the most common method used to choose the factor is iterative examination of difference spectra using the interactive graphics program supplied with many FTIR instruments (MACCARTHY, *et al.*, 1975; SPERLINE, *et al.*, 1986). The researcher adjusts the value of the factor and then determines the best difference spectrum by examining a visual display. POWELL, *et al.* (1986) showed that this method, which relies upon individual perceptions, is not reproducible, and does not necessarily result in the best choice of the difference factor.

To eliminate researcher bias and to incorporate statistical criteria for selecting the best difference factor, several researchers have developed least-squares minimization methods (DOUSSEAU, *et al.*, 1989; GILLETTE and KOENIG, 1984).

In the method used by DOUSSEAU, *et al.*, for protein solutions, residuals between 2650 cm^{-1} and 1750 cm^{-1} were calculated as the difference spectrum less the baseline. The difference factor was then adjusted and the process repeated until a minimum squared residual sum was achieved. At each iteration the baseline was estimated by a least-squares fit of the difference spectrum over the $2650 - 1750\text{ cm}^{-1}$ range. Their aqueous protein solutions were featureless in this region except for the ~ 2120 water peak which serves as an internal standard for the subtraction. Although this method provides a statistically defensible estimate of the difference factor, it does not guarantee a random distribution of residuals about the baseline. The minimum square residual sum may be the result of slight over- or under-subtraction, which can lead to significant errors in the difference spectrum of the solute.

A novel method for determining the difference factor was developed by POWELL, *et al.* (1986), in which the elimination of a trough, rather than a peak, was used as the criterion for subtraction. The range of their aqueous protein spectra was limited to $2000-900\text{ cm}^{-1}$, eliminating the 2120 cm^{-1} water band. The difference spectrum between $1990-1790\text{ cm}^{-1}$ was divided into two regions, each of which was approximated by a straight line segment. The difference factor was calculated iteratively using equality of the two line segment slopes as evidence of complete subtraction.

Several other approaches for choosing the difference factor have also been used. TEJEDOR-TEJEDOR and ANDERSON (1986) chose a difference factor of unity for their aqueous goethite suspensions. Another method approximates the factor as the ratio of a solution peak height to the corresponding solvent peak height (Perkin-Elmer software). These methods may perform well for particular solute-solvent systems, however, they are not generally applicable.

Clearly, no standard method for aqueous solvent subtraction of FTIR spectra exists. The method of choice should be reproducible and provide the best estimate of the difference factor with a minimal potential for over- or under-

subtraction. These requirements virtually necessitate the use of a computer algorithm.

Instrument requirements

For spectral subtraction to be successful, FTIR instrument parameters should be identical for both solution and solvent spectra (POWELL, *et al.*, 1986). Wavenumber scale reproducibility is particularly important because small wavenumber shifts between solution and solvent spectra result in spurious peaks in the difference spectrum (HIRSCHFELD, 1976). The same apodization function should be used for both spectra. High signal-to-noise ratios are required, especially to discern difference peaks in regions of high background absorbance, such as the 1640 cm^{-1} water band. If the background absorbance is extreme (*e.g.*, 3200 cm^{-1} water band), reliable spectral subtraction may not be possible (Paul Perkins, pers. comm.) Adequate purging with dry gas is essential to remove the sharp peaks due to water vapor ($1800\text{-}1400\text{ cm}^{-1}$). Sampling accessories should preserve the pathlength. For transmission cells, the same sealed cell should be used for both solution and solvent spectra. Attenuated total reflectance accessories should not be moved between the acquisition of solution and solvent spectra. Even small changes in the angle of the incident IR beam alter the pathlength by changing the depth of penetration of the evanescent wave (POWELL, *et al.*, 1986).

EXPERIMENTAL

Humic acid

The soil humic acid used was the same material described by BONN and FISH (1991). The total acidity of the material as measured by the barium acetate method was 7.3 ± 0.4 meq/g. Ash content was 1% (by weight) and the elemental composition (Huffman Laboratories, Golden, CO) was 58% C, 4% H, 35% O, 3% N. The freeze-dried humic acid was stored in a desiccator until use.

Twenty-four hours before acquiring spectra, the humic acid was dissolved in aqueous standardized base (LiOH, NaOH or KOH). After a 4 hr equilibration period, 2 mL aliquots of the dissolved humate were acidified with standardized HCl and shaken overnight. The average concentration of humic matter was 40 mg/mL. A pH meter (EA 920, Orion, Boston, MA) equipped with a micro-combination electrode (MI-410, Microelectrodes, Inc., Londonderry, NH) was used to measure the solution pH which was typically between 3 and 10. To minimize the potential for oxidation of the humic matter, all procedures were performed under N₂. Nitrogen-purged ultra-pure water (Nanopure System, Barnstead) and ACS Reagent Grade chemicals were used for all solutions.

Spectroscopy

Reflectance spectra were obtained using a cylindrical internal reflection (CIR) accessory, the micro CIRCLE® cell (Spectra-Tech, Stamford, CT). The CIRCLE® cell has been described in detail elsewhere (BRAUE and PANELLA, 1987; SPERLINE, *et al.*, 1986; PERKINS, 1987). Briefly, the cell consists of a cylindrical internal reflection crystal (ZnSe) suspended in a stainless steel sample boat. Teflon o-rings form a leak-proof seal between the crystal and the sample boat. Two Cassegrain mirrors on the optical bench focus the infrared beam on the conical ends of the ZnSe crystal. The accessory is aligned by adjusting the position of both the sample boat and the focusing mirrors so that the energy transmitted through the crystal is maximized. The maximum energy throughput with a dry CIRCLE® cell in place was about 15% of the open beam (without an accessory present) energy.

The spectra were recorded by a Perkin-Elmer 1800 Fourier Transform Infrared Spectrometer equipped with a globar source, a KBr beamsplitter, and a CsI TGS detector. Because of the inherent low throughput of the CIRCLE® cell, the mirror velocity was slowed to 0.25 cm/s to increase the energy reaching the detector. Two-hundred interferograms were coadded and convolved with

a weak Beer-Norton apodization function to yield a final spectrum with a resolution of 2 cm^{-1} .

To obtain the high quality spectra required for successful spectral subtraction a protocol for the analysis of a sample series was established. The instrument was purged with dry N_2 from liquid N_2 , until the water vapor peaks in the $1400\text{-}1800\text{ cm}^{-1}$ range disappeared. After adequate purging with N_2 an initial single beam background spectrum (transmittance format) of the dry CIRCLE® cell was recorded. All subsequent spectra were recorded in single beam ratio mode: single beam spectra were recorded relative to a reference spectrum (the spectrum of the dry CIRCLE® cell). This acquisition method removes the spectral features due to the CIRCLE® accessory from the transmittance spectrum of the solution. To avoid spurious trends due to instrument drift, humic spectra were recorded in random order, alternating with spectra of N_2 -purged ultrapure water. Each water spectrum served as the reference blank for the next humic spectrum, as well as an indicator of CIRCLE® cell contamination. Water-water difference spectra were formed by subtracting consecutive pairs of water spectra (interspersed with humic solution spectra) and then examined to assess the errors associated with water subtraction.

Sample introduction and cleaning between samples in a series were performed with the CIRCLE® cell in place so that the optical alignment of the cell was not altered. Samples were introduced into the open boat CIRCLE® cell using fine-tipped polyethylene transfer pipets taking care to completely fill the space near the ends of the cell and to avoid bubbles. Approximately 1 mL of sample was required for each spectrum. After each humic sample spectrum the CIRCLE® cell was cleaned by rinsing the cell first with ultrapure water, then with 2%(v/v) aqueous CONTRAD 70 CMS detergent (Decon Laboratories, Inc. Malvern, PA), then with 0.1 M phosphate (pH 9), and finally with ultrapure water. Fine tipped polyethylene transfer pipets were used to agitate the rinse solutions near the ends of the CIRCLE® cell where the o-rings meet the ZnSe

crystal. Rinsing the CIRCLE® cell with water alone did not prevent the slow accumulation of humic material on the crystal, especially in the vicinity of the o-rings.

After the spectra for a sample series were recorded, another spectrum of the dry CIRCLE® cell was obtained. This spectrum was compared with the dry cell spectrum recorded at the beginning of the series. If contamination or degradation of the ZnSe crystal was evident, the cell was dismantled and the ZnSe crystal removed for thorough cleaning, which involved polishing the crystal with plain toothpaste (Scott Strand pers. comm.) followed by rinsing with ultrapure water and finally acetone.

Infrared spectra of aqueous humic solutions were recorded in reflectance format on a Perkin-Elmer 8000 computer, and then translated into DOS-readable files. A BASIC program converted these spectra to absorbance format, digitally subtracted the background water spectra, and applied a baseline correction and normalization. The program source code is available from the authors. In all, 134 humic difference spectra were constructed over 4 months.

Choice of background spectrum

The background spectrum should contain all of the spectral features of the humic solution except those due only to the humic matter. The solution immediately surrounding the humic macromolecule would provide the most appropriate background spectrum. Unfortunately, isolating this solution is not feasible and usually the bulk solution is used for the background spectrum. In their spectroscopic studies of goethite suspensions, TEJEDOR-TEJEDOR and ANDERSON (1986) centrifuged aqueous samples to separate the bulk solution from the suspended solids. Centrifugation, however, cannot remove dissolved humic material from the bulk solution, and ultrafiltration is only effective for solutions that are far too dilute for FTIR analysis. Due to these problems, several researchers have used the spectrum of pure water for a background (MACCARTHY,

et al., 1975; DOUSSEAU, *et al.*, 1989). The difference spectra of aqueous humic-free salt solutions were examined to determine if using water for the background spectrum resulted in any artifacts due to pH effects or the omission of electrolyte.

SOLVENT-SUBTRACTION PROGRAM DESCRIPTION

Because correct subtraction of the water background is essential for examination of the carbonyl and carboxyl bands of humic spectra, we devised a method (inspired by that of POWELL, *et al.*, 1986) that minimizes the potential for over- or under-subtraction. As did MACCARTHY, *et al.* (1975) and DOUSSEAU, *et al.* (1989), we chose elimination of the combination water band (2120 cm^{-1}) from the difference spectrum as the criterion for the best difference factor. Absorbance data between 2250 and 1950 cm^{-1} ("fit region") were used (Figure 18a). The baseline in this narrow fit region can be adequately described by a straight line. The fit region was divided into two portions, left (2250 - 2120 cm^{-1}) and right (2100 - 1950 cm^{-1}). When the difference factor is chosen correctly, the difference spectrum in the fit region is identically the linear baseline and the left and right line segments are collinear (Figure 18c). Their slopes are equal and both extrapolate to the same absorbance value at 2110 cm^{-1} . If the factor is not optimal, the data from left and right portions sections of the fit region will describe two line segments with different slopes (Figures 18b and 18d). Least squares methods were used to obtain a system of equations for the difference factor and the absorbance value at 2110 cm^{-1} . To minimize numerical error, the absorbance values were scaled by a factor of 100, wavenumber values by a factor of 0.001. Double precision arithmetic was used for all calculations.

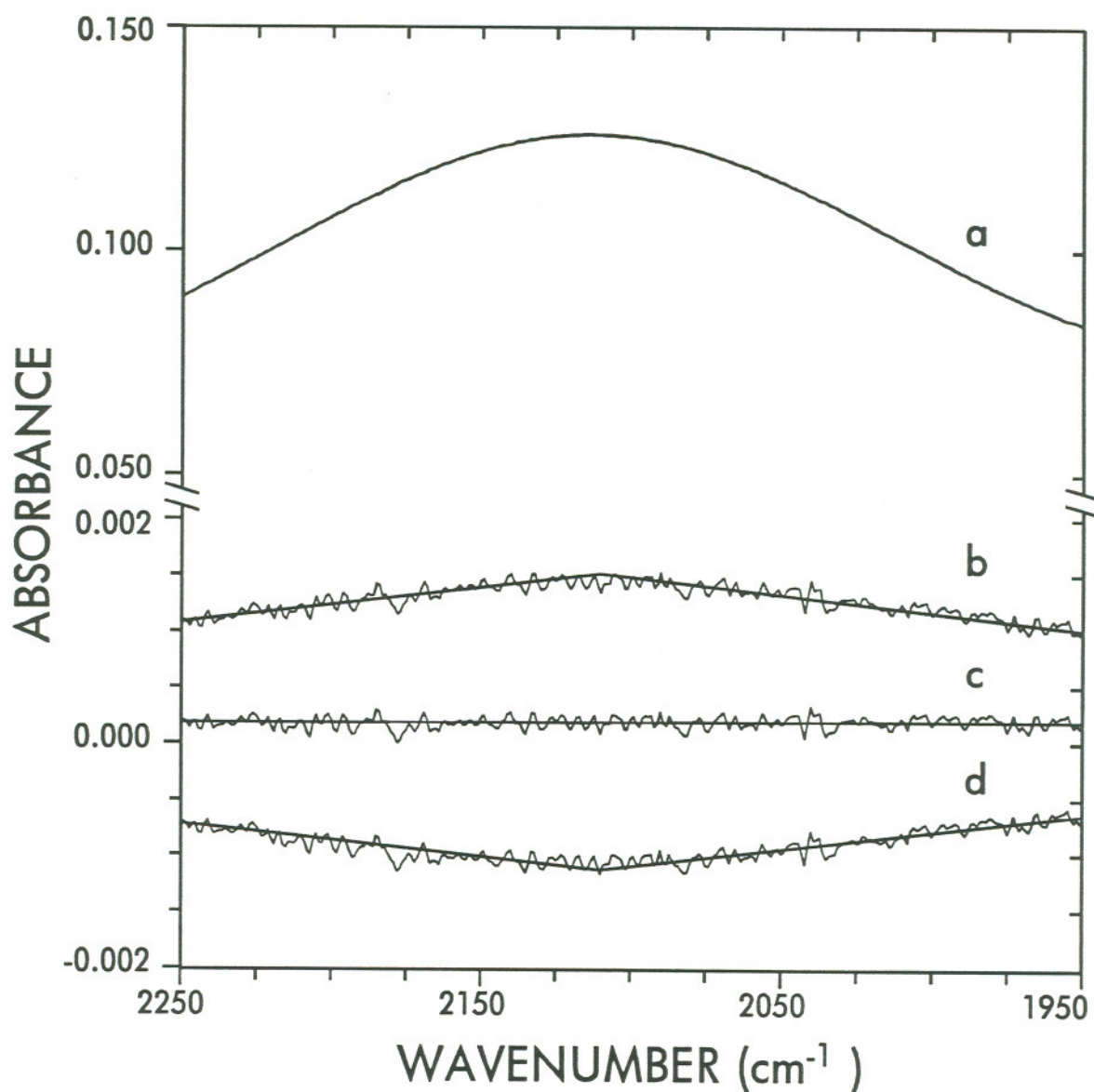


Figure 18. a) The infrared absorbance spectrum of water in the "fit region", 2250 - 1950 cm^{-1} . b) An undersubtracted difference spectrum and the best fit line segments in the fit region: -1% error in the factor "f" as described in the text. c) The difference spectrum and best fit line segments in the fit region: optimal factor. d) An oversubtracted difference spectrum and the best fit line segments in the fit region: +1% error in the factor "f".

The difference spectrum was expressed as

$$A_{Di} = A_{Si} - fA_{Wi} \quad (1)$$

where A_{Di} is the scaled absorbance of the difference spectrum at $i \text{ cm}^{-1}$, A_{Si} is the scaled absorbance of the humic solution spectrum at $i \text{ cm}^{-1}$, A_{Wi} is the scaled absorbance of the background water spectrum at $i \text{ cm}^{-1}$, and f is the difference factor. To calculate the best-fit linear baseline over the fit range, the sum of the square residuals was written for each line segment. For the left line segment, the expression is

$$\sum_{i=2120}^{2250} [A_{Si} - fA_{Wi} - A_{2110} - m(\frac{i}{1000} - 2.11)]^2 \quad (2)$$

where A_{2110} is the scaled absorbance at 2110 cm^{-1} and m is the slope. Equation (2) was differentiated with respect to m and set equal to zero. The resulting equation was solved for m in terms of f and A_{2110} to yield

$$m = \frac{\sum_{i=2120}^{2250} (A_{Si} - fA_{Wi} - A_{2110}) (\frac{i}{1000} - 2.11)}{\sum_{i=2120}^{2250} (\frac{i}{1000} - 2.11)^2} \quad (3)$$

An analogous equation was developed for the right line segment ($j = 1950$ to 2100) and solved for m . These two expressions were then equated (since the slopes must be equal) to yield an equation in f and A_{2110} which can be algebraically rearranged to obtain

$$C_1 f + C_2 A_{2110} + C_3 = 0 \quad (4)$$

where the constants C_1 , C_2 , and C_3 are given by

$$C_1 = \sum_{i=2120}^{2250} A_{Wi} \left(\frac{i}{1000} - 2.11\right) \sum_{j=1950}^{2100} \left(\frac{j}{1000} - 2.11\right)^2 - \sum_{j=1950}^{2100} A_{Wj} \left(\frac{j}{1000} - 2.11\right) \sum_{i=2120}^{2250} \left(\frac{i}{1000} - 2.11\right)^2$$

$$C_2 = \sum_{i=2120}^{2250} \left(\frac{i}{1000} - 2.11\right) \sum_{j=1950}^{2100} \left(\frac{j}{1000} - 2.11\right)^2 - \sum_{j=1950}^{2100} \left(\frac{j}{1000} - 2.11\right) \sum_{i=2120}^{2250} \left(\frac{i}{1000} - 2.11\right)^2$$

$$C_3 = \sum_{j=1950}^{2100} A_{Sj} \left(\frac{j}{1000} - 2.11\right) \sum_{i=2120}^{2250} \left(\frac{i}{1000} - 2.11\right)^2 - \sum_{i=2120}^{2250} A_{Si} \left(\frac{i}{1000} - 2.11\right) \sum_{j=1950}^{2100} \left(\frac{j}{1000} - 2.11\right)^2$$

A second equation was derived in the exact same manner, except that the partial derivatives were taken with respect to A_{2110} rather than m . After algebraic rearrangement, this equation is given by

$$D_1 f + D_2 A_{2110} + D_3 = 0 \quad (5)$$

where the constants D_1 , D_2 , and D_3 are given by

$$D_1 = \sum_{i=2120}^{2250} A_{Wi} \sum_{j=1950}^{2100} \left(\frac{j}{1000} - 2.11\right) - \sum_{j=1950}^{2100} A_{Wj} \sum_{i=2120}^{2250} \left(\frac{i}{1000} - 2.11\right)$$

$$D_2 = \sum_{i=2120}^{2250} 1 \sum_{j=1950}^{2100} \left(\frac{j}{1000} - 2.11\right) - \sum_{j=1950}^{2100} 1 \sum_{i=2120}^{2250} \left(\frac{i}{1000} - 2.11\right)$$

$$D_3 = \sum_{j=1950}^{2100} A_{Sj} \sum_{i=2120}^{2250} \left(\frac{i}{1000} - 2.11\right) - \sum_{i=2120}^{2250} A_{Si} \sum_{j=1950}^{2100} \left(\frac{j}{1000} - 2.11\right)$$

The value of f was calculated directly from the two simultaneous equations 4 and 5. Note that while the slopes of the left and right line segments must be equal to each other, equations 4 and 5 (obtained from different partial derivatives) do not generate the same slope.

Once the optimal factor was determined, a baseline correction was applied to the entire difference spectrum (4000-800 cm^{-1}). Examination of water-water difference spectra indicated that the baseline was curved. Unfortunately, the humic difference spectrum reaches the baseline only in the 4000-3800 cm^{-1} and 2250-1950 cm^{-1} regions, limiting the data used to fit the baseline correction to

these two regions. Because these baseline regions are relatively narrow and widely separated, they behave like two discrete points and, alone, do not provide sufficient information to determine curvature.

To determine the functionality of the baseline, single-beam 100% lines of the dry CIRCLE® cell were obtained by ratioing two single beam transmittance spectra to each other and converting the ratio spectrum to absorbance format. To accommodate for the typical range of instrument drift, the elapsed time between the acquisition of the single beam spectra varied from 30 minutes up to 9 hours. A number of functions, both linear and non-linear, were used to fit these 100% lines. Using a linear least-squares fitting routine and data from the entire 100% line (4000-800 cm^{-1}), several functions successfully fit the baseline. When only the limited spectral regions available in humic difference spectra were used to calculate the best fit, none of the functions performed well. Based upon further examination of the 100% lines, a third constraint was added to the baseline functions: the slope at 800 cm^{-1} must equal zero.

Using only the data in the 3800-4000 cm^{-1} and the 1950-2250 cm^{-1} regions, the new constrained functions were used to fit 30 different 100% lines. The function,

$$A_{Bi} = a(i - 40\sqrt{2i}) + b \quad (6)$$

was chosen as the best baseline approximation. A_{Bi} is the baseline absorbance at $i \text{ cm}^{-1}$ and a , and b are fitted constants. This function and the data in the 4000-3800 cm^{-1} and 2250-1950 cm^{-1} regions of the difference spectrum were used to approximate the baseline. The difference spectra were corrected by subtracting the baseline function. Each corrected difference spectrum was then normalized by a factor based upon the concentration of humic matter in the sample so that spectra of different humic solutions could be compared.

RESULTS AND DISCUSSION

Validation of the subtraction procedure

The excellent performance of the solvent subtraction method is shown by the flat and almost featureless baseline obtained when two water spectra are subtracted to yield a water-water difference spectrum (Figure 19a). The quality of the baseline is evident despite the extreme amplification of the absorbance scale. Good reproducibility is evidenced by the small magnitude of the standard deviation spectrum (Figure 19b). The 3400-3200 cm^{-1} region is associated with the noisiest signal and the greatest variability because of the very intense absorbance of water in this region. The $\sim 1640 \text{ cm}^{-1}$ water peak is evident in most water-water spectra, but its magnitude is small. Nonetheless, small changes in peak location or shape in aqueous difference spectra near 1640 cm^{-1} should be interpreted with caution because of the variability associated with subtracting the 1640 cm^{-1} water band.

The difference spectrum is dramatically affected by errors in the subtraction factor as small as $\pm 1\%$ (Figures 19c and 19d), even though such errors are barely detectable in the fit region (2250-1950 cm^{-1}). Not surprisingly, incorrect water-water difference spectra resemble a background water spectrum. Because the features produced by an incorrect water subtraction and those of the solute difference spectrum are of similar magnitude, a small error in the subtraction factor for a humic solution spectrum can result in a difference spectrum that is very misleading. Undersubtraction can result in spurious peaks or shoulders in the difference spectrum. The negative features associated with oversubtraction can decrease the intensity of an overlapping peak or split a single overlapping peak into two apparent peaks. Both errors can shift the apparent position and shape of an overlapping peak. In humic solution spectra, both major regions of interest (3600-2900 cm^{-1} : O-H, and 1800-1100 cm^{-1} : C=O and C-O) overlap regions that may contain interference from incorrect water subtraction. Consequently, a reliable method to determine the optimal difference factor is essential.

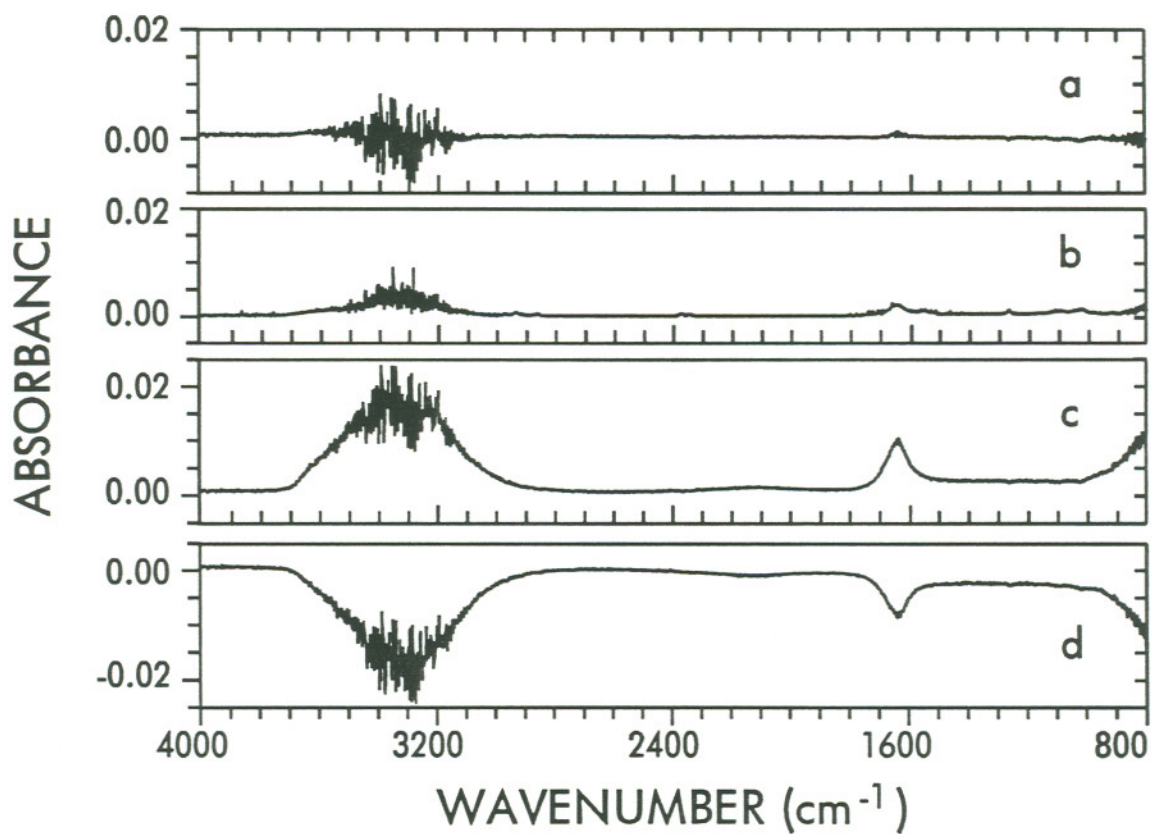


Figure 19. a) A representative water-water difference spectrum. b) The standard deviation of 6 water-water difference spectra. c) An undersubtracted water-water difference spectrum, -1% error in the factor, "f". d) An oversubtracted water-water difference spectrum, +1% error in the factor, "f".

The mean optimal subtraction factor for humic difference spectra ($\mu=0.992$) is significantly less ($\alpha=.01$) than the mean factor for water-water difference spectra ($\mu=1.007$). Although optimal factors differ from unity by only 1-2%, the assumption of a unit factor would lead to significant errors in the difference spectrum near 3400 cm^{-1} and 1640 cm^{-1} . The order in which spectra were collected had no effect on the subtraction factor with one exception. The value of the subtraction factor for the first water-water spectrum ($\mu=1.026$) is significantly greater ($\alpha=.01$) than the values of subsequent water-water spectra ($\mu=1.002$). This indicates that the first water spectrum exhibits slightly lower absorbance than the following spectra and may be due to incomplete wetting of the initially dry ZnSe crystal.

Reproducibility of spectra

The errors associated with solute difference spectra must be estimated if the difference spectra are to be compared. Three independent difference spectra were obtained on the same day for each of two humic solutions (pH 3.42 and pH 8.02). The presence of humic material does not significantly increase the variability in the difference spectrum at either pH as compared to water-water spectra (Figures 20 and 21). Interpretation of the spectral features in the $3600\text{-}2900\text{ cm}^{-1}$ region is limited by the error associated with water subtraction (up to 30% error). In contrast, the variability introduced by water subtraction is less than 4% of the difference spectrum signal between 1800 cm^{-1} and 1100 cm^{-1} . In this region difference spectra are reproducible enough for quantitative comparison.

Often it is desirable to compare spectra obtained from different sample series, recorded on different days. The FTIR instrument response might be different among such spectra, the CIRCLE® cell accessory position would likely not be identical, and the composition of the humic solution might be slightly different. To assess whether spectra are reproducible over time, the difference

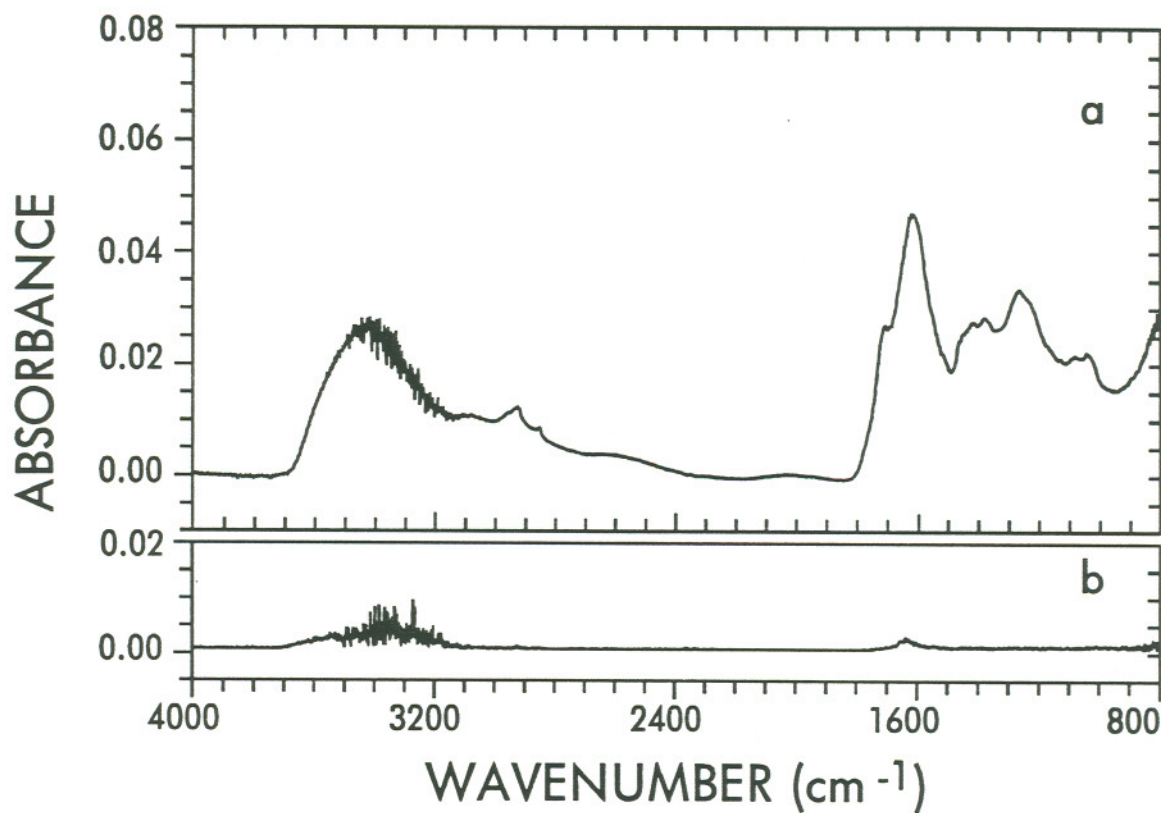


Figure 20. a) The mean of 3 lithium humate difference spectra obtained on the same day, pH 3.42. b) The standard deviation associated with the mean spectrum shown in a).

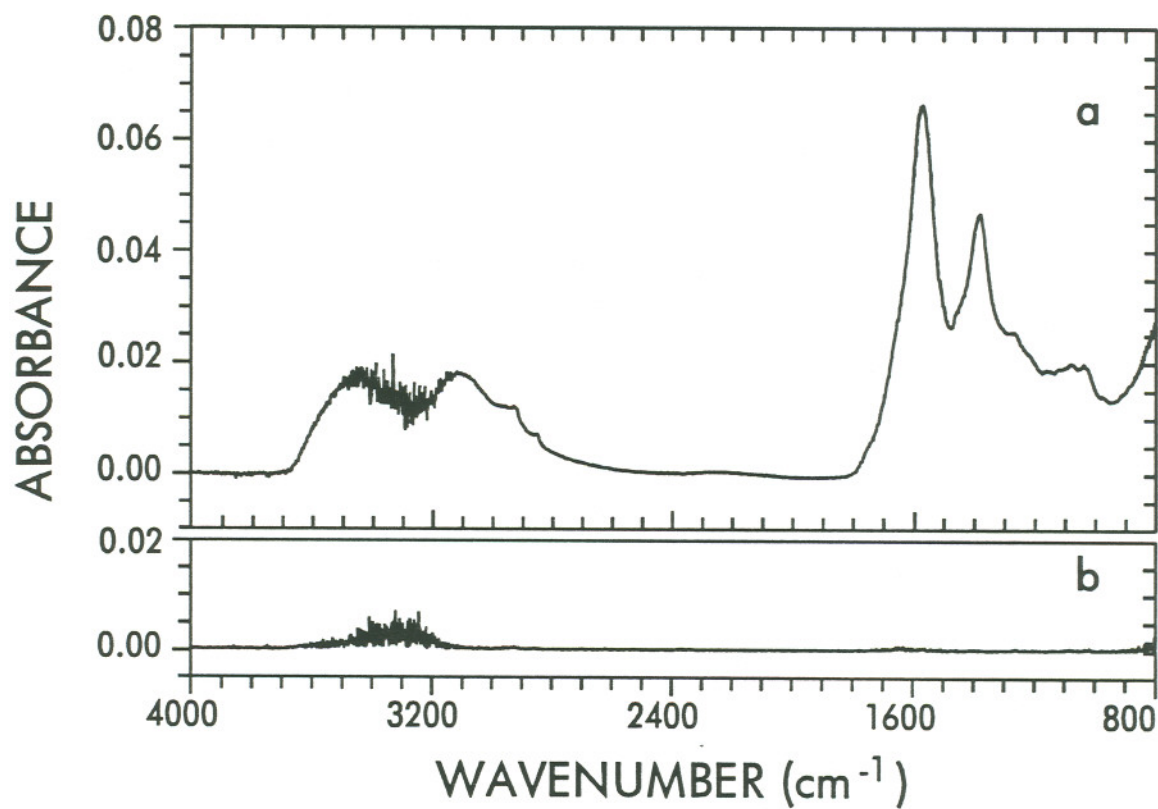


Figure 21. a) The mean of 3 lithium humate difference spectra obtained on the same day, pH 8.02. b) The standard deviation associated with the mean spectrum shown in a).

spectra of two different humic solutions (pH 3.91 and pH 3.92) collected 24 days apart were compared (Figure 22). During the time between the acquisition of these spectra, the CIRCLE® cell was dismantled, cleaned, reassembled, and realigned in the FTIR instrument. The two difference spectra are almost identical. Other comparable pairs of humic samples exhibited similar results at other pH values. Although the **difference spectra** are reproducible, the **unsubtracted solution spectra** are not. Using the water background spectrum obtained immediately prior to the solution spectrum effectively removes the variability associated with the instrument, the ambient environment and the sampling accessory.

Effects of electrolytes on background spectra

Changes in the pH of aqueous, humic-free salt solutions had no observable effect on the difference spectra over the range of pH used in this study (pH 3-10). In addition there was no interactive effect between the pH and the salt concentration. The spectra of dilute salt solutions (0.02 M) were indistinguishable from water spectra. The difference spectra of more concentrated NaCl and KCl solutions (0.1 M, pH 8), however, exhibit artifacts associated with wavenumber shifts (Figure 23). The effect is particularly pronounced in the 3500-2900 cm^{-1} region. The sinusoidal peak-trough pattern (characteristic of a wavenumber shift) observed in the NaCl and KCl difference spectra is absent from difference spectrum of 0.1 M LiCl. The spectrum of 0.1 M LiCl closely resembled water, although some increase in absorbance at $\sim 3400 \text{ cm}^{-1}$ was evident in the difference spectrum. At a higher concentration LiCl spectra may exhibit features similar to NaCl and KCl.

Changes in the extent of hydrogen bonding within the bulk solvent is the likely source of this apparent wavenumber shift. Hydrogen bonding between neighboring water molecules causes the frequency associated with O-H stretching (~ 3400 band) to decrease by effectively lowering the potential as the

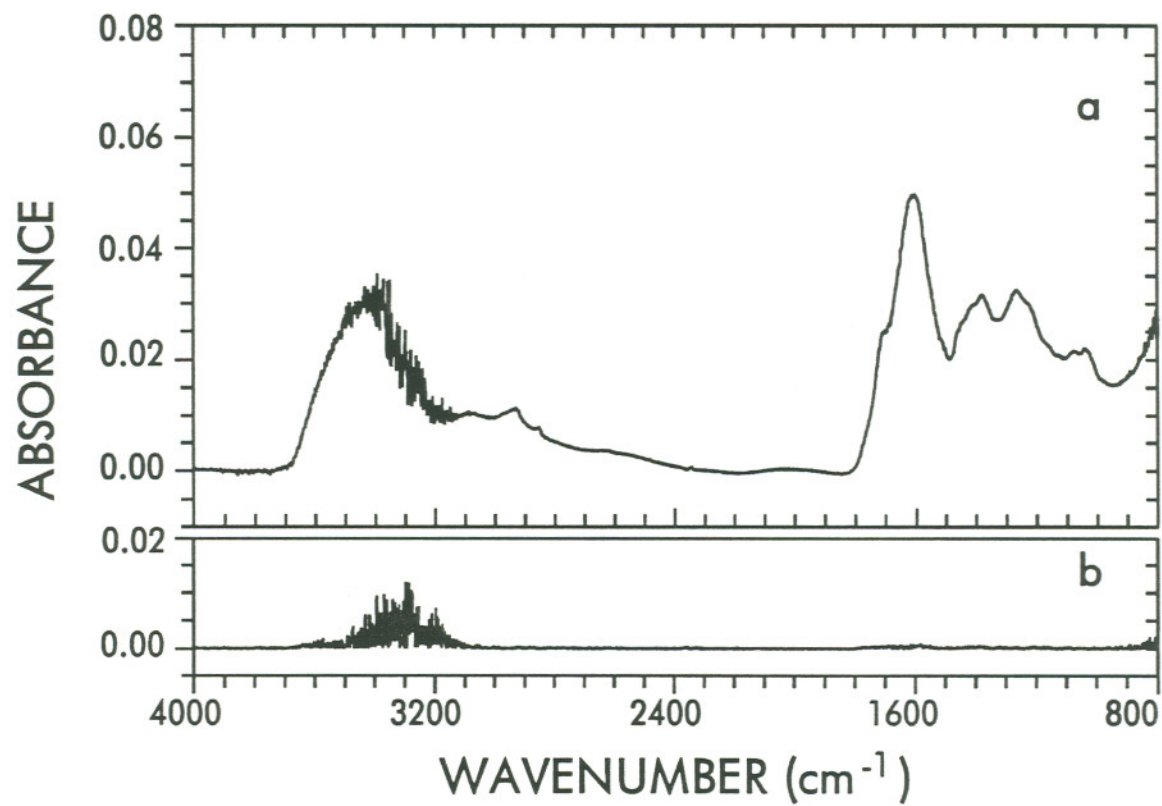


Figure 22. a) The mean of 2 lithium humate difference spectra prepared and recorded 24 days apart day, pH 3.91. b) The standard deviation associated with the mean spectrum shown in a).

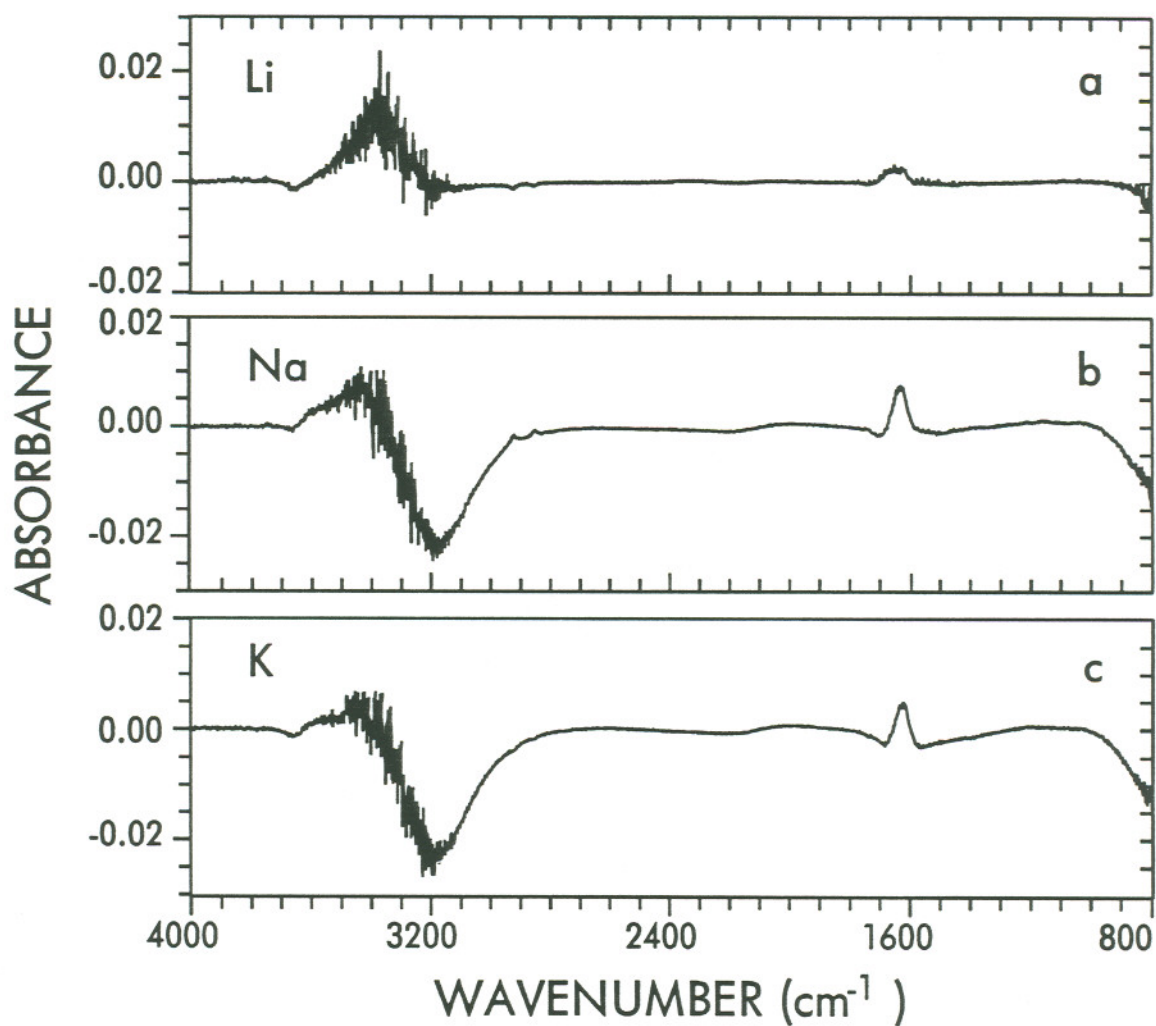


Figure 23. a) The difference spectrum between a 0.1 M solution of LiCl and a water background. b) The difference spectrum between a 0.1 M solution of NaCl and a water background. c) The difference spectrum between a 0.1 M solution of KCl and a water background.

H atom is displaced toward the hydrogen-bonded O atom. The frequency associated with the H-O-H bending mode (1640 cm^{-1}) increases due to hydrogen bonding because the H atom is now transversely interacting with two O atoms rather than one. Hydrogen bonding broadens both bands. The presence of cations and anions effectively decreases the extent of hydrogen bonding in the bulk solvent (CONWAY, 1981). Consequently the $\sim 3400\text{ cm}^{-1}$ band is shifted to a slightly higher frequency, while the 1640 cm^{-1} band shifts to a lower frequency. These frequency shifts are consistent with the appearance of the difference spectra in Figure 23. The $\sim 1640\text{ cm}^{-1}$ regions of these difference spectra also exhibit a pattern consistent with band narrowing in the salt solution spectra. The extent of these effects depends upon the identity of the cation and anion and their concentration. For alkali metal and alkaline earth cations, the ability to disrupt the structure of water in this manner increases in order of molecular weight ($\text{Li}^+ < \text{Na}^+ < \text{K}^+ < \text{Rb}^+$ and $\text{Mg}^{2+} < \text{Ca}^{2+} < \text{Sr}^{2+} < \text{Ba}^{2+}$). Unfortunately, no simple function has been found that describes the relationship between ion concentration and frequency shift.

The artifacts due to electrolyte effects are evident in humic difference spectra (Figure 24). Although it may be possible to eliminate these artifacts by using a salt solution for the background spectrum, choosing the correct salt concentration is not straightforward. The total salt concentration of the humic solution is known, but the degree of humic-cation association may not be known. Such association decreases the bulk solution salt concentration (recall Chapter III). Furthermore, the bulk solution concentration may not match the concentration of the solution immediately surrounding the humic moiety or the ZnSe crystal. Several solutions of varying salt concentration could be prepared and used as trial background spectra. The "best" background spectrum could then be chosen based upon selected characteristics of spectral subtraction. Rather than use such a trial-and-error approach, we chose to use water for all background spectra. The majority of humic samples were prepared using LiOH

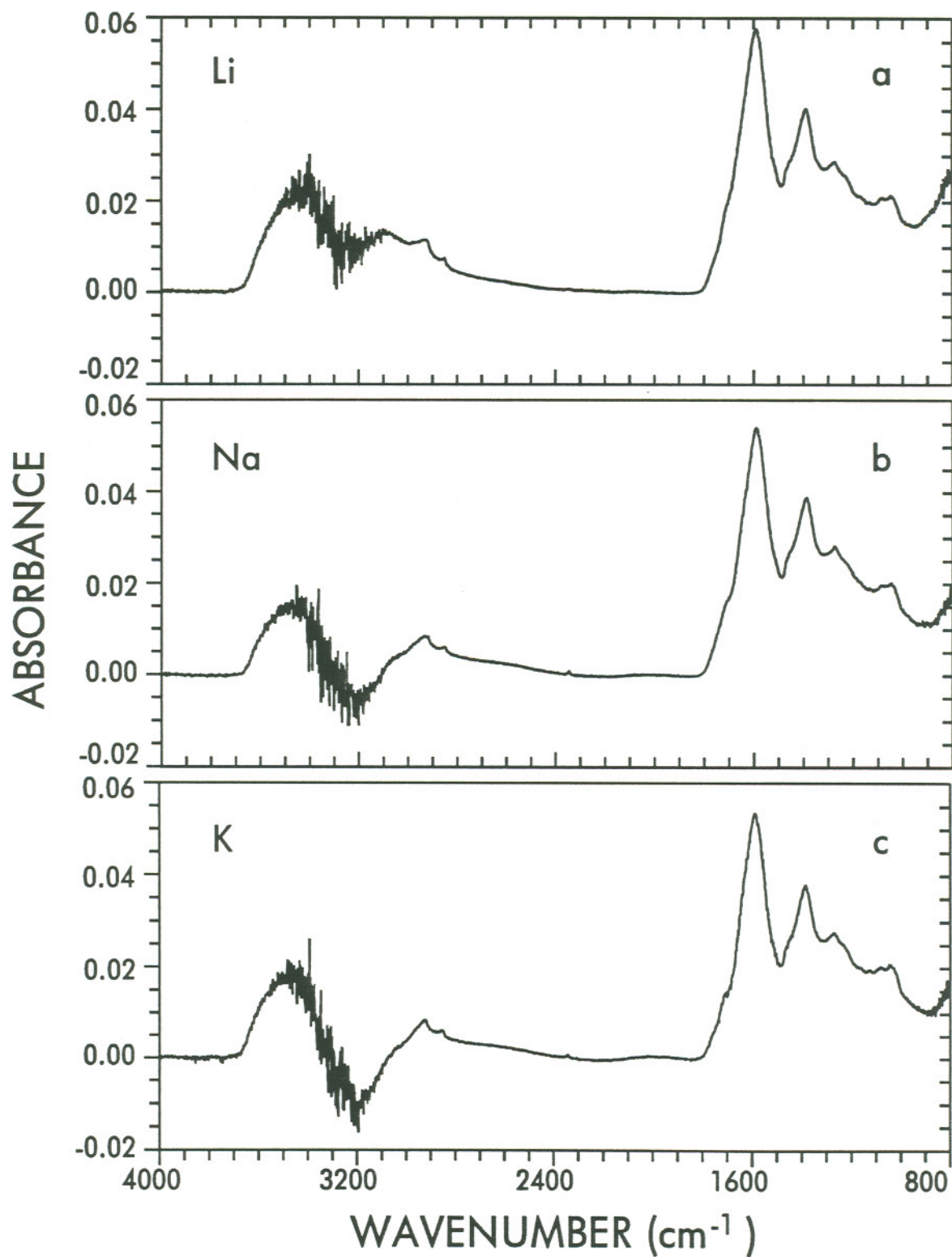


Figure 24. a) A Li-humate difference spectrum, pH 5.35. b) A Na-humate difference spectrum, pH 5.37. c) A K-humate difference spectrum, pH 5.45.

because Li-humate spectra are less subject to errors due to salt concentration. When Na-humate and K-humate solutions were analyzed, the difference spectra must be interpreted so that potential artifacts are taken into account.

CONCLUSIONS

We have described strategies using CIR-FTIR to acquire aqueous difference spectra of humic matter and evaluate the quality and reliability of those spectra. The CIR-FTIR technique is uncomplicated and facilitates the study of aqueous solutions. The following procedures are suggested to assist in obtaining reliable aqueous difference spectra with the CIR-FTIR method.

1) The solution and the background spectrum should be recorded under the most similar conditions possible. In particular, the CIR sampling accessory must not be moved between recording solution/background spectra pairs.

2) A routine cleaning procedure should be established for preventing contamination of the CIR crystal. The specific procedure depends upon the properties of the solute and CIR crystal. The condition of the CIR crystal should be evaluated daily.

3) An objective, reproducible method must be used to subtract the solvent spectrum from the solution spectrum. The method should minimize the potential for over- or under-subtraction of the solvent so that solvent features are completely removed from the solution spectrum. A program to perform aqueous solvent subtraction and baseline correction was described in this paper. This program uses elimination of the combination water band at $\sim 2120\text{ cm}^{-1}$ as the criterion for adequate solvent subtraction.

4) The assumption that the solvent spectrum is invariant with respect to the presence of solutes should be verified. If the spectrum of pure water is used as the background spectrum, artifacts due to the electrolyte concentration may occur. These artifacts must be considered when interpreting the difference

spectra. For aqueous humic solutions, artifacts arising from electrolyte effects can be minimized by using Li^+ salts rather than Na^+ or K^+ salts.

We have found the CIR-FTIR aqueous difference spectra of humic matter to be reproducible, allowing the reliable comparison of spectra obtained on different days. The variation in absorbance in the $1700\text{-}1500\text{ cm}^{-1}$ region is low enough to allow quantitative measurements. Caution, however, is advisable when interpreting these spectra. The $3600\text{-}2900\text{ cm}^{-1}$ region is associated with significant error and the potential for severe artifacts. Small shifts in difference spectrum peaks near the $\sim 1640\text{ cm}^{-1}$ water band also should be regarded with skepticism until the researcher determines that the effect is not due to errors in the subtraction of the solvent spectrum. With these caveats in mind, we believe that CIR-FTIR is a valuable technique for investigating the reactions and structure of many environmentally relevant materials in their natural hydrated state.

REFERENCES

- ANTOON M.K., D'ESPOSITO L. and KOENIG J.L. (1979) Factor analysis applied to Fourier transform infrared spectra. *Appl. Spec.* **33**, 351-357.
- BONN B.A. and FISH W. (1991) The variable nature of humic carboxyl content measurements *Environ. Sci. Technol.* **25**, 232-240.
- BRAUE E.H., JR., and PANELLA M.G. (1987) Imprecision in Circle cell FT-IR analysis of aqueous solutions. *Appl. Spec.* **41**, 1213-1216.
- CONWAY B.E. (1981) *Ionic Hydration in Chemistry and Biophysics* Elsevier, Chap. 7 pp. 113-137.
- DOUSSEAU F., THERRIEN M. and PÉZOLET M. (1989) On the spectral subtraction of water from the FT-IR spectra of aqueous solutions of proteins. *Appl. Spec.* **43**, 538-542.
- GILLETTE P.C. and KOENIG J.L. (1984) Objective criteria for absorbance subtraction. *Appl. Spec.* **38**, 334-337.

- GRIFFITHS P.R. and DEHASETH J.A. (1986) *Fourier Transform Infrared Spectroscopy*. Wiley-Interscience.
- HARRICK N.J. (1987) *Internal Reflection Spectroscopy*. Harrick Scientific.
- HIRSCHFELD T. (1976) Instrumental requirements for absorbance subtraction. *Appl. Spec.* **30**, 550-551.
- LEENHEER J.A. and NOYES T.I. (1989) Derivatization of humic substances for structural studies. In *Humic Substances II* (eds. M.H.B.HAYES, P.MACCARTHY, R.L.MALCOLM, and R.S.SWIFT), Chap.9, pp 257-280. Wiley.
- MACCARTHY P. and MARK H.B.JR. (1975) Infrared studies on humic acid in deuterium oxide. I. Evaluation and potentialities of the technique. *Soil Sci. Soc. Am. Proc.* **39**, 666-668.
- MACCARTHY P., MARK H.B.JR., and GRIFFITHS P.R. (1975) Direct measurement of the infrared spectra of humic substances in water by Fourier transform infrared spectroscopy. *J. Agric. Food Chem.* **23**, 600-602.
- MACCARTHY P. and RICE J.A. (1985) Spectroscopic methods (other than NMR) for determining functionality in humic substances. In *Humic Substances in Soil, Sediment, and Water* (eds. G.R.AIKEN, D.M.McKNIGHT, R.L.WERSHAW, and P.MACCARTHY), Chap.21, pp.527-559. Wiley-Interscience.
- MIELCZARSKI J.A., DEŃCA A., and STROJEK J.W. (1986) Application of attenuated total reflection infrared spectroscopy to the characterization of coal. *Appl. Spec.* **40**, 998-1004.
- PERKINS, P. Perkin-Elmer, San Jose, CA, (1991).
- PERKINS W.D. (1987) Fourier transform infrared spectroscopy. Part III. Applications. *J. Chem. Ed.* **64**, A296-A305.
- POWELL J.R., WASZ F.M. and JAKOBSEN R.J. (1986) An algorithm for the reproducible spectral subtraction of water from the FT-IR spectra of proteins in dilute solutions and adsorbed monolayers. *Appl. Spec.* **40**, 339-344.
- SPERLINE R.P., MURALIDHARAN S. and FREISER H. (1986) New quantitative technique for attenuated total reflection (ATR) spectrophotometry; Calibration of the "CIRCLE" ATR device in the infrared. *Appl. Spec.* **40**, 1019-1022.

STEVENSON F.J. (1985) Geochemistry of soil humic substances. In *Humic Substances in Soil, Sediment, and Water* (eds. G.R.AIKEN, D.M.McKNIGHT, R.L.WERSHAW, and P.MacCARTHY), Chap.2, pp.13-52. Wiley-Interscience.

STRAND, S. Spectra-Tech, Stamford, CT, (1991).

TEJEDOR-TEJEDOR M.I., YOST E.C. and ANDERSON M.A. (1990) Characterization of benzoic and phenolic complexes at the goethite-aqueous solution interface using cylindrical internal reflection Fourier transform infrared spectroscopy. Part 1. Methodology. *Langmuir* 6, 979-987.

TEJEDOR-TEJEDOR M.I. and ANDERSON M.A. (1986) "In Situ" attenuated total reflection fourier transform infrared studies of the goethite (α -FeOOH)-aqueous solution interface. *Langmuir* 2, 203-210.

CHAPTER V

Aqueous CIR-FTIR of Humic Acid II. Effects of pH, alkali metal cations, and alkaline earth cations

ABSTRACT

Cylindrical internal reflectance (CIR) Fourier transform infrared spectroscopy (FTIR) was used to obtain the spectra of aqueous humic solutions (pH 3 - 10) containing alkali metal cations or alkaline earth cations. Spectral subtraction was used to remove the peaks due to water. The spectral changes associated with the ionization of COOH were clearly observed, but overlap with other nearby peaks prevented the direct quantitation of COOH and COO⁻ concentrations. Second derivative spectra and curve-fitting methods were employed to improve peak resolution and quantitate highly overlapping peaks. Alkali-metal-humate mixtures of similar pH exhibited almost identical spectra, regardless of the cation identity or concentration. The spectra of humic solutions containing low concentrations of alkaline earth cations resembled alkali-metal-humate spectra. Unbound alkaline earth cations alter the spectrum of water, thereby creating artifacts the humic spectra which are indicators of cation binding. The extent of association of alkaline earth cations with humic material followed the order Ba²⁺ > Ca²⁺ > Mg²⁺. High concentrations of alkaline

earth cations caused a sharp decrease in the infrared spectrum intensity and a dramatic increase in the solution viscosity. The magnitude these sharp changes paralleled the apparent extent of cation binding: $Ba^{2+} > Ca^{2+} > Mg^{2+}$. The physical changes in the solutions were suggestive of humic conformational changes induced by the binding of divalent cations. No evidence of coordinative binding (peak shifts, changes in relative peak intensity) between either alkali metal cations or alkaline earth cations and humic material were observable via CIR-FTIR.

INTRODUCTION

The importance of humic substances in the biogeochemical cycling of cations in both aquatic and terrestrial environments is well known. Mathematical models have been formulated to describe the geochemically relevant acid-base chemistry and metal complexing reactions of humic substances. These empirical models are useful and often correctly represent the macroscopic effects of humic reactions, such as solution pH or free cation concentration. All mathematical models, however, are based upon assumptions concerning the precise chemical model of the reactions. A variety of chemical models have been proposed, ranging from a small set of discrete ligands (FISH, *et al.*, 1986), to a complex mixture of functional groups characterized as a continuum of ion-binding energies (PERDUE, *et al.*, 1984). In order to better delineate the actual chemical mechanisms of these reactions, the humic molecule must be probed at a molecular level. Infrared analysis is a particularly attractive method because it provides information concerning the most influential functional groups in humic matter.

Infrared spectra of humic substances exhibit a few broad, smeared features and lack the typical sharp peaks associated with the spectra of pure compounds. However, the spectral features include bands attributed to hydroxyl and carboxyl groups, aliphatic H, aromatic ring structures, and in some

cases amides and polysaccharides. By comparing the general shapes and intensities of these features researchers have characterized organic matter from different origins and described the changes that occur as a soil evolves or is subjected to different treatments (SENESI, *et al.*, 1989; BOYD, *et al.*, 1980; YONEBAYASHI and HATTORI, 1989). STEVENSON and GOH (1971) characterized three types of humic spectra: humic acids (I), fulvic acids (II) and humic acids with high nitrogen content (III).

Infrared spectroscopy yields information about the acid-base behavior of carboxyl groups. As the pH increases and the carboxyl groups ionize, the peak associated with the C=O bond of the COOH group gradually decreases with a concomitant increase in peaks due to COO⁻ stretching (BELLAMY, 1975). Humic spectra exhibit these characteristic pH-dependent changes. PAXÉUS and WEDBORG (1985) monitored changes in the COOH and COO⁻ peaks to determine a titration endpoint from which the carboxyl content of a fulvic acid was estimated. Several researchers have obtained good correlations between the carboxyl content (determined by wet chemical methods) and the size of the COOH spectral peak (IBARRA, 1989; THENG and POSNER, 1967). Recently, CABANISS (1992) used the relative peaks areas of COOH and COO⁻ peaks with potentiometric data to estimate carboxyl content. Although these empirical relationships are promising, they are complicated by the presence of overlapping spectral peaks. In addition, the extinction coefficients for humic COOH and COO⁻ groups have yet to be determined.

Infrared studies of metal-complexation by humic substances have also been reported, but most have been limited to demonstrating the importance of carboxyl groups in humic-Cu²⁺ and humic-Fe³⁺ complexation (BOYD, *et al.*, 1981; MACCARTHY, *et al.*, 1975; BYLER, *et al.*, 1987; SENESI, *et al.*, 1986). SENESI, *et al.*, (1981) used infrared spectra to show the reversibility of Cu²⁺ complexation. The separation of the asymmetric and symmetric carboxylate peaks is an indicator of the mode by which cations are complexed by the carboxylate group: unidentate,

bidentate or bridging. By comparing the frequency separation observed for Cu^{2+} -humate and Fe^{3+} -humate samples to that for simple organic salts, BOYD, *et al.* (1981) speculated that the humic complexes of Cu^{2+} and Fe^{3+} were unidentate. They did not, however, measure the frequency separation for humate solutions containing cations such as Li^+ or Na^+ for which strong complexation is not expected. Accurate measurement of peak separation is hampered by the poor resolution associated with all humic spectra.

Almost all infrared studies of humic matter have been performed using KBr pellets, which are associated with sampling artifacts and spectra of questionable reproducibility. Pellets must be extremely dry to avoid interference due to adsorbed moisture. STEVENSON and GOH (1974) suggest that in many spectra the broad band at 3400 cm^{-1} , that is usually attributed to the humic O-H group, might be mostly due to moisture. KBr-humic pellets can be heated to eliminate moisture, but prolonged heating causes the formation of acid anhydrides. In addition, thorough dehydration of organic matter alters its degree of dissociation (MACCARTHY and MARK, 1975). Interactions between the humic material and the salt matrix in the KBr pellet has also been suggested to cause interferences (BAES and BLOOM, 1989). Preparation of quantitatively reproducible KBr pellets may not be possible (PRICE, 1972). The degree of grinding affects the appearance of the spectrum and the optimal grinding time varies with the method and apparatus used (PAINTER, *et al.*, 1981). Quantitative comparisons among spectra obtained from KBr pellets, especially the calculation of difference spectra, are difficult or impossible. The problems associated with KBr pellets can be partially avoided by using diffuse reflectance spectroscopy and dry samples which are simply mixed with a salt matrix (BAES and BLOOM, 1989). This method, however, does not address the inherently unnatural state of dry humic material.

Only a few infrared spectroscopy studies have been performed with humic matter in its natural aqueous state. The water background absorbs

intensely in the same spectra regions as the oxygen-containing humic functional groups ($3500\text{-}2900\text{ cm}^{-1}$ and $1700\text{-}1600\text{ cm}^{-1}$). Two approaches to this problem were investigated by MACCARTHY and co-workers. MACCARTHY and MARK (1975) obtained the infrared spectra of humic matter in D_2O at both acidic and basic pH. In D_2O , the major solvent peaks are shifted and no longer obscure some of the humic functional groups. MACCARTHY and MARK noted that these spectra suggested that the humic carboxyl groups are partially dissociated at ambient pH. Such dissociation is suppressed in dry KBr pellets. The primary drawback to this method was the difficulty of eliminating ambient H_2O from the samples. Exchange of ^2H for ^1H was rapid in humic matter, and the contamination of D_2O with H_2O resulted in extra peaks due to HOD. In addition to their work in D_2O solution, MACCARTHY, *et al.* (1975) described the use of transmission cells with thin spacers to obtain aqueous (H_2O) humic spectra. A matched water background spectrum was digitally subtracted from the solution spectrum to eliminate interference from the very strong water bands. Infrared spectra of aqueous Cu^{2+} -humic solutions demonstrated the participation of carboxyl groups in Cu^{2+} complexation. The filling and cleaning of very thin transmission cells, however, was difficult with humic solutions or slurries. A demountable transmission cell rather than a sealed cell greatly facilitated cleaning, but the background subtraction technique was much less reliable when demountable cells were used.

In Chapter IV, a method was described for obtaining aqueous humic spectra using a circular internal reflectance accessory and a Fourier Transform infrared spectrometer (CIR-FTIR). CIR-FTIR techniques were also recently employed by CABANNIS (1992) to record the infrared spectra of a fulvic acid at several different pH values. CIR-FTIR is advantageous because path lengths are very short and reproducible, facilitating the reliable subtraction of the water background. In addition, no special sample preparation is required, and filling and cleaning the accessory are not difficult. Although the CIR-FTIR technique

is not complicated, care must be exercised to minimize artifacts due to incomplete background subtraction.

The broad peaks characteristic of humic infrared spectra are due to the overlap of many spectral features, each representing a functional group in the humic mixture. The assignment of one specific functional group vibration to a broad peak is flawed, and neglects the inherent nature of humic matter: humic material is a mixture containing many functional groups in a variety of chemical environments. Meaningful analysis of humic spectra requires the resolution of overlapping peaks so that the contributions of different functional groups can be separated. One method of resolution enhancement involves the use of the second derivative of the absorbance spectrum (MADDAMS, 1980). The second derivative function preserves the location of peak centers, while significantly reducing the half-widths of Lorentzian or Gaussian shaped peaks (Figure 25). By narrowing the half-width, peaks which overlap in the absorbance spectrum can be resolved in the second derivative curve. The resolving power of the second derivative is influenced by the relative broadness and intensity of the overlapping peaks. In general, peaks that are separated by at least 50% of their half-widths will be resolved by the second derivative. In addition to the major negative lobe, which corresponds to the spectral peak, the second derivative also exhibits two smaller positive lobes (Figure 25). The intensity of these positive lobes is 0.25 of the negative primary lobe for a Lorentzian shaped band and about 0.45 for a Gaussian shaped band. When the spectrum is a composite of many overlapping peaks, the positive lobe of one peak can coincide with the negative lobe of a neighboring peak, resulting in partial or complete cancellation and distortion of the second derivative. Consequently, the intensity of a second derivative minimum is an uninterpretable datum for complex, highly overlapping spectra. Because the broad features of humic infrared spectra probably contain several overlapping bands, the second derivative data should not be used quantitatively. Higher-order derivatives can also be used

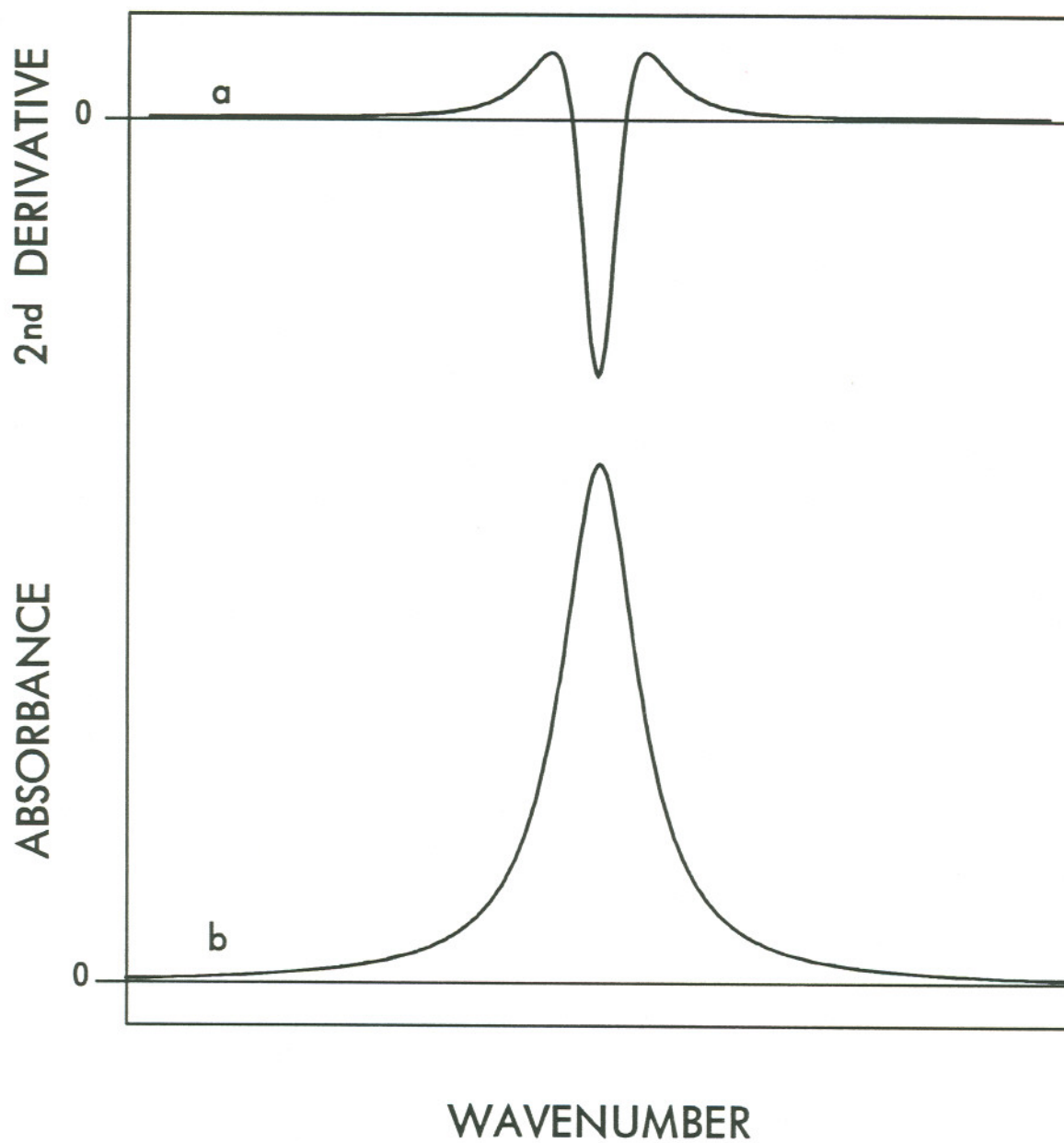


Figure 25. a) The second derivative spectrum of the Lorentzian shaped peak shown immediately below in b). b) A Lorentzian shaped peak.

diagnostically. The resolving power is successively greater for each higher even-order derivative, however, the noise approximately doubles with each derivative taken. This trade-off between increased noise and enhanced resolution effectively negates the utility of derivatives higher than fourth order.

The diagnostic ability of the second derivative has seldom been applied to humic spectra (BYLER, *et al.*, 1987; IBARRA, 1989). IBARRA (1989) used the second derivative to demonstrate that the absorbance at 1710 cm^{-1} , attributed to the C=O of the carboxyl group, was not entirely eliminated by reaction with barium acetate. Resolution enhancement and curve-fitting techniques have been more extensively used in the analysis of coal spectra which, like humic spectra, exhibit broad, composite peaks. Analysis of the second derivative of broad coal absorbance bands was used by PAINTER, *et al.* (1981) to obtain estimates for the number of overlapping peaks, their centers, and approximate half-widths. These estimates were then used as input parameters for curve-fitting routines. A similar approach was employed to quantitatively estimate the COOH content of coal samples (STARSINIC, *et al.*, 1984).

In this paper we will describe the changes in aqueous infrared spectra that occur over a range of pH values and in the presence of alkali metal and alkaline earth cations. Resolution enhancement using second derivative spectra will be used to demonstrate the complexity of seemingly simple humic spectra and the problems associated with interpreting these spectra. Both derivative and difference spectra indicate that the potential of infrared techniques for the quantitative examination of humic functional groups is limited.

EXPERIMENTAL

Humic acid

All spectra were obtained using samples of the same soil humic acid. The origin and isolation of this material has been described by BONN and FISH (1991).

The total acidity of the material as measured by the barium acetate method was 7.3 ± 0.4 meq/g. Ash content was 1% (by weight) and the elemental composition (Huffman Laboratories, Golden, CO) was 58% C, 4% H, 35% O, 3% N. The freeze-dried humic acid was stored in a desiccator.

Three types of humic solutions were prepared for infrared analysis: 1) variable acidity and constant total alkali metal cation concentration, 2) constant acidity, constant total Li^+ concentration, and variable total alkaline earth cation concentration, and 3) variable acidity, constant total Li^+ concentration, and constant total alkaline earth cation concentration. Sample series were prepared for each solution type. For the first series, humic acid was dissolved in aqueous standardized base (LiOH , NaOH or KOH ; $4.7 \pm 8\%$ meq base/g humic acid) and allowed to equilibrate for 4 hr. Varying amounts of standardized HCl were used to acidify 2 mL aliquots of the dissolved humate and the samples were shaken overnight. Sample pH was typically between 3 and 10. Only LiOH was used for the second sample series, and the dissolved Li-humate was not divided into aliquots before acidification. Rather, enough HCl was added to the entire sample so that the pH was approximately 6.6. This solution was then divided into aliquots and varying amounts of alkaline earth cations were added (0.4 to 2.5 mmol/g humic matter). One aliquot was retained as a control. The third series was prepared in manner similar to the first series, except that only aqueous LiOH was used in the initial dissolution step. The acidified aliquots were equilibrated for 1 hr after which each aliquot was divided and one portion retained as a control. An aqueous solution of alkaline earth metal (MgCl_2 , CaCl_2 or BaCl_2) was added to the remaining portion and all samples were mixed overnight. The average alkaline earth metal concentration was 2.2 mmol/g humic acid. For each cation of interest, every sample series was independently prepared and analyzed at least twice. The average concentration of humic matter was 40 mg/mL. All procedures were performed under N_2 . Nitrogen-purged ultra-pure water (Nanopure System, Barnstead) and ACS

Reagent Grade chemicals were used for all reagent solutions. A pH meter (EA 920, Orion, Boston, MA) equipped with a micro-combination electrode (MI-410, Microelectrodes, Inc., Londonderry, NH) was used to measure pH.

Spectroscopy

Reflectance spectra were obtained using a cylindrical internal reflection (CIR) accessory, the micro CIRCLE® cell (Spectra-Tech, Stamford, CT). The spectra were recorded by a Perkin-Elmer 1800 Fourier Transform Infrared Spectrometer equipped with a globar source, a KBr beamsplitter, and a CsI TGS detector. Two-hundred interferograms were coadded and convolved with a weak Beer-Norton apodization function to yield a final spectrum with a resolution of 2 cm^{-1} . The protocol used to obtain spectra that allowed successful background subtraction is described in Chapter IV.

Viscometry

Measurements of the viscosity of Ba^{2+} -humate solutions were performed using a Cannon-Fenske opaque viscometer (size 50, International Research Glassware, N.J.). The solutions were prepared in the same manner as the type 2 series for infrared analysis, except a much lower humic concentration was used (5 mg/mL). The concentrations of Li^+ and Ba^{2+} relative to the humic concentration were 4.5 and 0.0-6.0 mmol/g humic matter, respectively.

MATHEMATICAL DATA TREATMENT

Aqueous humic spectra

Aqueous humic spectra were obtained by digitally subtracting background water spectra from the humic solution spectra. The optimal subtraction factor was based upon the elimination of the $\sim 2120\text{ cm}^{-1}$ water band and determined using statistical criteria. The spectra were baseline corrected and normalized to the same humic concentration. The subtraction procedure is described in detail

in Chapter IV. In this paper, *aqueous humic spectrum* will refer to a spectrum obtained after water background subtraction, baseline correction and normalization have been applied.

Difference spectra

The differences between two spectra can be examined by calculating their difference spectrum. Difference spectra are particularly useful for distinguishing between peak broadening and the emergence of an additional peak. In this study, all difference spectra derived from two aqueous humic spectra were calculated using a subtraction factor of unity.

Derivative spectra

Second derivatives of the aqueous humic spectra were calculated using the formula $A''_i = A_{i+1} - 2A_i + A_{i-1}$, where A''_i and A_i are the second derivative value and the absorbance, respectively, at wavenumber i (SUSI and BYLER, 1983). The data points were spaced at whole number increments of wavenumber. Binomial smoothing was applied to the calculated second derivative to minimize the effects of noise (MARCHAND and MARMET, 1983).

Curve fitting

Synthetic spectra were created by fitting aqueous humic spectra with sums of individual idealized peaks (PAINTER, *et al.*, 1981, PIERCE, *et al.*, 1990). Each idealized peak was represented by a linear combination of Gaussian and Lorentzian functions given by

$$A = \alpha A_o \exp \left[-\ln 2 \left[\frac{2(X-X_o)}{\Delta X_{1/2}} \right]^2 \right] + \frac{(1-\alpha)A_o}{1 + [2(X-X_o)/\Delta X_{1/2}]^2}$$

where A is the absorbance at $X \text{ cm}^{-1}$, X_o is the peak center wavenumber, A_o is the maximum absorbance, $\Delta X_{1/2}$ is the width at half height, and α is the

Gaussian fraction. The number of peaks, as well as the peak positions, were fixed at values chosen by examining the second derivative spectra. All reproducible second derivative peaks were used regardless of their magnitude. A flat baseline was assumed and calculated as the mean absorbance in the range 1850-1825 cm^{-1} . Neither peak width nor peak shape can be reliably determined from the second derivative spectra and both must therefore be fitted. Non-linear least squares minimization (Gauss-Newton method) was used to calculate the optimal values of the parameters. The program, written in BASIC, was adapted from that given by FRASER and SUZUKI (1973).

Unfortunately, peak width, Gaussian fraction (α), and maximum absorbance do not act independently for highly overlapped spectra, and all values cannot be simultaneously fitted. We found that the value of α must be fixed for reliable convergence. The values of absorbance and peak width also interact, which causes the calculated parameter values to be affected by the initial estimates, especially if the estimates are poor. In addition, if the peak widths are allowed to vary, the width of one peak can expand and effectively devour a smaller neighboring peak. To prevent such problems and to increase the comparability of fitted synthetic spectra, fixed values of peak width were used.

The fixed values for the Gaussian fraction and the peak widths could not be determined solely by examining the standard error associated with the fitted spectra because an excellent fit was obtained for many different combinations of values. Better estimates of these fixed values can be obtained by fitting the smoothed, numerically approximated second derivatives in addition to the original spectra. An optimization scheme could be devised which incorporates both the spectra and its approximated derivatives. Such a routine, however, would be extremely computationally intensive and impractical, if not impossible, to implement on a desktop computer (i486 processor). Therefore, the numerically approximated second derivatives of the humic spectra were simply

compared visually to those of the synthetic spectra to evaluate the quality of the fixed values for peak width and Gaussian fraction. To minimize the influence of absorbance values on the peak width determination, preliminary absorbance values were calculated using a fixed width of 20 cm^{-1} for all peaks. These fitted absorbance values and 20 cm^{-1} peak widths were then used as the initial estimates for a second curve fit in which the peak width was allowed to vary. Using the fitted absorbances insures that the initial estimates will be "good enough" to minimize the potential for divergence. The second derivative spectra were examined and the fitted peak widths were adjusted to provide a better fit of the second derivative. A fixed Gaussian fraction of 0.4 was chosen after examining the spectra and second derivatives produced using several different Gaussian fractions.

Because the same fixed values for peak widths and Gaussian fraction were used for all spectra, the calculated optimal absorbance values obtained from different aqueous humic spectra can be reliably compared. The standard error associated with the fitted absorbance values was always less than 10%. The synthetic spectra presented in this paper are not unique; peak width, maximum absorbance and Gaussian fraction do not function as independent variables. The spectra here do, however, represent a first attempt to separate and quantitate the highly overlapping features in humic spectra.

RESULTS AND DISCUSSION

Lithium humate spectra

The spectral changes associated with changes in pH are evident in aqueous lithium humate spectra (Figure 26). In the pH 3.0 spectrum, a distinct shoulder at 1710 cm^{-1} is attributable to the C=O of the un-ionized carboxyl group. This shoulder gradually disappears with increasing pH and is imperceptible by pH 6.2. Similarly, the broad band associated with C-O

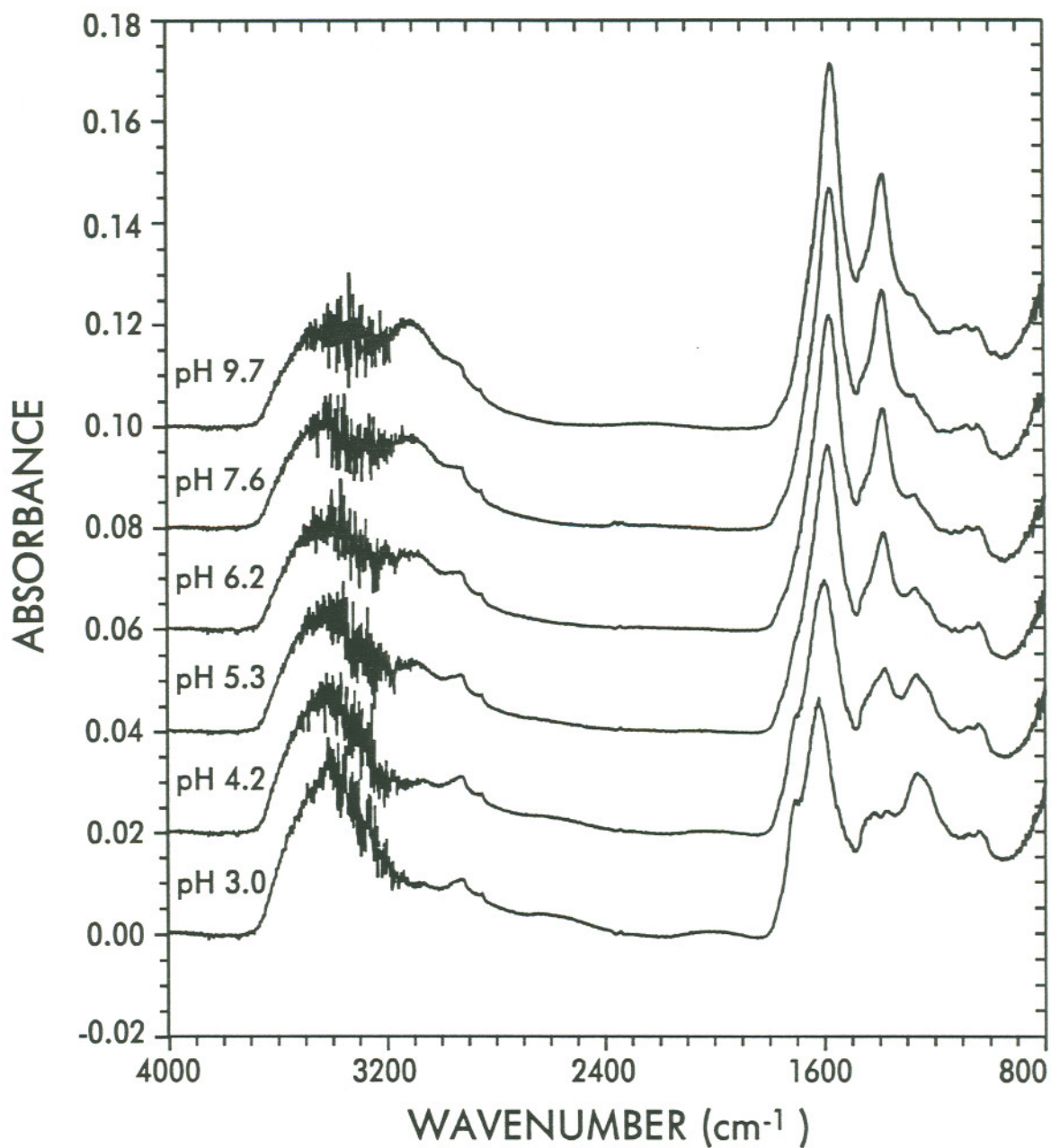


Figure 26. The aqueous spectra of six Li-humate solutions of different pH. All spectra have been background subtracted. The spectra are offset by 0.02 absorbance units for clarity. Humic acid concentration: 38.9 mg/mL; Total Li: 4.63 mmol/g HA.

stretching ($\sim 1230\text{ cm}^{-1}$) recedes into the background as the pH increases. A shallow broad peak at $\sim 2600\text{ cm}^{-1}$ is also present only at low pH and is probably indicative of strongly hydrogen-bonded O-H stretching in COOH. Concomitant with the disappearance of features associated with COOH, two other peaks ($\sim 1580\text{ cm}^{-1}$ and 1380 cm^{-1}) emerge and increase in intensity as the solution becomes more basic. These bands are associated with asymmetrical (ν_{as}) and symmetrical (ν_s) stretching of COO^- , respectively. The ν_{as} band at $\sim 1580\text{ cm}^{-1}$ appears to shift toward lower energy at higher pH. This shift, however, is probably an illusion due to overlap with the broad band at $\sim 1600\text{ cm}^{-1}$.

The broad $\sim 1600\text{ cm}^{-1}$ band is almost certainly due to the overlap of absorbances associated with a variety of structures such as aromatic C=C, strongly hydrogen-bonded C=O, and C=O conjugated with C=C. Hydrogen-bonded quinones, aryl ketones, $\alpha\beta$ unsaturated ketones and $\alpha\beta\alpha'\beta'$ unsaturated ketones also absorb in this region and may be present in humic matter (STEVENSON and GOH, 1974). The aromatic ring "breathing" mode is usually associated with weak absorbance near 1600 cm^{-1} , however, phenolic substituents can greatly enhance its intensity (PAINTER, *et al.*, 1981). In addition, the amide I band occurs near 1650 cm^{-1} and may be important for humic substances with high N content (BOYD *et al.*, 1980). The $\sim 1600\text{ cm}^{-1}$ band has also been attributed to COO^- , but its strong presence at very low pH contradicts that assignment (MACCARTHY and RICE, 1985). Water associated with the humic macromolecule could also contribute in this region via the H-O-H stretching mode at 1640 cm^{-1} . Unfortunately, bands in the $\sim 1600\text{ cm}^{-1}$ region severely overlap both of the important peaks associated with the ionization of COOH groups (1710 cm^{-1} and 1580 cm^{-1}), significantly complicating peak quantitation.

The very broad band at $\sim 3400\text{ cm}^{-1}$ is attributable to O-H stretching. The strong presence of this band at all pH values indicates that it may be primarily due to phenol or alcohol structures, rather than COOH groups. The two small peaks on the shoulder of this band (2920 and 2860 cm^{-1}) indicate the presence

of aliphatic C-H. The general changes in the shape of $\sim 3400\text{ cm}^{-1}$ band that occur with increasing pH might be interpreted as COOH ionization, however, attributing differences in this region to changes in humic structure is risky. The error associated with the aqueous humic spectrum in this region is large (± 0.02 absorbance units) because of the very strong absorbance of the water solvent. In addition, the presence of an aqueous electrolyte alters hydrogen-bonding in the water solvent and can create artifacts due to imperfect background subtraction (recall Chapter IV). At high pH, a considerable fraction of the Li^+ is associated with the negatively-charged humate macro-ion due to electrostatic attraction (recall Chapter III). As the pH decreases, the charge on the humate macro-ion also decreases, releasing Li^+ into the bulk solution. Even though the total Li^+ concentration is constant, the aqueous Li^+ concentration, and consequently the water solvent spectrum, vary with pH. Although Li^+ cations affect the structure of water less than other alkali metal cations, their effect cannot be disregarded and may be responsible for the observed pH dependence of the $\sim 3400\text{ cm}^{-1}$ band.

The spectral changes that accompany ionization (decreased absorbance at 1710 cm^{-1} and 1240 cm^{-1} , and increased absorbance at 1580 cm^{-1} and 1380 cm^{-1}) are clearly visible in difference spectra formed by subtracting pairs of aqueous humic spectra (Figure 27). Each of these difference spectra was calculated using the pH 3.0 spectrum as the reference. A negative band indicates a feature that is present in the pH 3.0 spectrum but absent in the higher pH spectrum, while a positive band indicates the opposite. The amplitudes of the difference spectra continue to increase for all ΔpH values, indicating that COOH ionization continues even between pH 7.6 and 9.7 (Figures 27d and 27e). Notice that difference spectra (Figure 27) clearly show COOH dissociation even when the shoulder at 1710 cm^{-1} band is imperceptible in the aqueous humic spectrum (Figure 26). The 1710 cm^{-1} band is much smaller than the 1580 cm^{-1} band, even though the loss of COOH and the gain of COO^- must be stoichiometrically

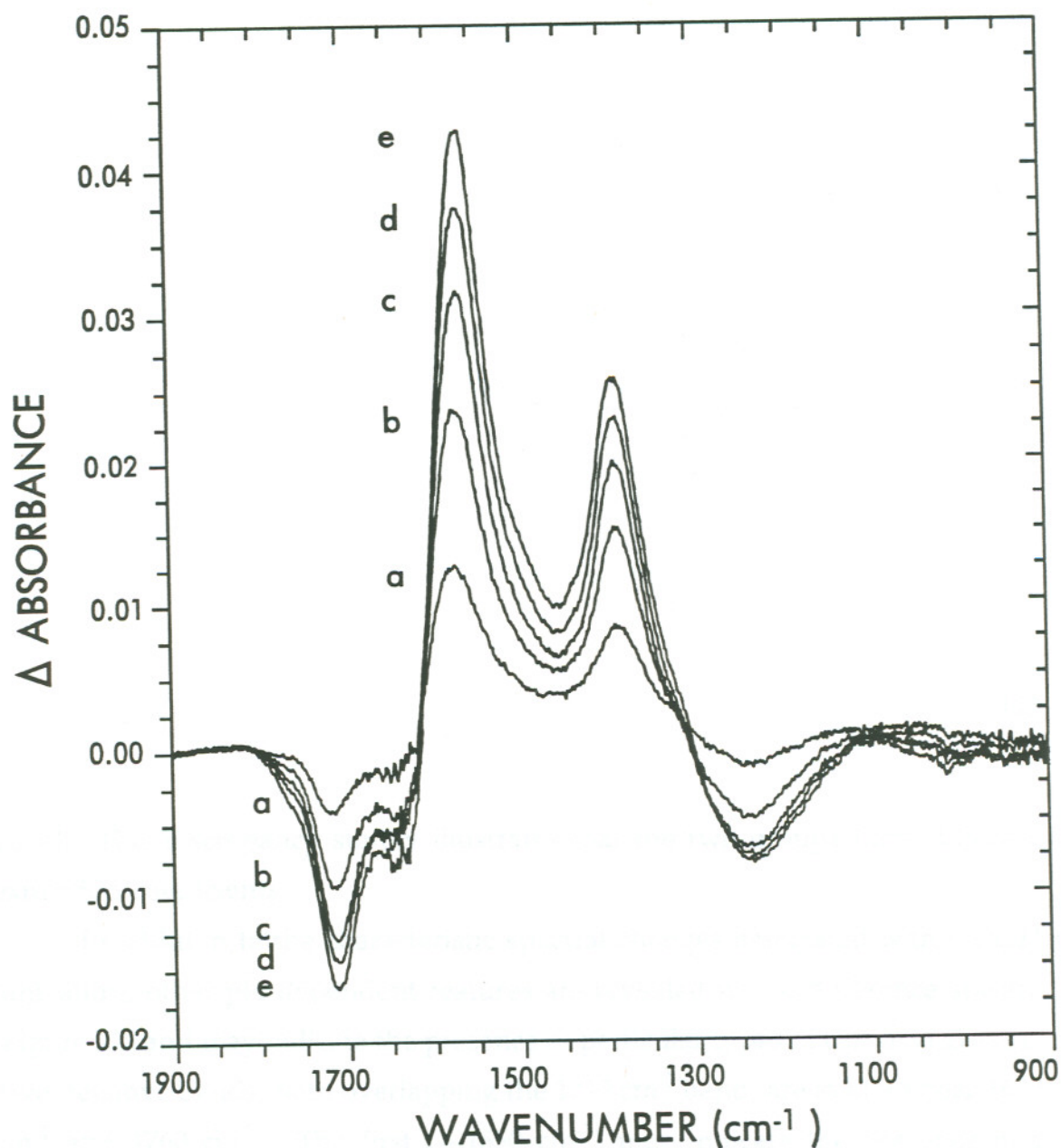


Figure 27. Difference spectra formed by subtracting the aqueous Li-humate spectrum at pH 3.0 from spectra of higher pH. Only the features that change with pH are visible. The negative bands are features present in the pH 3.0 spectrum but not in the higher pH spectrum. Similarly, positive bands are those features that are absent in pH 3 spectrum, but present in the higher pH spectrum. a) pH 4.2 - 3.0; b) pH 5.3 - 3.0; c) pH 6.2 - 3.0; d) pH 7.6 - 3.0; e) pH 9.7 - 3.0.

resolution from the 1710 cm^{-1} band. Very few groups exhibit pH dependent absorbances near 1760 cm^{-1} . One possible source of the 1760 cm^{-1} band is COOH groups that are intramolecularly hydrogen-bonded through the OH portion of the COOH rather than the C=O (e.g. *o*-methoxybenzoic acid). In this case the OH must assume a *trans* configuration which leads to a higher absorbance frequency than the preferred *cis* configuration (BELLAMY, 1980). The existence of such structures in humic acids is quite plausible.

Because difference spectra remove the pH invariant features that overlap the important COOH and COO⁻ peaks, they can be used to assess the chances for accurate quantitation of spectral changes. As the pH increases, the large positive peak at $\sim 1580\text{ cm}^{-1}$ appears to be displaced toward lower energy. This

equal. This discrepancy simply illustrates that the two groups have different extinction coefficients.

In addition to the characteristic spectral changes associated with COOH ionization, other pH dependent features are revealed in the difference spectra (Figure 27) and may indicate the presence of particular types of carboxyl groups. Two negative bands, both overlapping the 1710 cm^{-1} band, are evident near 1650 cm^{-1} and 1760 cm^{-1} . The first ($\sim 1650 \text{ cm}^{-1}$) may indicate the presence and ionization of COOH groups capable of participating in intramolecular hydrogen-bonding, such as *ortho*-hydroxy benzoic acids (*e.g.* salicylate). Intramolecular hydrogen-bonding shifts the frequency of the C=O vibration to the 1650-1670 range (BELLAMY, 1975). Based upon titration experiments, GAMBLE and co-workers (1980) postulated that salicylate-like groups occur in humic acids, however, spectroscopic evidence has been absent to date. Unfortunately, the difference spectrum is noisy in this region due to the strong absorbance of the water solvent at 1640 cm^{-1} . The second band, a small shoulder near 1760 cm^{-1} , is clearly greater in the pH 3.0 spectrum than in the spectra of more basic samples, but its precise pH dependence is indeterminate because of poor resolution from the 1710 cm^{-1} band. Very few groups exhibit pH dependent absorbances near 1760 cm^{-1} . One possible source of the 1760 cm^{-1} band is COOH groups that are intramolecularly hydrogen-bonded through the OH portion of the COOH rather than the C=O (*e.g.* *o*-methoxybenzoic acid). In this case the OH must assume a *trans* configuration which leads to a higher absorbance frequency than the preferred *cis* configuration (BELLAMY, 1980). The existence of such structures in humic acids is quite plausible.

Because difference spectra remove the pH invariant features that overlap the important COOH and COO^- peaks, they can be used to assess the chances for accurate quantitation of spectral changes. As the pH increases, the large positive peak at $\sim 1580 \text{ cm}^{-1}$ appears to be displaced toward lower energy. This peak is also somewhat asymmetrical and seems to be truncated on the left edge.

The negative band at 1650 cm^{-1} is also asymmetrical. Both the apparent peak shifts and asymmetry are probably caused by the superposition of the increasing 1580 cm^{-1} peak and the decreasing 1650 cm^{-1} peak. Of course, any calculation of the apparent peak area would underestimate the true peak area because of cancellation where the two peaks overlap. This overlap of peaks is also present in the aqueous humic spectra, but masked by overlap with peaks that are pH invariant. Consequently, the calculation of peak areas, either from the aqueous spectra or the difference spectra, will be inaccurate due to errors arising from the superposition of peaks.

Peaks that overlap in the absorbance spectrum (Figure 28) are partially resolved in their second derivative spectrum (Figure 29). Second derivative peak locations are remarkably constant among spectra of different pH. Furthermore, peaks associated with both ionized and un-ionized carboxyl groups are discernable in the second derivative spectra regardless of the pH indicating that complete dissociation is not achieved between pH 3 and 10. The C=O stretching band of COOH is resolved into at least two peaks, 1725 cm^{-1} and 1710 cm^{-1} . Similarly the band associated with asymmetrical COO^- stretching (ν_{as}) appears as a multiplet ($1583, 1567$ and 1551 cm^{-1}) which is poorly resolved from a shoulder at 1600 cm^{-1} . The symmetrical COO^- stretching vibration (ν_s) is also separated into a strong peak at 1383 cm^{-1} and a shoulder at 1402 cm^{-1} .

In addition to COOH-associated peaks, other patterns emerge in the second derivative spectra. Several small but consistent peaks occur between 1850 cm^{-1} and 1750 cm^{-1} which are probably associated with C=O stretching. These peaks may be due to esters, cyclic structures such as lactones, or possibly select COOH groups. The region between 1700 cm^{-1} and 1600 cm^{-1} also exhibits specific peaks, although the exact peak positions are slightly more variable in this region than elsewhere. As previously discussed, a wide variety of structures could give rise to spectral features in this region, so specific assignments cannot be given for these peaks. A shoulder at 1466 cm^{-1} is barely

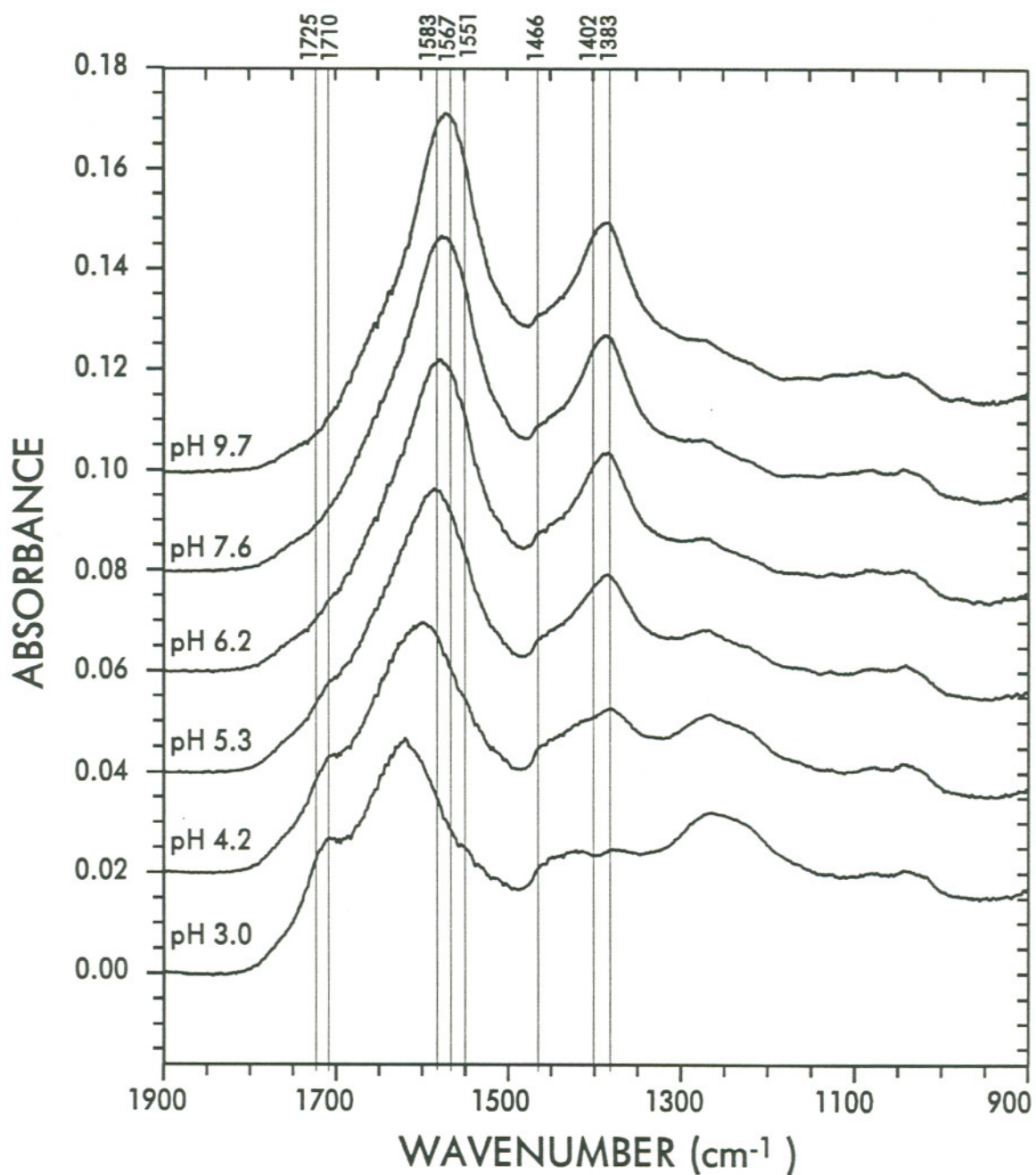


Figure 28. A detailed view of the carboxyl/carboxylate absorbance regions of Li-humate spectra of different pH. The spectra are offset by 0.02 absorbance units for clarity. The vertical lines indicate wavenumbers of peaks identified in the matched second derivative spectra (Figure 29).

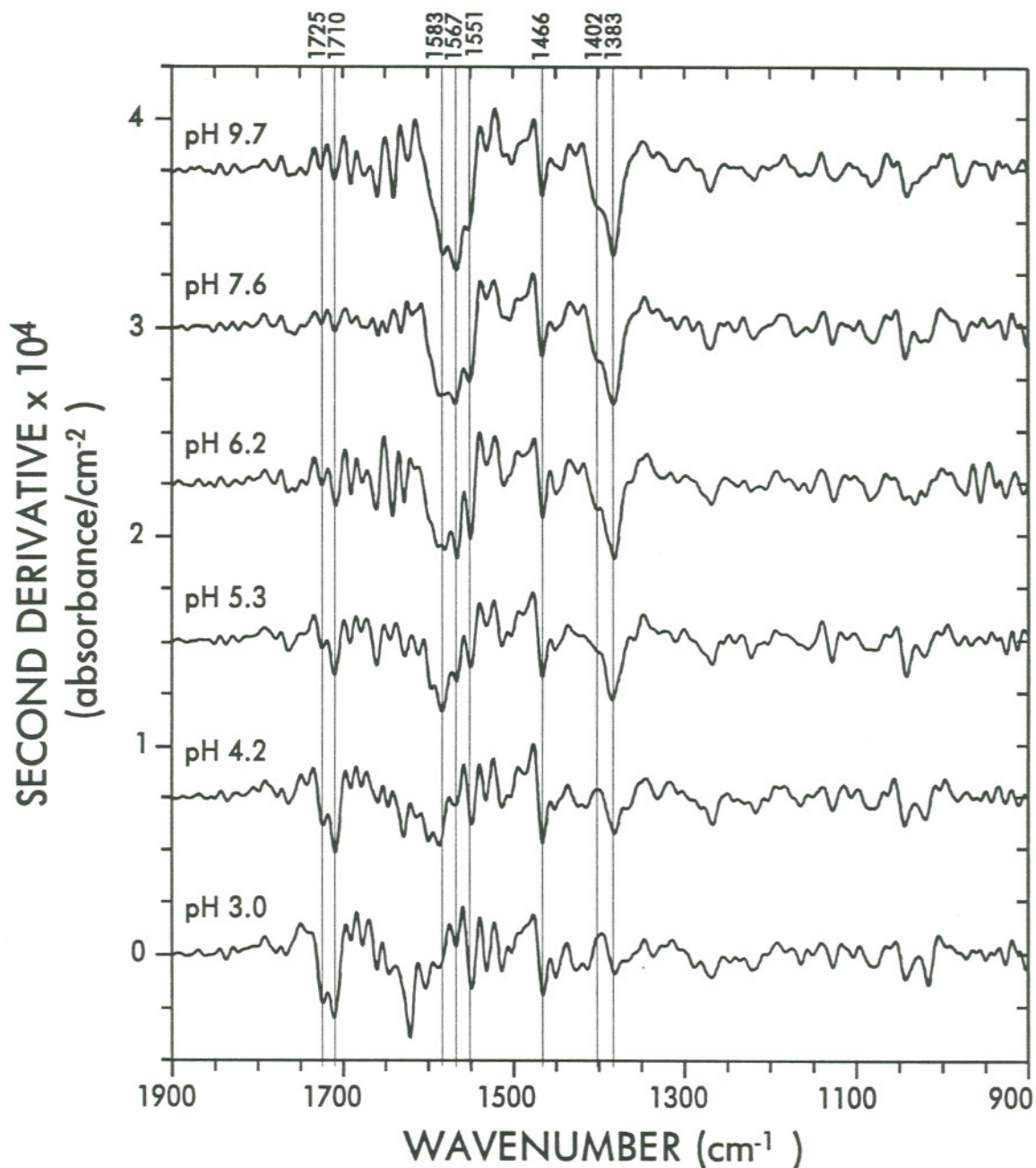


Figure 29. The numerically-approximated second derivatives of a set of Li-humate spectra of different pH. Only the carboxyl/carboxylate absorbance region is shown. The second derivative spectra are offset by 7.5×10^{-5} units for clarity. The vertical lines indicate wavenumbers of specific carboxyl and carboxylate peaks.

discernable in the absorbance spectrum, but is very sharp in the second derivative spectrum and indicative of aliphatic C-H stretching.

A modest amount of structure is evident in the absorbance spectrum between 1300 cm^{-1} and 900 cm^{-1} . Bands in this region are probably associated with C-O stretching in carboxylic, alcoholic and phenolic structures. Although in general C-O vibrations can be quite strong, peak positions are highly variable and dependent upon the nearby molecular structure. Consequently, the assignment of specific structures to individual peaks is unwise in this region. It is interesting to observe that the second derivative in this region is rather invariant with respect to pH. The very broad band associated with the C-O stretch of un-ionized COOH ($\sim 1240\text{ cm}^{-1}$) which is clearly visible in the humic difference spectra (Figure 27) is not apparent in the second derivative spectrum. The lack of pH-dependent peaks coupled with the overall weak nature of the features in this region suggests that these second derivative peaks are still highly overlapped.

Humic second derivative spectra cannot be used for quantitation of functional groups because of distortion produced by the highly overlapping absorbance spectrum peaks. To obtain quantitative estimates of the pH dependent COOH structures, curve fitting methods were used in the region 1800 cm^{-1} to 1480 cm^{-1} . Seventeen highly reproducible peaks were identified from the second derivative spectra (Table IV). The locations of these peaks were remarkably consistent among all spectra. Although the 1600 cm^{-1} peak seems less reproducible than other peaks, an unresolved shoulder near 1600 cm^{-1} was present in almost all of the lithium humate second derivative spectra. Because the humic spectrum does not reach a zero baseline at 1480 cm^{-1} , the peak at 1466 cm^{-1} was used to compensate for absorbance contributed the adjacent spectral region. Consequently, the fitted absorbance of this one peak is not meaningful.

Excellent fits were obtained for all lithium humate spectra (mean standard error = 3×10^{-4} a.u.). A representative pair of humic and synthetic spectra with

TABLE IV. Second derivative peaks of Li-humate spectra

center (cm ⁻¹)	s (cm ⁻¹)	frequency	width (cm ⁻¹)
1764	2	82%	28
1744	2	93%	28
1725	1	86%	28
1710	1	100%	30
1691	1	86%	30
1677	2	86%	30
1661	2	96%	30
1644	3	93%	30
1626	3	93%	43
1600	4	46%	44
1583	2	71%	34
1567	1	93%	34
1551	2	89%	34
1532	1	86%	38
1513	1	79%	20
1503	1	89%	36
1466	3	100%	53

the component peaks is shown in Figure 30a. The quality of the curve fit is evident in the tight, irregular residual spectrum of very low magnitude (Figure 30b). The fit of the numerically-approximated second derivatives is adequate (Figure 30c), especially considering that the second derivatives were not included in the least squares minimization routine.

The dependence of the individual, idealized peak areas upon pH is illustrated in Figure 31. All peaks of frequency 1690 cm^{-1} and greater exhibit a clear inverse relationship with increasing pH, indicating that all of these peaks result from C=O stretching within COOH groups. The absorbance values level off by pH 8, which is consistent with the titration of typical carboxylic acids. The absorbance decrease is not a sharp break, but rather smeared over a wide pH range (3-8). Each peak must, therefore, be interpreted as arising from a mixture of similar COOH groups, rather than one specific structure. In addition, absorbances remain significant at high pH values with the exception of the 1765 cm^{-1} peak. Either some of the COOH remains undissociated above pH 9 or these peaks include contributions from C=O vibrations not associated with COOH groups. The relatively strong intensity of the 1691 cm^{-1} peak, coupled with its weak pH dependence suggests that this peak probably arises from both carboxyl and ketonic C=O vibrations. In the case of the 1725 cm^{-1} and 1710 cm^{-1} peaks, data not shown suggest that a second region of decreasing absorbance occurs between pH 10 and 12. Such a region might indicate the dissociation of COOH groups that are in close proximity to already dissociated COO^- . The data, however, is inconclusive.

The assignment of carboxyl C=O to these peaks is confirmed by the presence of another set of peaks which are attributable to the COO^- structure. Peaks at 1583 , 1567 , 1551 , 1532 , and 1513 cm^{-1} increase in intensity as the pH increases. Again, no sharp break occurs in the absorbance-pH plot. No significant changes in the absorbances of the 1583 and 1551 cm^{-1} peaks occur after pH 8.5. The absorbance of the 1567 cm^{-1} peak, however, continues to

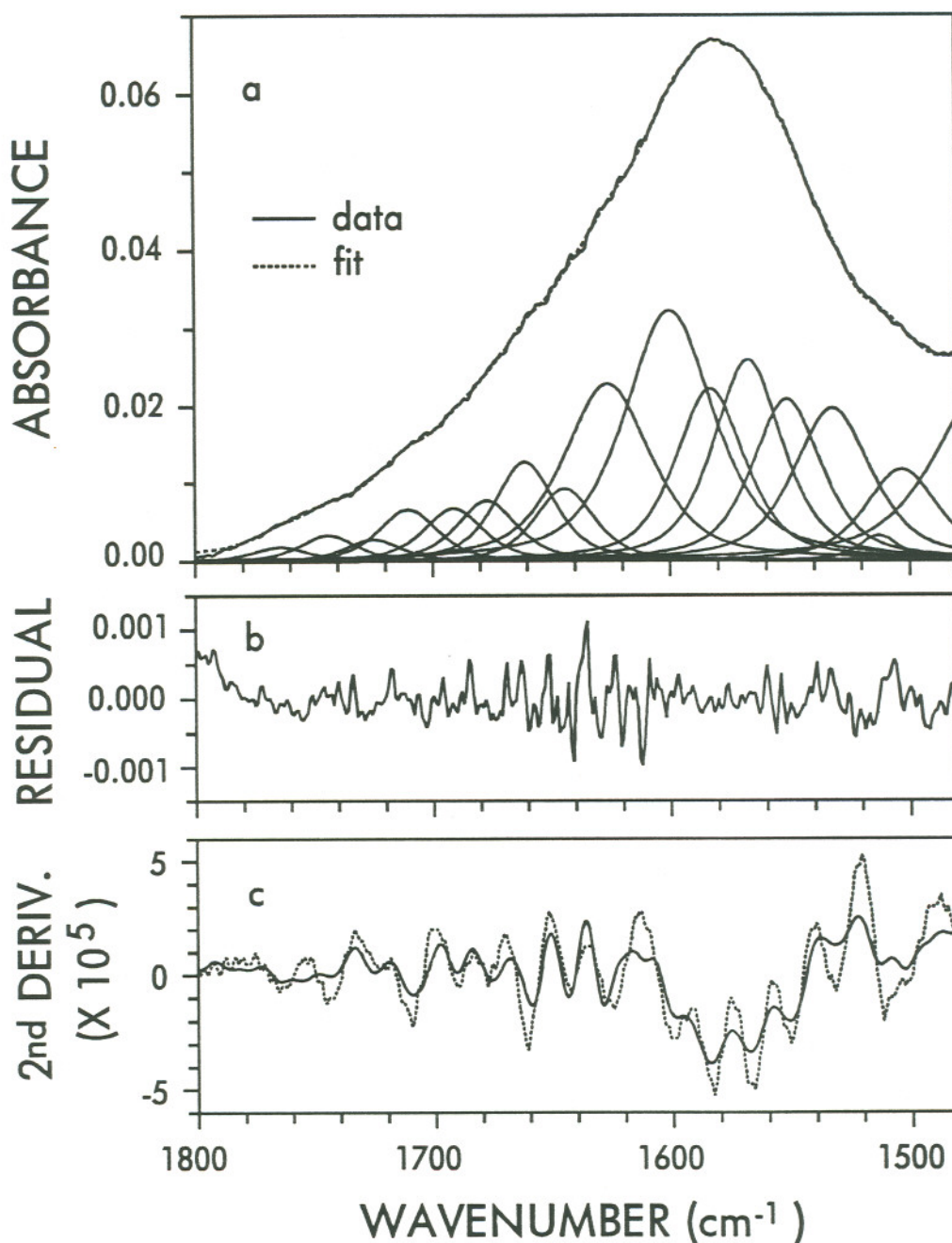


Figure 30. a) The absorbance spectrum of Li-humate (solid line) and the fitted synthetic spectrum (dashed line) in the region 1800-1480 cm⁻¹ with the 17 individual synthetic peaks (0.4 Gaussian fraction). Peak center locations and widths are given in Table IV. b) The residual spectrum, calculated as the difference of the absorbance data and the fitted values. c) The smoothed, numerically-approximated second derivatives of the absorbance spectrum (solid line) and the fitted spectrum (dashed line).

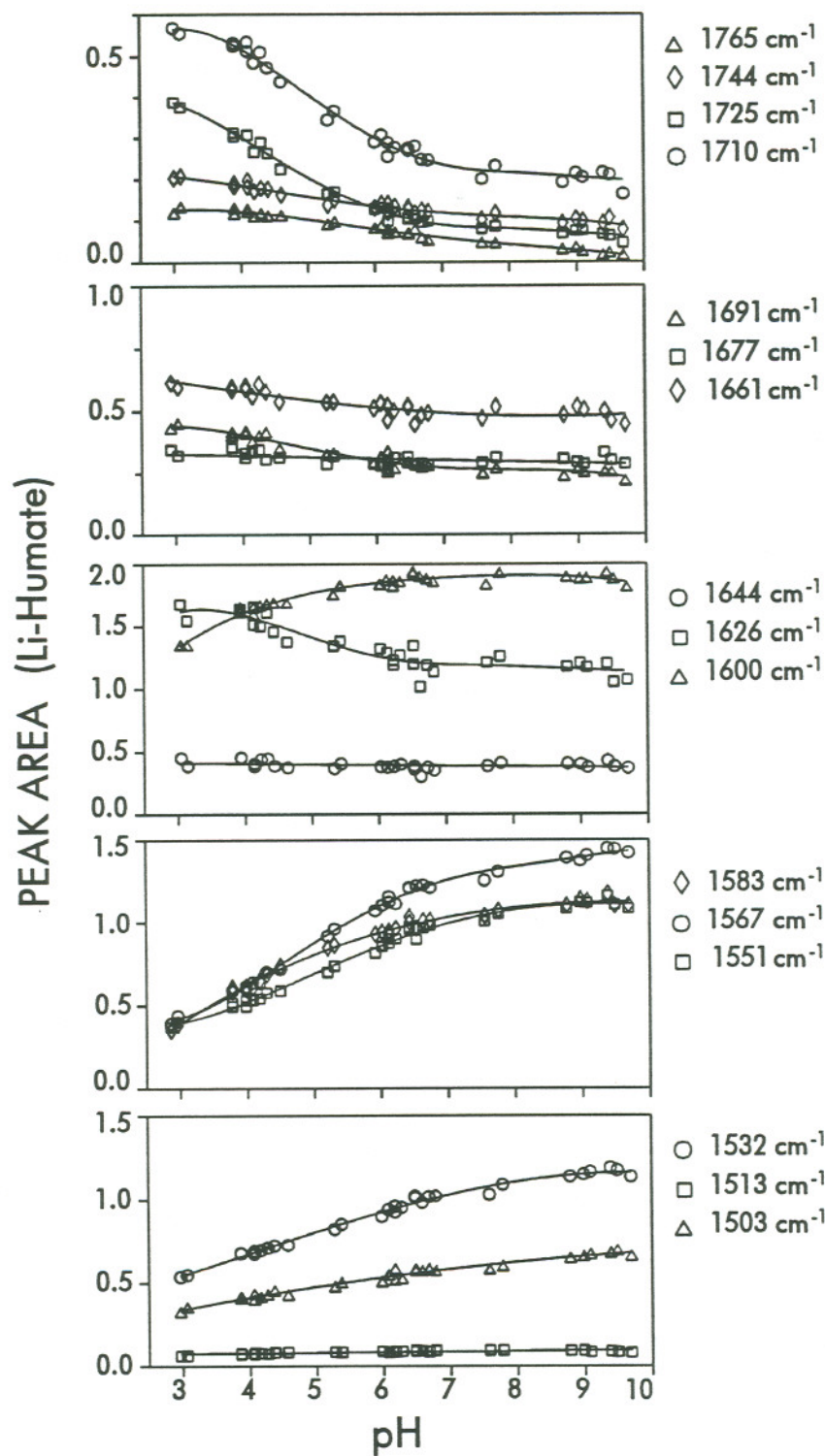


Figure 31. The pH dependence of the 16 fitted synthetic peaks for 28 Li-humate spectra.

increase. Absorbances are not negligible at low pH indicating that they probably include contributions from structures other than COO^- , or that detectable COO^- is present at pH 3 and less. As is the case with the carboxyl $\text{C}=\text{O}$ vibrations, these peaks cannot be identified with specific structures, but rather, arise from several similar structures. The asymmetrical vibrational frequency depends upon the moiety attached to the COO^- , and in general, decreases with increasing size. The following frequencies have been reported by BELLAMY (1980) using sodium salts and the KBr pellet technique: acetate (1583 cm^{-1}), propionate (1565 cm^{-1}), acrylate (1562 cm^{-1}), benzoate (1552 cm^{-1}) and α -dimethyl propionate (1551 cm^{-1}). Obviously, significant overlap would occur between the variety of possible humic carboxylate structures. In addition, hydrogen bonding typically decreases ν_{as} . There is some evidence that hydrogen bonding with the aqueous solvent has a similar effect. TACKETT (1989) measured ν_{as} of aqueous Na-acetate as 1551 cm^{-1} using CIR-FTIR, a 32 cm^{-1} decrease from the KBr pellet value.

Several peaks exhibit little or no pH dependence. Peaks at 1661 cm^{-1} and 1677 cm^{-1} are almost certainly due to α,β -unsaturated ketones, aryl ketones, or quinones. The 1644 cm^{-1} vibrational frequency is characteristic of unconjugated $\text{C}=\text{C}$ stretching. The constancy of the absorbance at 1644 cm^{-1} also supports the assignment of a skeletal structure. The peak at 1503 cm^{-1} is probably associated with the breathing mode of aromatic rings.

The assignment of plausible structures to the peaks at 1600 cm^{-1} and 1626 cm^{-1} is the most problematic. Several different structures could account for these absorbances, but few would exhibit the clear pH dependence observed. In addition, these are the most intense peaks in the $1800\text{-}1480\text{ cm}^{-1}$ region of the humic spectrum at any pH, and are the most variable in position. Therefore, it is likely that both peaks are composites of vibrations arising from several different structures, including $\text{C}=\text{C}$, $\text{C}=\text{O}$, aromatic rings and carboxylate. Conjugation of $\text{C}=\text{C}$ bonds with aromatic rings, or with $\text{C}=\text{O}$ or $\text{C}=\text{C}$ decreases their characteristic frequency to near 1625 cm^{-1} and 1600 cm^{-1} , respectively. The

intensity of the vibration is also enhanced by conjugation which could help explain the magnitude of the peaks in this region, although C=C absorbances would not be expected to be pH-dependent. Carbonyl vibrations, in general, shift to lower frequencies upon the formation of intramolecular hydrogen-bonds. Carboxylic C=O could account for the pH dependence, but vibrational frequencies less than 1650 cm^{-1} would be unusually low for carboxylic carbonyls. The carbonyl vibration is shifted to frequencies between 1650 and 1550 cm^{-1} in α,β -unsaturated β -hydroxy ketones and o -hydroxy quinones which form intramolecular hydrogen-bonded rings (BELLAMY, 1975). Changes in pH could disrupt the hydrogen bonding in such systems, thereby shifting the C=O vibrational frequency and creating apparent absorbance changes. The skeletal ring breathing mode also typically exhibits absorbance near 1600 cm^{-1} . The intensity of this absorbance is highly variable and increases as the the ring substituents become more polar. Consequently the weak pH dependence of the 1600 cm^{-1} peak could be explained by changes in the relative polarity of substituent groups related to the solvent pH. The asymmetric carboxylate stretching mode typically absorbs between 1610 and 1550 cm^{-1} and would be expected to be minimal at low pH. In α -amino acid structures, however, the dominant species at low pH is the zwitterion, $\text{R}_2\text{N}^+\text{H}-\text{CH}_2\text{COO}^-$, and ν_{as} is shifted to higher frequencies under the influence of the amino group. The complexation of a metal cation by COO^- also increases ν_{as} . TOMITA *et al.* (1965) studied the equilibrium complexation of Mg^{2+} by nitriloacetic acid (NTA) using aqueous infrared spectroscopy and found that as the pH increased, a band at 1625 cm^{-1} corresponding to $\text{HN}^+(\text{CH}_2\text{COO})_3^{2-}$ receded while a peak at 1610 cm^{-1} corresponding to $[\text{N}-(\text{CH}_2\text{COO})_3\text{Mg}]^-$ became stronger. The aqueous humic 1626 and 1600 cm^{-1} peaks display behavior similar to that of the NTA- Mg^{2+} system. Because the attraction of carboxylates to monovalent Li^+ is weaker than the attraction to Mg^{2+} , the frequency of carboxylate-lithium complexes would be expected to be slightly less than that of carboxylate-magnesium complexes. It

is unlikely, however, that the 1625 and 1600 cm^{-1} peaks are entirely due to amino-acid zwitterion/metal complex equilibria because of the low nitrogen content of the humic acid.

Sodium or potassium humate spectra

The spectra of aqueous sodium or potassium humate are virtually indistinguishable from aqueous lithium humate spectra at matched pH. The difference spectra of such matched samples, however, indicate that some differences do exist (Figure 32). Both the Na-Li and the K-Li humic difference spectra exhibit a pattern characteristic of a wavenumber shift. In fact, these difference spectra closely resemble the aqueous spectra of NaCl and KCl solutions (after water subtraction) which contain no humic material whatsoever (see Figure 23 in Chapter IV). The essential features of the humic spectrum have cancelled out, leaving only artifacts which are the result of changes in the extent of hydrogen-bonding within the water solvent caused by Na^+ and K^+ ions. Because both the Na- and K-humate spectra contain a similar wavenumber shift, the effects cancel out in the K-Na humic difference spectrum.

Although the artifact peaks are small, they can lead to severe problems when taking differences of humic spectra and can render such difference spectra uninterpretable (Figure 33). In the region near the important COOH and COO^- peaks, these artifacts coincide with both the COOH peak at 1710 cm^{-1} and the shoulder at 1650 cm^{-1} , altering both peak shape and size. The baseline is also affected. Unlike the Li-humate difference spectra (Figure 27), these difference spectra exhibit baselines that are neither flat nor centered at zero. The strong baseline curvature interferes with the negative 1240 cm^{-1} band enough to elevate it entirely above zero. These difference spectra are further complicated by the indirect dependence of the artifacts on pH. Although the total Na^+ concentration is constant, the extent of the wavenumber shift depends on the free Na^+ in solution, which in turn varies with pH. The apparent pH

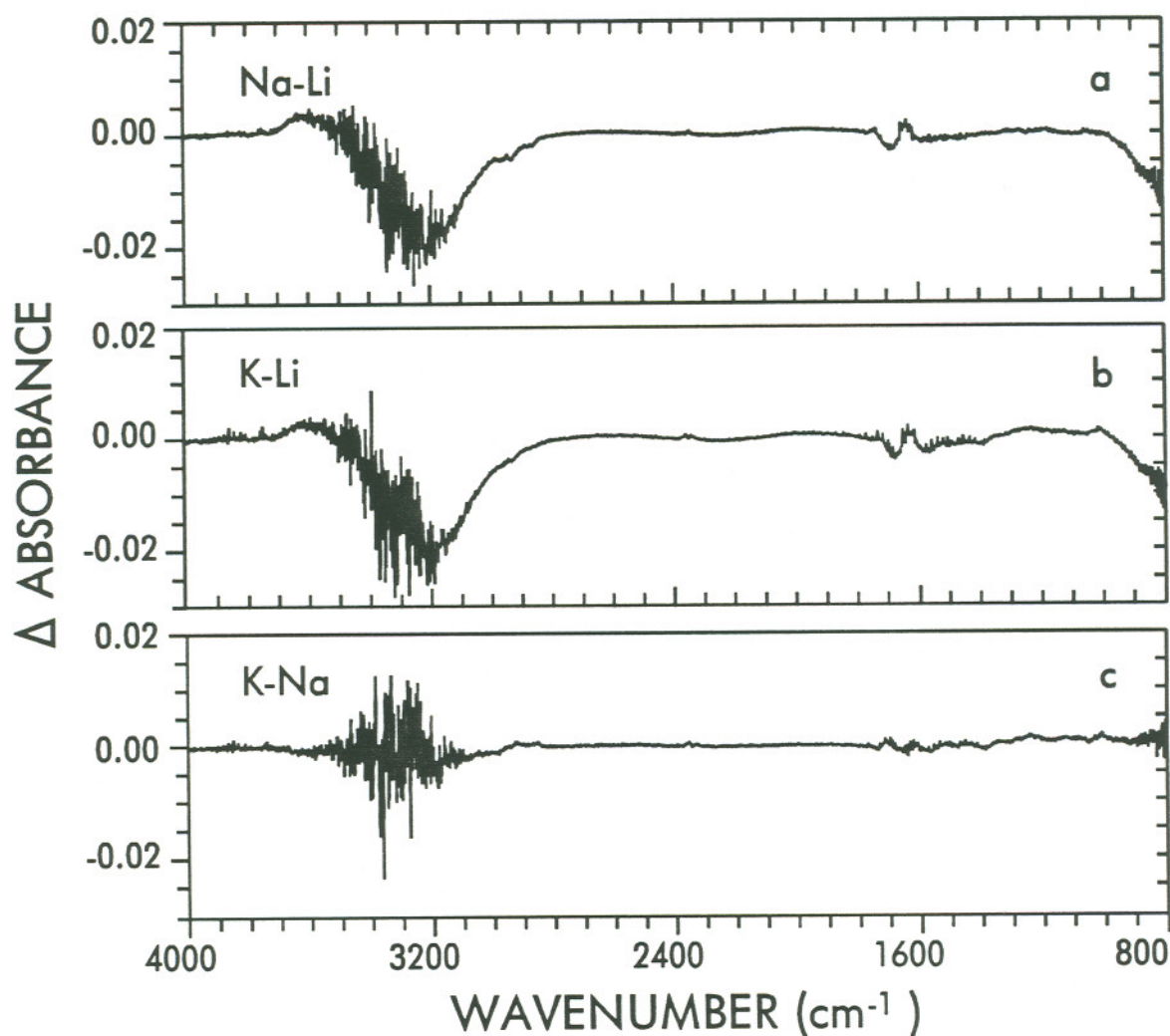


Figure 32. Three difference spectra formed by subtracting pH-matched (pH=4.6) aqueous spectra containing different alkali metal cations. A difference factor of unity was used. The aqueous spectra had been previously background subtracted. a) Na-humate - Li-humate. b) K-humate - Li-humate. c) K-humate - Na-humate.

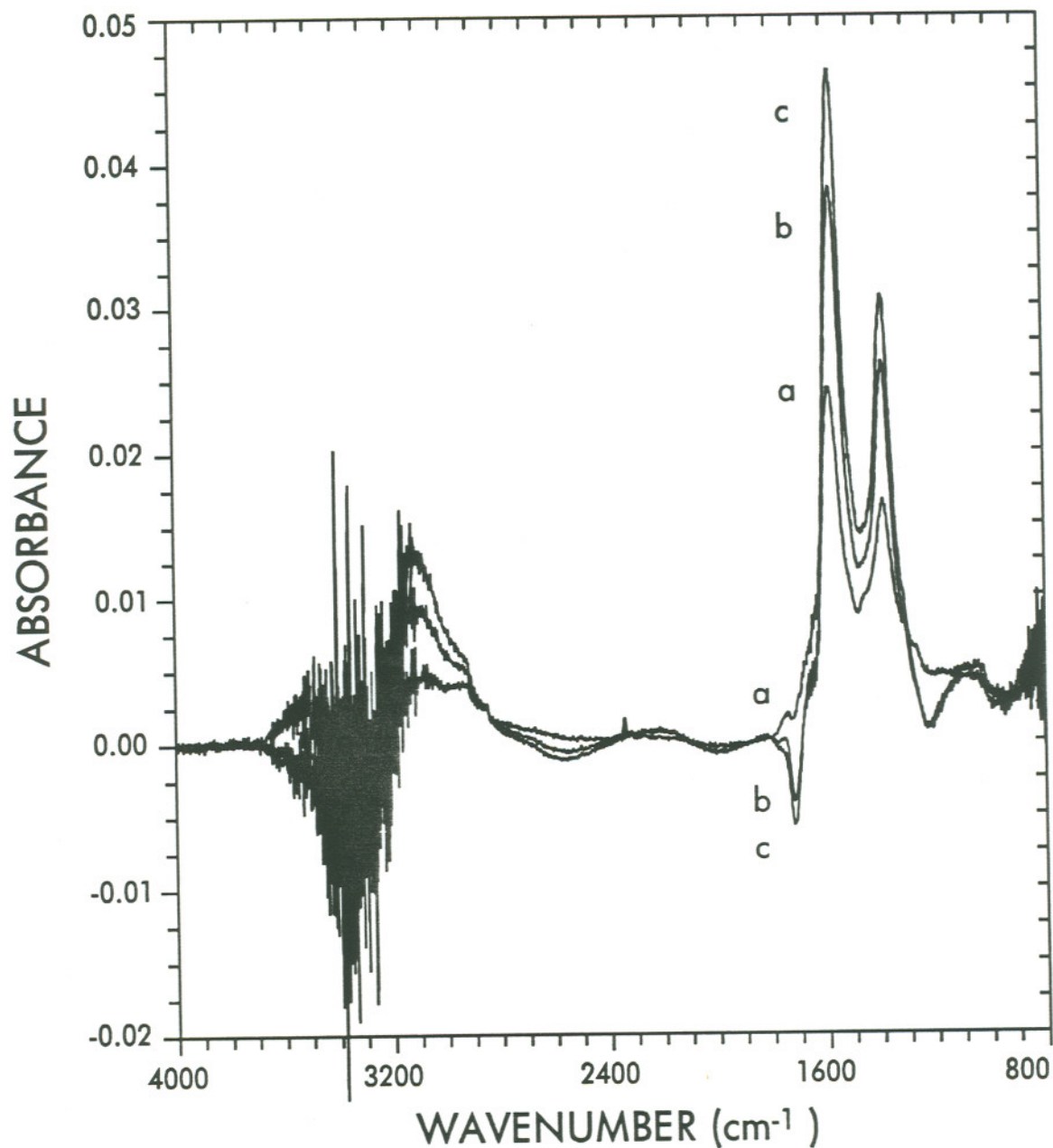


Figure 33. Difference spectra formed by subtracting an aqueous Na-humate spectrum (pH 3.1) from spectra of higher pH . Only the features that change with pH are visible. The negative bands are features present in the pH 3.1 spectrum but not in the higher pH spectrum. Similarly, positive bands are those features that are absent in pH 3.1 spectrum, but present in the higher pH spectrum. a) pH 4.6 - 3.1 b) pH 6.3 - 3.1 c) pH 7.9 - 3.1. Humic acid concentration: 39.4 mg/mL; Total Na: 4.48 mmol/g HA.

dependence of the extremely asymmetrical peak near 3300 cm^{-1} is entirely due to wavenumber shifts induced by changes in free Na^+ concentration. If the total Na^+ or K^+ is high enough, the aqueous cation concentration will be negligibly affected by association with humic matter, regardless of the pH. Wavenumber shifts would still occur, but should cancel out in the difference spectra. Of course, at high cation concentration, the ionic strength would be expected to influence the conformation of humic macro-ion.

The second derivative spectra of both Na- and K-humate are essentially the same as Li-humate second derivative spectra. No shifts in peak locations were observed. Such constancy indicates that the interactions between the humic macromolecule and Li^+ , Na^+ , and K^+ are of similar mechanism and strength.

Synthetic Na- and K-humate spectra were constructed for the region $1800\text{--}1480\text{ cm}^{-1}$ using the same fixed parameters as those used for the Li-humate spectra. As with the Li-humate spectra, excellent fits were obtained. The relationship between individual peak areas and pH is very similar for Na- and K-humate and at moderate to high pH resembles that of Li-humate (Figures 34 and 35). At low pH, however, the Na- and K-humate peaks are curiously reduced. This deviation is another artifact arising from hydrogen-bonding changes within the aqueous solvent. Close examination of Figures 32a and 32b show a mostly negative baseline between ~ 1750 and 1400 cm^{-1} due to a wavenumber shift that caused imperfect solvent subtraction. When an affected Na- or K-humate spectrum is fitted with a synthetic spectrum, the individual peak areas are less than those that would be obtained by fitting a similar Li-humate spectrum. A comparison of synthetic peak locations (Figures 34 and 35) with the artifact spectra (Figures 32a and 32b) also shows that the most severely affected peaks occur in the region of greatest artifact ($\sim 1750\text{--}1650\text{ cm}^{-1}$). At moderate to high pH values, the free Na^+ or K^+ concentration is low and minimally affects the solvent structure. Therefore, any artifacts are unnoticeable.

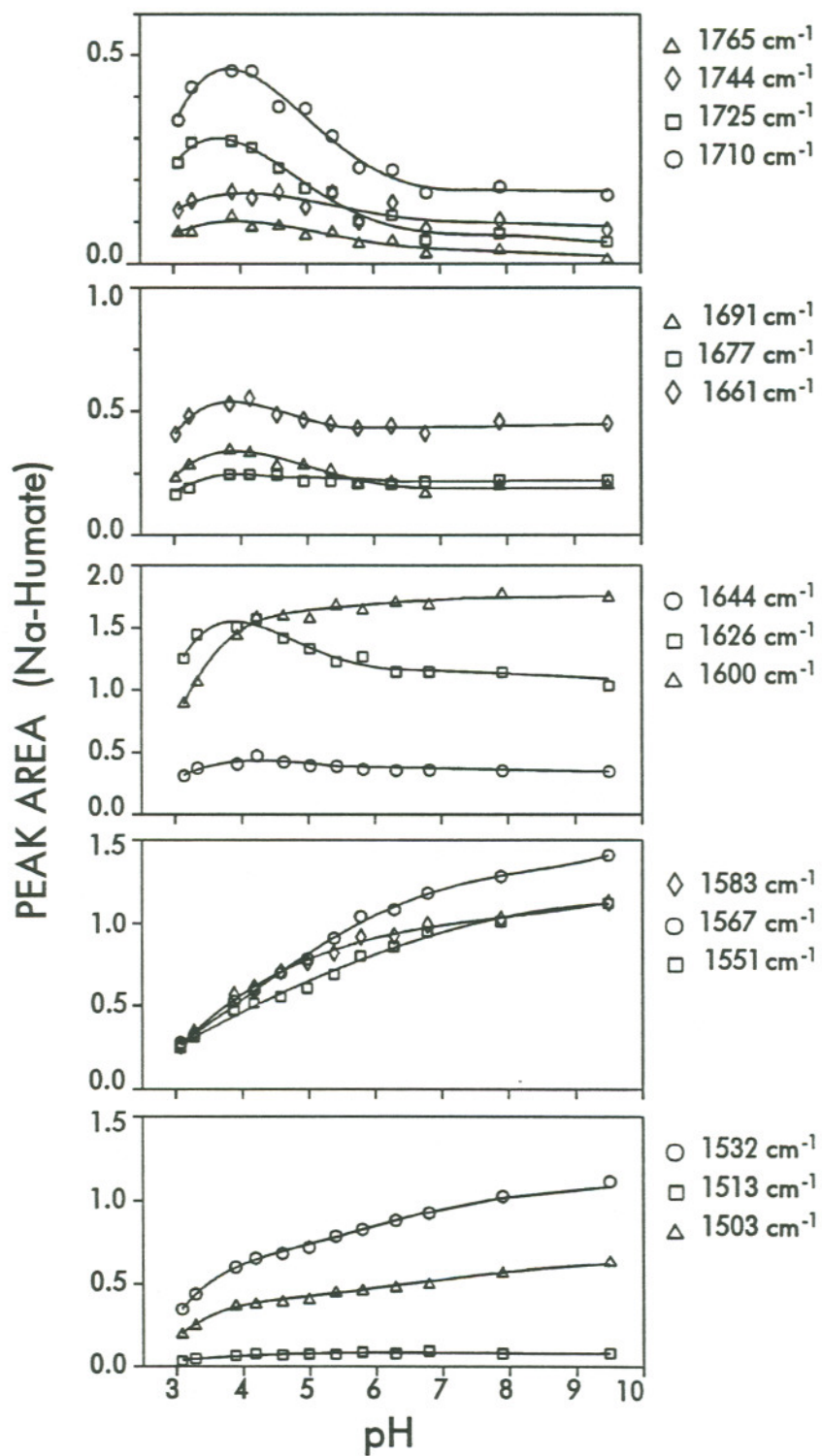


Figure 34. The pH dependence of the 16 fitted synthetic peaks for 12 Na-humate spectra.

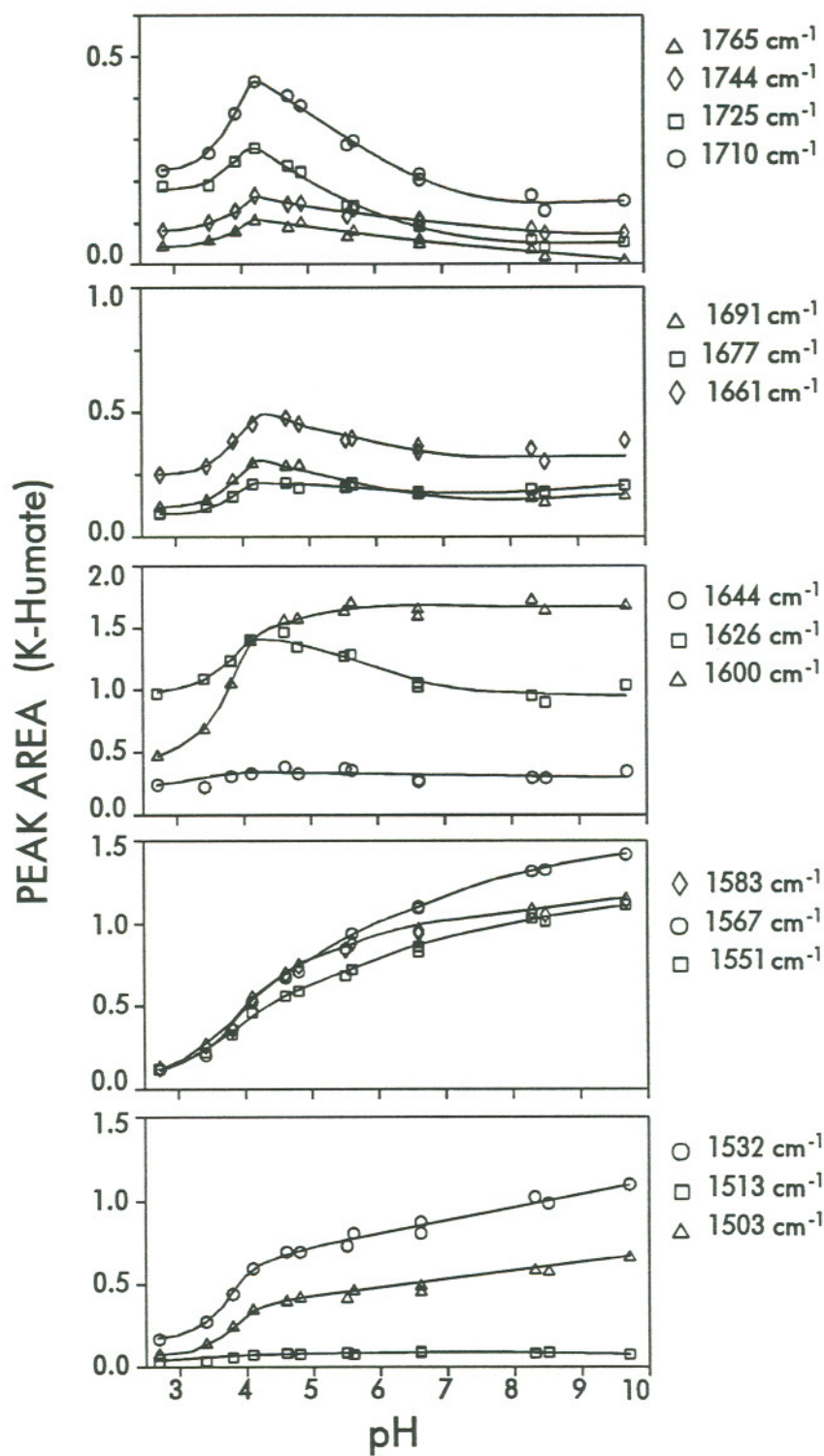


Figure 35. The pH dependence of the 16 fitted synthetic peaks for 13 K-humate spectra.

As the pH decreases, the free electrolyte concentration increases, disrupting the hydrogen-bonding of water. Greater free Na^+ or K^+ concentrations cause a larger wavenumber shift and hence poorer background solvent subtraction. Thus, the artifacts increase as the pH decreases.

Effects of alkaline earth cations

To investigate the interactions between alkaline earth cations (Mg^{2+} , Ca^{2+} , and Ba^{2+}) and humic material, increasing amounts of divalent cations were added to lithium humate (pH ~ 6.5). Because of their greater charge, these cations were expected to exhibit greater association with humate than any of the previously investigated alkali metal cations. The addition of Mg^{2+} , Ca^{2+} , or Ba^{2+} caused the pH to decrease, but not enough to expect significant pH-related changes in the humic infrared spectra. The magnitude of the pH change depends on the quantity of alkaline earth cation, rather than the identity (Figure 36). Similar additions of excess Li^+ did not affect the pH. The association of alkaline earth cations with humate must perturb the humic acid/humate equilibrium, causing further dissociation and the release of H^+ .

The mechanisms of cation-humate interaction may be different for alkaline earth cations and alkali metal cations. A shift in the position of one or more of the COO^- peaks would be evidence of such a mechanistic difference. The alkaline earth cations were not associated with any obvious shifts in peak positions; however, they did dramatically affect the humic spectra in another manner. A representative series of aqueous humate spectra illustrating the effects of increasingly larger Ba^{2+} concentrations is shown in Figure 37a. The aqueous humic spectrum does not appear to be influenced by low concentrations of Ba^{2+} . The humic spectrum is abruptly attenuated, however, if the Ba^{2+} concentration exceeds a threshold value (1.0-1.5 mmol Ba^{2+} /g HA). Even the C-H stretching bands at 2920 and 2860 cm^{-1} are diminished. Further increases in the Ba^{2+} concentration have little effect on the spectrum.

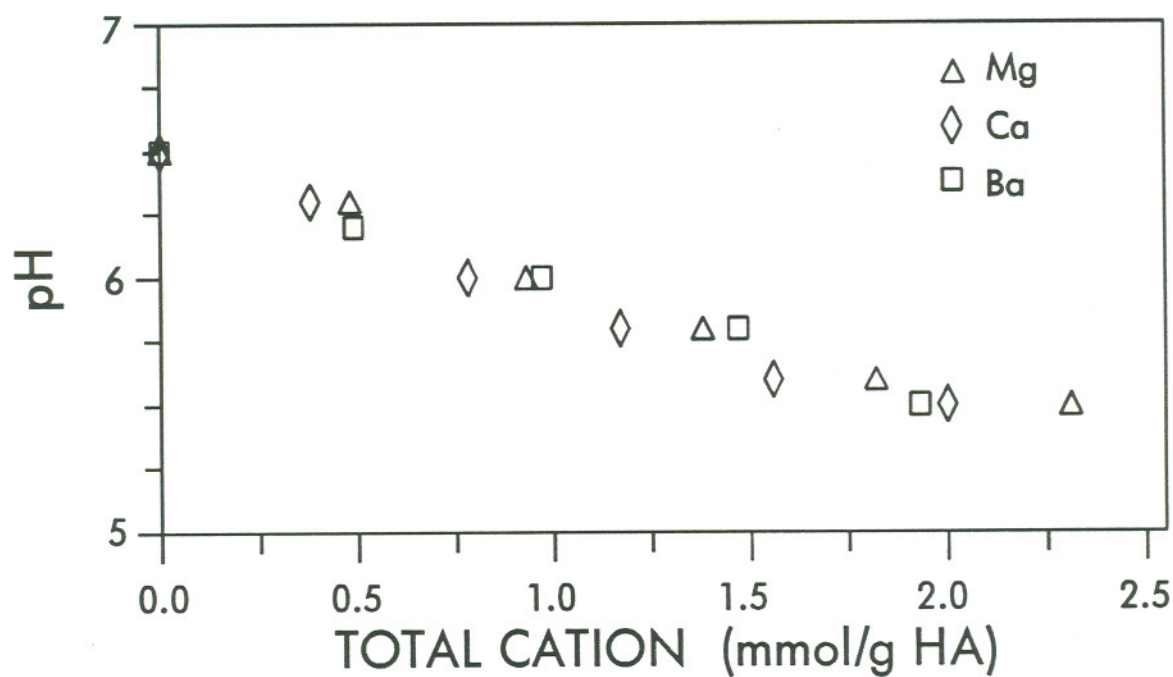


Figure 36. The dependence of the pH of Li-humate on the alkaline earth cation concentration. Humic acid concentration: 44.5 mg/ml. Total Li: 4.6 mmol/g HA for Ca and Mg and 4.7 mmol/g HA for Ba.

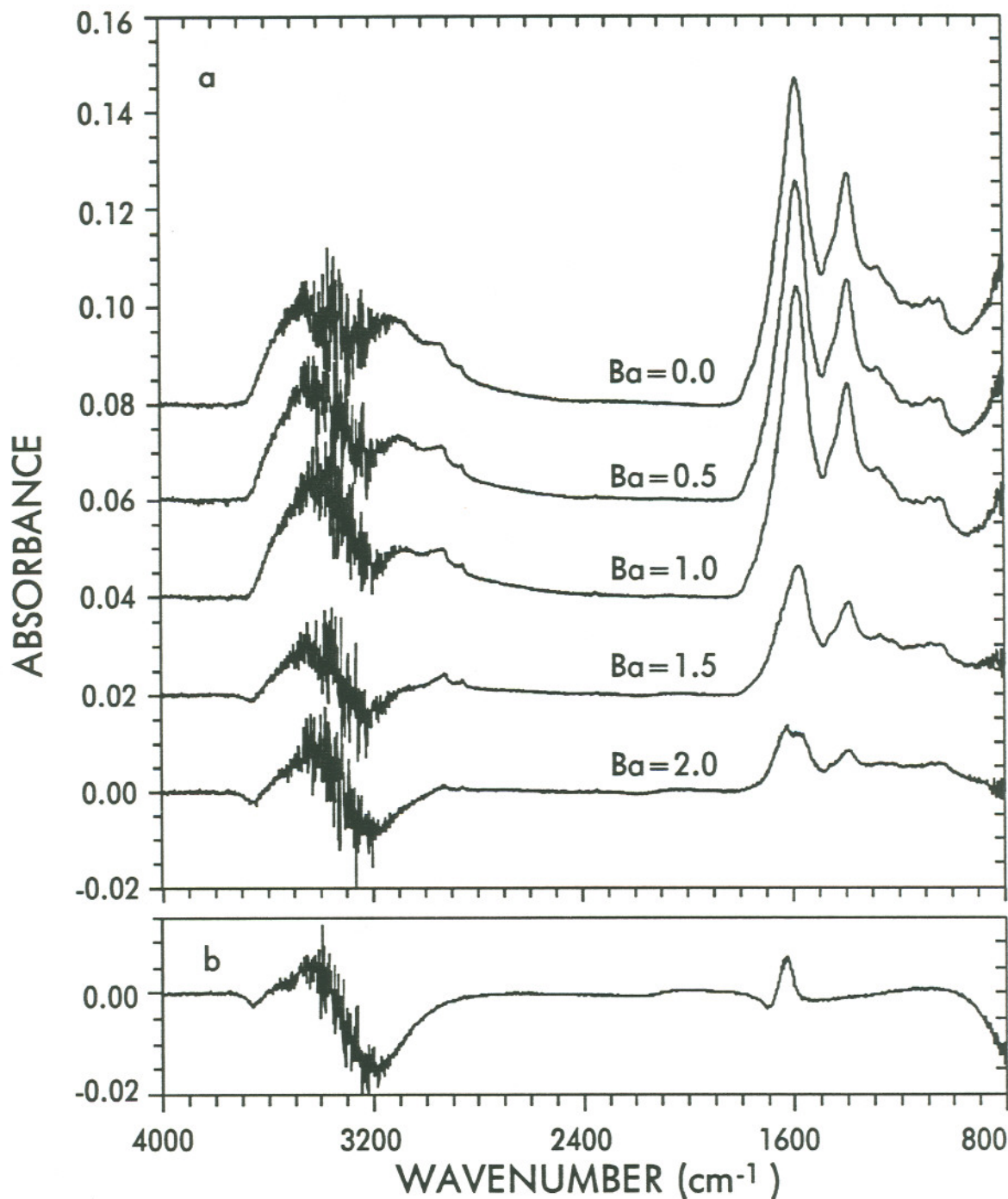


Figure 37. a) The aqueous spectra of five Li-humate solutions in the presence of increasing amounts of Ba²⁺. Total Ba²⁺ concentrations are expressed in units of mmol/g HA. All spectra have been background subtracted. The spectra are offset by 0.02 absorbance units for clarity. Humic acid concentration: 44.5 mg/mL; Total Li: 4.7 mmol/g HA. b) Background subtracted aqueous spectrum of 0.10 M BaCl₂ (humic-free).

The dramatic changes in humic spectra caused by the addition of Mg^{2+} , Ca^{2+} , or Ba^{2+} are most easily observed in difference spectra (Figure 38), calculated with reference to a Li^+ -humate spectrum. All three cations cause a similar sharp absorbance decrease with an increase in cation concentration. No wavenumber shifts are observable. Rather, the intensity of the entire spectrum is uniformly reduced. Different amounts of the three alkaline earth cations are required to induce the absorbance decrease; the required amounts increase in order Ba^{2+} (~ 1.0 mmol/gHA) $<$ Ca^{2+} (~ 1.2 mmol/gHA) $<$ Mg^{2+} (~ 1.5 mmol/gHA). The eventual absorbance reduction is greatest for Ba^{2+} (80%), followed by Ca^{2+} (60%), and Mg^{2+} (30%).

The spectral changes accompanying increases in the divalent cation concentration must be examined for possible artifacts caused by cation-induced changes in the hydrogen bonding of the water solvent. Such artifacts can be observed in the Mg difference spectra (Figure 38). Artifact peaks near 1690 and 1630 cm^{-1} are clearly visible in Mg difference spectrum C. Interestingly, artifact peaks are not noticeable in the Ca or Ba difference spectra, despite the fact that at similar concentrations, Ca^{2+} and Ba^{2+} disrupt the structure of water more than does Mg^{2+} . This could only occur if the free Mg^{2+} concentration were greater than the free Ca^{2+} or Ba^{2+} concentration. The fraction of cation associated with the humic matter, therefore, must be smaller for Mg^{2+} than for either Ca^{2+} or Ba^{2+} . Artifacts are not entirely absent in the (Ca+Li)-humate and (Ba+Li)-humate spectra. Artifacts can be observed in the (Ba+Li)-humate spectra (Figure 37a) by comparing them to the spectrum of a BaCl_2 solution after water subtraction (Figure 37b). The negative artifact near 3200 cm^{-1} in the BaCl_2 spectrum is clearly visible in aqueous humic spectra containing 1.5 and 2.0 mmol Ba^{2+} /g HA. The positive region of the S-shaped artifact at 1780-1580 cm^{-1} (Figure 37b) is just perceptible in the aqueous humic spectra. The negative region is masked in the humic spectra by the superposition of humic peaks.

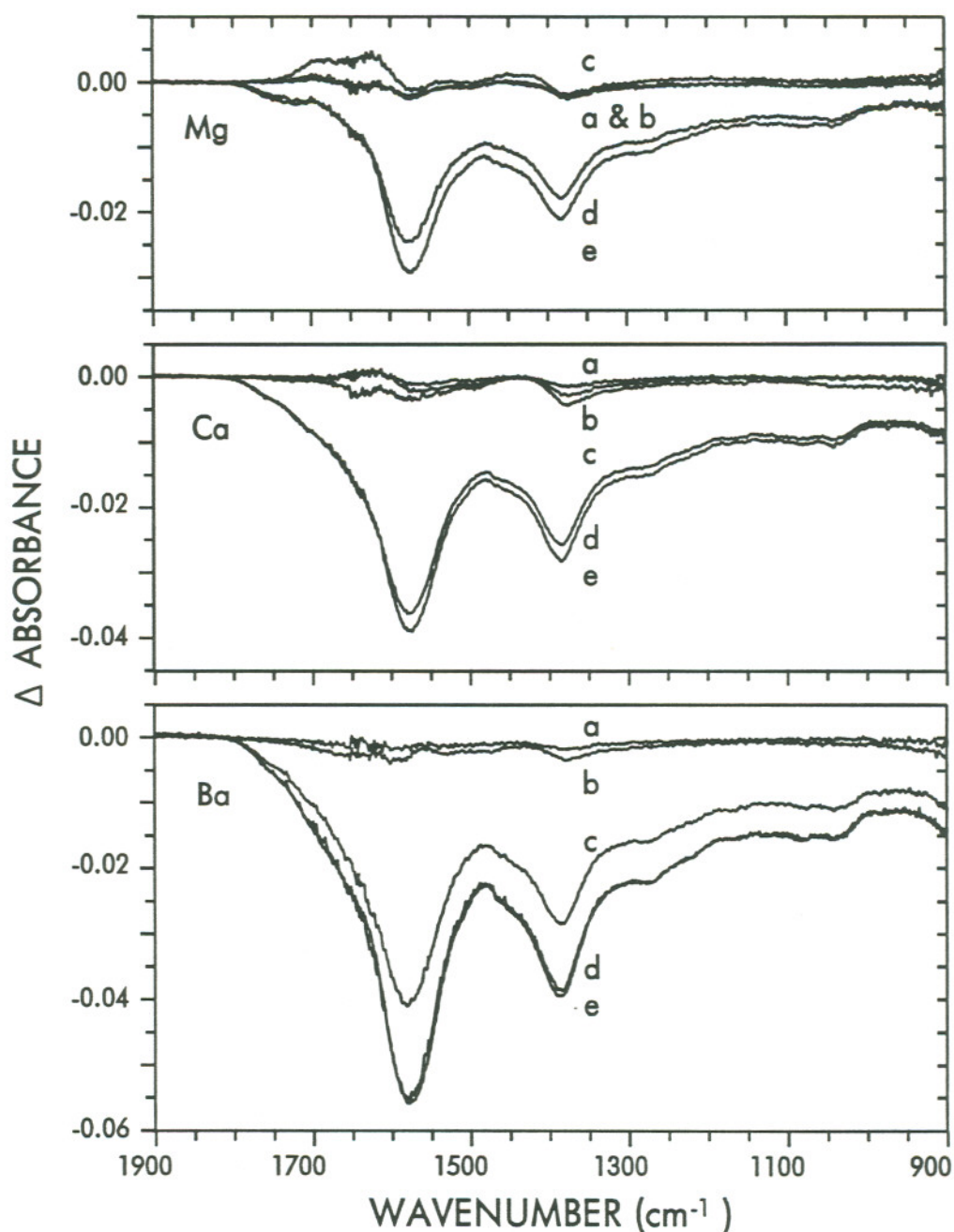


Figure 38. Difference spectra formed by subtracting the aqueous Li-humate spectrum (alkaline earth cation free) from spectra containing increasing amounts of Mg^{2+} , Ca^{2+} , or Ba^{2+} . Only the features that change are visible. The negative bands are features present in the Li-humate spectrum but absent in the spectra of Li-humate solutions containing the divalent cations. Divalent cation concentrations, expressed in units of mmol/g HA, are: **Mg**- a) 0.46, b) 0.92, c) 1.4, d) 1.8, e) 2.3; **Ca**- a) 0.38, b) 0.77, c) 1.2, d) 1.5, e) 1.9; **Ba**- a) 0.49, b) 0.97, c) 1.5, d) 1.9, e) 2.5.

The second derivatives of (Mg+Li)-, (Ca+Li)-, and (Ba+Li)-humate spectra were unexpectedly similar to those of alkali metal humate spectra. The positions of the second derivative peaks were essentially identical. Increased concentrations of the divalent cations did cause the absolute magnitudes of the second derivatives to decrease in the same manner as the peaks of aqueous spectra.

Synthetic spectra were fitted to the alkaline earth cation + Li-humate spectra to determine if the abrupt absorbance decrease was associated with particular functional groups. Because the amplitudes of these spectra depend so strongly on the divalent cation concentration, synthetic peak areas are best compared when expressed relative to the sum of all peak areas. Peak position, peak width, and Gaussian fraction were fixed at the same values previously used for Li-humate spectra. Again, excellent fits were obtained.

The fractional areas of most synthetic peaks are constant with respect to the total divalent cation concentration (Figures 39, 40, and 41). Only the peak at 1626 cm^{-1} exhibits a clear dependence on the concentration of Mg^{2+} , Ca^{2+} , or Ba^{2+} . The apparent increase in the relative area of this peak, however, is almost certainly an artifact related to cation-solvent interaction. The position of this peak coincides with the positive part of the previously-discussed artifact in Figure 37b. In addition, the strength of the dependence and the ability to disrupt hydrogen-bonding in water follow the same order, $\text{Mg}^{2+} < \text{Ca}^{2+} < \text{Ba}^{2+}$. For Mg and Ba, the increase at 1626 cm^{-1} does not coincide with the sharp absorbance (total area) decrease. In the Mg series, the increase in the fractional area of the 1626 cm^{-1} peak begins near $1\text{ mmol Mg}^{2+}/\text{g HA}$ and gradually continues as the total Mg^{2+} concentration increases. In the Ca series, a concentration of $1.5\text{ mmol Ca}^{2+}/\text{g HA}$ is required before changes in the relative area of the 1626 cm^{-1} peak are noticeable. In the Ba^{2+} series, the relative area of the 1626 cm^{-1} peak does not increase until *after* the break in the total area curve ($2.0\text{ mmol Ba}^{2+}/\text{g HA}$). The relative increase in the 1626 cm^{-1} peak,

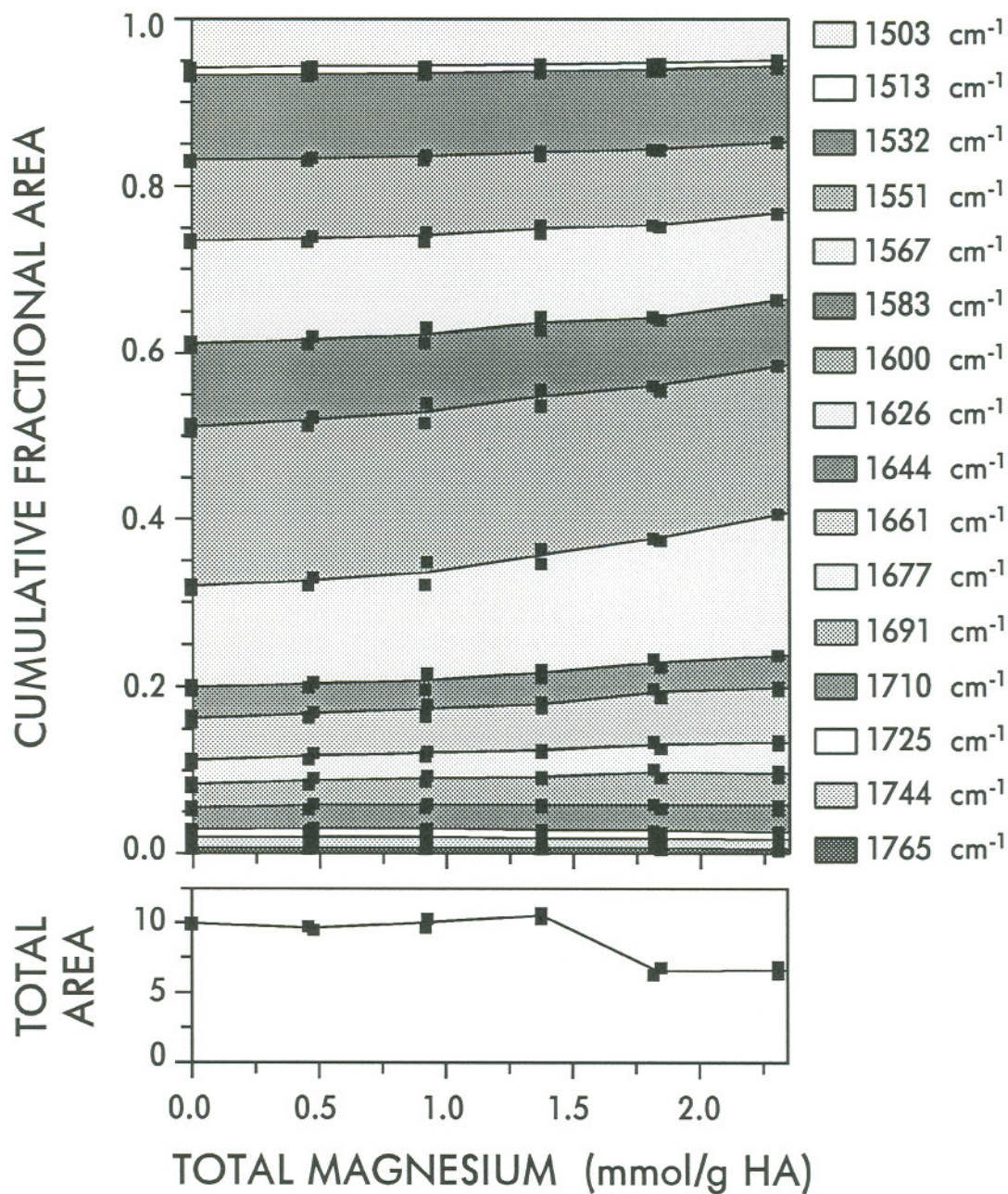


Figure 39. The dependence of the fitted synthetic peak areas on the total Mg^{2+} concentration for 12 aqueous Li-humate samples. Peak areas are normalized to the total area shown in the lower plot, and are displayed **cumulatively**. Because the areas are stacked, the ordinate values are arbitrary and comparisons should be based upon the height of the layer not the position.

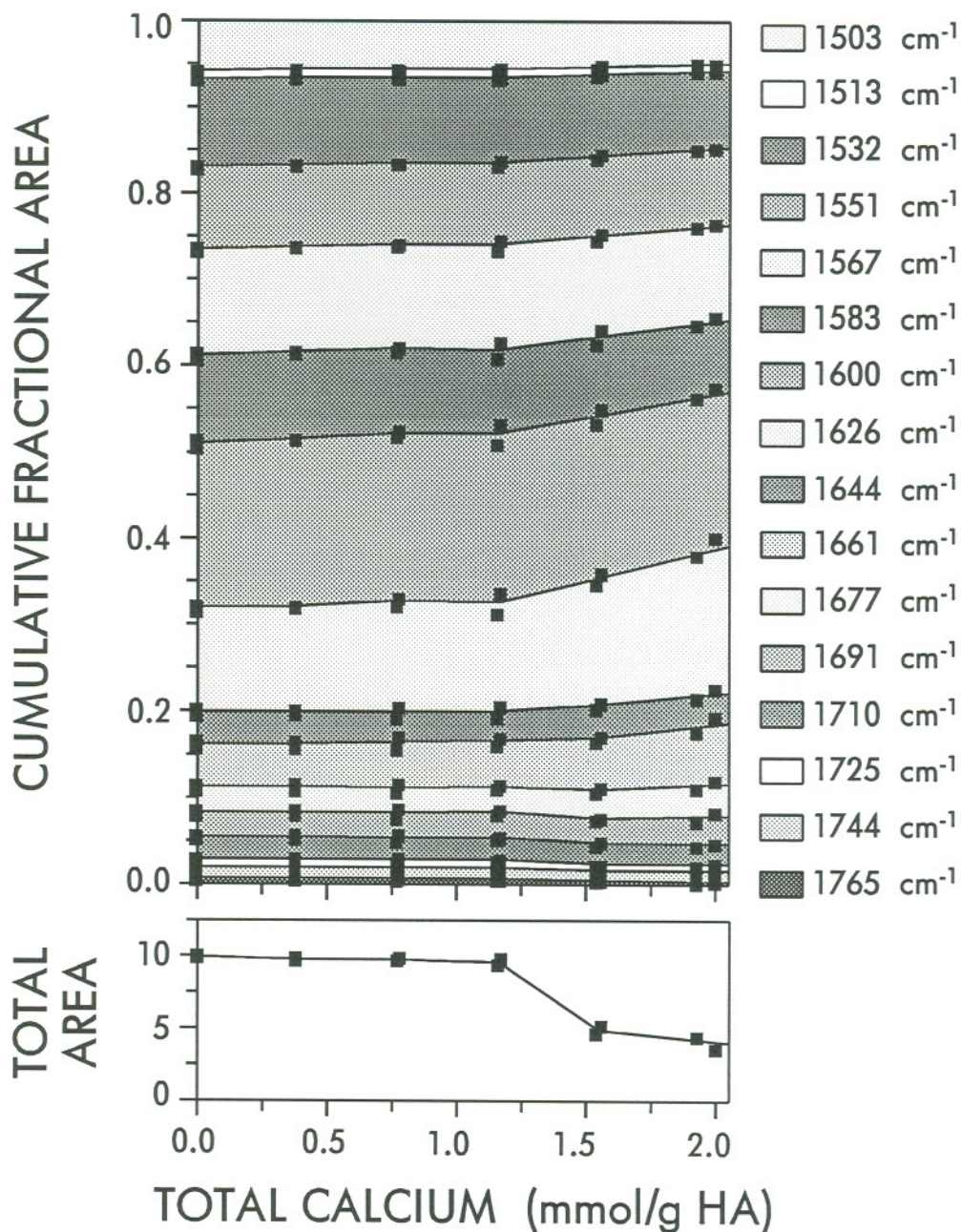


Figure 40. The dependence the fitted synthetic peak areas on the total Ca^{2+} concentration for 12 aqueous Li-humate samples. Peak areas are normalized to the total area shown in the lower plot, and displayed **cumulatively**. Because the areas are stacked, the ordinate values are arbitrary and comparisons should be based upon the height of the layer not the position.

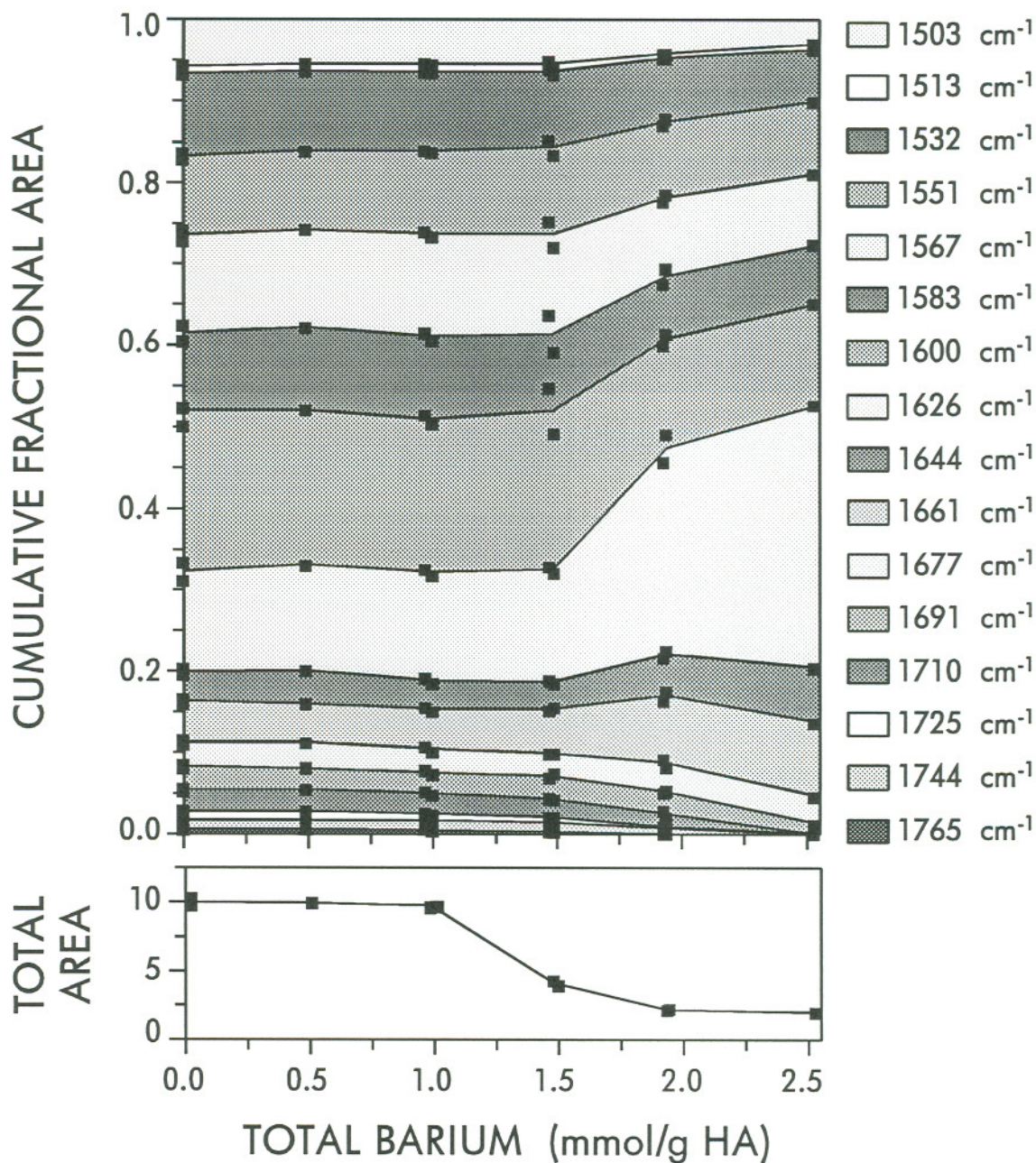


Figure 41. The dependence the fitted synthetic peak areas on the total Ba²⁺ concentration for 10 aqueous Li-humate samples. Peak areas are normalized to the total area shown in the lower plot, and displayed as **cumulatively**. Because the areas are stacked, the ordinate values are arbitrary and comparisons should be based upon the height of the layer not the position.

therefore, is probably not associated with changes in humic structure. Rather, it is an artifact indicating that the free cation concentration is greatest for Mg^{2+} and least for Ba^{2+} . This interpretation is consistent with previous experiments by (VAN DEN HOOP and VAN LEEUWEN, 1990) who showed that Ba^{2+} associated with humic matter more than did Ca^{2+} . The argument that the increase in the relative area of the 1626 cm^{-1} peak is due to imperfect solvent subtraction is supported by decreases in the relative peak areas at 1765, 1744, 1725, and 1710 cm^{-1} in the Ba^{2+} series. Recall that the solvent artifact ($1780\text{-}1580\text{ cm}^{-1}$) consists of both positive and negative features (Figure 37b). When the humic spectrum is superimposed on this artifact, relative increases and decreases must occur in the regions $1670\text{-}1580\text{ cm}^{-1}$ and $1780\text{-}1670\text{ cm}^{-1}$, respectively. Because Mg^{2+} and Ca^{2+} disrupt the structure of water less than does Ba^{2+} , the relative decreases between 1800 and 1670 cm^{-1} are smaller in the Mg^{2+} and Ca^{2+} series.

Several experiments were performed to determine if the presence of alkaline earth cations alters the pH-dependence of humic spectra. Four series of humate solutions were prepared (Li-, (Mg+Li)-, (Ca+Li)-, and (Ba+Li)-humates); each series was comprised of 3 solutions of different total acidity. The total Mg^{2+} , Ca^{2+} , or Ba^{2+} concentrations were sufficient to produce spectra with sharply reduced absorbance. The pH values differed for each cation series because of the influence of the additional divalent cation; the net acidities were the same. Difference spectra were constructed for each series by subtracting the spectrum of the most acidic sample in the series from the spectra of the other two samples of lower acidity. The overall shape of the difference spectra is similar for Li^+ and the three divalent cations (Figure 42). No peak positions change, no peaks are absent, and no new peaks emerge. The amplitudes of the spectra, however, decrease in the order $\text{Li}^+ > \text{Mg}^{2+} > \text{Ca}^{2+} > \text{Ba}^{2+}$. The magnitude of the negative band near 1630 cm^{-1} , however, seems little affected by the addition of divalent cations. The relative constancy of this negative band indicates the presence of an absorbance peak that is most intense at low pH

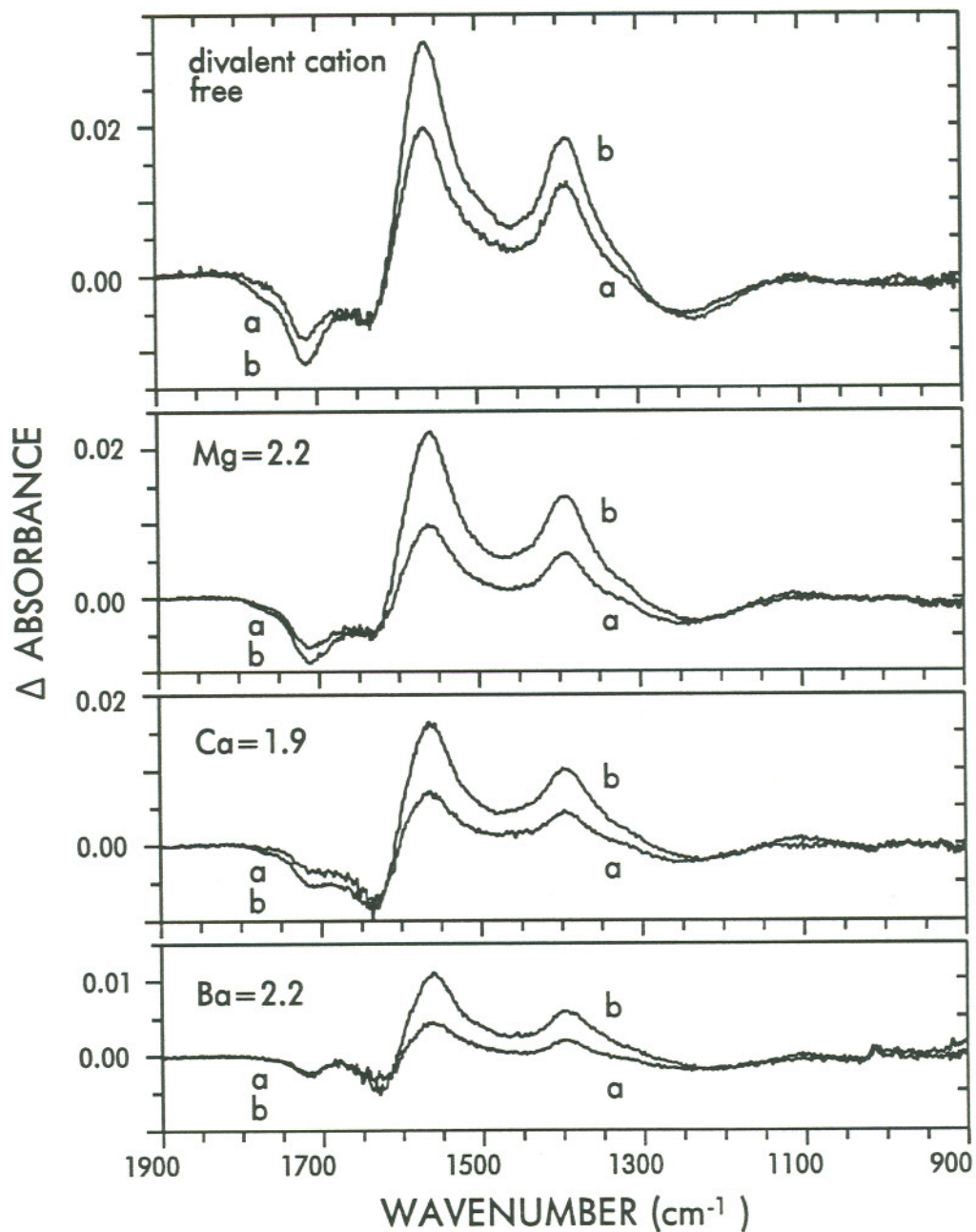


Figure 42. Four series of difference spectra formed by subtracting the aqueous spectrum of the most acidic sample in the series from the spectra of samples with higher pH. Only the features that change with pH are visible. Three of series contain divalent cations as indicated; total divalent cation concentrations are given units of mmol/g HA. Li (divalent cation free): a) pH 6.2 – 4.2, b) pH 9.1 – 4.2; Mg: a) pH 5.1 – 3.5, b) pH 7.6 – 3.5; Ca: a) pH 5.1 – 3.3, b) pH 7.9 – 3.3; Ba: a) pH 4.9 – 3.0, b) pH 7.7 – 3.0. The pH values are different for each cation series because of the influence of the additional divalent cation; the net acidities are the same. Humic acid concentration: 37 mg/mL; Total Li: 4.5 mmol/g HA for each series.

(pH < 4), and either absent or weaker and unchanging at higher pH (pH > 5). This peak is very near an intense solvent peak (1640 cm^{-1}) and could have easily resulted from a very small wavenumber shift in the water spectrum. Humic-free dilute acid solutions (pH 2-3) did not exhibit artifact peaks; however, the metal cations, H^+ , and humic matter may act in concert to disrupt hydrogen bonding in the water solvent.

The positions of the second derivative peaks of the (Mg+Li)-, (Ca+Li)-, and (Ba+Li)-humate spectra were very reproducible for solutions with pH > 4 and matched those of the Li-humate second derivatives. For (Ca+Li)- and (Ba+Li)-humate solutions with a low pH (~ 3), however, the absorbance in the COO^- region was extremely weak and second derivative peaks could not be discerned from noise. Synthetic spectra were not created due to the uncertain peak positions for the high acidity samples.

The infrared spectra of humic solutions containing alkaline earth cations paint a very consistent, but odd, picture. The humic material sampled by CIR-FTIR is little changed by the presence of Mg^{2+} , Ca^{2+} , or Ba^{2+} . The changes in the relative areas of absorbance peaks can be explained by solvent related artifacts. The pH-dependence of the spectra remains unchanged from that of Li-humate. At sufficiently high concentrations, however, the alkaline earth cations cause a significant fraction of the humic material to be undetectable in the mid-infrared region. The possibility that interactions between divalent cations and the humic molecule are able to shift the absorbance of every infrared-active humic structure outside of the $4000\text{-}800\text{ cm}^{-1}$ range is remote. Therefore, the decrease in absorbance is probably a physical, rather than a chemical, effect. This conclusion is supported by observations of viscosity differences among the humic solutions.

The viscosities of the humic solutions suddenly increased to an almost gelatinous state as the divalent cation concentration increased. The abrupt viscosity increase coincided with the sharp absorbance decrease in the humic

spectrum. The sharp changes in viscosity and absorbance also share other characteristics: increases in the divalent cation concentration beyond the threshold value had little effect, and the change was greatest for Ba^{2+} and smallest for Mg^{2+} . Quantitative viscosity measurements of more dilute humic solutions showed a similar relationship with the Ba^{2+} concentration. In these more dilute humic solutions, however, the abrupt viscosity increase was associated with a higher Ba^{2+}/HA ratio.

The changes in viscosity suggest that the dramatic decrease in infrared absorbance arises from intermolecular coordination of the humic material, which impairs the interactions between the ZnSe crystal and the humic sample. Inadequate contact between the crystal and the sample or the presence of bubbles would not result in reproducible spectra and can be ruled out. Gel formation due to cross-linking of the humic molecules by coordination with divalent cations is consistent with the sudden viscosity change. Such a reaction would depend on both humic and divalent cation concentrations. Interactions between a gelatinous humic phase and the ZnSe crystal could be impaired by the increased hydration of a gel phase, effectively decreasing the humic concentration near the crystal and yielding a spectrum similar to that of a more dilute aqueous phase humic solution. The size of the gel coagulate could also limit contact with the ZnSe crystal. In addition, if the aqueous phase humic matter is more attracted to the ZnSe crystal than is the gelatinous humic matter, the gel phase could be preferentially excluded. Unfortunately, the IR spectra shed little light on the changes induced by divalent cations because the structures that changed are no longer visible in the spectra.

CONCLUSIONS

CIR-FTIR methods were used to acquire the infrared spectra of aqueous humic material in the presence of alkali metal and alkaline earth cations over a range of pH values. Many of the chemical structures within the humic molecule

were clearly visible in these spectra, including COOH and COO⁻, aliphatic C-H, and aromatic rings. The following conclusions concerning the hydrated humic acid molecule and its interactions with alkali metal and alkaline earth cations can be drawn from this spectroscopic study.

1) *COOH/COO⁻*. The spectral changes associated with COOH dissociation were clearly observed with CIR-FTIR. Difference spectra and fitted synthetic spectra showed evidence of partial COOH dissociation at low pH (~3) and incomplete dissociation at high pH (~8). The intensity of the COOH peak in the absorbance spectrum was not an accurate indicator of complete dissociation because of other overlapping peaks. In addition, the extinction coefficient for the C=O stretch in COOH (~1710 cm⁻¹) was much smaller than those for either asymmetric or symmetric COO⁻ stretching.

Although CIR-FTIR provides useful information about the acid-base behavior of carboxyl groups, the infrared spectra cannot be used to directly quantify humic carboxyl content. Peaks in the humic spectra were highly overlapped, including COOH and COO⁻. Some COOH and COO⁻ may even overlap each other. Due to this superposition of peaks, calculation of peak areas directly from absorbance spectra does not yield an accurate measure of COOH or COO⁻ groups.

2) *Alkali metal cations*. Spectra of humic solutions containing three different alkali metal cations did not differ significantly from each other. Aqueous Na⁺ and K⁺ affect the water solvent and cause spectral artifacts due to imperfect background subtraction. The magnitude of this artifact depends upon the free Na⁺ or K⁺ concentration and is a qualitative measure of humic-cation association. The spectral similarities indicate that Li⁺, Na⁺, or K⁺ associate with humic matter via the same mechanism.

3) *Alkaline earth cations*. At low concentration, neither Mg²⁺, Ca²⁺, nor Ba²⁺ altered the spectra of Li-humate. Under these conditions, the mechanism of cation-humate association must be essentially the same for alkaline earth and

alkali metal cations. Spectral artifacts due to solvent-cation interactions provided indirect evidence that the fraction of the total cation associated with humate was greatest for Ba^{2+} and smallest for Mg^{2+} .

As the divalent cation concentration increased, the intensity of the humic spectrum abruptly decreased to a nearly constant low absorbance. The absorbance decrease was greatest for Ba^{2+} and smallest for Mg^{2+} . A simultaneous dramatic increase in the viscosity of the humic solution was also observed. Despite the dramatic physico-chemical changes, the relative intensities of peaks in the humic spectrum remained unchanged. This unusual behavior may be due to the formation of a gel phase which is not well-sampled by the ZnSe crystal. Mg^{2+} , Ca^{2+} , or Ba^{2+} could cause gel formation by cross-linking humic molecules, most likely through COO^- groups.

4) *Resolution enhancement.* The calculation of second derivative spectra and dramatically improved the resolution the highly overlapping peaks in humic spectra. Peak widths and areas could not be determined from the second derivatives, but curve fitting techniques provided estimates of these parameters. These fitted values were not unique, but did provide useful, semi-quantitative information about relative changes in peak magnitude as a function of solution pH. At this time, the synthetic peaks cannot be definitively correlated with specific chemical structures and some peaks almost certainly represent multiple functional groups.

5) *Spectral artifacts.* Aqueous cations can alter the extent of hydrogen-bonding in the water solvent, thus causing changes in the position or width of the absorption bands of water. Such changes in the water spectra induce artifacts in the humic spectra that correlate with the free cation concentration. Artifacts are most intense at low pH because the free cation concentration is highest in that region. As the pH increases, a greater fraction of the metal cations is associated with the humic material. Artifacts were negligible for Li^+ , but were clearly observed in spectra containing the other

cations with the effect increasing in the order $\text{Na}^+ < \text{K}^+$, and $\text{Mg}^{2+} < \text{Ca}^{2+} < \text{Ba}^{2+}$. Even small changes in the water background spectrum can significantly distort the aqueous humic spectrum. The potential for artifacts, therefore, must be assessed by examining humic-free solutions of the cations of interest.

In general CIR-FTIR was a reliable method which generated highly reproducible spectra of humic matter. The ability to obtain spectra in aqueous solution is a particular advantage. The greatest drawbacks are common to all humic IR spectra: poor resolution of overlapping peaks, and the inability to definitively correlate each peak with a chemical structure. These problems are at least partially inherent to the study of naturally heterogeneous humic matter and therefore cannot be completely overcome. A judicious choice of derivatization reactions might help in correlating peaks with chemical structures. Resolution enhancement by Fourier self-deconvolution may be helpful. A more sensitive FTIR detector (*e.g.*, Hg-Cd-Te) would decrease the apparent noise, especially near regions where water absorbs intensely. Curve fitting is a promising technique for extracting quantitative information from humic spectra. We feel that combining CIR-FTIR and curve-fitting with these other techniques could prove to be very powerful and could help elucidate the mechanisms of humic-cation interaction in aqueous solution.

REFERENCES

- BAES A.U. and BLOOM P.R. (1989) Diffuse reflectance and transmission Fourier transform infrared (DRIFT) spectroscopy of humic and fulvic acids. *Soil Sci. Soc. Am. J.* **53**, 695-700.
- BELLAMY L.J. (1975) *The Infrared Spectra of Complex Molecules*. Chapman and Hall.
- BELLAMY L.J. (1980) *The Infrared Spectra of Complex Molecules, Vol. 2*. Chapman and Hall.
- BONN B.A. and FISH W. (1991) The variable nature of humic carboxyl content. *Environ. Sci. Technol.* **25**, 232-240.

BOYD S.A., SOMMERS L.E. and NELSON D.W. (1980) Changes in the humic acid fraction of soil resulting from sludge application. *Soil Sci. Soc. Am. J.* **44**, 1179-1186.

BOYD S.A., SOMMERS L.E. and NELSON D.W. (1981) Copper(II) and iron(III) complexation by the carboxylate group of humic acid. *Soil Sci. Soc. Am. J.* **45**, 1241-1242.

BYLER D.M., GERASIMOWICZ W.V., SUSI H. and SCHNITZER M. (1987) FTIR spectra of soil constituents: fulvic acid and fulvic acid complex with ferric ions. *Appl. Spec.* **41**, 1428-1430.

CABANISS S.E. (in press) *Anal. Chim. Acta*

FISH W., DZOMBAK D.A. and MOREL F.M.M. (1986) Metal-humate interactions. 2. Application and comparison of models. *Environ. Sci. Technol.* **20**, 676-683.

GAMBLE D.S., UNDERDOWN A.W. and LANGFORD C.H. (1980) Copper(II) titration of fulvic acid ligand sites with theoretical, potentiometric, and spectrophotometric analysis. *Anal. Chem.* **52**, 1901-1908.

GERASIMOWICZ W.V., BYLER D.M. and PIOTROWSKI E.G. (1983) Infrared spectroscopic characterization of sludges and sludge extracts: comparison of several mild extraction procedures.

IBARRA J.V. (1989) Fourier transform infrared studies of coal humic acids. *Sci. Total Environ.* **81/82**, 121-128.

MACCARTHY P. and MARK H.B.JR. (1975) Infrared studies on humic acid in deuterium oxide: I. Evaluation and potentialities of the technique. *Soil Sci. Soc. Am. Proc.* **39**, 663-668.

MACCARTHY P., MARK H.B.JR. and GRIFFITHS P.R. (1975) Direct measurement of the infrared spectra of humic substances in water by Fourier transform infrared spectroscopy. *J. Agric. Food Chem* **23**, 600-602.

MACCARTHY P. and RICE J.A. (1985) Spectroscopic methods (other than NMR) for determining the functionality in humic substances. In *Humic Substances in Soil, Sediment, and Water* (eds. G.R.AIKEN, D.M.McKNIGHT, R.L. WERSHAW, and P.MACCARTHY), Chap.21, pp.527-559. Wiley-Interscience.

MADDAMS W.F. (1980) The scope and limitations of curve fitting. *Appl. Spec.* **34**, 245-267.

- MARCHAND P. and MARMET L. (1983) Binomial smoothing filter: a way to avoid some pitfalls of least-squares polynomial smoothing. *Rev. Sci. Instrum.* **54**, 1034-1041.
- PAINTER P.C., SNYDER R.W., STARSINIC M., COLEMAN M.M., KUEHN D. and DAVIS A. (1981) Concerning the application of FTIR to the study of coal: a critical assessment of band assignments and the application of spectral analysis programs. *Appl. Spec.* **35**, 475-485.
- PAXÉUS N. and WEDBORG M. (1985) Acid-base properties of aquatic fulvic acid. *Anal. Chim. Acta* **169**, 87-98.
- PERDUE E.M., REUTER J.H. and PARRISH R.S. (1984) A statistical model of proton binding by humus. **48**, 1257-1263.
- PIERCE J.A., JACKSON R.S., VAN EVERY K.W., GRIFFITHS, P.R. and HONGJIN G. (1990) Combined deconvolution and curve fitting for quantitative analysis of unresolved spectral bands. **62**, 477-484.
- PRICE W.J. (1972) Sample handling techniques. In *Laboratory Methods in Infraed Spectroscopy* (Eds. R.G.J. MILLER and B.C. STACE) Chap. 8. pp. 115-121.
- SENESI N., MIANO T.M., PROVENZANO M.R. and BRUNETTI G. (1989) Spectroscopic and compositional comparative characterization of IHSS reference and standard fulvic and humic acids of various origins. *Sci. Total Environ.* **81/82**, 143-156.
- SENESI N., SPOSITO G., and MARTIN J.P. (1986) Copper(II) and iron(III) complexation by soil humic acids: an IR and ESR study. *Sci. Total Environ.* **55**, 351-362.
- STARSINIC M., OTAKE Y., WALKER P.L.JR., and PAINTER P.C. (1984) Application of FT-i.r. spectroscopy to the determination of COOH groups in coal. *Fuel* **63**, 1002-1007.
- STEVENSON F.J. and GOH K.M. (1971) Infrared spectra of humic acids and related substances. *Geochim. Cosmochim. Acta* **35**, 471-483.
- STEVENSON F.J. and GOH K.M. (1974) Infrared spectra of humic acids: elimination of interference due to hygroscopic moisture and structural changes accompanying heating with KBr. *Soil Science* **117**, 34-41.
- SUSI H. and BYLER D.M. (1983) Protein structure by Fourier transform infrared spectroscopy: second derivative spectra. *Biochem. Biophys. Res. Comm.* **115**, 391-397.

TACKETT J.E. (1989) FT-IR Characterization of metal acetates in aqueous solution. *Appl. Spec.* **43**, 483-489.

TIMASHEFF S.N. (1972) Infrared titration of lysozyme carboxyls. *Archives Biochem. Biophys.* **150**, 318-323.

TOMITA K., ANDO T. and UENO K. (1965) Infrared spectra of nitrilotriacetate chelates in aqueous solution. *J. Phys. Chem.* **69**, 404-407.

VAN DEN HOOP M.A.G.T. and VAN LEEUWEN H.P. (1990) Study of the polyelectrolyte properties of humic acids by conductimetric titration. *Anal. Chim. Acta* **232**, 141-148.

YONEBAYASHI K. and HATTORI T. (1989) Chemical and biological studies on environmental humic acids II. ^1H -NMR and IR spectra of humic acids. *Soil Sci. Plant Nutrit.* **35**, 383-392.

CHAPTER VI

Summary

CONCLUSIONS

Every experimental result described in this work reflects the common characteristic of humic matter: heterogeneity. Heterogeneity influences all aspects of humic chemistry and its importance cannot be under-appreciated. Titrations of humic matter do not yield information concerning the association of either protons or metal cations with specific functional groups because all such groups react simultaneously. The extent of association may differ for each group, but only the total association is observable. Similarly, infrared spectra represent the humic molecule in its entirety. The absorbance bands corresponding to individual humic functional groups overlap each other and prevent the direct quantitation of individual features.

Humic association with alkali metal and alkaline earth metal cations

Both the wet-chemical experiments and the infrared spectra indicate that significant amounts of alkali metal cations associate with humic acid, and that the absolute amount of humic-associated cation depends on the solution alkalinity, rather than the cation concentration. These results were directly measured by discontinuous titration, and indirectly observed in the magnitude

of solvent-electrolyte artifacts in the IR spectra. Similarly, both experimental methods indicate that Li^+ , Na^+ , and K^+ behave equivalently and are essentially interchangeable. Humic infrared spectra were unaffected by the alkali metal cation identity, except for solvent artifact effects. In the discontinuous titrations, Li^+ , Na^+ , and K^+ competed equally. The results suggest a diffuse layer model for the association of alkali metal cations with humic matter. Cations in the diffuse layer do not form coordination complexes with the humate polyion, but are held near the humic structure by electrostatic attraction. Together, the diffuse layer and the humate polyion are electrically neutral. The diffuse layer is linked to the bulk solution by a Donnan equilibrium, and cations in the diffuse layer are very exchangeable.

A very small amount of site-specific binding of Na^+ and K^+ may also occur as evidenced by the desorption experiments at pH 1. The small extent of such binding prohibited confirmation by infrared spectroscopy. The number of sites was greater for K^+ than for Na^+ , indicating that the size of the hydrated cation is probably important. Large, highly-hydrated cations may be sterically excluded. The hydrated cation size decreases in order of molecular weight: $\text{Li}^+ > \text{Na}^+ > \text{K}^+$. No site-specific binding of Li^+ was detected.

The results of this study indicate that in certain situations alkali metal cations could affect the binding and transport of trace metal cations. Alkali metal cations will not compete with trace metal cations for specific sites, but will successfully exchange with any trace cations in the diffuse layer. The cation speciation in the diffuse layer will depend upon that in the bulk solution. In fresh water systems, the aqueous Na^+ or K^+ concentration might be low enough for a significant fraction of the trace metal cations to populate the diffuse layer. Upon an increase in the Na^+ concentration, such as might occur in an estuary, these trace cations would be released to the bulk solution.

The association of humic matter with alkaline earth cations is similar to that with alkali metal cations, but includes an additional mechanism. The

infrared spectra of humic solutions containing low concentrations of alkaline earth metal cations are essentially identical to those of humic solutions containing only alkali metal cations. Unlike the alkali metal cations, however, humic matter exhibits a preference among the alkaline earth cations, even at low concentration. The amount of humic-associated cation decreased in the order $\text{Ba}^{2+} > \text{Ca}^{2+} > \text{Mg}^{2+}$. The humic infrared spectra were mostly unaffected (except for solvent-electrolyte artifacts) by increases in the alkaline earth metal concentration until a threshold concentration was reached. At that concentration, the spectral intensity abruptly decreased and the solution became very viscous. The threshold concentration depended upon the humic acid concentration and the alkaline earth cation identity: Ba^{2+} was the most effective, then Ca^{2+} , then Mg^{2+} . The physical aspect of these changes and their precipitous nature suggest a conformational alteration. Because the alkaline earth cations could initiate this change and the alkali metal cations could not, cross-linking through the divalent cations might be responsible. Unfortunately, CIR-FTIR spectra offer little insight into this association mechanism because the altered humic matter is apparently "infrared invisible" to the ZnSe crystal.

CIR-FTIR of aqueous samples

Perhaps the most valuable aspect of my work is the description and evaluation of methods to acquire and analyze the infrared spectra of aqueous humic solutions. These methods are general and can be applied to a variety of environmentally relevant molecules. Because such molecules in their natural state are almost always hydrated, it is absolutely essential to use aqueous samples. Aqueous CIR-FTIR is an attractive method because sample handling is very easy and background subtraction seems to be very straightforward. This method can produce reliable, artifact-free difference spectra, but the process is not quite as simple as it initially appears.

To produce high quality difference spectra, the CIR accessory cannot be moved between the acquisition of the solution and background spectra. A background spectrum should be obtained for each sample, and, if possible, the background solution should match the bulk aqueous solution concentration. The infrared spectrum of water is altered by the presence of dissolved electrolytes. Any differences between the background solution spectrum and the bulk aqueous solution spectrum will appear as artifacts in the solute difference spectrum. To minimize such artifacts, Li^+ reagents should be used because Na^+ and K^+ disrupt the hydrogen bonding in water more than does Li^+ . An objective algorithm for spectral subtraction is required. Small errors in the choice of the scaling factor for background subtraction cause large errors in the difference spectra. The only method that insures a reproducible and optimal choice for the scaling factor is a statistically-based optimization routine.

Because the infrared absorbance peaks of individual humic functional groups are so highly overlapped direct peak quantitation is impossible. Resolution enhancement and curve fitting are promising techniques that can be used to analyze these spectra. Overlapping features were partially resolved in the second derivative spectrum. Peaks identified in the second derivative spectrum were then used in a curve-fitting routine to create synthetic humic spectra. The synthetic spectra are not unique, but do constitute a first estimate of resolved spectral features.

IMPLICATIONS FOR FURTHER RESEARCH

As is true of most scientific investigations, I find myself with more questions at the end of this work than I had at the beginning. These are suggestions for anyone who decides to continue this work.

Of the alkali metal cations, Li^+ seems to be the most inert. The use of LiOH in place of NaOH or KOH is advised for work with humic materials (including the initial fractionation procedure) and for aqueous infrared

spectroscopy. In addition, the lack of specific interactions between Li^+ and humic matter may allow it to be used to investigate the diffuse layer model more thoroughly. A set of experiments could be designed to investigate the diffuse layer through its dependence on Li^+ concentration, ionic strength, humic acid concentration, and alkalinity. A statistical optimization routine could be used to fit the diffuse layer model to the data and to calculate optimal values of humic charge and diffuse layer volume.

The aqueous infrared study of humic acid could be continued in a variety of ways. Well-characterized, site-specific derivatization or complexation reactions could be used prior to infrared analysis to help identify humic functional groups. Fourier self-deconvolution could be applied to humic spectra to improve resolution, investigate peak shape, and provide better constraints for fitting synthetic peaks. Fourier self-deconvolution of humic spectra would require the use of a detector that is more sensitive than a DTGS.

APPENDIX A

Computer Programs to Model Humic Carboxyl Acidity

Humic acid functional groups can be modeled with a set of discrete pK values or a continuous pK distribution. The computer programs included here were used to predict solution speciation for the acetate method of humic carboxyl content determination (Chapter II). All three programs were written in BASIC 7.1 (Microsoft, Redmond, WA). Input data is obtained from the keyboard at run time. The first two programs, DISCRETE.BAS and NORMAL.BAS, calculate the solution speciation for a set of discrete pK values and a set of continuous normal pK distributions, respectively. The pK values (mean and standard deviation for NORMAL.BAS) and the fractional pK composition must be provided. In addition, the normal distribution is truncated at pK values provided by the user. The concentration of acetate and humic carboxyl groups must be provided in units of molarity. Multiple humic carboxyl concentrations may be given for each run. All input is obtained via the keyboard and prompted by a screen message. Output is written to a file, the name of which is provided by the user. DISCRETE.BAS produces two output files. The suffix ".DAT" will be appended to the user-provided output file name and contains the output data in table format suitable for input to a graphing

program. The third program, SPEC-PDF.BAS, calculates the probability distribution function for total HA and for A⁻ at a given pH.

DISCRETE.BAS

```

DEFDBL A-Z
DIM A(20), HA(20), frac(20), per(20), logK(20), K(20)

/ ***** DEFINE CONSTANTS AND FORMAT STRINGS *****
Kac = 10# ^ (-4.74)
Kw = .000000000000001#
format1$ = "##.### "
format2$ = "##.###^ ^ ^ "

/ ***** COLLECT INPUT FROM THE SCREEN *****
10 CLS
PRINT "*** HUMIC ACID / ACETATE INTERACTIONS ***"
PRINT "      Discrete pK Distribution"
PRINT
INPUT ; "Number of Humic Acid ligands: ", num
LOCATE , 1: PRINT SPC(40); : LOCATE , 1
PRINT " #      log(Ka)      % of total"
PRINT " -----"
total = 0#
FOR i = 1 TO num
  PRINT USING " ##"; i;
  LOCATE , 11: INPUT ; "", logK(i)
  K(i) = 10# ^ (logK(i))
  IF num = 1 THEN
    per(i) = 100: LOCATE , 26: PRINT "100"
  ELSE
    LOCATE , 26: INPUT "", per(i)
  END IF
  frac(i) = per(i) / 100#
  total = total + per(i)
NEXT i
IF ABS(100# - total) > 1 THEN
  PRINT : PRINT "Percent total does not equal 100."
  GOTO 200
END IF
PRINT
INPUT "Normality of NaOAc: ", Na
INPUT "Starting Molarity of Humic Acid: ", Astart
INPUT "Ending Molarity of Humic Acid: ", Aend
INPUT "Total number of HA concentrations: ", Anum
PRINT
INPUT ; "File name for output: ", file$
data$ = file$ + ".dat"

/ ***** OPEN OUTPUT FILES AND WRITE HEADINGS *****
OPEN file$ FOR OUTPUT AS #1
OPEN data$ FOR OUTPUT AS #2
PRINT #1, "HUMIC CARBOXYL CONTENT BY ACETATE METHOD SIMULATION"
PRINT #1, "Humic Model: Discrete pK Values": PRINT #1,
PRINT #1, "Date = "; DATE$
PRINT #1, "Time = "; TIME$: PRINT #1,
PRINT #1, USING "&##.###&"; "Acetate Concentration: "; Na; " M"
PRINT #1, USING "&##"; "Number of Ligand Types: "; num
PRINT #1,
PRINT #1, "      Log(K)          K          percent"
PRINT #1, " -----"
FOR i = 1 TO num
  PRINT #1, USING " ##.##### #.###^ ^ ^ ##.###"; logK(i); K(i); per(i)

```

```

NEXT i
PRINT #1,

' CALCULATE SPECIATION FOR EACH VALUE OF TOTAL HUMIC ACID
logAstart = LOG(Astart) / LOG(10#)
logAend = LOG(Aend) / LOG(10#)
FOR j = 1 TO Anum
  IF Anum = 1 THEN
    logAtot = logAstart
  ELSE
    logAtot = logAstart + (j - 1) * (logAend - logAstart) / (Anum - 1)
  END IF
  Atot = 10# ^ (logAtot)
  PRINT #1,
  PRINT #1, USING "&&#.#####^&&"; RTRIM$(LTRIM$(STR$(j))); ". total HA = "; Atot; " M"
' Estimate the ionic strength.
Iest = Na
PRINT #1, USING "&&#.#####&"; "Estimate of Ionic Strength: "; Iest; " M"
LOCATE 1, 50: PRINT USING "&&#.#####&"; " I = "; Iest; " M"
' Calculate activity coefficients.
GOSUB COEFF
PRINT #1, USING "&&#.#####&"; "Activity coefficient: "; c1: PRINT #1,
LOCATE 2, 50: PRINT USING "&&#.#####&"; " gamma = "; c1
' Loop until an answer is found.
DO
' Calculate the residual at the first guess, pH = 3.00
pH1 = 3#
H = (10# ^ (-pH1)) / c1
GOSUB CALC
r1 = residual
' Calculate the residual at the second guess, pH = 10.00
pH2 = 10#
H = (10# ^ (-pH2)) / c1
GOSUB CALC
r2 = residual
IF r1 * r2 >= 0# THEN PRINT "Root not bracketed between pH 3 & 10. Program Stopped.": STOP
' Use the bisection method to find the root.
DO
  pH3 = (pH1 + pH2) / 2#
  H = (10# ^ (-pH3)) / c1
  GOSUB CALC
  r3 = residual
  IF r3 = 0# THEN EXIT DO
  IF r1 * r3 < 0# THEN
    pH2 = pH3
  ELSE
    pH1 = pH3: r1 = r3
  END IF
LOOP WHILE ABS(pH2 - pH1) > .00001#
pH = (pH1 + pH2) / 2#
pcH = pH + LOG(c1) / LOG(10#)
LOCATE 3, 50: PRINT USING "&&#.#####&"; " pH = "; pH
LOCATE 4, 50: PRINT USING "&&#.#####&"; " pcH = "; pcH
PRINT #1, USING "&&#.#####&"; " pH = "; pH
PRINT #1, USING "&&#.#####&"; " pcH = "; pcH
' Calculate the speciation.
H = (10# ^ (-pH)) / c1
OH = Kw / (H * c1 * c1)
HOAc = Na * H * c1 * c1 / (Kac + H * c1 * c1)
OAc = Na * Kac / (Kac + H * c1 * c1)
FOR i = 1 TO num
  HA(i) = frac(i) * Atot * H * c1 * c1 / (K(i) + H * c1 * c1)
  A(i) = frac(i) * Atot * K(i) / (K(i) + H * c1 * c1)
NEXT i
' Print the speciation to file
PRINT #1, USING "&&#.#####^&&"; " [H+] = "; H; " M"
PRINT #1, USING "&&#.#####^&&"; " [OH-] = "; OH; " M"
PRINT #1, USING "&&#.#####^&&"; " [HOAc] = "; HOAc; " M"

```

```

PRINT #1, USING "&##.#####^&"; " [OAc-] = "; OAc; " M"
FOR i = 1 TO num
  PRINT #1, USING "&##.#####^&"; "[HA("; i; ") = "; HA(i); " M"
  PRINT #1, USING "&##.#####^&"; "[A-("; i; ") = "; A(i); " M"
NEXT i
' Calculate the ionic strength and compare to the previous value.
Icalc = H + OH + OAc + Na
FOR i = 1 TO num
  Icalc = Icalc + A(i)
NEXT i
Icalc = Icalc / 2#
PRINT #1, USING "&##.#####"; "Ionic Strength = "; Icalc
PRINT #1,
LOCATE 1, 50: PRINT USING "&##.#####&"; "      I = "; Icalc; " M"
IF (ABS(Iest - Icalc)) / Iest <= .05 THEN
  EXIT DO
ELSE
  Iest = Icalc
' Re-calculate activity coefficients.
  GOSUB COEFF
  LOCATE 2, 50: PRINT USING "&##.#####"; " gamma = "; c1
END IF
LOOP

' Print the speciation to the screen
LOCATE 5, 50: PRINT USING "&##.#####^&"; "      [H+] = "; H; " M"
LOCATE 6, 50: PRINT USING "&##.#####^&"; "      [OH-] = "; OH; " M"
LOCATE 7, 50: PRINT USING "&##.#####^&"; "      [HOAc] = "; HOAc; " M"
LOCATE 8, 50: PRINT USING "&##.#####^&"; "      [OAc-] = "; OAc; " M"
FOR i = 1 TO num
  LOCATE 7 + 2 * i, 50
  PRINT USING "&##.#####^&"; "[HA("; i; ") = "; HA(i); " M";
  LOCATE 8 + 2 * i, 50
  PRINT USING "&##.#####^&"; "[A-("; i; ") = "; A(i); " M";
NEXT i
' Print a file of only data
PRINT #2, USING format2$; CSNG(Atot);
PRINT #2, USING format1$; pH;
PRINT #2, USING format2$; CSNG(H); CSNG(OH); CSNG(HOAc); CSNG(OAc);
FOR i = 1 TO num
  PRINT #2, USING format2$; CSNG(A(i));
NEXT i
FOR i = 1 TO num - 1
  PRINT #2, USING format2$; CSNG(HA(i));
NEXT i
PRINT #2, USING format2$; CSNG(HA(num))
NEXT j
CLOSE

200 LOCATE 25, 1: INPUT ; "Another run? (Y/N) ", A$
IF LEFT$(A$, 1) = "Y" OR LEFT$(A$, 1) = "y" THEN CLEAR : GOTO 10

END

COEFF:
logact = -.5# * (SQR(Iest) / (1# + SQR(Iest))) - .3# * Iest)
c1 = 10# ^ (logact)
RETURN

CALC:
residual = H + Na * H * c1 * c1 / (Kac + H * c1 * c1) - Kw / (H * c1 * c1)
FOR i = 1 TO num
  residual = residual - frac(i) * Atot * K(i) / (K(i) + H * c1 * c1)
NEXT i
RETURN

```

NORMAL.BAS

```

DEFDBL A-Z
DIM x(20), z(20), w(20)

/ ***** DEFINE GAUSS POINTS AND WEIGHTING FACTORS *****
z(0) = 0#: w(0) = .202578241925561#
z(1) = .201194094#: w(1) = .1984314853#
z(2) = .3941513471#: w(2) = .1861610001#
z(3) = .5709721726#: w(3) = .1662692058#
z(4) = .7244177313#: w(4) = .1395706779#
z(5) = .8482065834#: w(5) = .1071592204#
z(6) = .9372733924#: w(6) = .0703660474#
z(7) = .987992518#: w(7) = .030753242#

/ ***** DEFINE OTHER CONSTANTS AND FORMAT STRINGS *****
pi = 3.141592654#
Kw = .00000000000001#
Kac = .00001737801#
format1$ = "##.#### "
format2$ = "##.####^"

/ ***** DEFINE FUNCTIONS THAT PERTAIN TO NORMAL DISTRIBUTION *****
DEF FNnorm (x, mu, sigma)
  con = 1# / (sigma * SQR(2 * pi))
  arg = (-1 * ((x - mu) / sigma) * ((x - mu) / sigma)) / 2#
  FNnorm = con * EXP(arg)
END DEF
DEF FNalpha (x, mu, sigma, frac, H)
  alpha = 10 ^ -x / (10 ^ -x + H * c1 * c1)
  con = 1# / (sigma * SQR(2 * pi))
  arg = (-1 * ((x - mu) / sigma) * ((x - mu) / sigma)) / 2#
  FNalpha = frac * con * alpha * EXP(arg)
END DEF

/ ***** COLLECT INPUT FROM THE SCREEN *****
10 CLS
PRINT "***** HUMIC ACID / ACETATE INTERACTIONS *****"
PRINT "      Continuous Normal pK Distribution"
PRINT
INPUT "Maximum pK allowed: ", upper
INPUT "Minimum pK allowed: ", lower
INPUT "Number of distributions: ", num
PRINT
LOCATE , 1: PRINT SPC(40); : LOCATE , 1
PRINT " #          pK          S.D.      % of total"
PRINT " -----"
total = 0#
FOR i = 1 TO num
  PRINT USING " ##"; i;
  LOCATE , 12: INPUT ; "", pK(i)
  logK(i) = -1 * pK(i)
  k(i) = 10# ^ (logK(i))
  LOCATE , 22: INPUT ; "", SD(i)
  IF num = 1 THEN
    per(i) = 100: LOCATE , 35: PRINT "100"
  ELSE
    LOCATE , 35: INPUT "", per(i)
  END IF
  frac(i) = per(i) / 100#
  total = total + per(i)
NEXT i
IF ABS(100# - total) > 1 THEN
  PRINT : PRINT "Percent total does not equal 100."
  GOTO 200
END IF
PRINT

```

```

INPUT "Molarity of NaOAc: ", Na
INPUT "Starting Molarity of Humic Acid: ", Astart
INPUT "Ending Molarity of Humic Acid: ", Aend
INPUT "Total number of HA concentrations: ", Anum
PRINT
INPUT ; "File name for output: ", file$

/ ***** OPEN OUTPUT FILE AND WRITE HEADINGS *****
OPEN file$ FOR OUTPUT AS #1
PRINT #1, "HUMIC CARBOXYL CONTENT BY ACETATE METHOD SIMULATION"
PRINT #1, "Humic Model: Gaussian pK Distribution": PRINT #1,
PRINT #1, "Date = "; DATE$
PRINT #1, "Time = "; TIME$: PRINT #1,
PRINT #1, USING "&#.###^^^"; "Acetate Concentration: "; CSNG(Na)
PRINT #1, USING "&#.#####"; "Upper pK of normal distribution: "; upper
PRINT #1, USING "&#.#####"; "Lower pK of normal distribution: "; lower
PRINT #1, USING "&#.##"; "Number of Ligand Types: "; num
PRINT #1,
PRINT #1, "      pK          S.D.          percent"
PRINT #1, "-----"
FOR i = 1 TO num
PRINT #1, USING "  ###.#####  #.#####^^^  ###.###"; pK(i); SD(i); per(i)
NEXT i
PRINT #1,
PRINT #1,
PRINT #1, " Total HA    pH    -----    Speciation    -----"
PRINT #1, "              H      OH      HOAc      OAc      A      HA"
PRINT #1, "-----"

/ ***** CALCULATE CORRECTION FACTOR FOR TRUNCATED DISTRIBUTION *****
trun = 1#
FOR c = 1 TO num
tail1 = 0#: tail2 = 0#: k = 0#
DO
  p1 = ((2# * lower) - (2# * k * SD(c)) - SD(c)) / 2#
  p2 = SD(c) / 2#
  x(0) = p1
  sum = w(0) * FNnorm(x(0), pK(c), SD(c))
  FOR i = 1 TO 7
    i1 = (2 * i) - 1
    i2 = 2 * i
    x(i1) = p1 + p2 * z(i)
    sum = sum + w(i) * FNnorm(x(i1), pK(c), SD(c))
    x(i2) = p1 - p2 * z(i)
    sum = sum + w(i) * FNnorm(x(i2), pK(c), SD(c))
  NEXT i
  tail1 = tail1 + p2 * sum
  k = k + 1
LOOP WHILE sum > .0000001#
k = 0
DO
  p1 = (2# * upper + 2# * k * SD(c) + SD(c)) / 2#
  p2 = SD(c) / 2#
  x(0) = p1
  sum = w(0) * FNnorm(x(0), pK(c), SD(c))
  FOR i = 1 TO 7
    i1 = (2 * i) - 1
    i2 = 2 * i
    x(i1) = p1 + p2 * z(i)
    sum = sum + w(i) * FNnorm(x(i1), pK(c), SD(c))
    x(i2) = p1 - p2 * z(i)
    sum = sum + w(i) * FNnorm(x(i2), pK(c), SD(c))
  NEXT i
  tail2 = tail2 + p2 * sum
  k = k + 1
LOOP WHILE sum > .0000001#
trun = trun - frac(c) * (tail1 + tail2)
NEXT c

```

```

***** CALCULATE SPECIATION FOR EACH VALUE OF TOTAL HUMIC ACID *****
logAstart = LOG(Astart) / LOG(10#)
logAend = LOG(Aend) / LOG(10#)
FOR j = 1 TO Anum
  IF Anum = 1 THEN
    logAtot = logAstart
  ELSE
    logAtot = logAstart + (j - 1) * (logAend - logAstart) / (Anum - 1)
  END IF
  Atot = 10# ^ (logAtot)
  ' Estimate the ionic strength.
  Iest = Na
  LOCATE 1, 50: PRINT USING "&##.#####&"; "    I = "; Iest; " M"
  ' Calculate activity coefficients.
  GOSUB COEFF
  LOCATE 2, 50: PRINT USING "&##.#####"; "    gamma = "; c1
  ' Loop until an answer is found.
  DO
    ' Calculate the residual at the first guess, pH = 3.00
    pH1 = 3#
    H = (10# ^ (-pH1)) / c1
    GOSUB CALC
    r1 = residual
    ' Calculate the residual at the second guess, pH = 10.00
    pH2 = 10#
    H = (10# ^ (-pH2)) / c1
    GOSUB CALC
    r2 = residual
    IF r1 * r2 >= 0# THEN PRINT "Root not bracketed between pH 3 & 10. Program Terminated.": STOP
    ' Use the bisection method to find the root
    DO
      pH3 = (pH1 + pH2) / 2#
      H = (10# ^ (-pH3)) / c1
      GOSUB CALC
      r3 = residual
      IF r3 = 0# THEN EXIT DO
      IF r1 * r3 < 0# THEN
        pH2 = pH3
      ELSE
        pH1 = pH3: r1 = r3
      END IF
    LOOP WHILE ABS(pH2 - pH1) > .00001#
    pH = (pH1 + pH2) / 2#
    pcH = pH + LOG(c1) / LOG(10#)
    LOCATE 3, 50: PRINT USING "&##.#####"; "    pH = "; pH
    LOCATE 4, 50: PRINT USING "&##.#####"; "    pcH = "; pcH
    ' Calculate the speciation.
    H = (10# ^ (-pH)) / c1
    GOSUB CALC
    HA = Atot * (1# - al1)
    OAc = Na * Kac / (Kac + H * c1 * c1)
    ' Calculate the ionic strength and compare to the previous value.
    Icalc = (H + OH + A + OAc + Na) / 2#
    LOCATE 1, 50: PRINT USING "&##.#####&"; "    I = "; Icalc; " M"
    LOCATE 2, 50: PRINT USING "&##.#####"; "    gamma = "; c1
    IF (ABS(Iest - Icalc)) / Iest <= .05 THEN
      EXIT DO
    ELSE
      Iest = Icalc
    END IF
    ' Re-calculate activity coefficients.
    GOSUB COEFF
    LOCATE 2, 50: PRINT USING "&##.#####"; "    gamma = "; c1
  END IF
LOOP

' Print the speciation to the screen
LOCATE 5, 50: PRINT USING "&##.#####^&"; "    [H+] = "; H; " M"
LOCATE 6, 50: PRINT USING "&##.#####^&"; "    [OH-] = "; OH; " M"

```

```

LOCATE 7, 50: PRINT USING "&##.####^^^&"; " [HA] = "; HA; " M";
LOCATE 8, 50: PRINT USING "&##.####^^^&"; " [A-] = "; A; " M";
' Print the speciation to the output file
PRINT #1, USING format2$; CSNG(Atot);
PRINT #1, USING format1$; pH;
PRINT #1, USING format2$; CSNG(H); CSNG(OH); CSNG(HOAc); CSNG(OAc); CSNG(A); CSNG(HA)
NEXT j
CLOSE

200 LOCATE 25, 1: INPUT ; "Another run? (Y/N) ", AS
IF LEFT$(AS, 1) = "Y" OR LEFT$(AS, 1) = "y" THEN CLEAR : GOTO 10

END

COEFF:
logact = -.5# * (SQR(Iest) / (1# + SQR(Iest)) - .3# * Iest)
c1 = 10# ^ (logact)
RETURN

CALC:
al1 = 0#
integral = 0#
FOR d = 1 TO num
k = 0#: part = 0#:
DO
lo = lower + k * SD(d)
hi = lo + SD(d)
IF hi > upper THEN hi = upper
p1 = (hi + lo) / 2#
p2 = (hi - lo) / 2#
x(0) = p1
sum = w(0) * FNalpha(x(0), pK(d), SD(d), frac(d), H)
FOR i = 1 TO 7
i1 = (2 * i) - 1
i2 = 2 * i
x(i1) = p1 + p2 * z(i)
sum = sum + w(i) * FNalpha(x(i1), pK(d), SD(d), frac(d), H)
x(i2) = p1 - p2 * z(i)
sum = sum + w(i) * FNalpha(x(i2), pK(d), SD(d), frac(d), H)
NEXT i
part = part + p2 * sum
k = k + 1
LOOP UNTIL hi = upper
integral = integral + part
NEXT d
al1 = integral / trun
A = Atot * al1
HOAc = Na * H * c1 * c1 / (Kac + H * c1 * c1)
OH = Kw / (H * c1 * c1)
residual = HOAc + H - OH - A
RETURN

```

SPEC-PDF.BAS

```

5 DEFDBL A-Z
DIM x(20), z(20), w(20)

' ***** DEFINE GAUSS POINTS AND WEIGHTING FACTORS *****
z(0) = 0#: w(0) = .202578241925561#
z(1) = .201194094#: w(1) = .1984314853#
z(2) = .3941513471#: w(2) = .1861610001#
z(3) = .5709721726#: w(3) = .1662692058#
z(4) = .7244177313#: w(4) = .1395706779#
z(5) = .8482065834#: w(5) = .1071592204#
z(6) = .9372733924#: w(6) = .0703660474#
z(7) = .987992518#: w(7) = .030753242#

' ***** DEFINE OTHER CONSTANTS AND FORMAT STRINGS *****
pi = 3.141592654#
Kw = .000000000000001#
format1$ = "###.#### "
format2$ = "###.####^ ^ ^ ^ "
c1 = .75

' ***** DEFINE FUNCTIONS THAT PERTAIN TO NORMAL DISTRIBUTION *****
DEF FNnorm (x, mu, sigma)
  con = 1# / (sigma * SQR(2 * pi))
  arg = (-1 * ((x - mu) / sigma) * ((x - mu) / sigma)) / 2#
  FNnorm = con * EXP(arg)
END DEF
DEF FNalpha (x, mu, sigma, frac, H)
  alpha = 10 ^ -x / (10 ^ -x + H * c1 * c1)
  con = 1# / (sigma * SQR(2 * pi))
  arg = (-1 * ((x - mu) / sigma) * ((x - mu) / sigma)) / 2#
  FNalpha = frac * con * alpha * EXP(arg)
END DEF

' ***** COLLECT INPUT FROM THE SCREEN *****
10 CLS
PRINT "***** NORMAL DISTRIBUTION SPECIATION *****"
PRINT
INPUT "Maximum pK allowed: ", upper
INPUT "Minimum pK allowed: ", lower
INPUT "Number of distributions: ", num
PRINT
LOCATE , 1: PRINT SPC(40); : LOCATE , 1
PRINT " #          pK          S.D.          % of total"
PRINT " -----"
total = 0#
FOR i = 1 TO num
  PRINT USING " ##"; i;
  LOCATE , 12: INPUT ; "", pK(i)
  logK(i) = -1 * pK(i)
  k(i) = 10# ^ (logK(i))
  LOCATE , 22: INPUT ; "", SD(i)
  IF num = 1 THEN
    per(i) = 100: LOCATE , 35: PRINT "100"
  ELSE
    LOCATE , 35: INPUT "", per(i)
  END IF
  frac(i) = per(i) / 100#
  total = total + per(i)
NEXT i
IF ABS(100# - total) > 1 THEN
  PRINT : PRINT "Percent total does not equal 100."
  GOTO 5
END IF
PRINT
INPUT "pH: ", pH

```

```

INPUT "File name for output: ", file$

/ ***** OPEN OUTPUT FILES AND WRITE HEADINGS *****
OPEN file$ FOR OUTPUT AS #1
PRINT #1, "pH = "; pH
H = 10 ^ (-1 * pH)

/ ***** CALCULATE CORRECTION FACTOR FOR TRUNCATED DISTRIBUTION *****
trun = 1#
FOR c = 1 TO num
  tail1 = 0#: tail2 = 0#: k = 0#
  DO
    p1 = ((2# * lower) - (2# * k * SD(c)) - SD(c)) / 2#
    p2 = SD(c) / 2#
    x(0) = p1
    sum = w(0) * FNnorm(x(0), pK(c), SD(c))
    FOR i = 1 TO 7
      i1 = (2 * i) - 1
      i2 = 2 * i
      x(i1) = p1 + p2 * z(i)
      sum = sum + w(i) * FNnorm(x(i1), pK(c), SD(c))
      x(i2) = p1 - p2 * z(i)
      sum = sum + w(i) * FNnorm(x(i2), pK(c), SD(c))
    NEXT i
    tail1 = tail1 + p2 * sum
    k = k + 1
  LOOP WHILE sum > .0000001#
  k = 0
  DO
    p1 = (2# * upper + 2# * k * SD(c) + SD(c)) / 2#
    p2 = SD(c) / 2#
    x(0) = p1
    sum = w(0) * FNnorm(x(0), pK(c), SD(c))
    FOR i = 1 TO 7
      i1 = (2 * i) - 1
      i2 = 2 * i
      x(i1) = p1 + p2 * z(i)
      sum = sum + w(i) * FNnorm(x(i1), pK(c), SD(c))
      x(i2) = p1 - p2 * z(i)
      sum = sum + w(i) * FNnorm(x(i2), pK(c), SD(c))
    NEXT i
    tail2 = tail2 + p2 * sum
    k = k + 1
  LOOP WHILE sum > .0000001#
  trun = trun - frac(c) * (tail1 + tail2)
NEXT c
PRINT #1, USING "&##.####"; "correction factor: "; trun
PRINT #1,
PRINT #1, "  pK   freq(HA)  freq(A-)"

/ ***** CALCULATE AND PRINT THE SPECIATED DISTRIBUTION FUNCTIONS *****
FOR i = 1 TO 51 STEP 1
  increment = (upper - lower) / 50
  pK = lower + (i - 1) * increment
  Atot = 0: A1 = 0
  FOR c = 1 TO num
    Atot = Atot + frac(c) * FNnorm(pK, pK(c), SD(c))
    A1 = A1 + FNalpha(pK, pK(c), SD(c), frac(c), H)
  NEXT c
  Atot = Atot / trun
  A1 = A1 / trun
  PRINT #1, USING "##.####"; pK;
  PRINT #1, USING "##.###^^^"; CSNG(Atot); CSNG(A1)
NEXT i
CLOSE

END

```

APPENDIX B

Computer Programs to Calculate Langmuir Parameters

Desorption experiments with humic acid and Na^+ and K^+ exhibited dilution curves characteristic of Langmuir sorption (Chapter III). The computer program, FIT-WASH.BAS, fits experimental dilution curve data with a Langmuir-type sorption model coupled to a serial dilution calculation. The downhill simplex method is used to calculate the optimal values of the Langmuir parameters, M_s^∞ and b (the maximum sorbed concentration and the adsorption coefficient, respectively). The program WASH-LIM.BAS determines the approximate confidence limits of these optimized values. Both programs were written with the assistance of Stewart Rounds; the routines for the simplex method (FIT-WASH.BAS) and quadratic interpolation (WASH-LIM.BAS) were adapted from PRESS, *et al.* (1989). The programs are written in BASIC 7.1 (Microsoft, Redmond, WA). Input data is obtained from a file.

INPUT FILE

The same input file is used for FIT-WASH.BAS and WASH-LIM.BAS. The file must be named with the suffix ".IN" (*e.g.*, EXP1.IN). An output file will be created that has the same root name, but with the suffix ".FIT" (*e.g.*,

EXP1.FIT). The program WASH-LIM.BAS appends the output file from FIT-WASH.BAS. The input file format is

```

ncols  Kstart  Kend
nrows  Mstart  Mend
HA      Tot    Vin   nwash
W(1,1) W(1,2) W(1,3)
.
.
W(nwash,1) W(nwash,2) W(nwash,3)

```

where the variables are defined as follows. A simplex search is performed for $(ncols \times nrows)$ starting points defined by pairs of b and M_s^∞ values. The minimum and maximum values for b are K_{start} and K_{end} , respectively (expressed in g solution/mmol cation). The starting point values for M_s^∞ are similarly defined in terms of $nrows$, M_{start} , and M_{end} (expressed in mmol cation/g HA). HA is the mass (in grams) of dry humic acid. Tot is the initial milli-moles of sorbing cation. Vin is the initial mass (in grams) of wash solution added. The array $W(i,1)$, $W(i,2)$, $W(i,3)$ is $nwash$ lines long and contains, respectively, the mass of supernatant removed (in grams), the mass of wash solution added (in grams), and the cation concentration (in mmol cation/g supernatant) at each dilution step.

In addition to the input file, the program WASH-LIM.BAS requires three input parameters: the optimized values of b and M_s^∞ , and a target residual value related to the degree of confidence desired. These values are input from the keyboard at run time. The optimized values of b and M_s^∞ are obtained from the output of FIT-WASH.BAS. The target residual value (target SSR) is calculated using

$$\text{target SSR} = \text{SSR}_{\min} \left[1 + \frac{P}{N_p - P} F(p, N_p - p, \alpha) \right]$$

where SSR_{\min} is the minimum sum of squared residuals obtained from the output of FIT-WASH.BAS, N_p is the number of experimental data points, p is the number of fitted parameters, and F refers to the F-distribution at the α confidence level. For more information about these confidence limits see Box, *et al.* (1978) or ROUNDS (1992).

FIT-WASH.BAS

```

DECLARE FUNCTION FUNC# (P#())
DECLARE SUB SETUP ( )
DECLARE SUB AMOEBA (P#(), Y#(), ndim#, FTOL#, iter%)
/ ***** FIT-WASH.BAS *****

/ The search method is the downhill simplex method. This method is
/ described in Numerical Recipes by Press, Flannery, Teukolsky, and
/ Vetterling, Cambridge University Press, 1986, chapter 10. The code
/ here is a BASIC translation of routines that Stewart Rounds adapted
/ from Numerical Recipes. The search method is contained in the
/ the subroutine AMOEBA.

/ This optimization routine uses logarithmic values as the search
/ indices for the two fitting parameters, K and Max.

'DIMENSION THE VARIABLES & SET THE CONSTANTS
DEFINT I-J, N
DEFDBL A-H, M-Z
DIM Vect(3, 2), Value(3), V(20), W(20, 3)
COMMON SHARED /set1/ Kstart, Kend, Mstart, Mend, nrows, ncols, resid
COMMON SHARED /set2/ V(), W(), HA, Tot, nwash, Vin

CLS
LOCATE 1, 5: PRINT "*****"
LOCATE 2, 5: PRINT " FIT-WASH.BAS"
LOCATE 3, 5: PRINT "*****"

format1$ = "K: ##.###^"
format2$ = "Max: ##.###^"
ndim = 2
FTOL = .0000001#

'OBTAIN INPUT DATA & OPEN OUTPUT FILE
CALL SETUP

'SEARCH, SEARCH, SEARCH .....
/ For each starting point:
/ - Set the starting positions for beginning the search.
/ - Call AMOEBA to find the minimum.
/ - Report the number of iterations, the tolerance level, the
/ ending vertices, and the function values at those vertices.

Kinc = (LOG(Kend) / LOG(10) - LOG(Kstart) / LOG(10)) / (nrows - 1)
Minc = (LOG(Mend) / LOG(10) - LOG(Mstart) / LOG(10)) / (ncols - 1)
FOR irow = 1 TO nrows
FOR icol = 1 TO ncols
LOCATE 8, 5: PRINT USING "on #### of #### points"; (irow - 1) * ncols + icol; nrows * ncols

Vect(1, 1) = LOG(Kstart) / LOG(10) + (irow - 1) * Kinc
Vect(2, 1) = Vect(1, 1) + Kinc / 10#
Vect(3, 1) = Vect(1, 1)

Vect(1, 2) = LOG(Mstart) / LOG(10) + (icol - 1) * Minc
Vect(2, 2) = Vect(1, 2)
Vect(3, 2) = Vect(1, 2) + Minc / 10#

PRINT #1, USING "POINT&: Starting positions-"; STR$((irow - 1) * ncols + icol)
PRINT #1, " Vertex #1 Vertex #2 Vertex #3"
PRINT #1, USING format1$; 10 ^ Vect(1, 1); 10 ^ Vect(2, 1); 10 ^ Vect(3, 1)
PRINT #1, USING format2$; 10 ^ Vect(1, 2); 10 ^ Vect(2, 2); 10 ^ Vect(3, 2)

/ Find the best fit for K and Max.
CALL AMOEBA(Vect(), Value(), ndim, FTOL, iter)

```

```

PRINT #1, "Final positions-"
PRINT #1, USING format1$; 10 ^ Vect(1, 1); 10 ^ Vect(2, 1); 10 ^ Vect(3, 1)
PRINT #1, USING format2$; 10 ^ Vect(1, 2); 10 ^ Vect(2, 2); 10 ^ Vect(3, 2)
PRINT #1, USING "&Iterations: ### "; indent$; iter
PRINT #1, USING "&Sum square residuals: ##.###^^^"; indent$; resid
PRINT #1,
PRINT #1,

NEXT icol
NEXT irow
END

SUB AMOEBA (P(), Y(), ndim, FTOL, iter)
' Multidimensional minimization of the function FUNC(X) where X is
' an NDIM-dimensional vector, by the downhill simplex method of
' Nelder and Mead. Input is a matrix P whose NDIM+1 rows are NDIM-
' dimensional vectors which are the vertices of the starting
' simplex. [Logical dimensions of P are P(NDIM+1,NDIM)]. Also
' input is FTOL, the fractional convergence tolerance to be achieved
' in the function value. On output, P contains the coordinates of
' NDIM+1 new points all within FTOL of a minimum function value, Y
' contains the function values at those points, and ITER gives the
' number of iterations taken.

' ALPHA, BETA, and GAMMA are three parameters which define the
' expansions and contractions. ITMAX is the maximum allowed number
' of iterations. ND is the number of dimensions. This is awkward,
' but I want to try to match array sizes on function calls.

alpha = 1#: beta = .5#: gamma = 2#: itmax = 5000: nd = 2
DIM mpts AS INTEGER, PR(2), PRR(2), PBAR(2)

mpts = ndim + 1
iter = 0

' Evaluate the function FUNC at each of the vertices.
FOR i = 1 TO mpts
  FOR j = 1 TO ndim
    PR(j) = P(i, j)
  NEXT j
  Y(i) = FUNC(PR())
NEXT i

' First, determine which point has the highest (worst) value,
' the next-highest, and the lowest (best) value by looping over the
' points in the simplex.
10  ilo = 1
    IF Y(1) > Y(2) THEN
      ihi = 1
      inhi = 2
    ELSE
      ihi = 2
      inhi = 1
    END IF
    FOR i = 1 TO mpts
      IF Y(i) < Y(ilo) THEN ilo = i
      IF Y(i) > Y(ihi) THEN
        inhi = ihi
        ihi = i
      ELSEIF Y(i) > Y(inhi) THEN
        IF (i <> ihi) THEN inhi = i
      END IF
    NEXT i

' Compute the fractional range from highest to lowest and return
' if satisfactory.

```

```

RTOL = 2# * ABS(Y(ihi) - Y(ilo)) / (ABS(Y(ihi)) + ABS(Y(ilo)))
IF RTOL < FTOL THEN EXIT SUB

IF iter = itmax THEN
  PRINT "Amoeba exceeding maximum iterations."
  EXIT SUB
END IF

' Begin a new iteration. Compute the vector average of all points
' except the highest, i.e. the center of the "face" of the simplex
' across from the high point. We will subsequently explore along
' the ray from the high point through that center.

iter = iter + 1
FOR j = 1 TO ndim
  PBAR(j) = 0#
NEXT j
FOR i = 1 TO mpts
  IF i <> ihi THEN
    FOR j = 1 TO ndim
      PBAR(j) = PBAR(j) + P(i, j)
    NEXT j
  END IF
NEXT i

' Extrapolate by a factor ALPHA through the face, i.e. reflect the
' simplex from the high point.

FOR j = 1 TO ndim
  PBAR(j) = PBAR(j) / ndim
  PR(j) = (1# + alpha) * PBAR(j) - alpha * P(ihi, j)
NEXT j

' Evaluate the function at the reflected point.

YPR = FUNC(PR())
IF YPR <= Y(ilo) THEN

' Gives a result better than the best point, so try an additional
' extrapolation by a factor GAMMA.

FOR j = 1 TO ndim
  PRR(j) = gamma * PR(j) + (1# - gamma) * PBAR(j)
NEXT j

' ... and check out the function there.

YPRR = FUNC(PRR())
IF YPRR < Y(ilo) THEN

' The additional extrapolation succeeded, and the high point
' is replaced.

FOR j = 1 TO ndim
  P(ihi, j) = PRR(j)
NEXT j
Y(ihi) = YPRR
ELSE

' The additional extrapolation failed, but we can still use
' the reflected point.

FOR j = 1 TO ndim
  P(ihi, j) = PR(j)
NEXT j
Y(ihi) = YPR
END IF
ELSEIF YPR >= Y(inhi) THEN

```

```

' The reflected point is worse than the second-highest.
  IF YPR < Y(ihi) THEN
'   If it's better than the highest, then replace the highest.
    FOR j = 1 TO ndim
      P(ihi, j) = PR(j)
    NEXT j
    Y(ihi) = YPR
  END IF

' Look for an intermediate lower point. In other words, perform
' a contraction of the simplex along one dimension. Then evaluate
' the function.

  FOR j = 1 TO ndim
    PRR(j) = beta * P(ihi, j) + (1# - beta) * PBAR(j)
  NEXT j
  YPRR = FUNC(PRR())

  IF YPRR < Y(ihi) THEN
'   Contraction gives an improvement, so accept it.

    FOR j = 1 TO ndim
      P(ihi, j) = PRR(j)
    NEXT j
    Y(ihi) = YPRR
  ELSE

'   Can't seem to get rid of that high point. Better contract
'   around the lowest (best) point.

    FOR i = 1 TO mpts
      IF i <> ilo THEN
        FOR j = 1 TO ndim
          PR(j) = .5 * (P(i, j) + P(ilo, j))
          P(i, j) = PR(j)
        NEXT j
        Y(i) = FUNC(PR())
      END IF
    NEXT i
  END IF

  ELSE

'   We arrive here if the original reflection gives a middling
'   point. Replace the old high point and continue.

    FOR j = 1 TO ndim
      P(ihi, j) = PR(j)
    NEXT j
    Y(ihi) = YPR
  END IF
  GOTO 10

END SUB

FUNCTION FUNC (P()) STATIC
'Calculate the aqueous concentrations & residuals
K = 10 ^ P(1): Max = (10 ^ P(2))
resid = 0
Sum = Tot
FOR i = 1 TO nwash
  A = V(i) * K
  B = V(i) + Max * K * HA - K * Sum
  C = -Sum

```

```

aqplus = (-B + SQR(B ^ 2 - (4 * A * C))) / (2 * A)
aqminus = (-B - SQR(B ^ 2 - (4 * A * C))) / (2 * A)
IF aqplus >= 0 AND aqminus < 0 THEN
  aq = aqplus
ELSEIF aqplus < 0 AND aqminus >= 0 THEN
  aq = aqminus
ELSEIF aqplus >= 0 AND aqminus >= 0 THEN
  IF ABS(aqplus - W(i, 3)) <= ABS(aqminus - W(i, 3)) THEN
    aq = aqplus
  ELSE
    aq = aqminus
  END IF
ELSE
  PRINT "Both roots are negative. Program stopped."
  END
END IF
IF W(i, 3) > 1E-10 THEN resid = resid + ((aq - W(i, 3)) / aq) ^ 2
Sum = Sum - (W(i + 1, 1) * aq)
NEXT i
FUNC = resid
END FUNCTION

SUB SETUP
'THE INPUT VARIABLE LIST:
'mass of dry HA in grams: HA
'total initial mmol cation: Tot
'initial volume in ml: Vin
'number of washes: nwash
'volume of wash added in ml: W(i,1)
'volume of supernatant removed in ml: W(i,3)
'cation concentration in mmol/g at wash i: W(i,3)

format1$ = "##.####^ ^ ^ ^      ##.####^ ^ ^ ^      ##.####^ ^ ^ ^ ^"
LOCATE 5, 5
INPUT ; "What is the input file name? ", name$
in$ = name$ + ".in"
out$ = name$ + ".fit"

OPEN in$ FOR INPUT AS #1
  INPUT #1, nrows, Kstart, Kend
  INPUT #1, ncols, Mstart, Mend
  INPUT #1, HA, Tot, Vin, nwash
  FOR i = 1 TO nwash
    INPUT #1, W(i, 1), W(i, 2), W(i, 3)
  NEXT i
CLOSE #1

'Calculate the total volumes
V(1) = Vin
FOR i = 2 TO nwash
  V(i) = V(i - 1) + W(i, 2) - W(i, 1)
NEXT i

OPEN out$ FOR OUTPUT AS #1
PRINT #1, USING "2-D Simplex Optimization of file: &"; in$
PRINT #1,
PRINT #1, USING "Grid for Starting Points: ## K x ## Max"; nrows; ncols
PRINT #1, USING "  Range for K:   ##.####^ ^ ^ ^ to ##.####^ ^ ^ ^"; Kstart; Kend
PRINT #1, USING "  Range for Max:  ##.####^ ^ ^ ^ to ##.####^ ^ ^ ^"; Mstart; Mend
PRINT #1, : PRINT #1,
END SUB

```

WASH-LIM.BAS

```

DECLARE SUB SETUP ( )
DECLARE SUB BRAKET (A#(), B#(), FA#, FB#, icode%, idirect%, SUCCES$)
DECLARE SUB ZBRENT (A#(), B#(), FA#, FB#, icode%, tol#, iter%)
DECLARE FUNCTION FUNC# (P#())
'   PROGRAM WASH-LIM.BAS

'   This program finds the confidence limits on the optimized values
'   of K and Max that are needed to fit cation desorption data from
'   wash experiments. The program FIT-WASH is used as the fitting
'   function.

'   The values of the optimized K and Max are given as input.

'   The search method used here is Brent's method of parabolic
'   interpolation, as applied to finding roots. This method is
'   described in Numerical Recipes by Press, Flannery, Teukolsky, and
'   Vetterling, Cambridge University Press, 1989, chapter 9.

'   Logarithmic values of K and Max are used in finding the limits.

DEFINT I-J, N
DEFDBL A-H, K-M, O-Z
DIM P1(2), P2(2), W(20, 3), V(20)

COMMON SHARED /set1/ Kopt, Mopt, ftol
COMMON SHARED /set2/ Vin, V(), W(), HA, Tot, target, nwash

CLS
LOCATE 1, 5: PRINT "*****"
LOCATE 2, 5: PRINT "                               WASH-LIM.BAS"
LOCATE 3, 5: PRINT "*****"

' Get the input data
CALL SETUP
format1$ = "K: ##.###^ ^ Max: ##.###^ ^ residual: ##.###^ ^ iterations: ##"
tol = .0001

' Set up the values of K and Max
FOR icode = 1 TO 2
  FOR i = 1 TO 2
    P1(1) = LOG(Kopt) / LOG(10)
    P1(2) = LOG(Mopt) / LOG(10)
    idirect = (-1) ^ (i + 1)

    LOCATE 10, 5: PRINT USING "Searching for root: &      "; STR$(2 * icode - 2 + i)

'   Call BRAKET to bracket the root for ZBRENT.
    CALL BRAKET(P1(), P2(), F1, F2, icode, idirect, SUCCES$)

    IF SUCCES$ = "TRUE" THEN

'   Call ZBRENT to find the root.
      CALL ZBRENT(P1(), P2(), F1, F2, icode, ftol, iter)
'   Report the number of iterations, the tolerance level, the
'   root, and the residual at that value of Deff.
      PRINT #1, USING format1$; 10 ^ P2(1); 10 ^ P2(2); F2; iter

    ELSE
      PRINT #1, "Bracketing routine failed. Root not found."
    END IF
  NEXT i
NEXT icode
CLOSE 1
END

```

```

SUB BRAKET (A(), B(), FA, FB, icode, idirect, SUCCES$)
'
' Given a function FUNC and the point A(ICODE) which minimizes FUNC,
' this routine will search in either the positive or negative
' direction, as specified by IDIRECT, for a point B(ICODE) which will
' bracket the root between A(ICODE) and B(ICODE). The search range
' is expanded geometrically with each iteration. If the search
' fails in 50 iterations, or if FB becomes smaller than FA, then
' the routine returns a value of .FALSE. in the logical variable
' SUCCES. The vectors A and B as well as their function values
' are returned for use with a root-finding routine.

```

```

FACTOR = 1.6: ntry = 25
SUCCES$ = "TRUE"

```

```

B(1) = A(1)
B(2) = A(2)
B(icode) = B(icode) + idirect
FA = FUNC(A())
FB = FUNC(B())
FOR j = 1 TO ntry
  IF FA * FB < 0# THEN EXIT SUB
  B(icode) = B(icode) + FACTOR * (B(icode) - A(icode))
  FB = FUNC(B())
NEXT j
SUCCES$ = "FAIL"
EXIT SUB
END SUB

```

```

FUNCTION FUNC (P()) STATIC

```

```

'Calculate the aqueous concentrations & residuals
K = 10 ^ P(1): Max = (10 ^ P(2))
resid = 0
Sum = Tot
FOR i = 1 TO nwash
  A = V(i) * K
  B = V(i) + Max * K * HA - K * Sum
  C = -Sum
  aqplus = (-B + SQR(B ^ 2 - (4 * A * C))) / (2 * A)
  aqminus = (-B - SQR(B ^ 2 - (4 * A * C))) / (2 * A)
  IF aqplus >= 0 AND aqminus < 0 THEN
    aq = aqplus
  ELSEIF aqplus < 0 AND aqminus >= 0 THEN
    aq = aqminus
  ELSEIF aqplus >= 0 AND aqminus >= 0 THEN
    IF ABS(aqplus - W(i, 3)) <= ABS(aqminus - W(i, 3)) THEN
      aq = aqplus
    ELSE
      aq = aqminus
    END IF
  ELSE
    PRINT "Both roots are negative. Program stopped."
  END IF
  END IF
  IF W(i, 3) > 1E-10 THEN resid = resid + ((aq - W(i, 3)) / aq) ^ 2
  Sum = Sum - (W(i + 1, 1) * aq)
NEXT i
FUNC = resid - target

```

```

END FUNCTION

```

```

SUB SETUP

```

```

format2$ = "##.####^  ##.####^  ##.####^"
LOCATE 5, 5: INPUT "Optimized K = ", Kopt

```

```

LOCATE 6, 5: INPUT "Optimized Max = ", Mopt
LOCATE 7, 5: INPUT "Target value = ", target
LOCATE 9, 5: INPUT "Input file name: ", name$
in$ = name$ + ".in"
out$ = name$ + ".fit"

```

```

OPEN in$ FOR INPUT AS #1
  INPUT #1, nrows, Kstart, Kend
  INPUT #1, ncols, Mstart, Mend
  INPUT #1, HA, Tot, Vin, nwash
  FOR i = 1 TO nwash
    INPUT #1, W(i, 1), W(i, 2), W(i, 3)
  NEXT i
CLOSE #1

```

```

'Calculate the total volumes
V(1) = Vin
FOR i = 2 TO nwash
  V(i) = V(i - 1) + W(i, 2) - W(i, 1)
NEXT i

```

```

OPEN out$ FOR APPEND AS #1
PRINT #1,
PRINT #1, "Confidence Limits:"

```

```

END SUB

```

```

SUB ZBRENT (A(), B(), FA, FB, icode, tol, iter)

```

```

' Using Brent's method, find the root of a function FUNC known to
' lie between A(ICODE) and B(ICODE), whose function values are FA
' and FB, respectively. The root is returned as B(ICODE), and will
' be accurate to within an absolute error of TOL. This routine
' has been modified by SAR for use with a bracketing routine.

```

```

  itmax = 100: EPS = .00000003#

```

```

' itmax is the maximum number of iterations, and EPS is a
' representation of the machine floating point precision.

```

```

  FC = FB
  FOR iter = 0 TO itmax
    IF FB * FC > 0# THEN

```

```

'       Rename A(ICODE), B(ICODE), C, and adjust bounding interval D.

```

```

      C = A(icode)
      FC = FA
      D = B(icode) - A(icode)
      E = D
    END IF

```

```

    IF ABS(FC) < ABS(FB) THEN
      A(icode) = B(icode)
      B(icode) = C
      C = A(icode)
      FA = FB
      FB = FC
      FC = FA
    END IF
    TOL1 = 2# * EPS * ABS(B(icode)) + .5# * tol
    XM = .5# * (C - B(icode))

```

```

' Convergence check.

```

```

  IF ABS(XM) <= TOL1 OR FB = 0# THEN EXIT SUB

```

```

IF ABS(E) >= TOL1 AND ABS(FA) > ABS(FB) THEN
'
  Attempt the inverse quadratic interpolation.

  S = FB / FA
  IF A(icode) = C THEN
    P = 2# * XM * S
    Q = 1# - S
  ELSE
    Q = FA / FC
    R = FB / FC
    P = S * (2# * XM * Q * (Q - R) - (B(icode) - A(icode)) * (R - 1#))
    Q = (Q - 1#) * (R - 1#) * (S - 1#)
  END IF

'
  Check whether in bounds.

  IF P > 0# THEN Q = -Q
  P = ABS(P)
  IF (2# * P < 3# * XM * Q - ABS(TOL1 * Q)) AND 2# * P < ABS(E * Q)) THEN

'
    Accept the interpolation.

    E = D
    D = P / Q
  ELSE

'
    Interpolation failed, use bisection.

    D = XM
    E = D
  END IF
ELSE

'
  Bounds decreasing too slowly, use bisection.

  D = XM
  E = D
END IF

'
Move last best guess to A(ICODE).

A(icode) = B(icode)
FA = FB

'
Find the new value of the trial root.

IF ABS(D) > TOL1 THEN
  B(icode) = B(icode) + D
ELSE
  IF XM < 0 THEN
    B(icode) = B(icode) - ABS(TOL1)
  ELSEIF XM >= 0 THEN
    B(icode) = B(icode) + ABS(TOL1)
  END IF
END IF
FB = FUNC(B())
NEXT iter

PRINT "ZBRENT exceeding maximum iterations."

END SUB

```

REFERENCES

BOX G.E.P., HUNTER W.G., and HUNTER J.S. (1978) *Statistics for Experimenters, An Introduction to Design, Data Analysis, and Model Building*. Wiley, New York. Chap. 14.

PRESS W.H., FLANNERY B.P., TEULKOLSKY S.A. and VETTERLING W.T. (1989) *Numerical Recipes: the art of scientific computing*. Cambridge U. Press, New York. Chap. 10.

ROUNDS S.A. (1992) Ph.D. Thesis, Oregon Graduate Institute of Science & Technology.

APPENDIX C

Computer Programs for Aqueous Humic Infrared Spectral Analysis

During the course of this study several programs were used to manipulate infrared spectral files. The original files were translated from files that could be read by the Perkin-Elmer 1800 computer to MSDOS-readable files. The program to perform this translation is available from Perkin Elmer (WRSPEC). The files produced by the Perkin-Elmer program are written in 4-byte integer format. The computer programs included here perform the following functions: translate 4-byte integer format to ASCII format (READ.BAS), perform optimal subtraction of two spectra (BASEDIF.BAS), directly subtract two spectra (SIMPLDIF.BAS), take the second derivative of a spectrum (DERIV.BAS), fit a set of synthetic peaks to a spectrum (FITSPEC.BAS). All of the programs are written in BASIC 7.1 (Microsoft, Redmond, WA) and operate from a command line. The purpose, required input, and output for each program are summarized on the following page.

READ!.BAS

Purpose translate a Perkin-Elmer DOS-readable file to ASCII format
 Input NAME.SP (Perkin-Elmer IR spectra file)
 Output NAME.DAT
 Command Line *READ! NAME*

BASEDIF.BAS

Purpose perform optimal subtraction of two IR spectra
 Input SPEC.DAT (spectrum to subtract from, in ASCII format)
 BACK.DAT (spectrum to subtract, in ASCII format)
 NORM (normalization factor)
 Output OUT.DAT (difference spectrum)
 OUT.DOC (statistics file for optimized subtraction)
 Command Line *BASEDIF SPEC BACK OUT NORM*

SIMPLDIF.BAS

Purpose directly subtract two IR spectra (using a factor of 1)
 Input SPEC.DAT (spectrum to subtract from, in ASCII format)
 BACK.DAT (spectrum to subtract, in ASCII format)
 Output OUT.DAT (difference spectrum)
 Command Line *SIMPLDIF SPEC BACK OUT*

DERIV.BAS

Purpose calculate the smoothed second derivative spectrum between
 1900 and 800 cm^{-1}
 Input SPEC.DAT (spectrum to differentiate, SPEC is limited to 6
 characters in length)
 Output SPECDR.DAT (second derivative spectrum)
 SPECDR.DOC (list of second derivative minima and maxima)
 Command Line *DERIV SPEC*

FITSPEC.BAS

Purpose fits a spectral region with synthetic peaks
 Input NAME.IN (an input file containing the initial estimates of the
 synthetic peak parameters and the IR file name)
 SPEC.DAT
 Output NAME.DOC
 Command Line *FITSPEC NAME*

READ!.BAS

```

cl$ = COMMAND$
base$ = LTRIM$(RTRIM$(cl$))

CLS
LOCATE 1, 30: PRINT "**** READ ****"
LOCATE 2, 5: PRINT "a program to translate an IBM Perkin-Elmer IR file into ASCII format"

/*****   DEFINE FILE NAMES FOR INPUT AND OUTPUT   *****/
infile$ = base$ + ".sp"
outfile$ = base$ + ".dat"
LOCATE 5, 5: PRINT ; "Reading: "; infile$
LOCATE 6, 5: PRINT "Writing: "; outfile$
PRINT

/*****   OPEN THE PERKIN ELMER FILE   *****/
OPEN infile$ FOR INPUT AS #1

/*****   SEARCH FOR THE SCALE INFORMATION   *****/
c% = 0
DO
  INPUT #1, mark$
  c% = c% + 1
  IF c% = 9 THEN ident$ = mark$
  IF mark$ = "#GR" THEN
    INPUT #1, unit1$
    INPUT #1, unit2$
    INPUT #1, factor#
  EXIT DO
END IF
LOOP

/*****   SEARCH FOR SECTION CONTAINING BINARY DATA   *****/
i = 1
DO
  INPUT #1, mark$(i)
  IF mark$(i) = "#DATA" THEN EXIT DO
  byte = SEEK(1)
  i = 1 + i
LOOP
byte = SEEK(1)
CLOSE #1

start = VAL(mark$(2))
inc = VAL(mark$(3))
points = VAL(mark$(4))
finish = start + inc * (points - 1)
finish$ = LTRIM$(RTRIM$(STR$(finish)))

LOCATE 7, 5: PRINT USING "spectrum from & to & &"; mark$(2); finish$; unit1$
LOCATE 8, 5: PRINT USING "range: & to & &"; mark$(7); mark$(6); unit2$

OPEN outfile$ FOR OUTPUT AS #1 LEN = 2054
PRINT #1, USING "This file is an ASCII translation of the file &."; infile$
PRINT #1, USING "Perkin Elmer Description Line: '&'"; ident$
PRINT #1, USING "The spectrum domain is from & to & &"; mark$(2); finish$; unit1$
PRINT #1, USING "in increments of & &"; mark$(3); unit1$
PRINT #1, USING "The spectrum range is from & to & &"; mark$(7); mark$(6); unit2$

/*****   WRITE THE X-Y DATA POINTS FOR SPECTRUM   *****/
OPEN infile$ FOR BINARY AS #2
SEEK 2, byte
done% = 0: lastdone% = 0
FOR i = 1 TO points STEP 1

```

```

wavenum = start + inc * (i - 1)
done% = 10 * (INT(10 * i / points))
IF done% <> lastdone% AND done% <> 100 THEN
  LOCATE 10, 10: PRINT USING "## percent finished"; done%
ELSEIF done% = 100 THEN
  LOCATE 10, 10: PRINT "***** all done *****"
END IF
lastdone% = done%
GET #2, , n&
trans = n& * factor#
PRINT #1, USING "###.# ###.###"; wavenum; trans
NEXT i
CLOSE
END

```

BASEDIF.BAS

```

***** BASIC PRELIMINARY JUNK *****
DEFDBL A-H, L-Z
DEFINT I-K
DIM fit(601, 5), baseline(401, 5)
x1 = 5000#
DEF FNABS (x) = (LOG(100# / x)) / LOG(10#)

***** READ COMMAND LINE FOR FILENAME INPUTS *****
cl$ = COMMAND$: cl$ = RTRIM$(cl$)
blank$ = " "
k1 = INSTR(cl$, blank$)
k2 = INSTR(k1 + 1, cl$, blank$)
k3 = INSTR(k2 + 1, cl$, blank$)
spec$ = LEFT$(cl$, k1): spec$ = LTRIM$(RTRIM$(spec$))
bkgd$ = MID$(cl$, k1 + 1, k2 - k1): bkgd$ = LTRIM$(RTRIM$(bkgd$))
out$ = MID$(cl$, k2 + 1, k3 - k2): out$ = LTRIM$(RTRIM$(out$))
norm$ = RIGHT$(cl$, LEN(cl$) - k3): norm = VAL(LTRIM$(RTRIM$(norm$)))
IF norm = 0 THEN norm = 1#
CLS
LOCATE 1, 29: PRINT "**** BASEDIF.BAS ****"
LOCATE 2, 10: PRINT "a program to subtract two spectra including a curved baseline"
LOCATE 3, 5: PRINT "*****"

***** SET-UP THE FILE NAMES *****
LOCATE 5, 5: PRINT "Name of spectrum file to subtract from: "; spec$
LOCATE 6, 5: PRINT "Name of spectrum file to subtract: "; bkgd$
LOCATE 7, 5: PRINT "Name of file for the difference spectrum: "; out$
spec$ = spec$ + ".dat"
bkgd$ = bkgd$ + ".dat"
doc$ = out$ + ".doc"
out$ = out$ + ".dat"

***** BEGIN WRITING THE DOC FILE *****
OPEN doc$ FOR OUTPUT AS #1
PRINT #1, USING " _*_* Difference File: & _*_* "; out$
PRINT #1,

***** DETERMINE WHERE TO START READING DATA *****
OPEN spec$ FOR INPUT AS #2
OPEN bkgd$ FOR INPUT AS #3
FOR i = 1 TO 5
  LINE INPUT #2, text1$
  LINE INPUT #3, text2$
  IF i = 2 THEN
    PRINT #1, "Positive spectrum: "; spec$
    PRINT #1, USING " (&)"; text1$
    PRINT #1, "Subtracted spectrum: "; bkgd$
    PRINT #1, USING " (&)"; text2$

```

```

    PRINT #1,
  END IF
NEXT i
  start1! = SEEK(2)
  start2! = SEEK(3)

/***** READ IN TRANSMISSION DATA FOR THE FIT CRITERIA *****/
LOCATE 9, 5: PRINT "Reading data files..."
DO WHILE x1 > 1950
  INPUT #2, x1, spec
  INPUT #3, x2, bkgd
  IF x1 <> x2 THEN
    PRINT "file wavenumber mismatch"
  END
END IF
  IF x1 >= 3800 THEN
    ibase = ibase + 1
    baseline(ibase, 1) = x1 / 1000#
    baseline(ibase, 2) = 100# * FNABS(spec)
    baseline(ibase, 3) = 100# * FNABS(bkgd)
  ELSEIF x1 <= 2250 THEN
    ifit = ifit + 1
    fit(ifit, 1) = x1 / 1000#
    fit(ifit, 2) = 100# * FNABS(spec)
    fit(ifit, 3) = 100# * FNABS(bkgd)
  END IF
LOOP
CLOSE 2, 3

/***** CALCULATE THE LEFT & RIGHT HAND PRODUCT SUMS *****/
LOCATE 9, 5: PRINT "Calculating the factor..."
FOR i = 1 TO ifit
  IF fit(i, 1) >= 2.12 THEN
    leftN = leftN + 1
    leftN11 = leftN11 + (fit(i, 1) - 2.11) ^ 2
    leftN12 = leftN12 + (fit(i, 1) - 2.11) * (fit(i, 2))
    leftN13 = leftN13 + (fit(i, 1) - 2.11) * (fit(i, 3))
    leftN22 = leftN22 + (fit(i, 2)) ^ 2
    leftN23 = leftN23 + (fit(i, 2) * fit(i, 3))
    leftN33 = leftN33 + (fit(i, 3)) ^ 2
    leftN1 = leftN1 + (fit(i, 1) - 2.11)
    leftN2 = leftN2 + fit(i, 2)
    leftN3 = leftN3 + fit(i, 3)
  ELSEIF fit(i, 1) <= 2.1 THEN
    rightN = rightN + 1
    rightN11 = rightN11 + (fit(i, 1) - 2.11) ^ 2
    rightN12 = rightN12 + (fit(i, 1) - 2.11) * (fit(i, 2))
    rightN13 = rightN13 + (fit(i, 1) - 2.11) * (fit(i, 3))
    rightN22 = rightN22 + (fit(i, 2)) ^ 2
    rightN23 = rightN23 + (fit(i, 2) * fit(i, 3))
    rightN33 = rightN33 + (fit(i, 3)) ^ 2
    rightN1 = rightN1 + (fit(i, 1) - 2.11)
    rightN2 = rightN2 + fit(i, 2)
    rightN3 = rightN3 + fit(i, 3)
  END IF
NEXT i

/***** CALCULATE THE FACTOR *****/
A1 = rightN13 * leftN11 - leftN13 * rightN11
B1 = rightN1 * leftN11 - leftN1 * rightN11
C1 = rightN12 * leftN11 - leftN12 * rightN11
A2 = rightN3 * leftN1 - leftN3 * rightN1
B2 = rightN * leftN1 - leftN * rightN1
C2 = rightN2 * leftN1 - leftN2 * rightN1

det = A1 * B2 - A2 * B1
factor = -(B1 * C2 - B2 * C1) / det
mid = (A1 * C2 - A2 * C1) / det

```

```

LOCATE 10, 5: PRINT USING "      factor = #.#####          "; factor

/***** CHECK THE SLOPES, CALCULATE THE CORRELATIONS *****/
rightslope = (rightN12 - (factor * rightN13) - (mid * rightN1)) / rightN11
leftslope = (leftN12 - (factor * leftN13) - (mid * leftN1)) / leftN11
IF (leftslope - rightslope) / leftslope > .0001 THEN
  PRINT "slopes over fit range do not match"
  PRINT "leftslope = "; leftslope
  PRINT "rightslope = "; rightslope
END IF
lefttop = leftN * leftN12 - (leftN1 * leftN2) - factor * (leftN * leftN13 - (leftN1 * leftN3))
leftx = leftN * leftN11 - (leftN1 * leftN1)
lefty1 = leftN * ((leftN22) - (2 * factor * leftN23) + (factor * factor * leftN33))
lefty2 = (leftN2 * leftN2) - (2 * factor * leftN2 * leftN3) + (factor * factor * leftN3 * leftN3)
leftbottom = SQR((leftx) * (lefty1 - lefty2))
leftcorr = lefttop / leftbottom
righttop = rightN * rightN12 - (rightN1 * rightN2) - factor * (rightN * rightN13 - (rightN1 * rightN3))
rightx = rightN * rightN11 - (rightN1 * rightN1)
righty1 = rightN * ((rightN22) - (2 * factor * rightN23) + (factor * factor * rightN33))
righty2 = (rightN2 * rightN2) - (2 * factor * rightN2 * rightN3) + (factor * factor * rightN3 *
rightN3)
rightbottom = SQR((rightx) * (righty1 - righty2))
rightcorr = righttop / rightbottom

/***** CALCULATE THE BASELINE FIT *****/
LOCATE 9, 5: PRINT "Calculating the baseline fit..."
rootnum = -1 / (2 * SQR(.8))
FOR i = 1 TO ibase
  baseline(i, 4) = baseline(i, 2) - factor * baseline(i, 3)
  baseline(i, 5) = SQR(baseline(i, 1)) + rootnum * baseline(i, 1)
  baselinemean = baselinemean + baseline(i, 4)
  basismean = basismean + baseline(i, 5)
NEXT i
FOR i = 1 TO ifit
  fit(i, 4) = fit(i, 2) - factor * fit(i, 3)
  fit(i, 5) = SQR(fit(i, 1)) + rootnum * fit(i, 1)
  baselinemean = baselinemean + fit(i, 4)
  basismean = basismean + fit(i, 5)
NEXT i
baselinemean = baselinemean / (ibase + ifit)
basismean = basismean / (ibase + ifit)
FOR i = 1 TO ibase
  top = top + (baseline(i, 4) - baselinemean) * (baseline(i, 5) - basismean)
  bottom = bottom + (baseline(i, 5) - basismean) ^ 2
NEXT i
FOR i = 1 TO ifit
  top = top + (fit(i, 4) - baselinemean) * (fit(i, 5) - basismean)
  bottom = bottom + (fit(i, 5) - basismean) ^ 2
NEXT i
afit = top / bottom
cfit = baselinemean - afit * basismean
a = afit / (1000 * SQR(10))
b = -a / (2 * SQR(800))
c = cfit / 100
LOCATE 9, 5: PRINT "
LOCATE 11, 5: PRINT USING "      root coefficient = ##.####^^^          "; a
LOCATE 12, 5: PRINT USING "      linear coefficient = ##.####^^^          "; b
LOCATE 13, 5: PRINT USING "      constant = ##.####^^^          "; c

/***** CALCULATE THE STATISTICS ON THE FIT *****/
LOCATE 15, 5: PRINT "Calculating the fit statistics....."
oldresid = fit(1, 4) - afit * fit(1, 5) - cfit
runs! = 1
FOR i = 1 TO ifit
  resid = fit(i, 4) - afit * fit(i, 5) - cfit
  mean = mean + resid
  sqsum = sqsum + resid ^ 2
  IF resid < 0 THEN jneg = jneg + 1

```

```

IF resid > 0 THEN jpos = jpos + 1
IF oldresid * resid < 0 THEN runs! = runs! + 1
oldresid = resid
NEXT i
mean = mean / ifit
rmse = SQR(sqsum / ifit)
LOCATE 15, 5: PRINT "
LOCATE 16, 5: PRINT USING "          mean value over 1950-2250 = ##.###^"; mean / 100
LOCATE 17, 5: PRINT USING "          root mean square residual = ##.###^"; rmse / 100
LOCATE 18, 5: PRINT USING "          total points = ### (### positive ## negative) runs = ##"; ifit;
jpos; jneg; runs!

/***** FINISH WRITING THE .DOC FILE *****/
PRINT #1, USING "Difference factor = #.#####"; factor
PRINT #1, USING "Coefficient root x = ##.###^"; a
PRINT #1, USING "Linear coefficient = ##.###^"; b
PRINT #1, USING "Constant = ##.###^"; c
PRINT #1, USING "Normalization factor = #.#####"; norm
PRINT #1,
PRINT #1, "Statistics for the optimal factor determination:"
PRINT #1, "          2250-2120 wn 2100-1950 wn"
PRINT #1, USING "slopes          ##.###^ ##.###^"; leftslope; rightslope
PRINT #1, USING "correlations ##.##### ##.#####"; leftcorr; rightcorr
PRINT #1, USING "value at 2110 wn: ##.#####"; mid
PRINT #1,
PRINT #1, "Statistics for the 1950-2250 fit range after baseline correction:"
PRINT #1, USING " ## points"; ifit
PRINT #1, USING " Mean residual: ##.###^"; mean / 100
PRINT #1, USING " Root mean square residual: ##.###^"; rmse / 100
PRINT #1, USING " ## negative residuals ## positive residuals"; jneg; jpos
PRINT #1, USING " ## runs"; runs!
CLOSE 1

/***** CALCULATE & WRITE THE DIFFERENCE SPECTRUM *****/
PRINT
LOCATE 20, 5: PRINT "Writing the difference spectrum..."
OPEN spec$ FOR INPUT AS #2
OPEN bkgd$ FOR INPUT AS #3
OPEN out$ FOR OUTPUT AS #4 LEN = 2048
SEEK #2, start1!
SEEK #3, start2!
DO UNTIL EOF(2)
  INPUT #2, x1, spec
  INPUT #3, x2, bkgd
  IF x1 <> x2 THEN
    PRINT "file wavenumber mismatch"
  END
END IF
track! = (INT((x1 - 1) / 1000) + 1) * 1000
IF CINT(x1) = track! THEN
  LOCATE 20, 42
  PRINT USING "(wavenumber: #####)"; track!
ELSEIF x1 = 800 THEN
  LOCATE 20, 5
  PRINT "Done!"
END IF
spec = LOG(100# / spec) / LOG(10#)
bkgd = LOG(100# / bkgd) / LOG(10#)
diff = norm * (spec - (factor * bkgd) - a * SQR(x1) - b * x1 - c)
PRINT #4, USING "#####.## #.#####"; x1; diff
LOOP
END

```

SIMPLDIF.BAS

```

***** BASIC PRELIMINARY JUNK *****
DEFDBL A-Z

***** READ COMMAND LINE FOR FILENAME INPUTS *****
cl$ = COMMAND$: cl$ = RTRIM$(cl$)
blank$ = " "
k1 = INSTR(cl$, blank$)
k2 = INSTR(k1 + 1, cl$, blank$)
spec$ = LEFT$(cl$, k1): spec$ = LTRIM$(RTRIM$(spec$))
bkgd$ = MID$(cl$, k1 + 1, k2 - k1): bkgd$ = LTRIM$(RTRIM$(bkgd$))
out$ = RIGHT$(cl$, LEN(cl$) - k2): out$ = LTRIM$(RTRIM$(out$))
CLS

LOCATE 1, 29: PRINT "**** SIMPLDIF.BAS ****"
LOCATE 2, 10: PRINT "a program to subtract to spectra, factor =1, no tilt or offset"
spec$ = spec$ + ".dat"
bkgd$ = bkgd$ + ".dat"
out$ = out$ + ".dat"
LOCATE 5, 5: PRINT "Name of spectrum to subtract from: "; spec$
LOCATE 6, 5: PRINT "Name of spectrum to subtract: "; bkgd$
LOCATE 7, 5: PRINT "Name of file for the difference spectrum: "; out$

***** OPEN DOC FILE ****
OPEN out$ FOR OUTPUT AS #3 LEN = 2048
PRINT #3, USING "Difference file: & = & - &"; out$, spec$, bkgd$

***** DETERMINE WHERE TO START READING DATA *****
flag1$ = "number"
flag2$ = "number"
OPEN spec$ FOR INPUT AS #1
OPEN bkgd$ FOR INPUT AS #2
FOR i! = 1 TO 5
  INPUT #1, text1$
  IF VAL(text1$) = 0 THEN flag1$ = "header"
  INPUT #2, text2$
  IF VAL(text2$) = 0 THEN flag2$ = "header"
NEXT i!
IF flag1$ = "number" THEN
  CLOSE 1
  OPEN spec$ FOR INPUT AS #1
END IF
IF flag2$ = "number" THEN
  CLOSE 2
  OPEN bkgd$ FOR INPUT AS #2
END IF

***** WRITE THE DIFFERENCE SPECTRUM *****
LOCATE 9, 5: PRINT "writing the difference spectrum..."
DO UNTIL EOF(1)
  INPUT #1, x1, spec
  INPUT #2, x2, bkgd
  IF x1 <> x2 THEN
    PRINT "file wavenumber mismatch"
  END
END IF
track! = (INT((x1 - 1) / 1000) + 1) * 1000
IF CINT(x1) = track! THEN
  LOCATE 9, 42
  PRINT track!
ELSEIF x1 = 800 THEN
  LOCATE 9, 5
  PRINT "Done!"
END IF
diff = spec - bkgd
PRINT #3, USING "####.# #.#####"; x1; diff

```

```

LOOP
CLOSE
END

```

DERIV.BAS

```

***** BASIC PRELIMINARY JUNK *****
DEFDBL A-H, L-Z
DEFINT I-K
REM $DYNAMIC
DIM speclo(1 TO 1101), spechi(1 TO 1001, 2), derivlo(1 TO 1101), dumlo(1 TO 1101)
x1 = 5000#

***** READ COMMAND LINE FOR FILENAME INPUT *****
cl$ = COMMAND$
spec$ = LTRIM$(RTRIM$(cl$))
data$ = spec$ + ".dat"
CLS
LOCATE 1, 29: PRINT "**** DERIV.BAS ****"
LOCATE 2, 9: PRINT "calculates the second derivative of IR data 1900-900 wavenumbers,"
LOCATE 3, 12: PRINT "determines the minima and maxima of that second derivative,"
LOCATE 4, 5: PRINT "*****"
LOCATE 7, 5: PRINT USING "IR Spectrum: &"; data$

***** READ IN DATA TO BE SMOOTHED - DIFFERENCE SPECTRUM ASSUMED *****
LOCATE 9, 5: PRINT "Reading the data..."
OPEN data$ FOR INPUT AS #1
ilo = 0: ihi = 0
DO UNTIL EOF(1)
  INPUT #1, dumx, dummy
  IF (dumx <= 1950 AND dumx >= 850) THEN
    ilo = ilo + 1
    speclo(ilo) = dummy
  ELSEIF dumx >= 3000 THEN
    ihi = ihi + 1
    spechi(ihi, 1) = dummy
  ELSEIF dumx = 1951 THEN
    first = dummy
  ELSEIF dumx = 849 THEN
    last = dummy
  END IF
LOOP
CLOSE 1
LOCATE 9, 27: PRINT "Done."

***** CALCULATE THE SECOND DERIVATIVE OVER THE 1900-900 DATA RANGE *****
LOCATE 10, 5: PRINT "Calculating the second derivative...."
derivlo(1) = speclo(2) - 2 * speclo(1) + first
derivlo(ilo) = last - 2 * speclo(ilo) + speclo(ilo - 1)
FOR i = 2 TO ilo - 1
  derivlo(i) = speclo(i + 1) - 2 * speclo(i) + speclo(i - 1)
NEXT i
j = 0:
LOCATE 10, 45: PRINT "Done."

***** SMOOTH THE SECOND DERIVATIVE OVER 1900-900 - 40 PASSES *****
LOCATE 11, 5: PRINT "Smoothing the second derivative.... pass #"
FOR j = 1 TO 40
  LOCATE 11, 50: PRINT j
  FOR i = 1 TO ilo - 1
    dumlo(i) = (derivlo(i) + derivlo(i + 1)) / 2
  NEXT i
  FOR i = 2 TO ilo - 1
    derivlo(i) = (dumlo(i - 1) + dumlo(i)) / 2
  NEXT i

```

```

NEXT j
LOCATE 11, 42: PRINT "Done."          "

/***** PRINT THE SMOOTHED DATA SECOND DERIVATIVE *****/
LOCATE 12, 5: PRINT "Writing the derivative file..."
out$ = spec$ + "dr.dat"
OPEN out$ FOR OUTPUT AS #2
FOR i = 1 TO ilo
  wavenum = 1951 - i
  IF wavenum <= 1900 AND wavenum >= 900 THEN
    PRINT #2, USING "####.#  ##.###^"; wavenum; CSNG(derivlo(i))
  END IF
NEXT i
CLOSE 2
LOCATE 12, 38: PRINT "Done."

/***** FIND MINIMA AND MAXIMA OF THE SECOND DERIVATIVE IN THE 1900-900 RANGE *****/
LOCATE 13, 5: PRINT "Searching for derivative minima & maxima..."
out$ = spec$ + "dr.doc"
OPEN out$ FOR OUTPUT AS #2
FOR i = 52 TO ilo - 51
  IF derivlo(i - 1) < derivlo(i) THEN trend1$ = "up"
  IF derivlo(i - 1) > derivlo(i) THEN trend1$ = "down"
  IF derivlo(i) < derivlo(i + 1) THEN trend2$ = "up"
  IF derivlo(i) > derivlo(i + 1) THEN trend2$ = "down"
  IF trend1$ <> trend2$ THEN
    IF trend1$ = "up" AND trend2$ = "down" THEN
      type$ = "max"
    ELSE
      type$ = "min"
    END IF
    PRINT #2, USING "####  &  ##.###^"; 1951 - i; type$; derivlo(i)
  END IF
NEXT i
CLOSE 2
LOCATE 13, 51: PRINT "Done."

END

```

INPUT FILE FOR FITSPEC.BAS

An input file is required to run FITSPEC.BAS. The file contains the name of the file containing the IR spectra to be fitted, and the initial estimates for the parameters that characterize the synthetic peaks (peak centers, peak widths, absorbance at peak center, and the Gaussian character fraction). One or more of these values may be fixed by appending the initial value with the letter "f". If none of the values is fixed the likelihood of divergence dramatically increases. The program limits the number of synthetic peaks to 17, and the spectral region to 321 points. An example input file is given below.

```

306_1
306_1f
1480, 1800
17
.0010, 1764f, 28f
.0010, 1744f, 28f
.0010, 1725f, 28f
.0020, 1710f, 30f
.0020, 1691f, 30f
.0060, 1677f, 30f
.0150, 1661f, 30f
.0060, 1644f, 30f
.0170, 1626f, 43f
.0260, 1600f, 44f
.0260, 1583f, 34f
.0340, 1567f, 34f
.0240, 1551f, 34f
.0240, 1532f, 38f
.0030, 1513f, 20f
.0120, 1503f, 36f
.0260, 1466f, 53f
calcf, calcf
0.4f
50
0

```

The first two lines indicate the names of the input spectrum and output file respectively. The third line gives the wavenumber limits of the region to be fitted. The next line gives the number of synthetic peaks, in this case 17. The initial estimates of absorbance, center and width are next; a separate line is used for each peak. In this example the values of peak center and width are fixed. The line following the peak location information gives the values of the baseline at the wavenumber limits. In this case those values are given as `calcf` which instructs the program to use a horizontal baseline calculated as the mean absorbance between 1850 and 1800 cm^{-1} . The next line is the Gaussian character

fraction for the synthetic peaks (0.4 and fixed for this example); the Lorentzian character fraction is 1 - the Gaussian fraction (in this case 0.6). The next two lines are the maximum number of iterations allowed, and a code for the optimization method, respectively. The code for this program was adapted from FRASER and SUZUKI (1973).

FITSPEC.BAS

FITSPEC.BAS requires a VGA monitor.

```

DECLARE SUB autod (n%, x!(), y!(), tf!(), m%, p!(), lm%, d!, cmat!(), dmat!())
DECLARE SUB autos (n%, x!(), y!(), f!(), m%, p!(), dmat!())
DECLARE SUB dfcalc (n%, x!(), f!(), m%, p!(), df!())
DECLARE SUB dgcalc (m%, L%, ifp%(), dg!())
DECLARE FUNCTION drms! (n%, f!(), y!())
DECLARE SUB fcalc (n%, x!(), m%, p!(), f!())
DECLARE SUB fcalcp (n%, x!(), m%, p!(), f!())
DECLARE SUB gcalc (L%, g!())
DECLARE SUB jobend (n%, x!(), y!(), f!(), m%, L%, sd!, tcmat!(), tdmat!(), out$, p!())
DECLARE SUB matinv (a!(), b!(), n%, L%)
DECLARE SUB test (icycle%, ncycle%, sd!, it$, d!, m%, L%, ifp%(), tcmat!(), tdmat!())

REM $DYNAMIC
DEFSNG A-H, O-Z
DEFINT I-N
DIM x(321), y(321), f(321), p(54), g(53), df(321, 54), ifp(53)
DIM dg(53, 54), cmat(107, 107), dmat(107), tcmat(107, 107), tdmat(107)

CLS
LOCATE 1, 25: PRINT "***** FITSPEC *****"
LOCATE 2, 5: PRINT "a program to fit Lorentz-Gaussian sum peaks to absorbance data"
c1$ = COMMAND$
in$ = LTRIM$(RTRIM$(c1$)) + ".in"

/***** READ THE INPUT PARAMETERS FROM A FILE *****/
OPEN in$ FOR INPUT AS #1
' Set up the data file and output file names
LINE INPUT #1, data$
LINE INPUT #1, doc$
data$ = LTRIM$(RTRIM$(data$)) + ".dat"
doc$ = LTRIM$(RTRIM$(doc$)) + ".doc"
' Read the range to fit and the number of peaks
INPUT #1, wavemin, wavemax
INPUT #1, npeak
' Read the initial estimates of absorbance, center and half-width
L = 0
FOR i = 0 TO npeak - 1
INPUT #1, a$(1), a$(2), a$(3)
FOR j = 1 TO 3
IF INSTR(a$(j), "f") <> 0 THEN
a$(j) = LEFT$(a$(j), INSTR(a$(j), "f") - 1)
L = L + 1
ifp(L) = 3 * i + j
END IF
p(3 * i + j) = VAL(RTRIM$(LTRIM$(a$(j))))
NEXT j
NEXT i

```

```

' Read the initial estimates of the background absorbance
INPUT #1, a$(1), a$(2)
FOR j = 1 TO 2
  IF INSTR(a$(j), "f") <> 0 THEN
    a$(j) = LEFT$(a$(j), INSTR(a$(j), "f") - 1)
    L = L + 1
    ifp(L) = 3 * npeak + j
    IF a$(j) = "calc" THEN baseflag$ = "calc"
  END IF
  p(3 * npeak + j) = VAL(RTRIM$(LTRIM$(a$(j))))
NEXT j
' Read the input value for fraction Gaussian
INPUT #1, a$(1)
IF INSTR(a$(1), "f") <> 0 THEN
  a$(1) = LEFT$(a$(1), INSTR(a$(1), "f") - 1)
  L = L + 1
  ifp(L) = 3 * (npeak + 1)
END IF
p(3 * (npeak + 1)) = VAL(RTRIM$(LTRIM$(a$(1))))
' Read the input values for maximum iterations and mode
INPUT #1, ncycle
INPUT #1, mode
CLOSE 1

*****      CALCULATE REMAINING PARAMETERS      *****
m = npeak * 3 + 3
n = wavemax - wavemin + 1
lm = L + m
d = 0
' Scale the parameter estimates: wavenumber/100 & absorbance *1000
FOR i = 0 TO npeak - 1
  p(3 * i + 1) = p(3 * i + 1) * 1000#
  p(3 * i + 2) = p(3 * i + 2) / 100#
  p(3 * i + 3) = p(3 * i + 3) / 100#
NEXT i
p(m - 2) = p(m - 2) * 1000#
p(m - 1) = p(m - 1) * 1000#

*****      READ THE DATA FILE      *****
LOCATE 6, 5: PRINT "Reading the data file ..."
OPEN data$ FOR INPUT AS #1
i = 0
DO UNTIL EOF(1)
  INPUT #1, dumx, dumy
  IF baseflag$ = "calc" THEN
    IF dumx <= 1850 AND dumx >= 1825 THEN
      baseline = baseline + dumy
    END IF
  END IF
  IF dumx <= wavemax AND dumx >= wavemin THEN
    i = i + 1
    x(i) = dumx / 100#
    y(i) = dumy * 1000#
  END IF
LOOP
CLOSE 1
IF i <> n THEN
  PRINT " count error in reading input data file -- aborted"
  STOP
END IF
IF baseflag$ = "calc" THEN
  baseline = baseline * 1000# / 26#
  p(m - 2) = baseline: p(m - 1) = baseline
END IF
LOCATE 6, 27: PRINT " Done."

```

```

***** OPEN & BEGIN WRITING THE DOCUMENTATION FILE *****
OPEN doc$ FOR OUTPUT AS #2
PRINT #2, USING "DATA FILE: &"; data$
PRINT #2, USING " Range: ##### to #####"; wavemax; wavemin
PRINT #2, USING " Number of peaks: ### Gaussian fraction: #.###"; npeak; p(m)
PRINT #2,
PRINT #2, "Initial Values of Parameters:"
PRINT #2, " Absorbance Center Half-width"
FOR i = 0 TO npeak - 1
  id1$ = " ": id2$ = id1$: id3$ = id1$
  FOR j = 1 TO L
    IF ifp(j) = 3 * i + 1 THEN id1$ = "(fixed)"
    IF ifp(j) = 3 * i + 2 THEN id2$ = "(fixed)"
    IF ifp(j) = 3 * i + 3 THEN id3$ = "(fixed)"
  NEXT j
  PRINT #2, USING " ##.### & ##### & ### &"; p(3 * i + 1) / 1000#; id1$; p(3 * i + 2) *
100#; id2$; p(3 * i + 3) * 100#; id3$
NEXT i
PRINT #2,
id1$ = " ": id2$ = id1$: id3$ = id1$
FOR j = 1 TO L
  IF ifp(j) = m - 2 THEN id1$ = "(fixed)"
  IF ifp(j) = m - 1 THEN id2$ = "(fixed)"
NEXT j
PRINT #2, USING "Background absorbance- ##### cm-1: ##.### &"; wavemax; p(m - 2) / 1000#; id1$
PRINT #2, USING " ##### cm-1: #.### &"; wavemin; p(m - 1) / 1000#; id2$
PRINT #2, : PRINT #2,
PRINT #2, "BEGIN ITERATIONS:"
PRINT #2, " Cycle Standard Deviation Damping Factor"

***** BEGIN THE ITERATION PROCESS *****
  icycle = 0
' Set the graphics screen
SCREEN 12
CLS
DO
  CLS
  VIEW
  WINDOW (-wavemax / 100, 0)-(-wavemin / 100, 80)
  LOCATE 1, 1: PRINT data$
' Calculate the function values
  CALL fcalcp(n, x(), m, p(), f())
' Graph the data and the estimate on the screen
  COLOR 15
  PSET (-x(1), y(1))
  FOR i = 2 TO n
    LINE -(-x(i), y(i))
  NEXT i
  COLOR 13
  PSET (-x(1), f(1))
  FOR i = 2 TO n
    LINE -(-x(i), f(i))
  NEXT i
' Calculate the rms deviation and check the iteration
  sd = drms(n, f(), y())
  CALL test(icycle, ncycle, sd, it$, d, m, L, ifp(), tcmat(), tdmat())
' Write the new parameter estimates on the screen
  COLOR 7
  FOR i = 1 TO npeak
    LOCATE 1 + i, 1: PRINT USING "#.### ##### ###"; p(3 * i - 2) / 1000#; p(3 * i - 1) * 100#; p(3 *
i) * 100#;
  NEXT i

  IF it$ = "died" THEN
    LOCATE 2, 1: PRINT "...Terminated...";
    SCREEN 0
    END

```

```

ELSEIF it$ = "maxed" THEN
    LOCATE 2, 1: PRINT "maximum number of iterations completed";
    SCREEN 0
    STOP
END IF

' CALCULATE THE PARAMETER ADJUSTMENTS FOR A NEW ITERATION
' Calculate g for the fixed parameters
CALL gcalc(L, g())

' Calculate partial derivatives of f and g
CALL dfcalc(n, x(), f(), m, p(), df())
CALL dgcalc(m, L, ifp(), dg())

' Set up the constant vector, dmat
' dmat for the first m elements (from the parameter expressions)
FOR j = 1 TO m
    dmat(j) = 0#
    FOR i = 1 TO n
        dmat(j) = dmat(j) - df(i, j) * (f(i) - y(i))
    NEXT i
NEXT j
' dmat for the next L elements (from the added constraints)
FOR k = 1 TO L
    j = m + k
    dmat(j) = -g(k)
NEXT k

' Set up the coefficient matrix, cmat
FOR j = 1 TO lm
    FOR k = 1 TO lm
        cmat(j, k) = 0#
    NEXT k
NEXT j
' cmat for the first m x m section; it is symmetric
FOR j = 1 TO m
    FOR k = j TO m
        FOR i = 1 TO n
            cmat(j, k) = cmat(j, k) + df(i, j) * df(i, k)
        NEXT i
        cmat(k, j) = cmat(j, k)
    NEXT k
NEXT j
' cmat for the adjacent m x L and L x m sections;
' they are symmetric to each other
FOR i = 1 TO L
    j = m + i
    FOR k = 1 TO m
        cmat(j, k) = dg(i, k)
        cmat(k, j) = dg(i, k)
    NEXT k
NEXT i

' Store cmat and dmat arrays for calculation of inverse if needed
FOR j = 1 TO lm
    tdmatrix(j) = dmat(j)
    FOR k = 1 TO lm
        tcmatrix(j, k) = cmat(j, k)
    NEXT k
NEXT j

' Test for convergence
IF it$ = "converged" THEN
    LOCATE 2, 1: PRINT "Converged."
    LOCATE 3, 1: PRINT "Printing the parameters."
    CALL jobend(n, x(), y(), f(), m, L, sd, tcmatrix(), tdmatrix(), doc$, p())
    SCREEN 0
    END

```

```

END IF

' Optimize the damping factor and adjust matrix and solve for parameter adjustments
IF mode < 2 THEN CALL autod(n, x(), y(), f(), m, p(), lm, d, cmat(), dmat())
FOR j = 1 TO lm
  cmat(j, j) = (1# + d * d) * cmat(j, j)
NEXT j
CALL matinv(cmat(), dmat(), lm, 1)

' Optimize the scale of parameter adjustments and adjust parameters
IF mode = 2 OR mode = 0 THEN CALL autos(n, x(), y(), f(), m, p(), dmat())
FOR j = 1 TO m
  p(j) = p(j) + dmat(j)
NEXT j
icycle = icycle + 1
LOOP
END

REM $STATIC
SUB autod (n, x(), y(), tf(), m, p(), lm, d, cmat(), dmat()) STATIC

' The routine optimizes the damping factor (d)
DIM tcmat(107, 107), tdm(107), e(3), tp(54)
dmin = .000001#
dmax = 100#
dinc = 2#
IF d < dmin THEN d = 1#
IF d > dmax THEN d = dmax
k = 1
L = 3

' Calculate the standard deviation for .5d, d and 2d
1 FOR i = k TO L
  td = d * dinc ^ (i - 2)
  FOR j = 1 TO lm
    tdm(j) = dmat(j)
    FOR kk = 1 TO lm
      tcmat(j, kk) = cmat(j, kk)
    NEXT kk
    tcmat(j, j) = tcmat(j, j) * (1# + td * td)
  NEXT j
  CALL matinv(tcmat(), tdm(), lm, 1)
  FOR j = 1 TO m
    tp(j) = p(j) + tdm(j)
  NEXT j
  CALL fcalc(n, x(), m, tp(), tf())
  e(i) = drms(n, tf(), y())
NEXT i
k = 1

' Test to see if d is in the correct range
IF d < dmin OR d > dmax THEN
  PRINT USING "damping factor = ##.###^". Outside of range"; d
  IF d < dmin THEN d = dmin
  EXIT SUB
END IF

' Test to see if standard deviation is insensitive to d
IF ABS((e(3) - e(2)) / e(2)) < .000001# THEN EXIT SUB
IF ABS((e(1) - e(2)) / e(2)) < .000001# THEN EXIT SUB

' Test if minimum is detected
IF e(2) < e(1) AND e(2) < e(3) THEN EXIT SUB

' Test if the best d is greater than the current d
IF e(3) < e(1) THEN k = 3
L = 4 - k

```

```

    e(L) = e(2)
    e(2) = e(k)

' Choose a better d
d = d * dinc ^ (2 - L)
L = k
GOTO 1

END SUB

SUB autos (n, x(), y(), f(), m, p(), dmat()) STATIC

' Optimize the scale factor (h) of parameter adjustments
DIM e(3), ptemp(54)

k = 1
L = 3
h = 1#
hmin = .01#
hmax = 100#
hinc = 1.2#

' Calculate the standard deviation for the range of h values
101 FOR i = k TO L
    FOR j = 1 TO m
        ptemp(j) = dmat(j) * h * hinc ^ (i - 2) + p(j)
    NEXT j
    CALL fcalc(n, x(), m, ptemp(), f())
    e(i) = drms(n, f(), y())
NEXT i
k = 1

' Test if h is outside selected range
IF h < hmin OR h > hmax THEN GOTO 104

' Test if standard deviation is insensitive to h
IF ABS((e(1) - e(2)) / e(2)) <= .000001# THEN EXIT SUB
IF ABS((e(3) - e(2)) / e(2)) <= .000001# THEN EXIT SUB

' Test if a minimum is detected
IF e(2) < e(1) AND e(2) < e(3) THEN GOTO 106

' Test if the best h is greater than the current h
IF e(3) < e(1) THEN k = 3
L = 4 - k
e(L) = e(2)
e(2) = e(k)

' Choose the better h
h = h * hinc ^ (2 - L)
L = k
GOTO 101

104 PRINT "h is not with acceptable range"

' Multiply the parameters by the best h value
106 FOR j = 1 TO m
    dmat(j) = dmat(j) * h
NEXT j

END SUB

SUB dfcalc (n, x(), f(), m, p(), df()) STATIC

nb = (m - 3) / 3
q1 = LOG(2#)

```

```

FOR i = 1 TO n
  df(i, m) = 0#
  df(i, m - 1) = (x(i) - x(1)) / (x(n) - x(1))
  df(i, m - 2) = 1# - df(i, m - 1)
  FOR k = 1 TO nb
    j1 = 3 * k - 2
    j2 = 3 * k - 1
    j3 = 3 * k
    q2 = (x(i) - p(j2)) / p(j3)
    q3 = EXP(-4# * q1 * q2 * q2)
    q4 = 1# / (1# + 4# * q2 * q2)
    q5 = 8# * q1 * q2 * q3 * p(j1) / p(j3)
    q6 = 8# * q2 * q4 * q4 * p(j1) / p(j3)
    df(i, j1) = p(m) * q3 + (1# - p(m)) * q4
    df(i, j2) = p(m) * q5 + (1# - p(m)) * q6
    df(i, j3) = q2 * df(i, j2)
    df(i, m) = df(i, m) + p(j1) * (q3 - q4)
  NEXT k
NEXT i
END SUB

```

```

SUB dgcalc (m, L, ifp(), dg()) STATIC

```

```

FOR k = 1 TO L
  FOR j = 1 TO m
    dg(k, j) = 0#
    IF j = ifp(k) THEN dg(k, j) = 1
  NEXT j
NEXT k
END SUB

```

```

FUNCTION drms (n, f(), y())
  drms1 = 0#
  FOR i = 1 TO n
    drms1 = drms1 + (f(i) - y(i)) ^ 2
  NEXT i
  drms = SQR(drms1 / CDBL(n))
END FUNCTION

```

```

SUB fcalc (n, x(), m, p(), f()) STATIC

```

```

' Calculate the function values for Gauss + Lorentz curves

```

```

  nb = (m - 3) / 3
  q1 = p(m - 2)
  q2 = (p(m - 1) - q1) / (x(n) - x(1))
  FOR i = 1 TO n
    f(i) = q1 + q2 * (x(i) - x(1))
  NEXT i
  q1 = LOG(2#)
  FOR j = 1 TO nb
    q2 = 4# / (p(3 * j) ^ 2)
    q3 = p(3 * j - 2)
    q4 = p(3 * j - 1)
    FOR i = 1 TO n
      q5 = q2 * (x(i) - q4) ^ 2
      f(i) = f(i) + q3 * (p(m) * EXP(-q1 * q5) + (1# - p(m)) / (1# + q5))
    NEXT i
  NEXT j
END SUB

```

```

SUB fcalcp (n, x(), m, p(), f()) STATIC
' Calculate the function values for Gauss + Lorentz curves
' ... and plot the individual bands on the screen.

nb = (m - 3) / 3
q1 = p(m - 2)
q2 = (p(m - 1) - q1) / (x(n) - x(1))
FOR i = 1 TO n
    f(i) = q1 + q2 * (x(i) - x(1))
NEXT i
q1 = LOG(2#)
FOR j = 1 TO nb
    q2 = 4# / (p(3 * j) ^ 2)
    q3 = p(3 * j - 2)
    q4 = p(3 * j - 1)
    IF j > 15 THEN COLOR j - 15 ELSE COLOR j
    FOR i = 1 TO n
        q5 = q2 * (x(i) - q4) ^ 2
        fp = q3 * (p(m) * EXP(-q1 * q5) + (1# - p(m)) / (1# + q5))
        f(i) = f(i) + fp
        IF i = 1 THEN
            PSET (-x(i), fp)
        ELSE
            LINE -(-x(i), fp)
        END IF
    NEXT i
NEXT j

END SUB

SUB gcalc (L, g()) STATIC
FOR i = 1 TO L
    g(i) = 0#
NEXT i
END SUB

SUB jobend (n, x(), y(), f(), m, L, sd, tcmat(), tdmat(), out$, p()) STATIC
'Calculate the standard deviations of the parameter estimates
lm = L + m
CALL matinv(tcmat(), tdmat(), lm, 0)
FOR j = 1 TO m
    tdmat(j) = sd * SQR(ABS(tcmat(j, j) * CDBL(n) / CDBL(n + L - m)))
NEXT j
sd = sd * SQR(CDBL(n) / CDBL(n + L - m))

'Scale the parameters back to correct values
FOR i = 1 TO (m - 3) / 3
    p(3 * i - 2) = p(3 * i - 2) / 1000#
    p(3 * i - 1) = p(3 * i - 1) * 100#
    p(3 * i) = p(3 * i) * 100#
    tdmat(3 * i - 2) = tdmat(3 * i - 2) / 1000#
    tdmat(3 * i - 1) = tdmat(3 * i - 1) * 100#
    tdmat(3 * i) = tdmat(3 * i) * 100#
NEXT i
p(m - 2) = p(m - 2) / 1000#
p(m - 1) = p(m - 1) / 1000#
tdmat(m - 2) = tdmat(m - 2) / 1000#
tdmat(m - 1) = tdmat(m - 1) / 1000#

'Print the fitted parameters & their standard deviations
PRINT #2, USING "Unbiased estimate of standard deviation: ##.###^^^"; sd

```

```

PRINT #2,
PRINT #2, "Fitted Values of Parameters (standard deviation): "
PRINT #2, " Absorbance           Center           Half-width           Area"
format$ = " ##.#### (#.####)      ##### (####)      ##### (###.#)      ##.####"
factor = p(m) * SQR(3.141592654# / LOG(2)) + 3.141592654# * (1 - p(m))
FOR i = 1 TO (m - 3) / 3
  area = p(3 * i - 2) * p(3 * i) * (factor) / 2
  PRINT #2, USING format$; p(3 * i - 2); tdm(3 * i - 2); p(3 * i - 1); tdm(3 * i - 1); p(3 *
i); tdm(3 * i); area
NEXT i
PRINT #2, USING "Background absorbance- ##.#### (#.####)"; p(m - 2); tdm(m - 2)
PRINT #2, USING "                ##.#### (#.####)"; p(m - 1); tdm(m - 1)
PRINT #2, USING "Gaussian factor- ##.#### (#.####)"; p(m); tdm(m)
CLOSE 2
END SUB

```

```

SUB matinv (a(), b(), n, L) STATIC

```

```

DIM ip(107), in(107, 2)

```

```

FOR i = 1 TO n
  ip(i) = 0
NEXT i
FOR i = 1 TO n
  amax = 0#
  FOR j = 1 TO n
    IF ip(j) > 0 THEN GOTO 203
    IF ip(j) < 0 THEN GOTO 204
    FOR k = 1 TO n
      IF ip(k) = 1 THEN GOTO 202
      IF ip(k) > 1 THEN GOTO 204
      IF ABS(a(j, k)) <= amax THEN GOTO 202
      ir = j
      ic = k
      amax = ABS(a(j, k))
202  NEXT k
203  NEXT j
      ip(ic) = ip(ic) + 1
      IF amax <= 1D-30 THEN
204  LOCATE 1, 1: PRINT "singular matrix"
      SCREEN 0
      END
      END IF
      IF ir = ic THEN GOTO 208

' amax is not on the diagonal, so swap rows.
      FOR k = 1 TO n
        SWAP a(ir, k), a(ic, k)
      NEXT k
      IF L = 0 THEN GOTO 208
      SWAP b(ir), b(ic)

208  in(i, 1) = ir
      in(i, 2) = ic
      amax = a(ic, ic)
      a(ic, ic) = 1#
      FOR k = 1 TO n
        a(ic, k) = a(ic, k) / amax
      NEXT k
      IF L = 0 THEN GOTO 210
      b(ic) = b(ic) / amax

210  FOR j = 1 TO n
      IF j = ic THEN GOTO 212
      amax = a(j, ic)
      a(j, ic) = 0#

```

```

        FOR k = 1 TO n
            a(j, k) = a(j, k) - a(ic, k) * amax
        NEXT k
        IF L = 0 THEN GOTO 212
        b(j) = b(j) - b(ic) * amax
212 NEXT j
    NEXT i

    IF L = 1 THEN EXIT SUB
    FOR i = 1 TO n
        j = n + 1 - i
        IF in(j, 1) = in(j, 2) THEN GOTO 214
        ir = in(j, 1)
        ic = in(j, 2)
        FOR k = 1 TO n
            SWAP a(k, ir), a(k, ic)
        NEXT k
214 NEXT i

END SUB

SUB test (icycle, ncycle, sd, it$, d, m, L, ifp(), tcmat(), tdmat()) STATIC
/*****      CHECKS FOR CONVERGENCE & PRINTS UPDATES OF FIT PROGRESS      *****/
' Print the iteration # and the standard deviation on the screen & to the doc file
PRINT #2, USING "   ##          ##.###^    ^    ##.#####"; icycle; CSNG(sd); CSNG(d)
COLOR 7
LOCATE 1, 50: PRINT "iter  standard deviation";
LOCATE 2, 50: PRINT USING "_# ##          ##.#####^    ^    "; icycle; sd;

' Check to see if this iteration has just begun
IF icycle = 0 THEN
    it$ = "iterating"
    sdo = sd
    EXIT SUB
END IF

' Check for convergence and go to appropriate section
IF (sdo - sd) / sdo <= .005# AND (sdo - sd) / sdo >= -.000001# THEN
    it$ = "converged"
    EXIT SUB
ELSEIF (sdo - sd) / sdo > .005# THEN
    IF icycle = ncycle THEN
        it$ = "maxed"
    ELSE
        it$ = "iterating"
        sdo = sd
    END IF
    EXIT SUB
ELSE
    it$ = "died"
    PRINT "iteration diverged"
' Calculate the correlation coefficients
CALL matinv(tcmat(), tdmat(), L + m, 0)
FOR j = 2 TO m
    kk = j - 1
    FOR k = 1 TO kk
        tcmat(j, k) = 0#
        FOR i = 1 TO L
            IF j = ifp(i) OR k = ifp(i) THEN GOTO 9
        NEXT i
        tcmat(j, k) = tcmat(k, j) / SQR(ABS(tcmat(j, j) * tcmat(k, k)))
    NEXT k
9 NEXT j
FOR j = 1 TO m

```

```
    tcmat(j, j) = 1#  
  NEXT j  
  Print the correlation coefficient matrix  
  PRINT #2, "..... iteration diverged ....."  
  PRINT #2,  
  PRINT #2, "Correlation matrix:"  
  FOR i = 1 TO m  
    FOR j = 1 TO m - 1  
      PRINT #2, USING "##.###^" " "; tcmat(i, j);  
    NEXT j  
    PRINT #2, USING "##.###^"; tcmat(i, m)  
  NEXT i  
  EXIT SUB  
END IF  
END SUB
```

REFERENCES

FRASER R.D.B. and SUZUKI E. (1973) The use of least squares analysis in data analysis. In *Physical Principles and Techniques of Protein Chemistry, Part C* (Ed. S.J.LEACH), Academic Press, New York, Chap. 21.

VITA

The author was born in Portland, Oregon in 1957. She attended Sacred Heart Elementary School, where she was first introduced to science by a most extraordinary teacher, Sister Barbara Putnam. Her education continued at LaSalle High School. She graduated from the University of Portland, in 1979. She then spent 2 years working as a research assistant in pharmacology and oncology laboratories at the Oregon Health Sciences University. She returned to school to earn an Oregon teaching certificate in 1980 and taught chemistry and mathematics to 16 and 17 year olds at Beaverton High School for five very enjoyable years. (How **do** we know that atoms are not like blueberry muffins?)

She had almost finished a Master's Degree in Teaching when she enrolled in Jim Pankow's Aquatic Chemistry course at OGI and was persuaded to pursue a Ph.D. She was awarded an MAT degree from Lewis and Clark college in June of 1986 and became a full-time student at OGI in September of the same year. She successfully defended a thesis proposal in June of 1988 and has spent much of her time over the past three years working in the laboratory with humic material (*dirt*) and alkali metal cations (*salt*). With her husband, Stewart Rounds, she has written and published a computer program (*Dream*, 1990) that calculates groundwater flow for simple systems. She completed the requirements for the degree of Doctor of Philosophy in February of 1992.

After leaving OGI, the author hopes to rediscover the real world. She would like to teach undergraduate students about chemistry and environmental science.

BONN B.A. and ROUNDS S.A. (1990) *Dream*, Lewis Publishers, Chelsea, MI.